frontiers | Research Topics

Molecular pharmacological approaches against lung diseases: Targeted drug discovery

Edited by
Poonam Arora, Lalit Mohan Nainwal and Seyyed Shamsadin Athari

Published in
Frontiers in Pharmacology

ISSN 1664-8714
ISBN 978-2-8325-5070-0
DOI 10.3389/978-2-8325-5070-0

About Frontiers

Frontiers is more than just an open access publisher of scholarly articles: it is a pioneering approach to the world of academia, radically improving the way scholarly research is managed. The grand vision of Frontiers is a world where all people have an equal opportunity to seek, share and generate knowledge. Frontiers provides immediate and permanent online open access to all its publications, but this alone is not enough to realize our grand goals.

Frontiers journal series

The Frontiers journal series is a multi-tier and interdisciplinary set of open-access, online journals, promising a paradigm shift from the current review, selection and dissemination processes in academic publishing. All Frontiers journals are driven by researchers for researchers; therefore, they constitute a service to the scholarly community. At the same time, the *Frontiers journal series* operates on a revolutionary invention, the tiered publishing system, initially addressing specific communities of scholars, and gradually climbing up to broader public understanding, thus serving the interests of the lay society, too.

Dedication to quality

Each Frontiers article is a landmark of the highest quality, thanks to genuinely collaborative interactions between authors and review editors, who include some of the world's best academicians. Research must be certified by peers before entering a stream of knowledge that may eventually reach the public - and shape society; therefore, Frontiers only applies the most rigorous and unbiased reviews. Frontiers revolutionizes research publishing by freely delivering the most outstanding research, evaluated with no bias from both the academic and social point of view. By applying the most advanced information technologies, Frontiers is catapulting scholarly publishing into a new generation.

What are Frontiers Research Topics?

Frontiers Research Topics are very popular trademarks of the *Frontiers journals series*: they are collections of at least ten articles, all centered on a particular subject. With their unique mix of varied contributions from Original Research to Review Articles, Frontiers Research Topics unify the most influential researchers, the latest key findings and historical advances in a hot research area.

Find out more on how to host your own Frontiers Research Topic or contribute to one as an author by contacting the Frontiers editorial office: frontiersin.org/about/contact

Molecular pharmacological approaches against lung diseases: Targeted drug discovery

Topic editors

Poonam Arora — Shree Guru Gobind Singh Tricentenary University, India

Lalit Mohan Nainwal — GD Goenka University, India

Seyyed Shamsadin Athari — Zanjan University of Medical Sciences, Iran

Citation

Arora, P., Nainwal, L. M., Athari, S. S., eds. (2024). *Molecular pharmacological approaches against lung diseases: Targeted drug discovery*.

Lausanne: Frontiers Media SA. doi: 10.3389/978-2-8325-5070-0

Table of contents

frontiers | Frontiers in Pharmacology

TYPE Editorial
PUBLISHED 09 July 2024
DOI 10.3389/fphar.2024.1419138

OPEN ACCESS

EDITED AND REVIEWED BY
Heike Wulff,
University of California, Davis, United States

*CORRESPONDENCE
Poonam Arora,
poonamarora96@gmail.com

RECEIVED 17 April 2024
ACCEPTED 05 June 2024
PUBLISHED 09 July 2024

CITATION
Arora P, Nainwal LM and Athari SS (2024), Editorial: Molecular pharmacological approaches against lung diseases: targeted drug discovery.
Front. Pharmacol. 15:1419138.
doi: 10.3389/fphar.2024.1419138

Editorial: Molecular pharmacological approaches against lung diseases: targeted drug discovery

Poonam Arora[1]*, Lalit Mohan Nainwal[2] and Seyyed Shamsadin Athari[3]

[1]SGT College of Pharmacy, SGT University, Gurugram, India, [2]School of Medical and Allied Sciences, G. D. Goenka University, Gurugram, India, [3]Department of Immunology, School of Medicine, Zanjan University of Medical Sciences, Zanjan, Iran

KEYWORDS

respiratory disorders, molecular target based therapeutics, bispecific antibodies, monoclonal antibodies, RNA based therapeutics

Editorial on the Research Topic
Molecular pharmacological approaches against lung diseases: targeted drug discovery

Respiratory diseases represent a major global health and economic burden to society. The immunological complexity of asthma and chronic obstructive pulmonary disease, due to their considerable variation in phenotype and endotype, greatly hinders the identification of new therapeutic solutions (Arora et al., 2022a; Arora et al., 2022b). In recent years, increasing efforts by researchers to elucidate the molecular basis of disease pathology have coined the new concept of target-based molecular therapeutics. This approach has been exploited to tag small molecular agents obtained from biological and chemical studies that are patient-centric and have the potential to transform the course of a disease. Such therapies are efficient enough for disease treatment, mitigating side effects and reducing dose administration with better outcomes. Natural products have garnered significant attention in drug delivery due to their diverse chemical structures and inherent biological activity that can be harnessed for the development of targeted drug delivery systems (Nainwal and Arora, 2023).

The journal "Frontiers in Pharmacology" section Respiratory Pharmacology publishes high-quality research and review articles related to immunopharmacology, biology and therapeutic approaches in respiratory diseases. To introduce a special issue, the editorial "*Molecular pharmacological approaches against lung diseases: targeted drug discovery*" was published as a Research Topic in the journal, where we invited submissions ranging from original research to all types of review articles falling within the scope of the theme. The objective of this Research Topic was to shed light on the latest advancements in the use of molecular pharmacology to exploit the inherent capabilities of bioactive natural compounds for targeted drug delivery in lung diseases. A total of nine articles were selected, including original research articles, and two review articles.

The first review article by author Das et al. and collaborators explained the significant link between obesity and asthma pathophysiology. The manuscript critically discussed the

therapeutic role of medicinal plants and their phytoconstituents, including celastrol, tomatidine, resveratrol, quercetin, ascorbic acid, β-carotene, chrysophanol against obesity-associated asthma. In another article, Song et al. summarized the pharmacokinetics and molecular pharmacology of a flavonoid glycoside, Baicalin, in respiratory diseases. The researchers also discussed strategies that could be utilsed to improve the bioavailability of this flavonoid. Authors, further recommend further experimental studies for development of Baicalin into pharmaceutical drug product. Blanco et al. in their manuscript reported a persistent imbalance between cell proliferation and apoptosis as an underlying factor in the pathophysiology of pulmonary arterial hypertension. The authors demonstrated the role of survivin in the pathogenesis of pulmonary arterial hypertension and the potential of YM155, a novel compound as a significant inhibitor of survivin. Phulwanti Kumari Sharma studied the potential efficacy of *Withania sominifera* extract in reducing airway inflammation in cell-based assays and experimental models of LPS-induced inflammation. The findings reported in the research paper showed reduced levels of pharmacological markers and inflammatory cytokines in the lungs of animals treated with this plant extract, suggesting a therapeutic role of the plant in inflammatory disorders.

In a paper published by Wei et al., the authors proposed the protective efficacy of a new molecule, NRICM101 against COVID-19-induced lung injury. They proposed that the therapeutic role of NRICM101 in reversing pulmonary injury may be mediated by modulating the innate immune response and inhibiting pattern recognition receptor and toll-like receptor signaling. Ye et al. validated the therapeutic efficacy of a Chinese herbal formula, ECXB, in Chronic Obstructive Pulmonary Disease. The authors utilized multiple approaches such as network pharmacology, molecular docking, and molecular dynamic simulations to identify active components in the ECXB formula. The researchers suggested that the effects of the plant were due to the multi-target synergistic actions of the plant phytocomponents.

The role of Ferroptosis has been observed in the pathogenesis of inflammation and infection. In a research paper by Wang et al., the authors discovered ferroptosis-related hub genes, CAMKK2 and CISD1 and reported them as potential immunotherapy targets and prognostic markers for asthma. Chen et al. combined a Network pharmacology-based analytical approach and *in vivo* experimental methods to explore the mechanism of Cepharanthine in the treatment of acute respiratory distress syndrome. The researchers identified novel genes that play an important part in pathogenesis of inflammatory response. A study by Jin et al. examined the effects of the inhalation of PM@Cur-RV NPs poly (lactic-co-glycolic acid) nanoparticles in the management of pulmonary diseases. For this study, they designed curcumin and resveratrol PM@Cur-RV NPs by combining poly (lactic-co-glycolic acid) nanoparticles coated with platelet membrane vesicles (PM) for targeted delivery in inflammatory lungs.

Recent advancements in understanding of the pathophysiology of chronic respiratory diseases aim towards identification of potential novel targets for pharmacological interventions. The molecular target-based therapeutics approach will open new avenues for personalised therapies that may have potential to transform patient outcomes in the management of chronic disease cases. The articles included in this Research Topic provide scientific information related to pharmacological effects of bioactives obtained from natural products that could provide endless opportunities in the design of biologically active lead molecules for utilisation in targeted drug discovery.

Author contributions

PA: Conceptualization, Writing–original draft. LN: Conceptualization, Writing–review and editing. SA: Resources, Writing–review and editing.

Conflict of interest

The authors declare that the research was conducted in the absence of any commercial or financial relationships that could be construed as a potential conflict of interest.

Publisher's note

References

Arora, P., Athari, S. S., and Nainwal, L. M. (2022a). Piperine attenuates production of inflammatory biomarkers, oxidative stress and neutrophils in lungs of cigarette smoke-exposed experimental mice. *Food Biosci.* 49, 101909. doi:10.1016/j.fbio.2022.101909

Arora, P., Nainwal, L. M., Gupta, G., Singh, S. K., Chellappan, D. K., Oliver, B. G., et al. (2022b). Orally administered solasodine, a steroidal glycoalkaloid, suppresses ovalbumin-induced exaggerated Th2-immune response in rat model of bronchial asthma. *Chemico-Biological Interact.* 366, 110138. doi:10.1016/j.cbi.2022.110138

Nainwal, L. M., and Arora, P. (2023). "Dietary polyphenols in arthritis and inflammatory disorders," in *Book: dietary polyphenols in human diseases advances and challenges in drug discovery*. Editor M. Rudrapal 1st Edition (United States: CRC Press).

frontiers | Frontiers in Pharmacology

TYPE Original Research
PUBLISHED 26 October 2022
DOI 10.3389/fphar.2022.1054339

OPEN ACCESS

EDITED BY
Lalit Mohan Nainwal,
GD Goenka University, India

REVIEWED BY
Mukesh Kumar Kumawat,
Apeejay Stya University, India
Ashok Kumar,
University of Kansas Medical Center, United States

*CORRESPONDENCE
Ye Zhang,
zhangy@ahmu.edu.cn
Chunhui Wang,
wangchhaymz@163.com
Jian Huang,
876886365@qq.com

†These authors have contributed equally to this work

SPECIALTY SECTION
This article was submitted to Ethnopharmacology, a section of the journal Frontiers in Pharmacology

RECEIVED 26 September 2022
ACCEPTED 17 October 2022
PUBLISHED 26 October 2022

CITATION
Chen C, Wang N, Wang B, Zhang Q, Hu Y, Cheng G, Tao S, Huang J, Wang C and Zhang Y (2022), Network analysis-based strategy to investigate the protective effect of cepharanthine on rat acute respiratory distress syndrome. *Front. Pharmacol.* 13:1054339. doi: 10.3389/fphar.2022.1054339

Network analysis-based strategy to investigate the protective effect of cepharanthine on rat acute respiratory distress syndrome

Chen Chen[1,2,3†], Ning Wang[1,2†], Bingjie Wang[3,4†], Qiaoyun Zhang[3,4], Yuexia Hu[3,4], Gao Cheng[3,4], Shaoyi Tao[3,4], Jian Huang[5]*, Chunhui Wang[3,4]* and Ye Zhang[1,2]*

[1]Department of Anesthesiology, The Second Affiliated Hospital of Anhui Medical University, Hefei, China, [2]Key Laboratory of Anesthesiology and Perioperative Medicine of Anhui Higher Education Institutes, Anhui Medical University, Hefei, China, [3]Anhui Public Health Clinical Center, Hefei, China, [4]Department of Anesthesiology, The First Affiliated Hospital of Anhui Medical University, Hefei, China, [5]Department of Thoracic Surgery, First Affiliated Hospital of Anhui Medical University, Hefei, Anhui, China

Combined with Network Analysis (NA) and *in vivo* experimental methods, we explored and verified the mechanism of Cepharanthine (CEP) involved in the treatment of acute respiratory distress syndrome (ARDS). Potential targets of CEP were searched using the SwissTargetPrediction database. The pathogenic genes related to ARDS were obtained using the DisGeNET database. A protein-protein interaction network of common target genes of disease-compound was subsequently built and visualised. Functional enrichment analysis was performed through the Enrichr database. Finally, for *in vivo* experimental verification, we established an oleic acid-induced ARDS rat model, mainly through histological evaluation and the ELISA method to evaluate both the protective effect of CEP on ARDS and its effect on inflammation. A total of 100 genes were found to be CEP targeted genes, while 153 genes were found to be associated with ARDS. The PPI network was used to illustrate the link and purpose of the genes associated with CEP and ARDS, which contained 238 nodes and 2,333 links. GO and KEGG analyses indicated that inflammatory response and its related signalling pathways were closely associated with CEP-mediated ARDS treatment. Thus, a key CEP–gene–pathway-ARDS network was constructed through network analysis, including 152 nodes (5 targets and 6 pathways) and 744 links. The results of *in vivo* experiments showed that CEP could alleviate histopathological changes and pulmonary edema related to ARDS, in addition to reducing neutrophil infiltration

Abbreviations: ADME, absorption, distribution, metabolism, and excretion; ARDS, acute respiratory distress syndrome; BALF, broncho-alveolar lavage fluid; BP, biological processes; CC, cellular components; CEP, cepharanthine; DisGeNET, disease target genes; ELISA, enzyme-linked immunosorbent assay; GO, gene ontology; H&E, hematoxylin-eosin; IHC, immunohistochemical; KEGG, kyoto encyclopedia of genes and genomes; MF, molecular function; MPO, myeloperoxidase; NA, network Analysis; PI3P, phosphatidylinositol-3-phosphate; PI3K, phosphatidylinositol 3-kinase; PIP, phosphatidylinositol phosphate; PPI, protein-protein interactions; Res D1, ResolvinD1; Res E1, ResolvinE1; SARS-CoV-2, severe acute respiratory syndrome coronavirus 2; TCM, traditional Chinese medicines.

and secretion of inflammatory cytokines, whilst increasing serum contents of ResolvinD1 and ResolvinE1. Thus, these effects enhance the anti-inflammatory responses. Thus, our results show that CEP can treat oleic acid-induced ARDS in rats *via* ResolvinE1 and ResolvinD1 signalling pathways that promote inflammation resolution, providing a new avenue to explore for the clinical treatment of ARDS.

KEYWORDS

cepharanthine, ARDS, inflammation, traditional Chinese medicine, network analysis

1 Introduction

Acute respiratory distress syndrome (ARDS) is a rapidly progressing disease, which can be divided into two categories according to its underlying diseases: direct ARDS is a result of lung pathology, whilst indirect ARDS is caused by systemic inflammation (Monahan, 2013; Dickson et al., 2016). ARDS is a refractory disease associated with a high mortality (van Gemert et al., 2021). In the ICU, ARDS was reported to be the cause of 10.4% of admissions. Up to the 2000s, the mortality rate for ARDS was reported to be as high as 40%–70%. (Mane and Isaac, 2021). Although several ARDS treatments have been developed, none show the efficacy needed to reduce mortality or prolong the lives of ARDS patients.

Traditional Chinese medicine (TCM) has been widely used to treat lung diseases (Tsai et al., 2013). Relevant studies have shown that TCM has obvious effects in alleviating ARDS pulmonary inflammation, reducing mortality and improving prognosis (Yeh et al., 2021; Ting et al., 2022). Cepharanthine (CEP), a monomer component of TCM, is a natural alkaloid extracted from *Stephania cepharantha Hayata*, which has anti-inflammation, immunomodulation, antioxidation, anti-parasitic and anti-virus effects (Murakami et al., 2000; Furusawa and Wu, 2007; Kudo et al., 2011). Rat pharmacokinetics demonstrate that after a single dose of intravenous administration of 1 mg/kg, CEP achieved a 153.17 ± 16.18 ng/ml maximum plasma concentration and the $t_{1/2}$ was 6.76 ± 1.21 h. Bioavailability of CEP in rats after administration oral bioavailability of CEP was 5.65% ± 0.35%, which showed that oral bioavailability was low (Deng et al., 2017). As early as 2020, Tong et al. (Fan et al., 2020) has reported the research results of anti-Coronavirus Disease 2019 drugs, and found that CEP is a potential drug for the treatment of severe acute respiratory syndrome coronavirus 2 (SARS-CoV-2) infection. Recently, the scientific research team in China has successfully obtained the national invention patent authorization of CEP (Jiang et al., 2022). The patent specification shows that CEP 10 μmol/L inhibits SARS-CoV-2 replication by 15,393 times, showing a strong ability to inhibit viruses (Fan et al., 2020). Although CEP has the aforementioned beneficial characteristics, its role in the treatment of ARDS has not been reported. Network Analysis (NA) is a cross-discipline, that is, based on system biology, combining polypharmacology, molecular network data, bioinformatics and computer simulation (Gao et al., 2020; Sakle et al., 2020). It uses the database information of drugs, compounds, genes, and diseases to construct the interaction network of drug targets, disease targets and signal pathways, so as to reveal the complex mechanism of multi-components and multi-target characteristics of TCM (Saberian et al., 2019; Zhang et al., 2021). It provides the basis for the transformation of TCM from empirical medicine to evidence-based medicine, and provides some guidance for the development and application of new clinical drugs.

Based on the above research background, this study used NP to predict the potential target and pathway of CEP in the treatment of ARDS. We carried out *in vivo* experiments to verify the mechanism of CEP in the treatment of ARDS, which provided a research foundation for its clinical application.

2 Materials and methods

2.1 Absorption, distribution, metabolism and excretion screening

Common ADME characteristics include lipophilicity, water solubility, pharmacokinetics and drug-likeness (Nainwal et al., 2020; Nabi et al., 2022). We looked into the properties of CEP's ADME using the SwissADME database. Since 2017, SwissADME has been a Web application that provides free access to a collection of quick, yet reliable, predictive models to assess physicochemical properties, pharmacokinetics, drug-likeness, and synthetic accessibility, including in-house effective techniques like iLOGP (a physics-based model for lipophilicity) (Daina et al., 2017). The 2D structure of CEP is obtained by using chemdraw software (Ultra 8.0).

2.2 Acquisition target genes of cepharanthine

Utilising the PubChem (https://pubchem.ncbi.nlm.nih.gov) website, the structural formula of CEP was obtained in the Canonical SMILES format, and used as input for SwissTargetPrediction free webserver to predict potential molecular targets of CEP.

2.3 Disease-related target genes

The pathogenic genes related to ARDS were obtained by using the DisGeNET database (Piñero et al., 2021), which is one of the

largest publicly accessible datasets of genes and variations linked to human disorders. Data from expert-curated sources, GWAS catalogues, animal models, and scientific literature are all combined *via* DisGeNET. DisGeNET data are uniformly labeled using community-driven ontologies and controlled vocabularies. A number of unique measures are also offered to help with prioritising genotype-phenotype connections.

2.4 Common target genes of disease-compound

By creating venn diagrams, the targets of ARDS were intersected with the targets of active compound. Finally, the common targets of ARDS and the potential targets of CEP (in the treatment of ARDS) were obtained.

2.5 Discovery of protein-protein interactions network

To identify the network PPI, we utilised STRING11.0 (Szklarczyk et al., 2017) (https:/string-db.org/), an online tool for investigating protein interactions. The "Homo sapiens" sample type was chosen, and all gene symbols for ARDS and CEP were entered. For the PPI network development, a minimum interaction score requirement of 0.7 was used, and unconnected nodes were buried in the network for future presentation. The initial information on protein interactions was downloaded. Cytoscape v3.9.1 (Shannon et al., 2003) (https://www.cytoscape.org/), a tool used to visually analyse networks of protein interaction, portrayed the nodes and links in networks of protein interaction; this was used to visualise the PPI network.

2.6 Functional analysis

Gene Ontology (GO) enrichment analysis of biological processes (BP), cellular composition (CC), and molecular function (MF) of the common target genes of disease-compounds identified above were carried out using the Enrichr database (Kuleshov et al., 2016). Also examined were the common target genes pertaining to the Kyoto Encyclopedia of Genes and Genomes (KEGG) pathways and Jensen tissue. The analysis cutoff threshold, $p < 0.05$, was established.

2.7 Construction of key CEP–gene–pathway-acute respiratory distress syndrome network

Based on the aforementioned analysis, a CEP–gene–pathway-ARDS network was constructed using Cytoscape v3.9.1.

3 *In vivo* experimental verification

3.1 Experimental animals

Fifteen Sprague-Dawley rats (320 ± 30 g) were used as experimental animals in this study. They were randomly divided into three groups: Control (n = 5), ARDS (n = 5) and ARDS + CEP (n = 5). During the experiment, animals were placed in enriched cages with access to water and food. The cage was a temperature and hygrometry-controlled vicinity. The study protocol was approved by the Laboratory Animal Ethics Committee of Anhui Medical University (No. LLSC20190476) and performed according to the ARRIVE guidelines (https://www.nc3rs.org.uk/arrive-guidelines) for animal experiments.

3.2 Experimental protocol

CEP (purity 99.82%, Cat# HY-N6972, Selleck, Huston, TX, United States) was dissolved in sterile saline to a final concentration of 1.07×10^4 μmol/mol prior to the experiment. The rats were anaesthetised with pentobarbital (30 mg/kg intraperitoneally). After local disinfection of the right groin, 0.5% lidocaine anaesthesia was injected, penetrating layer-by-layer, in order to expose and separate the right femoral artery and vein. Next, a rat ARDS model was established according to the previous study (Li et al., 2021; Huang et al., 2022a; Huang et al., 2022b). Highly pure (99.9%) oleic acid (100 mg/kg) (Sigma, St. Louis, MO, United States) was slowly injected into the rat body through the femoral vein with a microsyringe. CEP (10 mg/kg) was injected intraperitoneally 1 h after oleic acid injection in the ARDS + CEP group, and the dose was determined according to previous reports (Murakami et al., 2000; Kudo et al., 2011; Chang et al., 2016). The Control and ARDS groups were injected with the same amount of sterile saline. 24 h after the intraperitoneal injection, rats were sacrificed by CO_2 narcosis and cervical dislocation. Subsequently, broncho-alveolar lavage fluid (BALF), in addition to serum and lung tissues, were collected for use in subsequent experiments.

3.3 BALF protein concentration and the Wet/Dry weight ratio

After the left main bronchus was clamped, BALF of the right lung was performed with 2 ml of pre-cooled sterile saline through a tracheal cannula. According to the manufacturer's instructions, we measured the BALF protein concentration using a bicinchoninic acid protein assay kit (Solaibao, Beijing, China). In the measurement of the Wet/Dry ratio, the left lower lobe of the lung was taken and weighed wet. The lung dry weight was recorded after being placed in an oven for 48 h. The Wet/Dry weight ratio of lung was subsequently calculated.

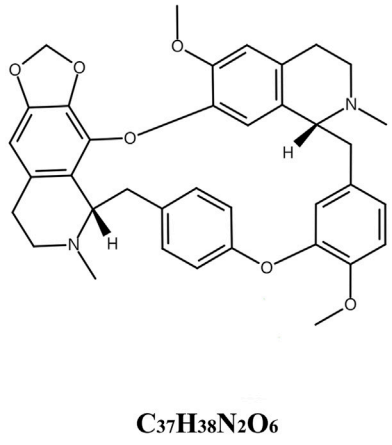

$C_{37}H_{38}N_2O_6$

Physicochemical Properties	
Formula	C37H38N2O6
Molecular weight	606.71 g/mol
Num. heavy atoms	45
Num. arom. heavy atoms	24
Fraction Csp3	0.35
Num. rotatable bonds	2
Num. H-bond acceptors	8
Num. H-bond donors	0
Molar Refractivity	179.15
TPSA	61.86 Å²
Lipophilicity	
Log $P_{o/w}$ (iLOGP)	4.98
Log $P_{o/w}$ (XLOGP3)	6.54
Log $P_{o/w}$ (WLOGP)	5.46
Log $P_{o/w}$ (MLOGP)	3.96
Log $P_{o/w}$ (SILICOS-IT)	5.71
Consensus Log $P_{o/w}$	5.33
Druglikeness	
Lipinski	Yes; 1 violation: MW>500
Ghose	No; 3 violations: MW>480, MR>130, #atoms>70
Veber	Yes
Egan	Yes
Muegge	No; 3 violations: MW>600, XLOGP3>5, #rings>7
Bioavailability Score	0.55

Pharmacokinetics	
GI absorption	High
BBB permeant	No
P-gp substrate	No
CYP1A2 inhibitor	No
CYP2C19 inhibitor	No
CYP2C9 inhibitor	No
CYP2D6 inhibitor	No
CYP3A4 inhibitor	No
Log K_p (skin permeation)	-5.36 cm/s
Water Solubility	
Log *S* (ESOL)	-7.98
Solubility	6.29e-06 mg/ml ; 1.04e-08 mol/l
Class	Poorly soluble
Log *S* (Ali)	-7.64
Solubility	1.40e-05 mg/ml ; 2.31e-08 mol/l
Class	Poorly soluble
Log *S* (SILICOS-IT)	-10.32
Solubility	2.88e-08 mg/ml ; 4.74e-11 mol/l
Class	Insoluble
Medicinal Chemistry	
PAINS	0 alert
Brenk	0 alert
Leadlikeness	No; 2 violations: MW>350, XLOGP3>3.5
Synthetic accessibility	7.01

FIGURE 1
Chemical structure and ADME parameters of CEP.

3.4 Histological evaluation

A paraffin embedding procedure was performed on the left superior lobes of the lung that were fixed in 10% buffered formalin for 48 h. Hematoxylin-eosin (H&E) staining and Immunohistochemical (IHC) staining was performed on 5 μm paraffin-embedded sections. For H&E staining, paraffin-embedded tissues were de-waxed, rehydrated, HE stained, and dehydrated. The lung sections were scored by a pathologist in a blinded fashion. The degree of lung injury was scored based on the following variables: hemorrhage, lung edema, inflammatory cell infiltration, hyaline membrane, and atelectasis. For IHC analysis, sections were incubated with Myeloperoxidase (MPO) (1:200, Cat# ab208670, Abcam, United States) antibodies at 4°C overnight followed by the secondary antibody. Diaminobenzidine substrate kits (Vector Laboratories, Burlingame, CA) were used to reveal the IHC reaction. For cell count, 10 high-power fields at a magnification of ×400, were randomly selected, and ~200 cells were counted in each field. All the sections were observed under an optical microscope.

3.5 Enzyme-linked immunosorbent assay

After the experiment, rat blood was collected from the inferior vena cava, then centrifuged at 3500 rpm for 15 min at 4°C. To assess the degree of inflammation, level of inflammatory cytokines such as TNF-α, IL-1β, IL-6, IL-8, ResolvinD1 (ResD1) and ResolvinE1 (ResE1) in the serum, lung and BALF were measured using ELISA assay kit (Bioexcellence, Beijing, China) according to the manufacturer's instructions.

3.6 Statistical analysis

We used the SPSS 22.0 statistical software (SPSS Inc., Chicago, IL, United States) to carry out statistical analysis and we created graphs using GraphPad Prism 7.0 (GraphPad, United States). Measurement data were expressed as mean ± standard deviation (SD). The normality of distribution was studied using the Shapiro-Wilk test. Independent sample *t*-test and/or one-way ANOVA were used to compare data between the two groups. p values <0.05 were considered statistically significant.

4 Results

4.1 Evaluation of acute respiratory distress syndrome parameters of CEP

CEP is a bisbenzylisoquinoline alkaloid from *Stephania cepharantha Hayata,* whose chemical formula is $C_{37}H_{38}N_2O_6$. Through the SwissADME database, the associated ADME characteristics of CEP were examined. SwissADME screening criteria: a. Gastrointestinal absorption (GI absorption) is "high"; b. 2 out of 5 gastric drug properties (Lipinski, Ghose, Veber, Egan, Muegge) results are "yes"; c. Lipophilicity is less than 5.5; d. Water solubility is less than −6. The findings revealed that the CEP's lipophilicity value was 5.36 and its water solubility value was −7.98. GI absorption was high, and the bioavailability score was 0.55. These values demonstrate the compound's enormous potential to be develop as a therapeutic molecule (Figure 1).

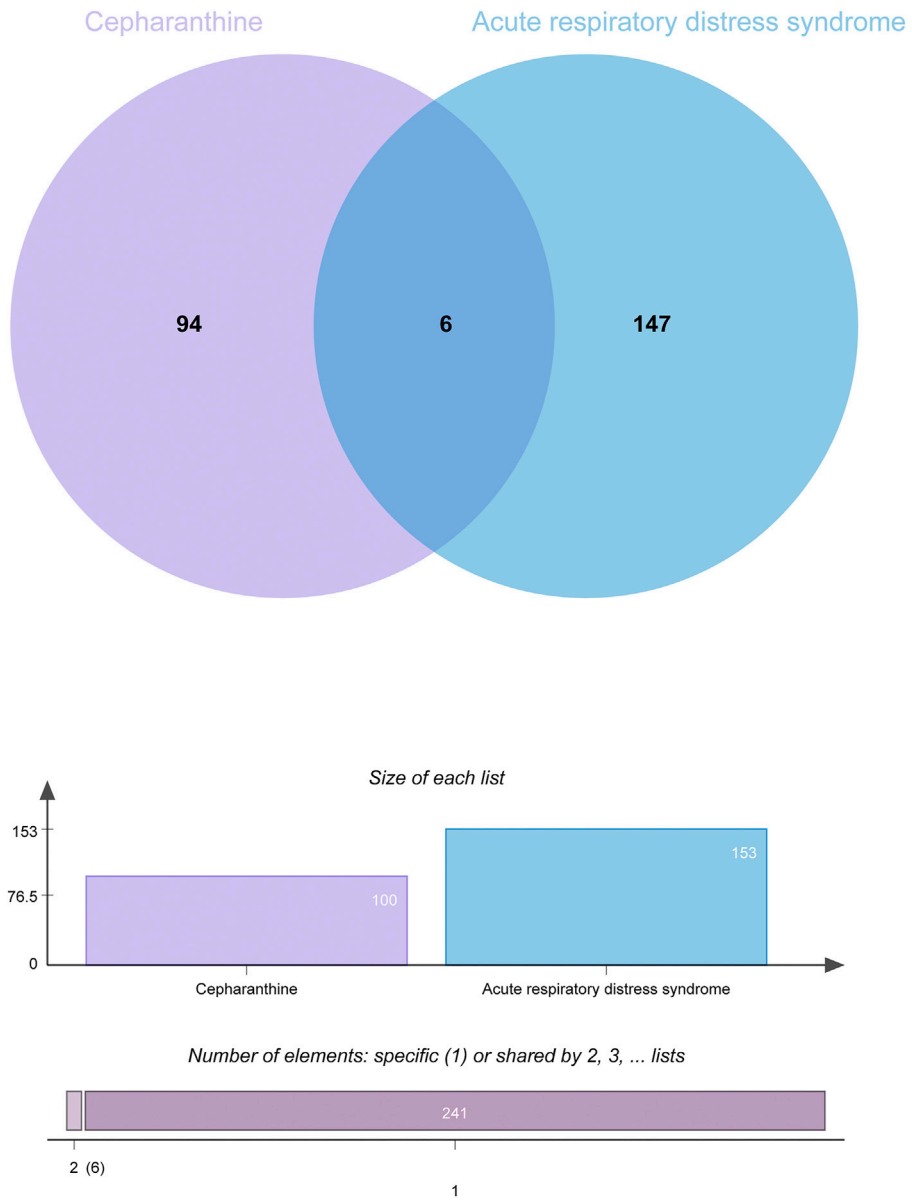

FIGURE 2
Venn diagram of the interactions of CEP targeted genes and genes associated with ARDS.

4.2 Identification of common target genes of disease-compound

A total of 100 genes were found to be CEP-targeted genes, while 153 genes were found to be associated with ARDS. A total of 6 genes were identified by the intersection between CEP's target genes and ARDS-related genes. In Figure 2, the target genes of disease-compounds were shown.

4.3 Construction of the PPI network

To collect PPI information, the discovered genes were submitted to the STRING database. In order to create the PPI network, we utilised Cytoscape (version 3.9.1). The PPI network (developed after the elimination of isolated nodes) was used to illustrate the link and purpose of the genes associated with CEP and ARDS. There were 238 nodes and 2333 links in the PPI network (Figure 3).

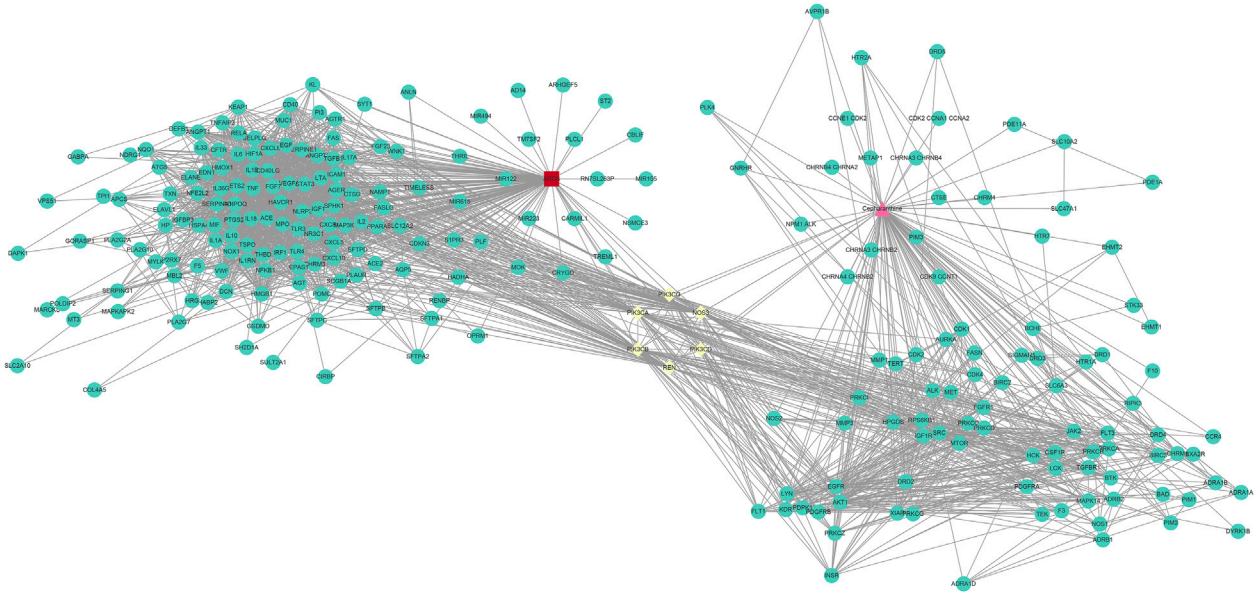

FIGURE 3
PPI network of CEP's targeted genes and genes associated with ARDS.

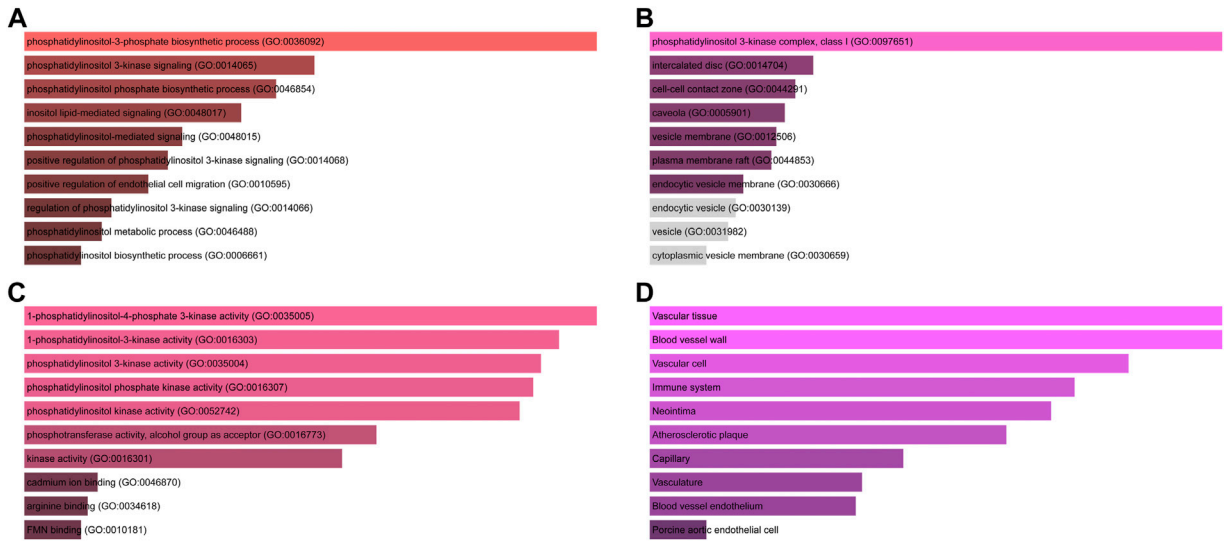

FIGURE 4
GO functional and tissue annotation for the common target genes of disease-compounds. **(A)** BP; **(B)** CC; **(C)** MF; **(D)** tissue. Ranking by-log10 (*p*-value).

4.4 GO enrichment analysis and tissue analysis of common target genes of disease-compounds

Initial common target genes of disease-compound were discovered for GO enrichment analysis to categorise the potential functions of these important common target genes of disease-compounds. Four types of outcomes, namely, BP, CC, MF, and tissues, were created from the data. The top ten phrases for GO enrichment of common target genes of disease-compounds in each category are displayed. The common target genes of disease-compounds, primarily enriched in the BP

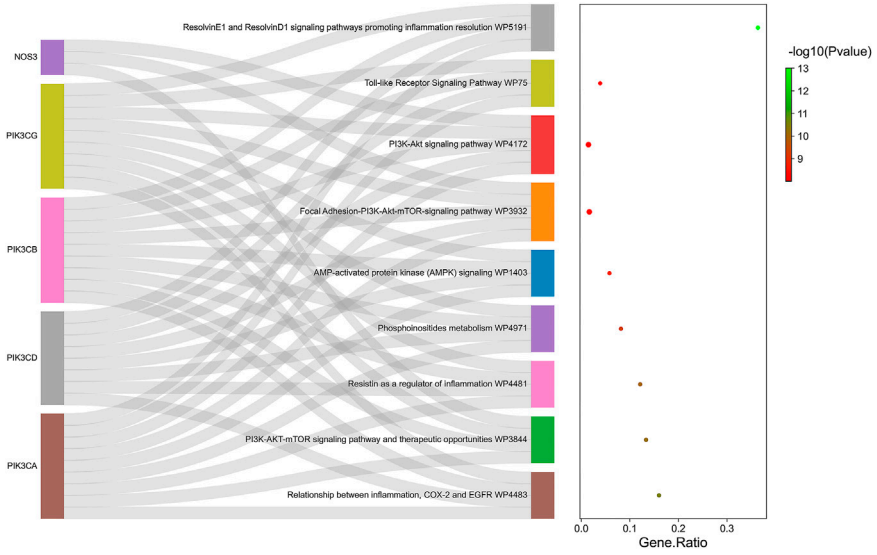

FIGURE 5
KEGG pathway enrichment analysis for the common target genes of disease-compound. Ranking by-log10 (*p*-value).

TABLE 1 Top ten KEGG pathways terms of common target genes of disease-compound.

Term	Overlap	*p*-value	Adjusted *p*-value	Odds Ratio	Combined Score	Genes
Relationship between inflammation, COX-2 and EGFR WP4483	4/25	2.84E-11	2.09E-09	1902.19	46,192.98	PIK3CA; PIK3CD; PIK3CB; PIK3CG
PI3K-AKT-mTOR signaling pathway and therapeutic opportunities WP3844	4/30	6.15E-11	2.09E-09	1536	36,113.53	PIK3CA; NOS3; PIK3CB; PIK3CG
Resistin as a regulator of inflammation WP4481	4/33	9.19E-11	2.34E-09	1376.897	31,821.11	PIK3CA; PIK3CD; PIK3CB; PIK3CG
Phosphoinositides metabolism WP4971	4/49	4.75E-10	5.38E-09	886.6222	19,033.66	PIK3CA; PIK3CD; PIK3CB; PIK3CG
AMP-activated protein kinase (AMPK) signaling WP1403	4/69	1.94E-09	1.97E-08	613.2	12,302.66	PIK3CA; PIK3CD; PIK3CB; PIK3CG
Focal Adhesion-PI3K-Akt-mTOR-signaling pathway WP3932	5/303	4.58E-09	3.59E-08	330.4698	6345.799	PIK3CA; NOS3; PIK3CD; PIK3CB; PIK3CG
PI3K-Akt signaling pathway WP4172	5/340	8.16E-09	5.55E-08	293.4179	5464.679	PIK3CA; NOS3; PIK3CD; PIK3CB; PIK3CG
Toll-like Receptor Signaling Pathway WP75	4/103	9.87E-09	6.29E-08	401.9192	7408.86	PIK3CA; PIK3CD; PIK3CB; PIK3CG
ResolvinE1 and ResolvinD1 signaling pathways promoting inflammation resolution WP5191	4/11	1.00E-13	2.51E-09	254.3333	9059.458	PIK3CA; PIK3CB; PIK3CD; PIK3CG

category, were the phosphatidylinositol-3-phosphate biosynthetic process, phosphatidylinositol 3-kinase signalling, and the phosphatidylinositol phosphate biosynthetic process (Figure 4A and Supplementary Table S1). The CC category included the phosphatidylinositol 3-kinase complex, class I, intercalated disc, and the cell-cell contact zone (Figure 4B and Supplementary Table S2). MF category included 1-phosphatidylinositol-4-phosphate 3-kinase activity, 1-phosphatidylinositol-3-kinase activity, and phosphatidylinositol 3-kinase activity (Figure 4C and Supplementary Table S3). The common target genes of disease-compounds, primarily enriched in the Jensen tissue category, were vascular tissue, blood vessel wall, and vascular cell (Figure 4D and Supplementary Table S4).

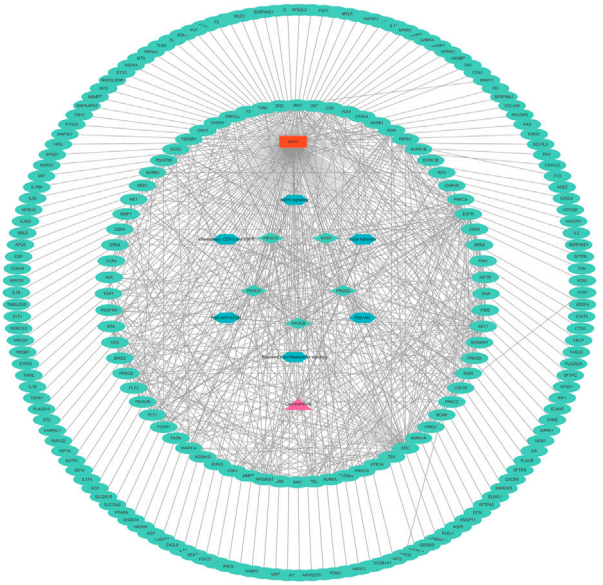

FIGURE 6
Key CEP–gene–pathway-ARDS network.

4.4.1 KEGG pathway analysis of common target genes of disease-compound

KEGG enrichment was then conducted on the common target genes of disease-compound. The common target genes of disease-compounds primarily enriched in the KEGG category were ResolvinE1 and ResolvinD1 signalling pathways (promoting inflammation resolution), the PI3K-Akt signalling pathway, the focal Adhesion-PI3K-Akt-mTOR-signalling pathway, AMP-activated protein kinase (AMPK) signalling, therapeutic opportunities, the PI3K-AKT-mTOR signalling pathway, as well as the relationship between inflammation, COX-2 and EGFR (Figure 5 and Table 1).

4.4.2 Construction of the key CEP–gene–pathway-ARDS network

A key CEP–gene–pathway-ARDS network was constructed, including 152 nodes (5 targets and 6 pathways) and 744 links (Figure 6).

4.5 CEP alleviated oleic acid induced-ARDS lung injury in rats

H&E staining showed the pathological changes of lung tissue in each group. Lung histopathology in the ARDS group showed clear alveolar inflammatory cell infiltration, edema and interstitial thickening, which was significantly alleviated after CEP treatment (Figure 7A). The lung injury score quantification confirmed that oleic acid-induced severe lung damage and was substantially attenuated by treatment with CEP (Figure 7B). Lung edema was quantified using the Wet/Dry weight ratio (Figure 7C). As we expected, the Wet/Dry ratio of lung tissues in the ARDS group was higher than that in the Control group, and was significantly decreased after the CEP treatment. In addition, we detected the BALF protein concentration and found that the ARDS group BALF protein concentration significantly increased, while it reduced in the ARDS + CEP group (Figure 7D).

4.6 Effects of CEP on ARDS-induced inflammation

To identify the inflammatory infiltrate, standard IHC was performed to stain for neutrophil-specific marker, MPO. MPO staining in lung tissues of each group was shown in Figure 8A. The positive expression of MPO in the ARDS + CEP group was significantly lower than that in the ARDS group (Figure 8B). However, the levels of serum Res D1 and Res E1 were significantly higher in the Control and ARDS + CEP group, compared with the ARDS group (Figure 8C). In terms of proinflammatory cytokines, the levels of TNF-α, IL-1β, IL-6, and IL-8 in BALF and lung tissues were higher in the ARDS group compared with the Control group; moreover, CEP treatment decreased their levels (Figures 8D,E).

5 Discussion

ARDS is a common critical illness, characterised by a large number of inflammatory reactions, which play an important role in its occurrence and development (Dickson et al., 2016). Therefore, effective suppression of inflammatory response is the basic treatment strategy for ARDS. TCM is widely used in the treatment of various diseases, among which it shows unique advantages in the treatment of lung diseases (Jin et al., 2021). However, several issues remain to be resolved, among them, the effective components and target genes of TCM have always been the key issues in the research of TCM (Jin et al., 2021). Based on NA and *in vivo* experimental verification, this study confirmed that CEP, an active component of TCM, played a significant role in improving the treatment of inflammation in ARDS.

The success of a medicinal drug depends not only on good efficacy, but also on the acceptable characteristics of ADME (Vaou et al., 2021). The ADME characteristics of CEP were analyzed based on the SwissADME database, as well as parameters including good lipophilicity, water solubility, GI absorption and bioavailability, which provide a basis for CEP as a molecular therapy for disease. We carried out NA analysis in order to further evaluate the therapeutic effect of CEP on ARDS

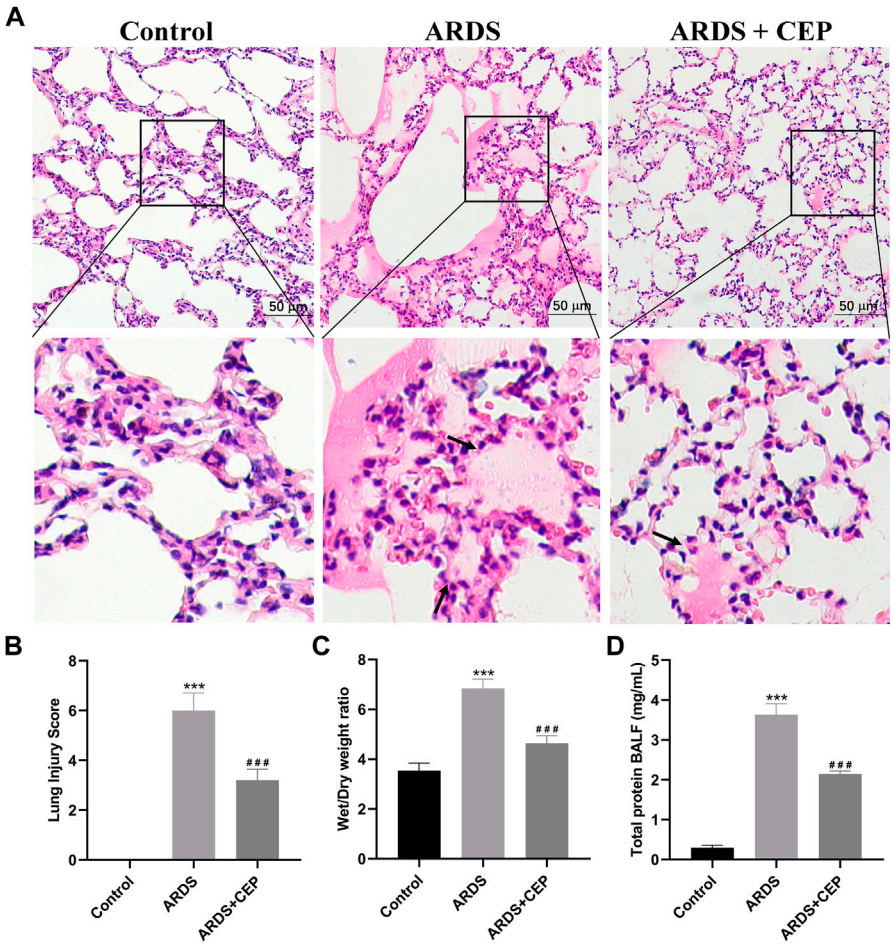

FIGURE 7
Evaluation of the CEP alleviation of oleic acid induced-ARDS lung injury *in vivo*. **(A)** Representative histological images of lung in each group (scale bar = 50 μm). Arrows represent exudative lesions and bleeding. **(B)** Lung injury scores according to the degree of lung damage in each group. **(C)** Wet/Dry weight ratios of lungs as an index of lung edema. **(D)** Total protein concentration in the BALF. Data are presented as the mean ± SD. ***$p < 0.001$, compared with the Control group; $^{###}p < 0.001$, compared with the ARDS group.

and predict its therapeutic target. Firstly, we constructed the PPI network that identified PIK3CA PIK3CB, PIK3CD, PIK3CG, NOS3, and REN are core targets in the context of CEP-mediated ARDS treatment. Subsequently, in order to clarify the multiple mechanisms of CEP on ARDS, we analyzed the enrichment of these targets by GO and KEGG. GO analysis showed that the treatment of CEP on ARDS was mainly related to phosphatidylinositol-3-phosphate (PI3P), phosphatidylinositol 3-kinase (PI3K) and the phosphatidylinositol phosphate (PIP) biosynthetic process. For PI3P, many steps of autophagy require the involvement of PI3P (Steinfeld et al., 2021). Many studies have shown that autophagy is associated with various lung diseases, including ARDS (Schuliga et al., 2021; Tomer et al., 2021). For PI3K, it plays an important role in inflammatory response, which promotes the production of a variety of pro-inflammatory cytokines (Cianciulli et al., 2016). In addition, PIP was reported to be essential in vesicular trafficking, organelle biogenesis and autophagy (Nascimbeni et al., 2017). Further KEGG analyses found that the role of CEP was mainly concentrated in the inflammatory factor signalling pathway of ResE1 and ResD1, as well as the apoptotic signalling pathway of PI3K-Akt. Next, in the rat ARDS model induced by oleic acid, it was further confirmed that CEP alleviated lung injury by inhibiting lung inflammatory response.

The animal model induced by oleic acid is a well-recognized animal model of ARDS (Fan et al., 2015; Huang et al., 2022a; Matute-Bello et al., 2008; Puuvuori et al., 2022). The destruction of alveolar capillary barrier, microvascular thrombosis and massive inflammation, are the main pathophysiological features of oleic acid-induced ARDS (Matute-Bello et al., 2008). Our study demonstrated that CEP treatment significantly ameliorated lung inflammation, reduced pulmonary edema, and improved

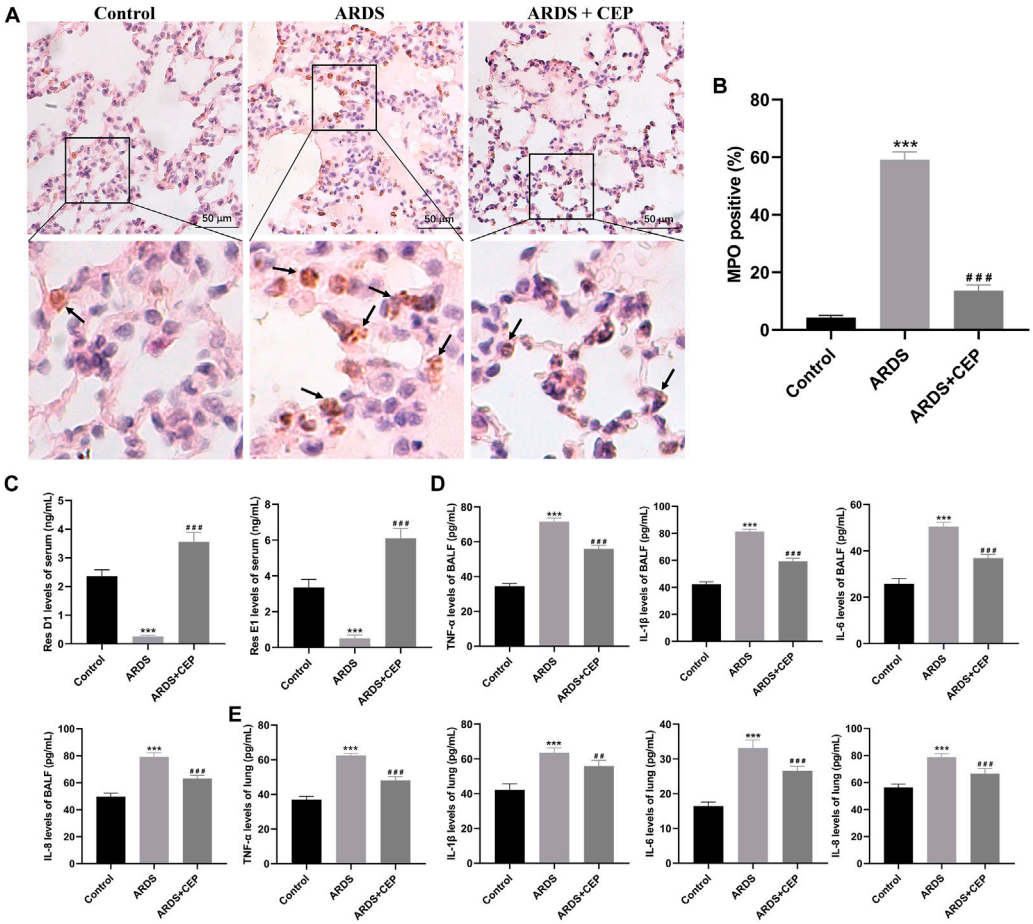

FIGURE 8
Effects of CEP on oleic acid induced-ARDS inflammation in rats. **(A,B)** Representative images of IHC staining for MPO (brown), a marker of neutrophils and their quantification in each group. Scale bar = 50 μm. **(C)** Levels of serum Res D1 and Res E1 assessed by ELISA. **(D,E)** Levels of TNF-α, IL-1β, IL-6, and IL-8 in BALF and lung tissues assessed by ELISA. Data are presented as the mean ± SD. ***$p < 0.001$, compared with the Control group; $^{\#\#}p < 0.01$, $^{\#\#\#}p < 0.001$, compared with the ARDS group.

histologic lung injury scores. MPO is a pro-inflammatory enzyme, mainly produced by activated neutrophils, which can promote the aggravation and prolongation of inflammation (Koyani et al., 2015). Previous studies have found that oleic acid, injected into lung tissue, can stimulate neutrophil accumulation (Ito et al., 2005; El Ayed et al., 2017). We found that CEP can significantly reduce the expression of MPO positive cells in lung tissue. In the above KEGG enrichment, significant enrichment belongs to ResE1 and ResD1 signalling pathways promoting inflammation resolution. Resolvins are potent short-lived autacoids that belong to a novel family of bioactive lipids and participate in the resolution process (Xie et al., 2016). Resolvins play an important role in orchestrating inflammation resolution (Guo et al., 2020). ResD1 and ResE1, as important members of the Resolvins family, have received more and more attention in the field of lung injury research (Seki et al., 2010; Wang et al., 2011; Thankam et al., 2022). Previous studies have shown that ResD1 protects the integrity of endothelial cell adhesion and barrier function from inflammatory mediators by inhibiting ROS production and preventing SHP2 inactivation (Wang et al., 2011). ResE1 is produced at the site of inflammation through transcellular metabolism and has been shown to effectively inhibit the migration of neutrophils across endothelial cells (Siddiquee et al., 2019). Our study found that the serum levels of ResD1 and ResE1 in CEP-treated rats were significantly increased. The proinflammatory mediator promote recruitment of inflammatory cells particularly, neutrophils and eosinophils, into the airways by its direct and indirect chemotactic properties (Arora et al., 2022a). IL-1β is a pro-inflammatory cytokine, which can trigger immune and inflammatory responses, and can be synthesised and secreted by a variety of cells (He et al., 2015). Pro-inflammatory cytokines IL-6 and IL-8 are important mediators of inflammation locally and systemically

(Wang et al., 2009). Antioxidants can prevent the enzymatic and non-enzymatic production of oxidant molecules and protect against the injurious effects of ROS (Arora et al., 2022b). As CEP can reduce the production of oxidants, it is reasonable to speculate that CEP may very likely act through oxidant production inhibition to exert its effects on downregulating inflammatory molecule expression (Chang et al., 2016). The expression levels of TNF-α, IL-1β, IL-6, and IL-8 in lung tissue and BALF were detected by ELISA *in vivo*. The results showed that CEP inhibited the expression of these inflammatory factors. Therefore, the data indicates that CEP effectively suppresses the inflammatory response of lung injury and confirms the results relating to the function of enrichment analysis.

Although this study has obtained a lot of effective information on the basis of NA and has been verified by experiments, there are still some limitations. Firstly, we collected all the relevant targets of CEP and ARDS from databases (as much as possible), however, we were not able to collect the latest research results. Secondly, although CEP can be administered safely over a range of doses without evident side effects, our study used only a single dose (10 mg/kg) for the CEP treatment. Thirdly, in terms of experimental verification, we only confirmed the therapeutic effect of CEP on the inflammatory response of ARDS, and no further research on the mechanism has been carried out, which will be the focus of future research work.

6 Conclusion

To sum up, this study preliminarily determined the key targets and important signalling pathways of CEP in the treatment of ARDS, based on NA. We verified the accuracy of the above results through *in vivo* experiments, which laid a theoretical foundation for the clinical application of CEP.

Data availability statement

The datasets presented in this study can be found in online repositories. The names of the repository/repositories and accession number(s) can be found in the article/ Supplementary Material.

Ethics statement

The animal study was reviewed and approved by Committee of Ethics on Animal Experiments at the Anhui Medical University.

Author contributions

JH, YZ, and CW designed the study. CC, BW, and NW performed the experiments. BW, QZ, and JH performed the statistical analysis. YH, GC, and ST drafted the article. CC, JH, YZ, and CW supervised the experimental work. All authors contributed to the article and approved the submitted version.

Funding

This work was supported by the National Natural Science Foundation of China (81970231), the Basic and Clinical Cooperative Research Promotion Program of Anhui Medical University (2020xkjT046), the Research Fund Of Anhui Medical University (2019xkj144, 2020xkj047), the Open Research fund of Key Laboratory of Anesthesiology and Perioperative Medicine of Anhui Higher Education Institutes, Anhui Medical University (MZKF202003), the Anhui Public Health Clinical Center Scientific Research Cultivating Fund (2022YKJ05).

Acknowledgments

We would like to thank Home for Researchers for providing language help and writing assistance.

Conflict of interest

The authors declare that the research was conducted in the absence of any commercial or financial relationships that could be construed as a potential conflict of interest.

Publisher's note

Supplementary material

The Supplementary Material for this article can be found online at: https://www.frontiersin.org/articles/10.3389/fphar.2022.1054339/full#supplementary-material

References

Arora, P., Athari, S.S., and Nainwal, L.M. (2022a). Piperine attenuates production of inflammatory biomarkers, oxidative stress and neutrophils in lungs of cigarette smoke-exposed experimental mice. *Food Biosci.* 49, 101909. doi:10.1016/j.fbio.2022.101909

Arora, P., Nainwal, L.M., Gupta, G., Singh, S.K., Chellappan, D.K., Oliver, B.G., et al. (2022b). Orally administered solasodine, a steroidal glycoalkaloid, suppresses ovalbumin-induced exaggerated Th2-immune response in rat model of bronchial asthma. *Chem. Biol. Interact.* 366, 110138. doi:10.1016/j.cbi.2022.110138

Chang, Y.K., Huang, S.C., Kao, M.C., and Huang, C.J. (2016). Cepharanthine alleviates liver injury in a rodent model of limb ischemia-reperfusion. *Acta Anaesthesiol. Taiwan* 54, 11–15. doi:10.1016/j.aat.2015.11.004

Cianciulli, A., Calvello, R., Porro, C., Trotta, T., Salvatore, R., and Panaro, M.A. (2016). PI3k/Akt signalling pathway plays a crucial role in the anti-inflammatory effects of curcumin in LPS-activated microglia. *Int. Immunopharmacol.* 36, 282–290. doi:10.1016/j.intimp.2016.05.007

Daina, A., Michielin, O., and Zoete, V. (2017). SwissADME: a free web tool to evaluate pharmacokinetics, drug-likeness and medicinal chemistry friendliness of small molecules. *Sci. Rep.* 7, 42717. doi:10.1038/srep42717

Deng, Y., Wu, W., Ye, S., Wang, W., and Wang, Z. (2017). Determination of cepharanthine in rat plasma by LC-MS/MS and its application to a pharmacokinetic study. *Pharm. Biol.* 55, 1775–1779. doi:10.1080/13880209.2017.1328446

Dickson, R.P., Singer, B.H., Newstead, M.W., Falkowski, N.R., Erb-Downward, J.R., Standiford, T.J., et al. (2016). Enrichment of the lung microbiome with gut bacteria in sepsis and the acute respiratory distress syndrome. *Nat. Microbiol.* 1, 16113. doi:10.1038/nmicrobiol.2016.113

El Ayed, M., Kadri, S., Smine, S., Elkahoui, S., Limam, F., and Aouani, E. (2017). Protective effects of grape seed and skin extract against high-fat-diet-induced lipotoxicity in rat lung. *Lipids Health Dis.* 16, 174. doi:10.1186/s12944-017-0561-z

Fan, H.H., Wang, L.Q., Liu, W.L., An, X.P., Liu, Z.D., He, X.Q., et al. (2020). Repurposing of clinically approved drugs for treatment of coronavirus disease 2019 in a 2019-novel coronavirus-related coronavirus model. *Chin. Med. J.* 133, 1051–1056. doi:10.1097/cm9.0000000000000797

Fan, X.F., Xue, F., Zhang, Y.Q., Xing, X.P., Liu, H., Mao, S.Z., et al. (2015). The Apelin-APJ axis is an endogenous counterinjury mechanism in experimental acute lung injury. *Chest* 147, 969–978. doi:10.1378/chest.14-1426

Furusawa, S., and Wu, J. (2007). The effects of biscoclaurine alkaloid cepharanthine on mammalian cells: implications for cancer, shock, and inflammatory diseases. *Life Sci.* 80, 1073–1079. doi:10.1016/j.lfs.2006.12.001

Gao, K., Song, Y.P., and Song, A. (2020). Exploring active ingredients and function mechanisms of Ephedra-bitter almond for prevention and treatment of Corona virus disease 2019 (COVID-19) based on network pharmacology. *BioData Min.* 13, 19. doi:10.1186/s13040-020-00229-4

Guo, Y., Tu, Y.H., Wu, X., Ji, S., Shen, J.L., Wu, H.M., et al. (2020). Extracellular Vesicles Released From the Skin Commensal Yeast Malassezia sympodialis Activate Human Primary Keratinocytes. *Front. Cell. Infect. Microbiol.* 10, 6. doi:10.3389/fcimb.2020.00006

He, W.T., Wan, H., Hu, L., Chen, P., Wang, X., Huang, Z., et al. (2015). Gasdermin D is an executor of pyroptosis and required for interleukin-1β secretion. *Cell Res.* 25, 1285–1298. doi:10.1038/cr.2015.139

Huang, J., Wang, B., Tao, S., Hu, Y., Wang, N., Zhang, Q., et al. (2022a). D-tagatose protects against oleic acid-induced acute respiratory distress syndrome in rats by activating PTEN/PI3K/AKT pathway. *Front. Immunol.* 13, 928312. doi:10.3389/fimmu.2022.928312

Huang, J., Zhang, R., Zhai, K., Li, J., Yao, M., Wei, S., et al. (2022b). Venovenous extracorporeal membrane oxygenation promotes alveolar epithelial recovery by activating Hippo/YAP signaling after lung injury. *J. Heart Lung Transplant.* 41, 1391–1400. doi:10.1016/j.healun.2022.06.005

Ito, K., Mizutani, A., Kira, S., Mori, M., Iwasaka, H., and Noguchi, T. (2005). Effect of Ulinastatin, a human urinary trypsin inhibitor, on the oleic acid-induced acute lung injury in rats via the inhibition of activated leukocytes. *Injury* 36, 387–394. doi:10.1016/j.injury.2004.06.018

Jiang, P., Ye, J., Jia, M., Li, X., Wei, S., and Li, N. (2022). The common regulatory pathway of COVID-19 and multiple inflammatory diseases and the molecular mechanism of cepharanthine in the treatment of COVID-19. *Front. Pharmacol.* 13, 960267. doi:10.3389/fphar.2022.960267

Jin, D., An, X., Zhang, Y., Zhao, S., Duan, L., Duan, Y., et al. (2021). Potential Mechanism Prediction of Herbal Medicine for Pulmonary Fibrosis Associated with SARS-CoV-2 Infection Based on Network Analysis and Molecular Docking. *Front. Pharmacol.* 12, 602218. doi:10.3389/fphar.2021.602218

Koyani, C.N., Flemmig, J., Malle, E., and Arnhold, J. (2015). Myeloperoxidase scavenges peroxynitrite: A novel anti-inflammatory action of the heme enzyme. *Arch. Biochem. Biophys.* 571, 1–9. doi:10.1016/j.abb.2015.02.028

Kudo, K., Hagiwara, S., Hasegawa, A., Kusaka, J., Koga, H., and Noguchi, T. (2011). Cepharanthine exerts anti-inflammatory effects via NF-κB inhibition in a LPS-induced rat model of systemic inflammation. *J. Surg. Res.* 171, 199–204. doi:10.1016/j.jss.2010.01.007

Kuleshov, M.V., Jones, M.R., Rouillard, A.D., Fernandez, N.F., Duan, Q., Wang, Z., et al. (2016). Enrichr: a comprehensive gene set enrichment analysis web server 2016 update. *Nucleic Acids Res.* 44, W90–97. doi:10.1093/nar/gkw377

Li, Y., Huang, J., Zhang, R., Wang, S., Cheng, X., Zhang, P., et al. (2021). Establishment of a venovenous extracorporeal membrane oxygenation in a rat model of acute respiratory distress syndrome. *Perfusion* 2676591211031468, 026765912110314. doi:10.1177/02676591211031468

Mane, A., and Isaac, N. (2021). Synopsis of Clinical Acute Respiratory Distress Syndrome (ARDS). *Adv. Exp. Med. Biol.* 1304, 323–331. doi:10.1007/978-3-030-68748-9_16

Matute-Bello, G., Frevert, C.W., and Martin, T.R. (2008). Animal models of acute lung injury. *Am. J. Physiol. Lung Cell. Mol. Physiol.* 295, L379–399. doi:10.1152/ajplung.00010.2008

Monahan, L.J. (2013). Acute respiratory distress syndrome. *Curr. Probl. Pediatr. Adolesc. Health Care* 43, 278–284. doi:10.1016/j.cppeds.2013.10.004

Murakami, K., Okajima, K., and Uchiba, M. (2000). The prevention of lipopolysaccharide-induced pulmonary vascular injury by pretreatment with cepharanthine in rats. *Am. J. Respir. Crit. Care Med.* 161, 57–63. doi:10.1164/ajrccm.161.1.9808142

Nabi, S.A., Ramzan, F., Lone, M.S., Beg, M.A., Hamid, A., Nainwal, L.M, et al. (2022). Synthesis, crystallographic study, molecular docking, ADMET, DFT and biological evaluation of new series of aurone derivatives as anti-leishmanial agents. *J. Mol. Struct.* 1256, 132528. doi:10.1016/j.molstruc.2022.132528

Nainwal, L.M., Shaququzzaman, M., Akhter, M., Husain, A., Parvez, S., Khan, F., et al. (2020). Synthesis, ADMET prediction and reverse screening study of 3, 4, 5-trimethoxy phenyl ring pendant sulfur-containing cyanopyrimidine derivatives as promising apoptosis inducing anticancer agents. *Bioorg. Chem.* 104, 104282. doi:10.1016/j.bioorg.2020.104282

Nascimbeni, A.C., Codogno, P., and Morel, E. (2017). Phosphatidylinositol-3-phosphate in the regulation of autophagy membrane dynamics. *Febs j* 284, 1267–1278. doi:10.1111/febs.13987

Piñero, J., Saüch, J., Sanz, F., and Furlong, L.I. (2021). The DisGeNET cytoscape app: Exploring and visualizing disease genomics data. *Comput. Struct. Biotechnol. J.* 19, 2960–2967. doi:10.1016/j.csbj.2021.05.015

Puuvuori, E., Chiodaroli, E., Estrada, S., Cheung, P., Lubenow, N., Sigfridsson, J., et al. (2022). PET imaging of neutrophil elastase with 11C-GW457427 in Acute Respiratory Distress Syndrome in pigs. *J. Nucl. Med.* doi:10.2967/jnumed.122.264306

Saberian, N., Peyvandipour, A., Donato, M., Ansari, S., and Draghici, S. (2019). A new computational drug repurposing method using established disease-drug pair knowledge. *Bioinformatics* 35, 3672–3678. doi:10.1093/bioinformatics/btz156

Sakle, N.S., More, S.A., and Mokale, S.N. (2020). A network pharmacology-based approach to explore potential targets of Caesalpinia pulcherima: an updated prototype in drug discovery. *Sci. Rep.* 10, 17217. doi:10.1038/s41598-020-74251-1

Schuliga, M., Read, J., and Knight, D.A. (2021). Ageing mechanisms that contribute to tissue remodeling in lung disease. *Ageing Res. Rev.* 70, 101405. doi:10.1016/j.arr.2021.101405

Seki, H., Fukunaga, K., Arita, M., Arai, H., Nakanishi, H., Taguchi, R., et al. (2010). The anti-inflammatory and proresolving mediator resolvin E1 protects mice from bacterial pneumonia and acute lung injury. *J. Immunol.* 184, 836–843. doi:10.4049/jimmunol.0901809

Shannon, P., Markiel, A., Ozier, O., Baliga, N.S., Wang, J.T., Ramage, D., et al. (2003). Cytoscape: a software environment for integrated models of biomolecular interaction networks. *Genome Res.* 13, 2498–2504. doi:10.1101/gr.1239303

Siddiquee, A., Patel, M., Rajalingam, S., Narke, D., Kurade, M., and Ponnoth, D.S. (2019). Effect of omega-3 fatty acid supplementation on resolvin (RvE1)-mediated suppression of inflammation in a mouse model of asthma. *Immunopharmacol. Immunotoxicol.* 41, 250–257. doi:10.1080/08923973.2019.1584903

Steinfeld, N., Lahiri, V., Morrison, A., Metur, S.P., Klionsky, D.J., and Weisman, L.S. (2021). Elevating PI3P drives select downstream membrane trafficking pathways. *Mol. Biol. Cell* 32, 143–156. doi:10.1091/mbc.E20-03-0191

Szklarczyk, D., Morris, J.H., Cook, H., Kuhn, M., Wyder, S., Simonovic, M., et al. (2017). The STRING database in 2017: quality-controlled protein-protein

association networks, made broadly accessible. *Nucleic Acids Res.* 45, D362–d368. doi:10.1093/nar/gkw937

Thankam, F.G., Wilson, V.E.D., Radwan, M.M., Siddique, A., and Agrawal, D.K. (2022). Involvement of ischemia-driven 5-lipoxygenase-resolvin-E1-chemokine like receptor-1 axis in the resolution of post-coronary artery bypass graft inflammation in coronary arteries. *Mol. Biol. Rep.* 49, 3123–3134. doi:10.1007/s11033-022-07143-4

Ting, N.C., Chen, Y.H., Chen, J.C., Huang, W.C., Liou, C.J., Chen, L.C., et al. (2022). Perilla Fruit Water Extract Attenuates Inflammatory Responses and Alleviates Neutrophil Recruitment via MAPK/JNK-AP-1/c-Fos Signaling Pathway in ARDS Animal Model. *Evid. Based. Complement. Alternat. Med.* 2022, 4444513. doi:10.1155/2022/4444513

Tomer, Y., Wambach, J., Knudsen, L., Zhao, M., Rodriguez, L.R., Murthy, A., et al. (2021). The common ABCA3(E292V) variant disrupts AT2 cell quality control and increases susceptibility to lung injury and aberrant remodeling. *Am. J. Physiol. Lung Cell. Mol. Physiol.* 321, L291–l307. doi:10.1152/ajplung.00400.2020

Tsai, W.H., Yang, C.C., Li, P.C., Chen, W.C., and Chien, C.T. (2013). Therapeutic potential of traditional chinese medicine on inflammatory diseases. *J. Tradit. Complement. Med.* 3, 142–151. doi:10.4103/2225-4110.114898

van Gemert, J.P., van den Berk, I.A.H., Nossent, E.J., Heunks, L.M.A., Jonkers, R.E., Vlaar, A.P., et al. (2021). Cyclophosphamide for interstitial lung disease-associated acute respiratory failure: mortality, clinical response and radiological characteristics. *BMC Pulm. Med.* 21, 249. doi:10.1186/s12890-021-01615-2

Vaou, N., Stavropoulou, E., Voidarou, C., Tsigalou, C., and Bezirtzoglou, E. (2021). Towards Advances in Medicinal Plant Antimicrobial Activity: A Review Study on Challenges and Future Perspectives. *Microorganisms* 9, 2041. doi:10.3390/microorganisms9102041

Wang, B., Gong, X., Wan, J.Y., Zhang, L., Zhang, Z., Li, H.Z., et al. (2011). Resolvin D1 protects mice from LPS-induced acute lung injury. *Pulm. Pharmacol. Ther.* 24, 434–441. doi:10.1016/j.pupt.2011.04.001

Wang, X.M., Hamza, M., Wu, T.X., and Dionne, R.A. (2009). Upregulation of IL-6, IL-8 and CCL2 gene expression after acute inflammation: Correlation to clinical pain. *Pain* 142, 275–283. doi:10.1016/j.pain.2009.02.001

Xie, W., Wang, H., Liu, Q., Li, Y., Wang, J., Yao, S., et al. (2016). ResolvinD1 reduces apoptosis and inflammation in primary human alveolar epithelial type 2 cells. *Lab. Invest.* 96, 526–536. doi:10.1038/labinvest.2016.31

Yeh, Y.C., Doan, L.H., Huang, Z.Y., Chu, L.W., Shi, T.H., Lee, Y.R., et al. (2021). Honeysuckle (Lonicera japonica) and Huangqi (Astragalus membranaceus) Suppress SARS-CoV-2 Entry and COVID-19 Related Cytokine Storm *in Vitro*. *Front. Pharmacol.* 12, 765553. doi:10.3389/fphar.2021.765553

Zhang, M., Li, P., Zhang, S., Zhang, X., Wang, L., Zhang, Y., et al. (2021). Study on the Mechanism of the Danggui-Chuanxiong Herb Pair on Treating Thrombus through Network Pharmacology and Zebrafish Models. *ACS Omega* 6, 14677–14691. doi:10.1021/acsomega.1c01847

frontiers | Frontiers in Pharmacology

TYPE Original Research
PUBLISHED 29 November 2022
DOI 10.3389/fphar.2022.1050224

OPEN ACCESS

EDITED BY
Lalit Mohan Nainwal,
GD Goenka University, India

REVIEWED BY
Mithun Rudrapal,
Rasiklal M. Dhariwal Institute of Pharmaceutical Education and Research, India
Zhiyu Dai,
University of Arizona, United States

*CORRESPONDENCE
Hua Jin,
jinhua0413@gdmu.edu.cn
Gonghua Huang,
gonghua.huang@gdmu.edu.cn

†These authors have contributed equally to this work

SPECIALTY SECTION
This article was submitted to Respiratory Pharmacology, a section of the journal Frontiers in Pharmacology

RECEIVED 21 September 2022
ACCEPTED 16 November 2022
PUBLISHED 29 November 2022

CITATION
Jin H, Luo R, Li J, Zhao H, Ouyang S, Yao Y, Chen D, Ling Z, Zhu W, Chen M, Liao X, Pi J and Huang G (2022), Inhaled platelet vesicle-decoyed biomimetic nanoparticles attenuate inflammatory lung injury.
Front. Pharmacol. 13:1050224.
doi: 10.3389/fphar.2022.1050224

Inhaled platelet vesicle-decoyed biomimetic nanoparticles attenuate inflammatory lung injury

Hua Jin[1,2*†], Renxing Luo[1,3†], Jianing Li[1,3], Hongxia Zhao[4], Suidong Ouyang[1], Yinlian Yao[1,2], Dongyan Chen[2], Zijie Ling[2], Weicong Zhu[2], Meijun Chen[2], Xianping Liao[2], Jiang Pi[2] and Gonghua Huang[1*]

[1]Guangdong Provincial Key Laboratory of Medical Molecular Diagnostics, The First Dongguan Affiliated Hospital, Guangdong Medical University, Dongguan, China, [2]School of Pharmacy, Guangdong Medical University, Dongguan, China, [3]School of Medical Technology, Guangdong Medical University, Dongguan, China, [4]School of Biomedical and Pharmaceutical Science, Guangdong University of Technology, Guangzhou, China

Acute lung injury (ALI) is an inflammatory response which causes serious damages to alveolar epithelia and vasculature, and it still remains high lethality and mortality with no effective treatment. Based on the inflammatory homing of platelets and cell membrane cloaking nanotechnology, in this study we developed a biomimetic anti-inflammation nanoparticle delivery system for ALI treatment. PM@Cur-RV NPs were designed by combining the poly (lactic-co-glycolic acid) nanoparticles (NPs) coated with platelet membrane vesicles (PM) for the purpose of highly targeting delivery of curcumin (Cur) and resveratrol (RV) to inflammatory lungs. PM@Cur-RV NPs showed good biocompatibility and biosafety both *in vitro* and *in vivo*. Accumulation of NPs into lung tract was observed after inhaled NPs. Remarkably, the inhalation of PM@Cur-RV NPs effectively inhibited lung vascular injury evidenced by the decreased lung vascular permeability, and the reduced proinflammatory cytokine burden in an ALI mouse model. The analysis of infiltrated macrophages in the lungs showed that the Cur-RV-modulated macrophage polarized towards M2 phenotype and the decreased histone lactylation might contribute to their anti-inflammation effects. Together, this work highlights the potential of inhalation of biomimetic nanoparticle delivery of curcumin and resveratrol for the treatment of pulmonary diseases.

KEYWORDS

acute lung injury, biomimetic nanoparticle, Chinese herbal medicine (CHM), platelet membrane coating, macrophage polarization (MP), histone lactylation

Introduction

Acute lung injury (ALI) or acute respiratory distress syndrome (ARDS) is characterized by respiratory distress, refractory hypoxemia, and non-cardiogenic pulmonary edema, with significantly high morbidity and mortality in critically ill patients (Zhang et al., 2021a). COVID-19 is associated with acute respiratory distress and cytokine release syndrome. In the later stage of disease, some COVID-19 patients may develop into ALI/ARDS or even multiple organ failure. Despite an improvement in the lung protective ventilation and a fluid conservative strategy, the mortality rate remains as high as 40% (Prasanna et al., 2021). In clinics, ALI/ARDS treatment is mainly relying on hormone drugs, such as glucocorticoids, antibiotics and supportive care (Fernando et al., 2021). Although all of these drugs demonstrate significantly anti-inflammatory effects, their off-targeting in the body determines their seriously systemic immunosuppressive side effects (Oray et al., 2016). Therefore, the findings of new targets and the development of targeting strategies are of great significance for controlling clinical pneumonia from mild to severe, reducing severe mortality, shortening hospitalization time, and improving the life quality of patients during treatment.

Macrophages are one of the most important immune cells in the body to control the inflammatory responses. Abundance of studies has shown that macrophages are key mediators in the pathogenesis of ALI/ARDS (Huang et al., 2018a), which demonstrates that regulation of macrophage polarization might be an important strategy to improve the prognosis. Under different local environmental stimuli, macrophages can be divided into two distinct polarization states: classically activated phenotype (M1), and the alternatively activated phenotype (M2) (Chen et al., 2020). Substantial evidences have shown that M1 is associated with pro-inflammatory responses, while M2 makes a great contribution to anti-inflammatory reactions (Sica and Mantovani, 2012; Arora et al., 2018). This demonstrates that employment of novel drugs or strategy to regulate macrophage towards M2 phenotype might be an effective treatment for ALI/ARDS.

Curcumin (Cur), a diarylheptanoid, which is produced from plants of the curcuma longa species, has been shown excellent inhibition effects in inflammation, metabolic syndrome, pain, various of cancers, etc (Hewlings and Kalman, 2017). In recent years, Cur has been reported to inhibit the inflammation through the modulation of macrophage autophagy (Shakeri et al., 2019). Although most of these pharmacological activities of curcumin demonstrate to play roles at the cellular level, it can't achieve expective improvements in clinical therapeutics due to its poor absorption, rapid metabolism, and rapid elimination (Ghalandarlaki et al., 2014).

Resveratrol (3, 5, 4' -trihydroxystilbene, RV) is a natural phytoalexin which is widely presents in grapes, peanuts, berries and especially Chinese herbal medicine Polygonum cuspidatu. Resveratrol is attracting increasing attentions in many fields, such as medicine, pharmacy, etc, because of its good anti-proliferative, anti-oxidative and anti-inflammatory activity (Zhang et al., 2021b). It has been found that RV could attenuate lung vascular hyperpermeability during ventilator-induced lung injury. However, its poor solubility in aqueous solvents greatly restricts its efficiency, bioavailability and application in clinics.

Therefore, the targeted delivery and enhancing the bioavailability of anti-inflammatory agents to the local inflammation sites represent a promising strategy for disease treatment. Recently, cell membrane coating-based biomimetic nanodrug delivery system has attracted increasing attentions in the field of nanomedicine (Fang et al., 2018). Cell membrane coated nanoparticles (NPs) are developed combining a NP core coated with membrane or membrane vesicles derived from natural cells such as erythrocytes, endothelial cells, cancer cells, stem cells, platelets or bacterial cells. This kind of biomimetic engineered device has proven to possess the functions of proteins from source cell membrane and drugs loaded in nanoparticles. The targeting ability of these biomimetic nanoparticles is often mediated by proteins that are expressed on the source cells, and this facilitates the NPs with the ability to specifically adhere to various disease substrates. In the past decade, various of cell membranes from erythrocytes to cancer cells have been coated onto the surface of nanoparticles to obtain nano-formulations with enhanced functionality that can be custom-tailored to specific applications (Park et al., 2021). Among these, nanoparticles coated with the membrane derived from platelets were develop to target damaged vasculature or inflammation sites in the lungs because platelets have the intrinsic affinity to the site of inflammation (Ma et al., 2020).

In this work, to improve the bioavailability and facilitate delivery of Cur and RV to the lung inflammations sites, poly (lactic-co-glycolic acid) (PLGA) nanoparticles were synthesized to co-encapsulate Cur and RV, and platelet membrane were isolated from healthy mouse blood and coated onto the Cur-RV NPs to form the inflammation targeting PM@Cur-RV NPs. *In vitro*, PM@Cur-RV NPs showed good dispersity, excellent biocompatibility and biosafety. *In vivo* studies demonstrated that PM@Cur-RV NPs could target and accumulate into the inflammatory lungs. In LPS-induced ALI mouse model, the PM@Cur-RV NPs demonstrated enhanced inhibiting effects on lungs vascular permeability and impressive improvement in anti-inflammation of lungs compared with other formulations of Cur and RV (i.e., Free Cur-RV and Cur-RV NPs). Interestingly, the PM@Cur-RV NPs could induce macrophages towards M2 polarization in pulmonary alveoli. Collectively, our study demonstrates that this kind of biomimetic nano-platform might be an efficient strategy to deliver drugs for treating infectious diseases, such as pneumonia.

Methods and materrials

Preparation of Cur and RV-coloaded PLGA nanoparticles

The Cur-RV NPs were synthesized using emulsification and evaporation method as previously described (Jin et al., 2017) with a little modification. Briefly, 20 mg of Curcumin ((Sigma, United States), 20 mg of resveratrol (Shanghai yuanye Bio-Technology Co., Ltd) and 160 mg PLGA-PEG (lactide: glycolide 50:50, sigma, United States) were co-dissolved in 5 ml of dichloromethane (Tianjin Damao Chemical Reagent Factory, China) as oil phase (O), 20 ml of PVA (1%, w/w, from sigma, United States) was as external water phase (W). Firstly, the O phase was ultrasonic for 40 s on ice bath to form the first emulsification. Then, the first emulsification was dropped in W phase and ultrasonicated for another 40 s to form the second emulsification. After that, the second emulsification was added to 100 ml water and stirred for 6 h for organic regent evaporation and nanoparticle hardening. Finally, the nanoparticles were harvested by centrifuging at 12,000 rpm for 20 min and washed 3 times using ultrapure water. The harvested NPs were lyophilized for 48 h for storage in powdered form.

Isolation of platelets

Fresh whole blood samples were drawn from healthy mice. Platelets from whole blood were isolated through gradient centrifugation [15]. Briefly, 0.5 ml whole blood (from five mice) was centrifuged at 200 g for 10 min and isolated the supernatant as platelet-rich plasma (PRP). Then, the PRP was centrifuged at 1800 g for 20 min, remove the supernatant and the precipitation was platelets. Wash it with PBS two times before using.

Preparation of platelet membrane-coated Cur and RV-coloaded NPs

Platelets were suspended in deionized water with protease inhibitor, frozen at −80°C, thawed at room temperature for use. The process of frozen-thawing was repeated for three times. A BCA protein assay kit (Solarbio, China) was used to determine the protein concentration of isolated PM. Finally, the mixture was extruded *via* a Hand Extruder to obtain uniform particles.

Characterization of NPs

Size distribution of NPs was measured using a Zetasizer Nano ZS. NPs were visualized by scanning electron microscopy (Philips Co., Holland). The encapsulation of Cur and RV was detected using an ultraviolet and visible spectrophotometer (UV 6000). To measure the drug (Cur and RV) loading rate of Cur-RV NPs, 10 mg lyophilized nanoparticles were dissolved in 1 ml of methanol, and then the amount of Cur or RV in solution was determined by High Pressure Liquid Chromatography (HPLC). HPLC detection was performed using a C18 column (5 μm, 250 mm × 4.6 mm). Whereas the mobile phase, consisting of methanol and 0.1% acetic acid (88:12) (v/v), was maintained at a flow rate of 1.0 ml/min. The ultraviolet detector wavelength was 218 nm (for Cur) and 210 nm (for RV) and the injection volume was 20 μl. The loading of Cur and RV was calculated the concentration of Cur and RV based on the standard curve.

SDS-PAGE analysis of retention proteins from cell membranes and NPs

Retained membrane proteins were examined by SDS-PAGE. Stem cell membrane protein samples and PM@Cur-RV NPs were mixed with loading buffer (Beyotime, China) and denatured at 95°C. 30 μg of protein samples was separated by 10% SDS-PAGE gel, and then the gel was stained with Coomassie Blue for 2 h and decolored overnight for imaging.

Hemolysis assay

To determine the *in vivo* biosafety of the compounds, hemolysis of red blood cells treated with the designated compounds was determined. Erythrocytes were originated from normal healthy C57BL/6J mice through washing the anticoagulant whole blood with PBS at 3,500 rpm for 5 min. Then, a 4% red blood cell suspension (v/v, in PBS) was blended with different compounds, including nanoparticles, MLT, and different formulations of DOX and ICG. The erythrocyte sample lysed using pure water was used as positive control, and erythrocyte sample diluted using PBS was used as negative control group. After incubating with 100ug/mL of compounds at 37°C for 4 h, all the samples were centrifuged at 3,500 rpm, 4°C, for 5 min to collect the supernatant and measured its absorbance value at 550 nm by a microplate reader. Also, the red blood cells were added into 12-well plate and imaged using a Living cell imaging system (EVOSFL Auto, Invitrogen, United States).

Cell viability assay

Cell Counting Kit-8 assay was used to detect cell viability according to the manufacturer's instruction. Primary cultures of Human umbilical vein endothelial cell (HUVECs) and human bronchial epithelial cell line (HBE cells) were cultured at 37°C in a humidified atmosphere of 5% CO_2 and 95% air. HUVECs or HBE cells were seeded into 96-well plates at a density of 10^4 cells/

well in 100 μl of RPMI medium with 10% FBS and incubated for 24 h. Then, the medium was replaced with 100 μl of fresh culture medium containing LPS (1ug/mL) plus either PBS with 5% of DMSO (vehicle) or different formulations of Cur and RV for another 24 h. Cell viability was then estimated by CCK-8 assay (Beyotime institute of biotechnology, China)) according to the manufacturer's protocol.

Cellular uptake

The green fluorescence of Cur was as the fluorescent marker of the different formulations of Cur and RV. Human bronchial epithelial cells (HBE) were bought from ATCC (Shanghai, China). The cells were cultured in DMEM (Gibco, United States) with 10% fetal bovine serum (Gibco) containing 100 μg/ml streptomycin and 100 IU/ml penicillin at 5% CO_2 and 37°C. The cells were cultured with free Cur-RV, Cur-RV NPs and PM@Cur-RV NPs for 4 h, separately, and then washed twice with PBS to remove unbound nanoparticles and added into PBS. The cells were imaged using a Live Cell Imaging System (EVOSFL Auto, Invitrogen, United States).

Animal study

8–12-week-age female C57/6J mice were purchased from SPF biotechnology co., LTD., Beijing, China. Experimental procedures using mice in this work were reviewed and approved by the ethical review board of Guangdong Medical University, and all the experiments were performed in accordance with relevant guidelines and regulations of Animal Ethics Committee of Guangdong province, China.

Mouse model of acute lung injury

Lipopolysaccharide (LPS, *E.coli* 0111:B4, L2630) was bought from Sigma (United States). To induce acute lung injury, LPS was dissolved in PBS and administered by intraperitoneal injection (i.p.) to mice at 5 mg/kg body weight in 150 μl PBS.

In vivo imaging of NPs in mice

LPS-induced C57BL/6J mouse sepsis model were intranasally administered with 50 μl of differently modified nanoparticles. Indocyanine green (ICG) was loaded into the NPs as fluorescence marker. For semiquantitative analysis, the image and fluorescence intensities of mice were collected 2 h after intranasal administration of NPs and determined using the Kodak Multi Mode Imaging System.

Assessment of lung vascular permeability

The Evans blue-conjugated albumin (EBA) extravasation assay was used to assess pulmonary vascular permeability (Zhao et al., 2014). Briefly, EBA (20 mg/kg) was injected retro-orbitally at 30 min before sacrifice and lung collection following perfusion free of blood with PBS. The extravasated EBA in lung homogenates was expressed as μg of EBA per mg of lung. Briefly, lung homogenates were incubated with two volumes of formalin for 18 h at 60°C, centrifuged at 5,000 g for 30 min, and the optical density (OD) of the supernatant was determined spectrophotometrically at 620 nm.

Total protein levels in bronchiolar alveolar lavage fluid (BALF) were measured *via* bicinchoninacid-assay (BCA) according to the manufacturer's instructions (Pierce BCA Protein Assay, Thermo Scientific, United States).

RT-PCR analysis of cytokines in lung tissues

To determine the expression of mRNA in lungs, lungs from asthmatic mice were lysed with a tissue homogenizer in TRIzol (Invitrogen). Total RNA was extracted by TRIzol according to the manufacturer's instructions. Real-time PCR analysis was performed with primers using Power SYBR Green Master Mix from Life Technologies. All gene expression results (mRNA abundances) were expressed as arbitrary units relative to the abundance of GADPH mRNA. The fold change was calculated through the $2^{-\Delta\Delta CT}$ method. The primers used were as follows: The primers used were as follows: TNF-α, forward primer: CCC TCACACTCAGATCATCTTCT, reverse primer: GCTACG ACGTGGGCTACAG; IL-6, forward primer: TAGTCCTTC CTACCCCAATTTCC, reverse primer: TTGGTCCTTAGC CACTCCTTC; iNOS, forward primer: TACTGAGACAGG GAAGTCTGAA, reverse primer: AGTAGTTGCTCCTCTTCC AAGGT; ICAM1, forward primer: GTGATGCTCAGGTAT CCATCCA, reverse primer: CACAGTTCTCAAAGCACAGCG.

Histology

Lung tissue and other organs (liver, spleen, kidney) were fixed and processed for H and E staining. Briefly, lung tissues were fixed by 5 min instillation of 10% PBS-buffered formalin through trachea catheterization at a transpulmonary pressure of 15 cm H_2O, and then overnight at 4°C with agitation. The other organs (liver, spleen, kidney) were isolated and fixed using 10% of formalin at 4°C with agitation for 48 h. After paraffin processing, the tissues were cut into 5 μm thick and stained with H&E for histological analysis. Inflammation scores were determined as: grade 0, no inflammation; grade 1, occasional cuffing with inflammatory cells; and grades 2, 3, and 4 indicated that most bronchi or vessels were surrounded by a thin 1–2 cell layer, a moderate 3–5 cell layer, or a thick (>5) cell layer of inflammatory cells, respectively (Xing et al., 2019).

Assay of aspartate aminotransferase and alanine transam

The levels of AST and ALT were determined using Elisa kit (Nanjing Jiancheng Bioengineering Institute, Nanjing, China)) according to the manufacturer's instructions. Take 100 mg of liver tissue and add 900 μl of saline, and then homogenized, centrifugated, and the supernatant was kept for test.

Lung mononuclear cells isolation

Lung mononuclear cells were prepared as previously described (Han et al., 2022). Briefly, lung tissues were sliced into small pieces and incubated at 37°C for 45 min with collagenase IV (1 mg/ml; Life Technologies) in RPMI-1640 medium (HyClone) supplemented with 5% fetal bovine serum (FBS; HyClone), and cells were isolated by gradient centrifugation over 38% Percoll (GE Healthcare Life Sciences). After erythrocyte lysis with ACK lysis buffer (Gibco), the cells were harvested for analyses.

Flow cytometric analysis for macrophage polarization in lung

For surface staining, lung mononuclear cells were labeled with FITC-mouse CD11b (48-0112-82, eBioscience)PE/cyanine7-anti-mouse CD11c (117317; Biolegend), APC-anti-mouse F4/80 (123115; Biolegend) and FITC-anti-mouse CD206 (141703; Biolegend) and the matching control isotype IgG (MCA421; AbD Serotec) in FACS buffer (PBS with 2% FBS) for 30 min at 4°C. M1 macrophages were identified as F4/80+CD11c+CD206− and M2 macrophages were identified as F4/80 + CD11c−CD206+ cells. Flow cytometry data were acquired on BD LSRFortessa X-20 and analyzed using FlowJo software (Tree Star).

Western blot

Whole proteins extracted from lung and protein concentrations were determined using BCA protein assay. Samples containing 40 μg of protein were fractionated by SDS-polyacrylamide gel electrophoresis (PAGE) and electro-transferred to a PVDF membrane. The blocked membranes were then immunoblotted with primary antibodies Anti-L-Lactyl Lysine Rabbit mAb (1:1,000, PTMBIO Inc., China) and anti-β-actin (1:1,000, Cell Signaling Technology Inc. United States). The proteins were visualized using enhanced chemiluminescence by secondary antibody. WB bands were scanned and analyzed for optical density using ImageJ software.

Statistical analysis

Pairwise comparisons were analyzed using non-parametric unpaired Student's t-tests for equal variance. Multiple comparisons were assessed using ANOVA with Bonferroni post-tests. p values of less than 0.05 were considered statistically significant. Values are mean ± standard deviation (SD).

Results

Characterization of PM@Cur-RV NPs

A classical emulsification-evaporation method was used to prepare the PLGA NPs. During the synthesis process, the compounds Cur and RV were added into the oil phase of the PLGA NPs. The harvested PM@Cur-RV NPs were mixed with platelet membrane and extruded through a polycarbonate porous membrane to form PM@Cur-RV NPs (shown in Figure 1A). This as-synthesized biomimetic nano-system was supposed to achieve inflammation targeting, and facilitate the delivery of drugs (Cur and RV) into the lungs in LPS-induced sepsis mice.

Nano Particle Analyzer SZ-100 (Horiba Scientific) and scanning electron microscope (SEM) were employed to characterize the size and morphology of Cur-RV NPs and PM@Cur-RV NPs. As shown in Figure 1A, the sizes of Cur-RV NPs were around 100 nm, and the sizes were remarkably increased into 450 nm with the membrane coating. The SEM image (Figure 1C) indicated that these NPs presented a spherical and uniform morphology, and PM@Cur-RV NPs demonstrated a better dispersion.

The UV-vis spectrum of the NPs was measured to determine the loading of Cur and RV in NPs. As shown in Figure 1D, the absorption spectrum of Cur or RV exhibited the characteristic absorption peaks at 210 nm. The absorption spectrum of the PM@Cur-RV NPs was closely consistent with that of free Cur or RV, indicating a successful encapsulation of Cur and RV into the PM@Cur-RV NPs. The loading capacity of Cur and RV was ~70% and ~75% in Cur-RV NPs and PM@Cur-RV NPs, which was calculated based on the standard curve of Cur and RV at their UV absorption peak of 425 nm and 208 nm, separately.

For further confirmation of the PM coating onto the Cur-RV NPs, the protein ingredients of PM and PM@Cur-RV NPs were analyzed by SDS-gel electrophoresis (Huang and Zhao, 2012). As shown in Figure 1E, PM@Cur-RV NPs contained characteristic proteins preserved by stem cell membrane (indicated by red circle). Collectively, these results indicate that the proteins of PM are successfully coated or conjugated on the surface of the Cur-RV NPs.

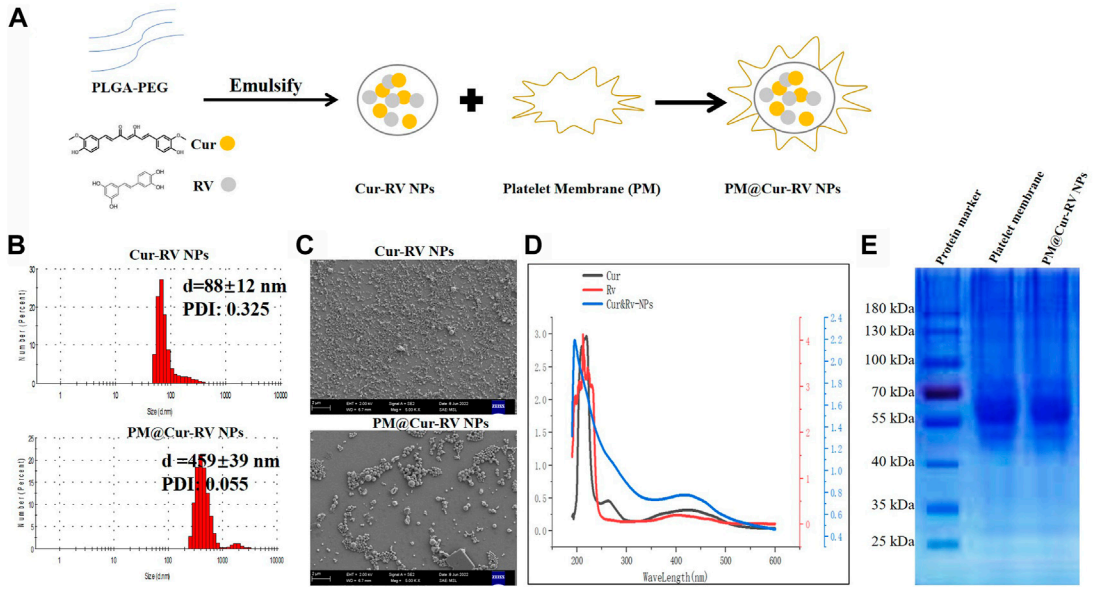

FIGURE 1
Characterization of Cur and RV-coloaded PLGA nanoparticles. **(A)** Scheme illustrates the preparation of Cur-RV NPs and PM@Cur-RV NPs using emulsification method. **(B)** Size distribution of Cur-RV NPs and PM@Cur-RV NPs, respectively. **(C)** Representative morphology photos of Cur-RV NPs and PM@Cur-RV NPs imaged by scanning electron microscope (1bar = 2 μm). **(D)** UV-vis spectrum of free Cur, RV and Cur-RV NPs indicated that Cur and RV were both successfully encapsulated in Cur-RV NPs, which shown by the similar absorption peaks at around 210 nm. **(E)** SDS-PAGE protein analysis of platelet membrane (PM), and PM@Cur-RV NPs (the samples were determined at same protein concentrations).

Biocompatibility and biosafety of the NPs

Giving that the biocompatibility and biosafety of nanoparticle-based systems have been known as the most important factors for their clinical application, the effects of free Cur and/or Cur-RV NPs were performed by using alveolar epithelial cell line (HBE cells) and endothelial cell line (HUVECs). As shown in Figure 2A, the same concentration of Cur-RV NPs and PM@ Cur-RV NPs did not induce significant cytotoxicity of macrophages, and only slightly inhibited the cell viability of HBE cells and HUVECs. Notably, 100 μg/ml of free Cur and RV had significant inhibiting effects on the viability of HBE cells and HUVECs, implying that the high dose of free Cur and RV could induce toxic effects on lung epithelia and endothelia. This result indicates that nano-formulation of compounds can significantly decrease their toxicity and increase their biosafety.

To further confirm the biosafety of Cur and RV, we evaluated their hemolytic properties using healthy mouse red blood cells. The erythrocytes lysed by water were used as the hemolysis positive group and the erythrocytes dispersed in PBS buffer were used as the normal control group. The free compounds, Cur-RV NPs and PM@Cur-RV NPs were used at the same concentration of 100 μg/ml (calculated based on the Cur and RV loading into NPs). As shown in Figures 2B,C, the free compounds showed slightly hemolysis. Interestingly, after being formulated into the NPs, the erythrocytes treated with Nar-NPs or CM@Nar-NPs did not show hemolysis. In addition, the shapes of erythrocytes under different treatments were also imaged under a light microscope. The same numbers of erythrocytes were added into 12-well plate, and 100 μg/ml different formulations of compounds were added and cultured for 30 min in 37°C, with pure water or PBS as hemolysis positive or normal control group, separately. As shown in Figure 2C, the water-lysis erythrocytes were almost completely destructed with a few of cell fragments, while the PBS-treated group showed normal, healthy erythrocytes with intact double concave disc shapes. In free compound group, the erythrocytes showed slightly decreased in the number and deformed in the shapes, while erythrocytes co-cultured with Cur-RV NPs and PM@Cur-RV NPs showed the intact membrane and healthy shapes. Collectively, these data indicate that nanoparticle-based platform can significantly improve the biocompatibility and biosafety of free Cur and RV.

In vivo targeting of PM@Cur-RV NPs

To confirm the effect of PM@Cur-RV NPs on targeting inflammatory lungs, an IVIS imaging system was performed. Indocyanine green (ICG) was co-loaded onto the nanoparticles as the fluorescent marker. The protocol and time-axis of *in vivo* targeting tests were shown in Figure 3A. Mice were intraperitoneal

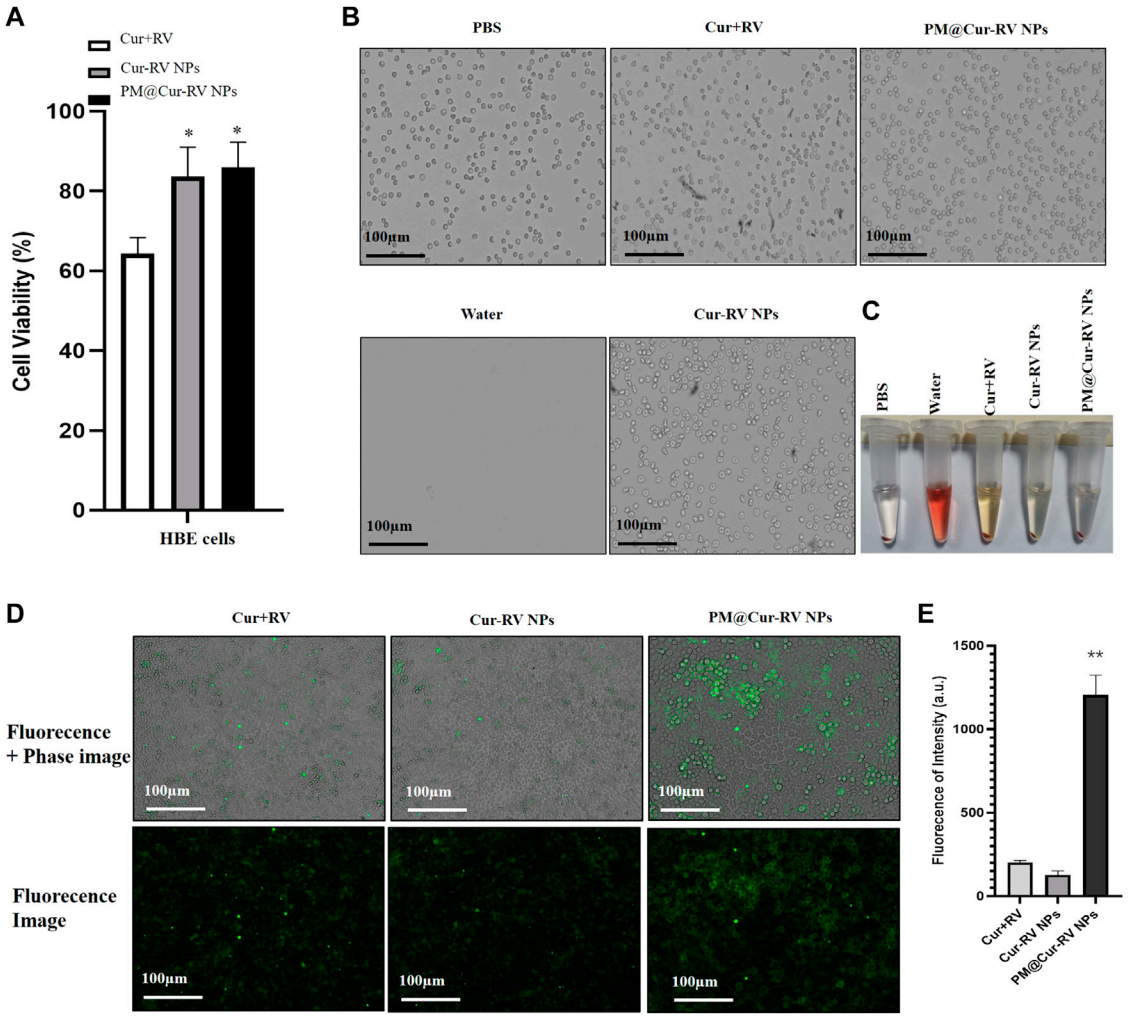

FIGURE 2
Biocompatibility and biosafety of different formulations of Cur and RV. **(A)** Cell viability of human bronchial epithelial cell line (HBE cells) treated with different formulations of Cur and RV at 100 μg/ml for 24 h, which implied that low dose of Cur and RV will not cause cytotoxicity to cells. **(B)** The images of hemolysis assay of free Cur and RV, Cur-RV NPs and PM@Cur-RV NPs, separately. **(C)** The morphology of erythrocytes co-cultured with free Cur and RV, Cur-RV NPs and PM@Cur-RV NPs, separately. **(D)** The typical images of HBE cell uptake of free Cur-RV, Cur-RV-NPs and PM@Cur-RV NPs (green fluorescence resulted from Cur). **(E)** The fluorescence intensity in HBE cells cocultured with different formulations of Cur-RV.

injected (*i.p.*) with LPS (8 mg/kg) to induce ALI. Fluorescent (ICG) mixed with free Cur-RV, Cur-RV NPs or PM@Cur-RV NPs were then *i. n.* Administered to visualize the tracks of NPs in the lungs. Figure 3 showed the distribution of NPs in the body at different time points after inhalation of NPs. Figure 3C showed that PM-coated biomimetic nanoparticles significantly promoted the accumulation and retention in inflammatory lungs. At 4 h of inhalation of NPs, mouse organs were collected for IVIS imaging. As shown in Figure 4D, all formulations of drugs were accumulated in the lungs but not in other organs, and the Cur-RV NPs, particularly PM@Cur-RV NPs, showed more stronger MFI in the lungs than other main organs. The decreased MFI of free ICG/Cur-RV could be due to the fast clearing out by the immune system. These results demonstrate that platelet membrane decoration of NPs has improved drug delivery and accumulation in inflammatory lungs.

PM@Cur-RV NPs significantly reduce lung injury and vascular permeability

ALI is characterized by leukocyte accumulation, epithelial injury, pulmonary edema, and increased alveolar permeability, as well as diffuse alveolar damage. It usually leads to ARDS,

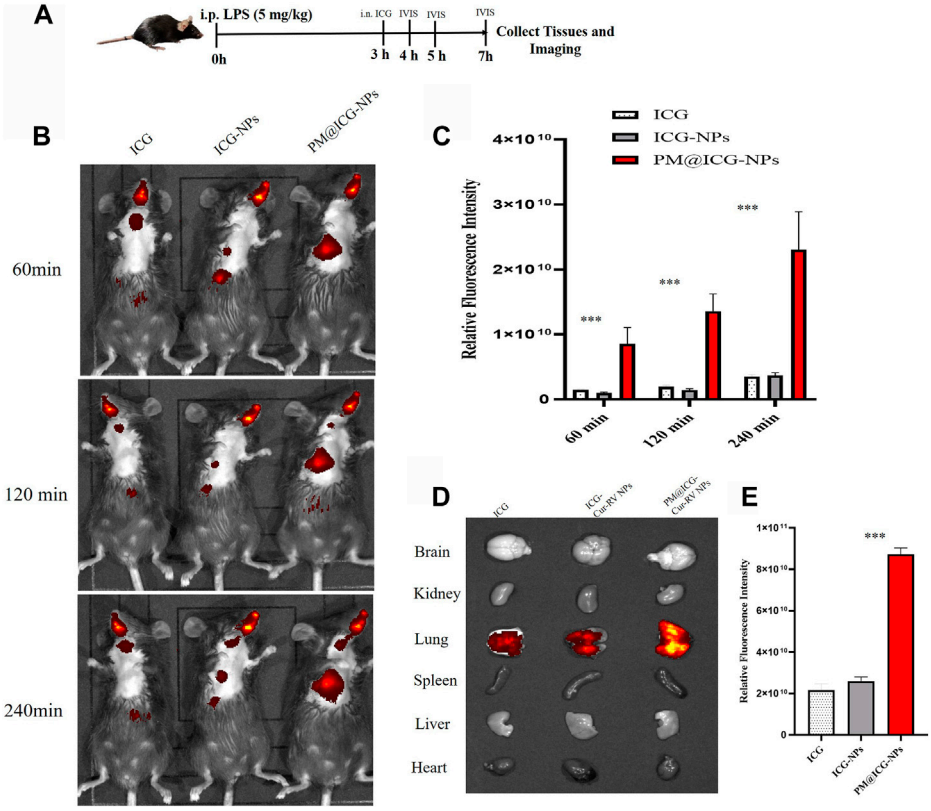

FIGURE 3
In vivo targeting of different modified NPs. Indocyanine green (ICG) were co-loaded into the NPs as a fluorescent marker of nanoparticles. **(A)** Scheme of time axis shows the IVIS imaging of ALI mice: the mice were intraperitoneal (i.p.) administrated with LPS (5 mg/kg) to induce ALI model and at 3 h post LPS challenging, the mice were intranasally administrated with different formulations of ICG. **(B)** Representative IVIS imaging of free ICG, ICG-NPs or PM@ICG-NPs distributed in sepsis mice at 1, 2, and 4 h after intranasal administration of ICG. **(C)** Relative fluorescence intensity of ICG in Figure B, which was measured with Living Image 4.5 software. Data are expressed as mean ± SD (n = 4). $*p < 0.05$, $**p < 0.01$ *versus* ICG group. **(D)** Typical fluorescence imaging of main organs originated from ALI mice after intranasal of Nar-NPs with or without PM modification for 4 h. **(E)** Relative fluorescence intensity of ICG in Figure D, calculating with Living Image 4.5 software.

and is the primary cause of death in critical patients (Butt et al., 2016). We explored the lung vascular permeability by determining the Evans blue albumin (EBA) flux (permeability to protein) (Nidavani RBM and Shalawadi, 2014; Wick et al., 2018). Figure 4A illustrated the experimental scheme of the lung vascular permeability assay. The mice were *i. p.* Administrated with LPS (5 mg/kg), and then different drugs were *i. n.* Administrated 3 h-post LPS challenge. At 23.5 h LPS challenge, the mice were intravascular injected with EBA. After 30 min, mouse lungs were collected to determine the EBA flux. Figure 4B showed the representative images of the lungs extracted from the EBA-injected-mice. As expected, LPS treatment resulted in increased EBA flux at 24 h post-LPS compared to the basal controls. Mice received the free Cur and RV treatment were no discernable improvements in lung permeability compared to the vehicle treatment. However, mice received Cur-RV NPs, especially PM@Cur-RV NPs, showed remarkably decreased EBA flux levels of lung vascular permeability (Figure 4C). These results demonstrate that nasally administered PM@Cur-RV NPs leads to targeted delivery of Cur and RV to inflammatory lungs and effectively inhibits pneumonia permeability. The protein levels in broncholveolr lvge fluid (BALF) and wet/dry ratio were also detected to evaluate the severity of pulmonary edema. Figures 4D,E demonstrated that NPs treatment was significantly attenuated the pulmonary edema in ALI mice.

Anti-inflammatory efficacy of PM@Cur-RV NPs in LPS-Induced ALI mice

The therapeutic effect of Cur and RV was examined in an LPS-induced ALI model. Mice were *i. p.* Injected with LPS at 5 mg/kg, and drugs were *i. n.* Administrated at 3 h-post LPS

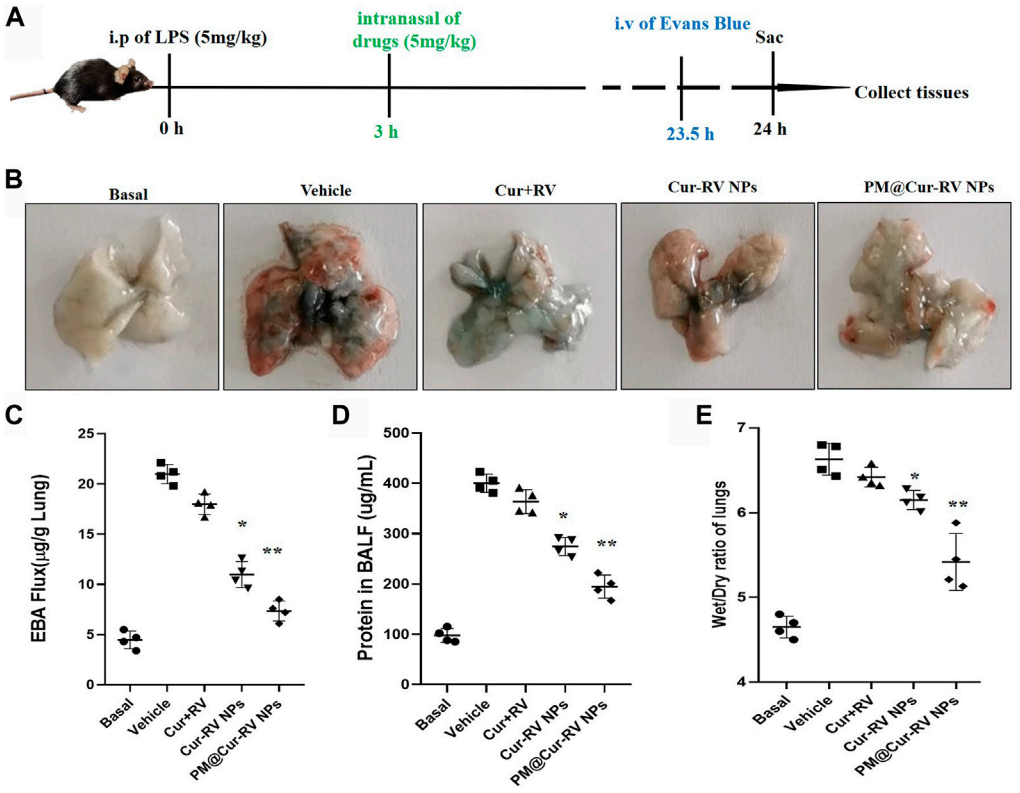

FIGURE 4
Cur-RV NPs, especially PM@Cur-RV NPs significantly inhibit lung vascular permeability in LPS-challenged mice. **(A)** Time-axis of lung vascular permeability determined by EBA (Evans blue-conjugated albumin) extravasation assay. At 3 h post-LPS challenge (5 mg/kg, i. p.), drugs (5 mg/kg, i. n.) were administered to mice. The same volume of PBS (5% of DMSO were included) was administrated to a group of mice as controls. Lungs were collected at 24 h post-LPS challenging for quantitative tests. **(B)** Representative photos demonstrated that curcumin-NPs could significantly inhibited lung vascular injury comparing with that of curcumin group. At 24 h post-LPS challenge, mouse lungs 30 min after i. v. Of EBA were perfused to remove blood and imaged. **(C)** The amounts of Evans Blue (EB) fluxed in lungs were assayed to evaluate the permeability of lung vessels. **(D)** The quantitative analysis of protein level in broncholveolr lvge fluid (BALF) of mice treated with different formulations of Cur and RV. **(E)** The wet/dry ratio of lungs from LPS-challenged mice treated with different formulations of Cur and RV. Data were expressed as mean ± SD (n = 4/group). $*p < 0.05$, $**p < 0.001$ *versus* vehicle group.

challenge. In Figures 5B,C, hematoxylin and eosin (H&E) staining showed that Cur-RV NPs, particularly PM@Cur-RV NPs-treated mice exhibited less alveolar wall thickening and inflammatory cell infiltration in the pulmonary alveoli and attenuated inflammatory cell recruited to lung tissues, indicating a protection effect of Cur-RV NPs against lung injury. Moreover, the proinflammation cytokines in ALI mice, such as TNFα, IL-6, ICAM1 and iNOS, were significantly increased (Figure 5D). However, all these cytokines were significantly inhibited after treated with Cur-RV NPs, especially PM@Cur-RV NPs. Collectively, PM@Cur-RV NPs show a higher efficacy therapeutic benefit in the ALI model by inhibiting the infiltration of inflammatory cell and relieving proinflammatory cytokines.

Toxicological studies in ALI mice

The biosafety of drugs is very important in their clinical applications. We analyzed the cytotoxicity of PM@Cur-RV NPs *in vivo* by histological analysis of the major organs (kidney, spleen, liver) (Huang et al., 2018b). H&E staining revealed that no significant tissue damage and adverse effect to these organs in all test groups (Figure 6A). We also explored the levels of aspartate aminotransferase (AST) and alanine transam (ALT) of livers to evaluate the effects of drugs to liver functions (Figure 6B) (Zhao et al., 2020). There was no statistical significance among all the treated groups of ALI mice. This result implies that PM@Cur-RV NPs possess excellent biocompatibility and biosafety, indicating a promising potential in clinical applications.

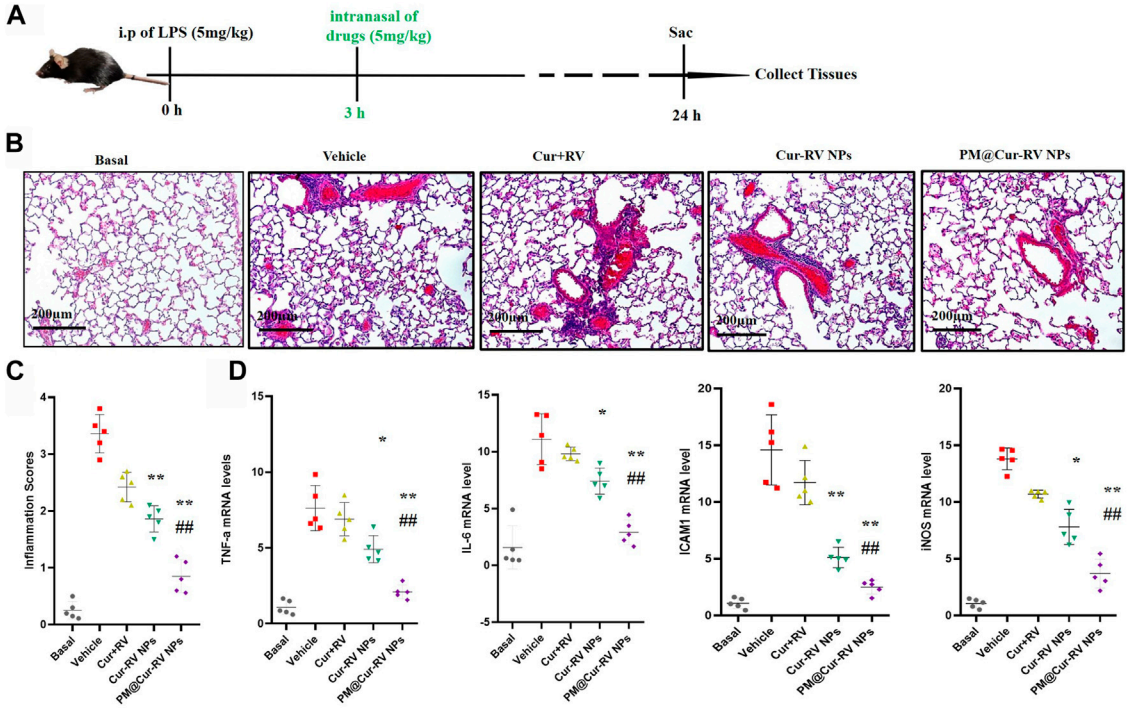

FIGURE 5
Cur-RV NPs, especially PM@Cur-RV NPs significantly promote resolution of lung inflammation in LPS-induced septic mice. **(A)** Time-axis of lung inflammation determination. The mice were intranasally administrated different formulations of Cur and RV at 3 h post-LPS challenge (5 mg/kg), and bronchiolar alveolar lavage fluid (BALF), blood, and lung tissues were collected at 24 h post-LPS challenge (5 mice/group). **(B)** Representative micrographs of lung tissue cross-sections at 24 h post-LPS challenge stained by H&E. Magnification (×400). **(C)** Inflammation scores in the different treated groups. **(D)** Expression levels of pro-inflammation cytokines TNF-a, IL-6, ICAM1 and iNOS, respectively. *$p < 0.05$, **$p < 0.001$ versus vehicle group.

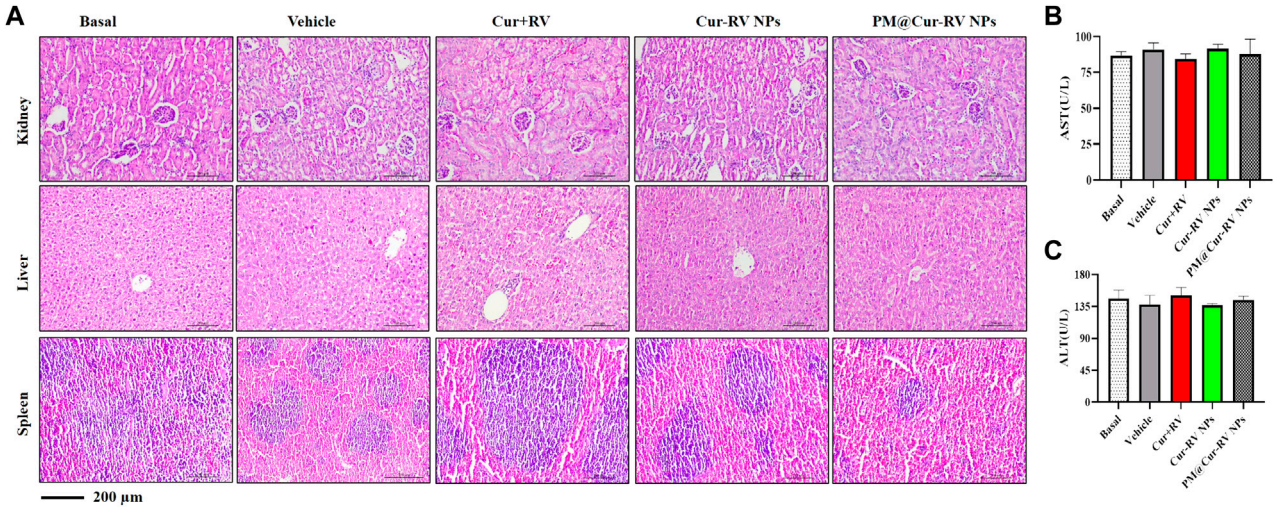

FIGURE 6
Toxicological studies in ALI mice. **(A)**Pathological data using H&E staining of different organs (Kidney, Liver and Spleen) originated from ALI mice inhaled with different compounds. No obvious toxicity was observed. Magnification (×400). **(B–C)** The levels of aspartate aminotransferase (AST) and alanine transam (ALT) of livers were tested to evaluate the toxicity of different formulations of Cur-RV. There was no statistical significance among the groups.

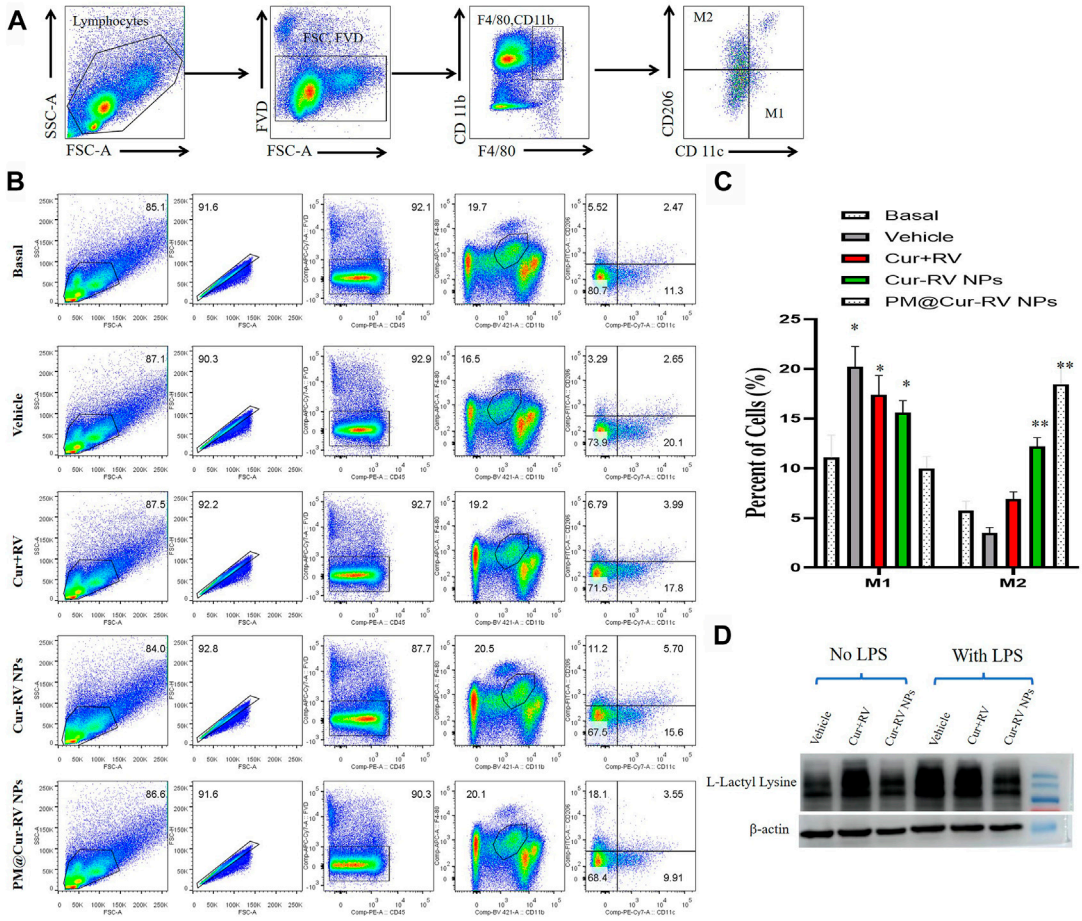

FIGURE 7
PM@Cur-RV NPs reduce lung inflammation by inducing macrophage towards to M2 polarization. Flow cytometric analysis of macrophages derived from inflammatory lungs treated with different formulations of Cur and RV for 24 h. **(A)** The scheme illustrates the selection of M1-or M2-positive cells from isolated single cells of lung tissues. In brief, we first gated out the live cells, and then gated out the F4/80-positive cells. In this subgroup, we used CD11c and CD206 as markers to identify M1 or M2 macrophages. F4/80+, CD11c+, CD206-cells are zoned as M1 cells, F4/80+, CD11c-, CD206+ cells are marked as M2 cells. **(B)** The representative images of cell distribution pattern in sepsis mice treated with different formulations of drugs. **(C)** The quantitative analysis of percentage of total M1 (F4/80+) macrophages and M2 (CD206+) macrophages in LPS-challenged lungs (n = 4/group; $^{**}p < 0.01$, $^{***}p < 0.0001$ *versus* PBS-treated group; $^{\#\#}p < 0.001$, $^{\#\#\#}p < 0.001$ *versus* Nar-treated group). **(D)** Representative western blot of L-Lactyl Lysine expression in RAW264.7 cells after 24 h treatment with vehicle or different formulations of Cur-RV. β-actin was used as a loading control. It shows that Cur-RV significantly decreased the lactic acid modification in LPS-induced macrophages.

PM@Cur-RV NPs induce macrophage polarization towards M2 in ALI mice

Activated macrophages are polarized into two categories: M1 ($F4/80^{+}CD11c^{+}CD206^{-}$) macrophages, which are mainly associated with pro-inflammatory responses; and M2 ($F4/80^{+}CD11c^{-}CD206^{+}$) macrophages, which are mainly associated with anti-inflammatory responses. Figure 6A demonstrated the method to analyze M1 and M2 cells in all isolated monocytes from lung tissues. As shown in Figure 7B, macrophages in the lung tended to polarize to M1 phenotype in LPS-challenged ALI mice. After treatment with Cur and RV, we found that all formulations of Cur and RV-treated group, especially PM@Cur-RV NPs, significantly decreased the number of M1 macrophages, and oppositely increased the number of M2 macrophages in the lungs (Figures 7B,C), suggesting that Cur and RV-treatment induces alveolar macrophages polarized from M1-type to M2-type.

Huge amount of studies indicate that elevated and impaired clearance of blood lactate are independently involved in increased mortality in septic patients (Marty et al., 2013). Thus, the use of lactate clearance as a treatment guideline for sepsis has gained increasing attractions in adult and pediatric patients in clinics (Marty et al., 2013). Figure 7D showed that Cur-RV treatment significantly decreased the levels of histone lactylation in LPS-induced macrophages.

This indicates that Cur- RV attenuates ALI might be through the pathway of decreased histone lactylation and regulating macrophage to M2 polarization, however, further study need to be done in future study.

Discussion

The respiratory system plays crucial roles in the biology of vertebrate animals. Injuries of the respiratory system caused by bacterial or viral infections (e.g., by COVID-19 and SARS) can lead to severe or lethal conditions. To date, there are no effective treatments for respiratory injuries. Recently, the COVID-19 pandemic caused a huge economic and medical burden to the whole world. Therefore, it is impressive to develop effective drugs and strategies to fight against infection-induced respiratory injuries. In the past decades, the rapid development of bio-nanotechnology provides new ideas for people to fight diseases. Nanomedicines are utilized to deliver a variety of therapeutic agents, including corticosteroids, chemotherapy drugs, herbal extract and nucleic acids (Blanco et al., 2015).

Actively targeting strategies aim at improving drug homing simultaneously reducing systemic toxicity (Bazak et al., 2015). Interestingly, cell membrane-cloaked biomimetic nano-formulations are capable of possessing the properties of the inherent tropisms of the host cells and the therapeutic function of drugs encapsulates in the nano-core (Tan et al., 2015). In this work, we develop a biomimetic nano-delivery system for localizing the therapeutic payloads to the lungs. Platelet cell vesicles, homing to the inflammation sites, are employed to coat nanoparticle cores loaded with the anti-inflammatory herbal ingredients-Cur and RV. The as-synthesized PM@Cur-RV NPs are used to treat ALI mice through inhaled administration.

In clinics, most of drugs are currently administrated intravenously. Topical administration of drugs to the disease sites highlights a better safety and efficacy. In the current study, the efficacy of inhaled PM@Cur-RV NPs demonstrates a high efficiency in anti-inflammation and attenuation of ALI. Comparing with an intraperitoneally administration of Cur at 200 mg/kg (Kim et al., 2016) or RV at 30 mg/kg (Li et al., 2013), the 20-fold lower dose administered by inhalation represents a comparable curative effect in ALI mice. This result supports further clinical development of inhalation nano-drugs against pulmonary disease.

Vascular permeability is characterized by the plasma and its solutes cross the vascular barrier. It is essential for the health of normal tissues and is also a vital factor in many disease states such as tumors, wounds, and inflammatory diseases. The acute inflammatory response quickly induces the increased vascular permeability, and leukocytosis into the injured tissues (Zhao et al., 2014). In the pathological processes of ALI, the increase in lung vessel permeability and loss of alveolar-capillary membrane integrity are closely associated with neutrophils infiltration and cytokine storm release in the lungs (Mammoto et al., 2013).

Recent studies demonstrate that high dose of Cur and RV can effectively inhibit the production of pro-inflammatory cytokines, however, their anti-inflammatory effects are greatly limited *in vivo* and must need high dose for that purpose (>100 mg/kg) (Li et al., 2013; Kim et al., 2016). Only the high dose could achieve the curative effects in experimental animal models, due to their poor water solubility, lower biocompatibility and bioavailability. Using nano-formulation, 5 mg/kg of PM@Cur-RV NPs can reach high treatment efficiency on ALI. Disruption of endothelial barrier leads to lung edema and injury, and PM@Cur-RV NPs might regulate endothelial barrier function and decrease vascular permeability in our study.

Macrophages in the lungs sustain the homeostasis *via* phagocytosing the inhaled particulate, foreigner pathogens and inducing cytokine production or antigen presentation, which facilitates the clearance of particulate antigens (Puttur et al., 2019). Macrophage polarization is a process in which macrophages phenotypically mount a specific phenotype and functional response under different pathophysiological conditions and microenvironments (Biswas et al., 2012). The balance of M1 and M2 macrophages could help to avoid excessive inflammatory responses which can lead to tissue damage. Macrophages are usually polarized to M1 phenotype in response to microbial stimuli including lipopolysaccharide (LPS) and Th1-related cytokines such as IFNγ and TNFα (Murray et al., 2014). M1 macrophages produce large amounts of inflammatory mediators and cytokines such as TNFα, IL-1, IL-6, IL-12, iNOS, reactive oxygen species (ROS), *etc.* These inflammatory mediators simultaneously promote inflammatory response and Th1 immune response and even cause tissue damage (Aggarwal et al., 2014). In the early stage of ALI/ARDS, alveolar macrophages are M1-polarized and release several pro-inflammatory factors, which facilitate to clear pathogenic microorganisms and recruit neutrophils. However, the excessive accumulation of pro-inflammatory cytokines and inflammatory cells reversely leads to lung tissue injury (Huang et al., 2018a). M2 macrophages contribute to promoting the recovery of host tissues through releasing anti-inflammatory mediators, inhibiting the production of proinflammatory cytokines, and removing apoptotic neutrophils from the inflammatory sites (Wynn and Vannella, 2016). Thus, the regulation of macrophage polarization from M1 towards M2 macrophages is the key regulator of tissue repair during ALI/ARDS recovery.

Moreover, our study have reported that lactate is elevated in ALI, and it might influence the function of immune cells (Caslin et al., 2021). Lactic acid-mediated glycolytic inhibition may suppress the function of inflammatory immune cells and promote their regulatory function (Nolt et al., 2018). It has been reported that the acute hospital mortality is significantly higher in patients with higher serum lactate level than those with

lower serum lactate level (Lee and An, 2016). Decreased or normalized the lactate levels are an important sign of recovery from septic shock, and lactate clearance at a discrete time point is an important prognostic factor compared to the initial serum lactate level in severe sepsis (Lee et al., 2015). In this study, we have found that Cur-RV especially PM@Cur-RV NPs treatment significantly decrease the lactylation modification in macrophages and might regulate them into M2 phenotype. These results demonstrate a potential application of PM@Cur-RV NPs for fighting against inflammatory pulmonary disease, such as ALI.

Conclusion

In this study, we developed a platelet membrane-cloaked nanoplatform to deliver anti-inflammation drugs for ALI treatment. The as-synthesized PM@Cur-RV NPs exhibited excellent dispersion, good biocompatibility and increased biosafety *in vitro* and *in vivo*. This biomimetic nanoplatform could successfully target and accumulate into inflammatory lungs in ALI mice. In LPS-induced ALI mice, the PM@Cur-RV NPs significantly improved the anti-inflammatory efficiency, suppressed the vascular permeability of lung edema, and decreased the inflammatory cells infiltration, which demonstrated an excellent enhanced therapeutic efficiency comparing with the free Cur-RV. Furthermore, flow cytometry analysis indicated that PM@Cur-RV NPs polarized lung macrophages from M1 to M2 type. Notably, the effective dose of Cur or RV in this work (1 mg/kg) was decreased more than 20-fold comparing with their effective doses reported in the previous studies (10 mg/kg for inhalation (Kumari et al., 2015) and 100 mg/kg for intraperitoneal injection (Guzel et al., 2013), which highlighted the merits of nanoplatform-based system in drug delivery to disease location. Together, this work provides a promising biomimetic nanoplatform for targeting treatment of inflammatory pulmonary disease, and this strategy shows potential clinical application in the future.

Data availability statement

The original contributions presented in the study are included in the article/supplementary material, further inquiries can be directed to the corresponding authors.

Ethics statement

The animal study was reviewed and approved by Experimental procedures using mice in this study were reviewed and approved by the ethical review board of Guangdong Medical University, and all the experiments were performed in accordance with relevant guidelines and regulations of Animal Ethics Committee of Guangdong Province, China. Animals and protocol were approved by the Ethics Committee of Guangdong Medical University (Approval No: GDY2002004).

Author contributions

HJ and GH were responsible for the conception of the study. HJ, RL, SO, JL, DC, ZL, WZ, MC, JP, and XL were responsible for data collection and analysis. HJ, RL, and SO participated in processing the images. YY, JL, YZ, HJ, and GH contributed to the revision. HJ, HZ, and GH wrote the manuscript. All authors have read and approved the final manuscript.

Funding

This work was supported by the Guangdong Basic and Applied Basic Research Foundation (2021B1515130004), the Natural Science Foundation of Guangdong Province (2021A1515011595), the Scientific research project of general universities in Guangdong province (2021KTSCX033), the Science Foundation of Dongguan Science and Technology Bureau (2020717152117, 20211800905092), Guangdong Medical Research Fund (A2021188, 20211226), the Two Universities' Paired and Cooperated Research Team Project of Guangdong Medical University (4SG22261G).

Conflict of interest

The authors declare that the research was conducted in the absence of any commercial or financial relationships that could be construed as a potential conflict of interest.

Publisher's note

References

Aggarwal, N. R., King, L. S., and D'alessio, F. R. (2014). Diverse macrophage populations mediate acute lung inflammation and resolution. *Am. J. Physiol. Lung Cell. Mol. Physiol.* 306 (8), L709–L725. doi:10.1152/ajplung.00341.2013

Arora, S., Dev, K., Agarwal, B., Das, P., and Syed, M. A. (2018). Macrophages: Their role, activation and polarization in pulmonary diseases. *Immunobiology* 223 (4-5), 383–396. doi:10.1016/j.imbio.2017.11.001

Bazak, R., Houri, M., El Achy, S., Kamel, S., and Refaat, T. (2015). Cancer active targeting by nanoparticles: A comprehensive review of literature. *J. Cancer Res. Clin. Oncol.* 141 (5), 769–784. doi:10.1007/s00432-014-1767-3

Biswas, S. K., Chittezhath, M., Shalova, I. N., and Lim, J. Y. (2012). Macrophage polarization and plasticity in health and disease. *Immunol. Res.* 53 (1-3), 11–24. doi:10.1007/s12026-012-8291-9

Blanco, E., Shen, H., and Ferrari, M. (2015). Principles of nanoparticle design for overcoming biological barriers to drug delivery. *Nat. Biotechnol.* 33 (9), 941–951. doi:10.1038/nbt.3330

Butt, Y., Kurdowska, A., and Allen, T. C. (2016). Acute lung injury: A clinical and molecular review. *Arch. Pathol. Lab. Med.* 140 (4), 345–350. doi:10.5858/arpa.2015-0519-RA

Caslin, H. L., Abebayehu, D., Pinette, J. A., and Ryan, J. J. (2021). Lactate is a metabolic mediator that shapes immune cell fate and function. *Front. Physiol.* 12, 12688485. doi:10.3389/fphys.2021.688485

Chen, X., Tang, J., Shuai, W., Meng, J., and Han, Z. (2020). Macrophage polarization and its role in the pathogenesis of acute lung injury/acute respiratory distress syndrome. *Inflamm. Res.* 69 (9), 883–895. doi:10.1007/s00011-020-01378-2

Fang, R. H., Kroll, A. V., Gao, W., and Zhang, L. (2018). Cell membrane coating nanotechnology. *Adv. Mat.* 30 (23), e1706759. doi:10.1002/adma.201706759

Fernando, S. M., Ferreyro, B. L., Urner, M., Munshi, L., and Fan, E. (2021). Diagnosis and management of acute respiratory distress syndrome. *CMAJ* 193 (21), E761–E768. doi:10.1503/cmaj.202661

Ghalandarlaki, N., Alizadeh, A. M., and Ashkani-Esfahani, S. (2014). Nanotechnology-applied curcumin for different diseases therapy. *Biomed. Res. Int.* 2014, 2014394264. doi:10.1155/2014/394264

Guzel, A., Kanter, M., Guzel, A., Yucel, A. F., and Erboga, M. (2013). Protective effect of curcumin on acute lung injury induced by intestinal ischaemia/reperfusion. *Toxicol. Ind. Health* 29 (7), 633–642. doi:10.1177/0748233711430984

Han, M., Ma, J., Ouyang, S., Wang, Y., Zheng, T., Lu, P., et al. (2022). The kinase p38α functions in dendritic cells to regulate Th2-cell differentiation and allergic inflammation. *Cell. Mol. Immunol.* 19 (7), 805–819. doi:10.1038/s41423-022-00873-2

Hewlings, S. J., and Kalman, D. S. (2017). Curcumin: A review of its effects on human health. *Foods* 6 (10), E92. doi:10.3390/foods6100092

Huang, R., Li, J., Kebebe, D., Wu, Y., Zhang, B., and Liu, Z. (2018). Cell penetrating peptides functionalized gambogic acid-nanostructured lipid carrier for cancer treatment. *Drug Deliv.* 25 (1), 757–765. doi:10.1080/10717544.2018.1446474

Huang, X., Xiu, H., Zhang, S., and Zhang, G. (2018). The role of macrophages in the pathogenesis of ALI/ARDS. *Mediat. Inflamm.* 2018, 20181264913. doi:10.1155/2018/1264913

Huang, X., and Zhao, Y. Y. (2012). Transgenic expression of FoxM1 promotes endothelial repair following lung injury induced by polymicrobial sepsis in mice. *PLoS One* 7 (11), e50094. doi:10.1371/journal.pone.0050094

Jin, H., Pi, J., Zhao, Y., Jiang, J., Li, T., Zeng, X., et al. (2017). EGFR-targeting PLGA-PEG nanoparticles as a curcumin delivery system for breast cancer therapy. *Nanoscale* 9 (42), 16365–16374. doi:10.1039/c7nr06898k

Kim, J., Jeong, S. W., Quan, H., Jeong, C. W., and Bae, H. B. (2016). Effect of curcumin (Curcuma longa extract) on LPS-induced acute lung injury is mediated by the activation of AMPK. *J. Anesth.* 30 (1), 100–108. doi:10.1007/s00540-015-2073-1

Kumari, A., Tyagi, N., Dash, D., and Singh, R. (2015). Intranasal curcumin ameliorates lipopolysaccharide-induced acute lung injury in mice. *Inflammation* 38 (3), 1103–1112. doi:10.1007/s10753-014-0076-y

Lee, S. M., and An, W. S. (2016). New clinical criteria for septic shock: Serum lactate level as new emerging vital sign. *J. Thorac. Dis.* 8 (7), 1388–1390. doi:10.21037/jtd.2016.05.55

Lee, S. M., Kim, S. E., Kim, E. B., Jeong, H. J., Son, Y. K., and An, W. S. (2015). Lactate clearance and vasopressor seem to Be predictors for mortality in severe sepsis patients with lactic acidosis supplementing sodium bicarbonate: A retrospective analysis. *PLoS One* 10 (12), e0145181. doi:10.1371/journal.pone.0145181

Li, T., Zhang, J., Feng, J., Li, Q., Wu, L., Ye, Q., et al. (2013). Resveratrol reduces acute lung injury in a LPS-induced sepsis mouse model via activation of Sirt1. *Mol. Med. Rep.* 7 (6), 1889–1895. doi:10.3892/mmr.2013.1444

Ma, Q., Fan, Q., Xu, J., Bai, J., Han, X., Dong, Z., et al. (2020). Calming cytokine storm in pneumonia by targeted delivery of TPCA-1 using platelet-derived extracellular vesicles. *Matter* 3 (1), 287–301. doi:10.1016/j.matt.2020.05.017

Mammoto, A., Mammoto, T., Kanapathipillai, M., Wing, Y. C., Jiang, E., Jiang, A., et al. (2013). Control of lung vascular permeability and endotoxin-induced pulmonary oedema by changes in extracellular matrix mechanics. *Nat. Commun.* 4, 41759. doi:10.1038/ncomms2774

Marty, P., Roquilly, A., Vallee, F., Luzi, A., Ferre, F., Fourcade, O., et al. (2013). Lactate clearance for death prediction in severe sepsis or septic shock patients during the first 24 hours in intensive care unit: An observational study. *Ann. Intensive Care* 3 (1), 3. doi:10.1186/2110-5820-3-3

Murray, P. J., Allen, J. E., Biswas, S. K., Fisher, E. A., Gilroy, D. W., Goerdt, S., et al. (2014). Macrophage activation and polarization: Nomenclature and experimental guidelines. *Immunity* 41 (1), 14–20. doi:10.1016/j.immuni.2014.06.008

Nidavani, R. B. M., A. M., and Shalawadi, M. (2014). Vascular permeability and Evans blue dye: a physiological and pharmacological approach. *J. Appl. Pharm. Sci.* 4 (11), 106–113. doi:10.7324/JAPS.2014.41119

Nolt, B., Tu, F., Wang, X., Ha, T., Winter, R., Williams, D. L., et al. (2018). Lactate and immunosuppression in sepsis. *Shock* 49 (2), 120–125. doi:10.1097/SHK.0000000000000958

Oray, M., Abu Samra, K., Ebrahimiadib, N., Meese, H., and Foster, C. S. (2016). Long-term side effects of glucocorticoids. *Expert Opin. Drug Saf.* 15 (4), 457–465. doi:10.1517/14740338.2016.1140743

Park, J. H., Jiang, Y., Zhou, J., Gong, H., Mohapatra, A., Heo, J., et al. (2021). Genetically engineered cell membrane-coated nanoparticles for targeted delivery of dexamethasone to inflamed lungs. *Sci. Adv.* 7 (25), eabf7820. doi:10.1126/sciadv.abf7820

Prasanna, P., Rathee, S., Upadhyay, A., and Sulakshana, S. (2021). Nanotherapeutics in the treatment of acute respiratory distress syndrome. *Life Sci.* 276, 276119428. doi:10.1016/j.lfs.2021.119428

Puttur, F., Gregory, L. G., and Lloyd, C. M. (2019). Airway macrophages as the guardians of tissue repair in the lung. *Immunol. Cell Biol.* 97 (3), 246–257. doi:10.1111/imcb.12235

Shakeri, A., Cicero, A. F. G., Panahi, Y., Mohajeri, M., and Sahebkar, A. (2019). Curcumin: A naturally occurring autophagy modulator. *J. Cell. Physiol.* 234 (5), 5643–5654. doi:10.1002/jcp.27404

Sica, A., and Mantovani, A. (2012). Macrophage plasticity and polarization: *In vivo* veritas. *J. Clin. Invest.* 122 (3), 787–795. doi:10.1172/JCI59643

Tan, S., Wu, T., Zhang, D., and Zhang, Z. (2015). Cell or cell membrane-based drug delivery systems. *Theranostics* 5 (8), 863–881. doi:10.7150/thno.11852

Wick, M. J., Harral, J. W., Loomis, Z. L., and Dempsey, E. C. (2018). An optimized Evans blue protocol to assess vascular leak in the mouse. *J. Vis. Exp.* doi:10.3791/57037

Wynn, T. A., and Vannella, K. M. (2016). Macrophages in tissue repair, regeneration, and fibrosis. *Immunity* 44 (3), 450–462. doi:10.1016/j.immuni.2016.02.015

Xing, Q. Q., Liu, L. W., Zhao, X., Lu, Y., Dong, Y. M., and Liang, Z. Q. (2019). Serum proteomics analysis based on label-free revealed the protective effect of Chinese herbal formula Gu-Ben-Fang-Xiao. *Biomed. Pharmacother.* 119, 119109390. doi:10.1016/j.biopha.2019.109390

Zhang, J., Huang, X., Ding, D., Zhang, J., Xu, L., Hu, Z., et al. (2021). Comparative study of acute lung injury in COVID-19 and non-COVID-19 patients. *Front. Med. (Lausanne).* 8, 8666629. doi:10.3389/fmed.2021.666629

Zhang, L. X., Li, C. X., Kakar, M. U., Khan, M. S., Wu, P. F., Amir, R. M., et al. (2021). Resveratrol (RV): A pharmacological review and call for further research. *Biomed. Pharmacother.* 143, 143112164. doi:10.1016/j.biopha.2021.112164

Zhao, L., Zhao, J., Gao, R., Tian, Y., Zhang, Y., Tang, W., et al. (2020). Intrabody against prolyl hydroxylase 2 ameliorates acetaminophen-induced acute liver injury in mice via concomitant promotion of angiogenesis and redox homeostasis. *Biomed. Pharmacother.* 123, 123109783. doi:10.1016/j.biopha.2019.109783

Zhao, Y. D., Huang, X., Yi, F., Dai, Z., Qian, Z., Tiruppathi, C., et al. (2014). Endothelial FoxM1 mediates bone marrow progenitor cell-induced vascular repair and resolution of inflammation following inflammatory lung injury. *Stem Cells* 32 (7), 1855–1864. doi:10.1002/stem.1690

frontiers | Frontiers in Pharmacology

TYPE Original Research
PUBLISHED 10 February 2023
DOI 10.3389/fphar.2023.1087557

OPEN ACCESS

EDITED BY
Lalit Mohan Nainwal,
GD Goenka University, India

REVIEWED BY
Poonam Arora,
Shree Guru Gobind Singh Tricentenary University, India
Kamal Dua,
University of Technology Sydney, Australia

*CORRESPONDENCE
Shouwei Yue,
shouweiy@sdu.edu.cn
Ou Chen,
chenou@sdu.edu.cn

SPECIALTY SECTION
This article was submitted to Respiratory Pharmacology, a section of the journal Frontiers in Pharmacology

RECEIVED 02 November 2022
ACCEPTED 30 January 2023
PUBLISHED 10 February 2023

CITATION
Wang H, Jia Y, Gu J, Chen O and Yue S (2023), Ferroptosis-related genes are involved in asthma and regulate the immune microenvironment.
Front. Pharmacol. 14:1087557.
doi: 10.3389/fphar.2023.1087557

Ferroptosis-related genes are involved in asthma and regulate the immune microenvironment

Haixia Wang[1], Yuanmin Jia[1], Junlian Gu[1], Ou Chen[1]* and Shouwei Yue[1,2]*

[1]School of Nursing and Rehabilitation, Cheeloo College of Medicine, Shandong University, Jinan, Shandong, China, [2]Rehabilitation Center, Qilu Hospital of Shandong University, Jinan, Shandong, China

Background: Asthma was a chronic inflammatory illness driven by complicated genetic regulation and environmental exposure. The complex pathophysiology of asthma has not been fully understood. Ferroptosis was involved in inflammation and infection. However, the effect of ferroptosis on asthma was still unclear. The study was designed to identify ferroptosis-related genes in asthma, providing potential therapeutic targets.

Methods: We conducted a comprehensive analysis combined with WGCNA, PPI, GO, KEGG, and CIBERSORT methods to identify ferroptosis-related genes that were associated with asthma and regulated the immune microenvironment in GSE147878 from the GEO. The results of this study were validated in GSE143303 and GSE27066, and the hub genes related to ferroptosis were further verified by immunofluorescence and RT-qPCR in the OVA asthma model.

Results: 60 asthmatics and 13 healthy controls were extracted for WGCNA. We found that genes in the black module ($r = -0.47$, $p < 0.05$) and magenta module ($r = 0.51$, $p < 0.05$) were associated with asthma. CAMKK2 and CISD1 were discovered to be ferroptosis-related hub genes in the black and magenta module, separately. We found that CAMKK2 and CISD1 were mainly involved in the CAMKK-AMPK signaling cascade, the adipocytokine signaling pathway, the metal cluster binding, iron-sulfur cluster binding, and 2 iron, 2 sulfur cluster binding in the enrichment analysis, which was strongly correlated with the development of ferroptosis. We found more infiltration of M2 macrophages and less Tregs infiltration in the asthma group compared to healthy controls. In addition, the expression levels of CISD1 and Tregs were negatively correlated. Through validation, we found that CAMKK2 and CISD1 expression were upregulated in the asthma group compared to the control group and would inhibit the occurrence of ferroptosis.

Conclusion: CAMKK2 and CISD1 might inhibit ferroptosis and specifically regulate asthma. Moreover, CISD1 might be tied to the immunological microenvironment. Our results could be useful to provide potential immunotherapy targets and prognostic markers for asthma.

Abbreviations: CAMKK2, Calcium/calmodulin-dependent protein kinase 2; ceRNA, competing endogenous; CISD1, CDGSH iron sulfur domain 1; FDR, false discovery rate; FEV1, forced expiratory volume in 1 s; GEO, Gene Expression Omnibus; GO, Gene Ontology; GS, gene significance; KEGG, Kyoto Encyclopedia of Genes and Genomes; MAD, median absolute deviation; MM, module membership; OCS, oral corticosteroid; PEF, peak expiratory flow; PPI, Protein-Protein Interaction network; RMA, robust multi-array average; RNAInter, RNA Interactome Database; ROS, reactive oxygen species; RT-qPCR, RNA real-time quantitative PCR; Tregs, Regulatory T-cell; WGCNA, Weighted Gene Co-expression analysis.

KEYWORDS

asthma, ferroptosis, immune infiltration, co-expression network analysis, tregs (regulatory T-cell)

1 Introduction

Asthma was recognized as one of the most common chronic diseases driven by interactions between genetic regulation and environmental exposure (Vos et al., 2012; Kaur and Chupp, 2019). Current asthma therapy was based mainly on inhaled corticosteroids and bronchodilators to suppress symptoms, and the symptoms of about 5%–10% of patients with asthma were not adequately controlled (Papi et al., 2018). Little success has been achieved in developing drugs that target the underlying mechanisms of asthma, which implied that understanding the genetic basis of asthma might unravel many disease-causing mechanisms (El-Husseini et al., 2020).

Ferroptosis after being first reported by Dixon et al., in 2012 has been recognized as a potential therapeutic target in many diseases (Hassannia et al., 2019; Qiu et al., 2020; Ma et al., 2021). Ferroptosis was a unique intracellular iron-dependent form of non-apoptotic cell death that occurred through excessive peroxidation of polyunsaturated fatty acids (Dixon et al., 2012). Recent studies have also indicated that ferroptosis played a critical role in the pathogenesis of lung diseases (Xu et al., 2021). Some researchers have also initially explored the role that ferroptosis acted in asthma. Wu et al. (2020) found that the induction of ferroptosis alleviated allergic inflammation in the OVA asthma model. In contrast, Zeng et al. (2022) showed that ferroptosis might occur in airway epithelial cells, and the inhibitors of ferroptosis could reduce levels of IL4, IL5, and IL13 in the HDM asthma model. Most of the currently published research on ferroptosis and asthma has focused on animal models of asthma, and only Nagasaki et al. have explored the potential mechanisms of ferroptosis in asthmatics (Bao et al., 2022; Nagasaki et al., 2022). Furthermore, the results of the relationship between ferroptosis and asthma were controversial.

FerrDb was the first database of experimentally validated ferroptosis regulators and markers and ferroptosis-disease associations (Zhou and Bao, 2020). Several researchers took advantage of this database in recent years to select ferroptosis-related genes in various diseases. In addition, Weighted Gene Co-expression analysis (WGCNA) was used as a data exploratory tool or as a gene screening method and aimed to provide potential disease-related molecular targets (Langfelder and Horvath, 2008). Therefore, we first screened for asthma-related specific modules using the WGCNA approach, and then further filtered for ferroptosis genes associated with asthma in combination with the FerrDb database. In this way, we want to clarify the molecular process by which genes associated with ferroptosis were engaged in asthma, which might help us find molecular targets that might aid in the early diagnosis of asthma and improve patient treatment.

2 Methods

2.1 Data download and processing

GSE147878 was downloaded from the Gene Expression Omnibus (GEO) database (https://www.ncbi.nlm.nih.gov/geo). It was part of the U-BIOPRED cohort and the Australian Newcastle severe asthma cohort including endobronchial biopsies of 60 asthmatics (including 18 mild/moderate asthma and 42 severe asthma) and 13 healthy controls. The criteria for diagnosis of asthma were agreed upon at the U-BIOPRED consensus meeting. (1) Airflow reversibility: Participants with asthma had an increase in forced expiratory volume in 1 s (FEV_1) >12% predicted or 200 mL after inhaling 400 μg salbutamol; (2) Airway hyperresponsiveness: methacholine provocative concentration caused a 20% fall in FEV_1 <8 $mgmL^{-1}$, or diurnal peak expiratory flow (PEF) amplitude >8% of mean; (3) Participants with asthma had a decrease in FEV_1 of 12% predicted or 200 mL within 4 weeks after tapering maintenance treatment. Healthy controls had no history of asthma or wheezing, no other chronic respiratory disease, and their pre-bronchodilator FEV1 was ≥80% pred (Shaw et al., 2015).

First, we used the GEOquery package of the R software (version 4.1.0) to download the GSE147878 from the GEO database. Second, the raw gene expression data were normalized by the robust multi-array average (RMA) method by the R Bioconductor package affy (Bolstad et al., 2003). Third, we used the annotation information to map gene IDs to microarray probes. Probes matching more than one gene were excluded and the mean expression value of genes measured by multiple probes was calculated. Four, the top 5,000 genes were screened using the median absolute deviation (MAD) value (Zhao et al., 2021). Finally, we imported data on clinical characteristics including age, atopy, oral corticosteroid (OCS), gender, prednisone, and smokers. The false discovery rate (FDR) technique modified the *p*-value.

2.2 Network construction and consensus module detection

WGCNA was used to separate genes into various clusters and further explore the connection between co-expression modules and clinical characteristics. All co-expression networks were created using the Bioconductor WGCNA package (Langfelder and Horvath, 2008). (1) Samples were clustered and looked for outliers using the hclust function. (2) The pickSoftThreshold function of WGCNA, which computed the scale-free topology fit index for a set of candidate powers ranging from 1 to 20, was used to determine the soft-thresholding power in the building of each module. If the index value for the reference dataset was more than 0.85, the appropriate power was found. (3) Co-expression modules were discovered using one-step network construction, with a minimum gene number of 50.

2.3 Relating modules to external clinical traits

The gene significance (GS) and module membership (MM) were used to identify the gene of high group significance and module membership in the modules. The significant module for asthma was identified if: $|GS| \geq 0.5$ and $|MM| \geq 0.5$, and hub genes were visualized in the Protein-Protein Interaction (PPI) network based on the

STRING database. The relationship between MM and GS in the module was statistically significant ($p < 0.05$).

2.4 Identification of hub genes related to ferroptosis

FerrDb V2 was the first database of experimentally validated ferroptosis regulators and markers and ferroptosis-disease associations (Zhou and Bao, 2020). The ferroptosis-related genes were downloaded to the FerrDb database (http://www.zhounan.org/ferrdb/), including the driver, suppressor, and marker genes. These genes were compared to asthma-related genes generated from WGCNA. The overlapping genes were described by the Venn diagram.

2.5 Enrichment analysis

To further visualize the biological function of key genes related to ferroptosis in the key module, Gene Ontology (GO) and Kyoto Encyclopedia of Genes and Genomes (KEGG) enrichment analyses were identified in the Cytoscape plug-in ClueGo. The *p*-value of less than 0.05 was identified as a significant term.

2.6 Construction of ceRNA network

The RNA Interactome Database (RNAInter) was a comprehensive resource for RNA interactome data obtained from the literature and other databases, containing over 41 million RNA-associated interactions (Lin et al., 2020). CDGSH iron sulfur domain 1 (CISD1) and Calcium/calmodulin-dependent protein kinase 2 (CAMKK2) were entered into the RNAInter website respectively to get miRNA with a confidence score >0.5 related to the CISD1 and CAMKK2. We then entered these miRNAs into RNAInter to search for miRNA-associated lncRNAs with a confidence score >0.5. The result of ceRNA was visualized by a Sankey diagram in the river plot package.

2.7 Immune infiltrating

CIBERSORT was a deconvolution method for accurately quantifying cell fractions from gene expression profiles (Newman et al., 2015; Chen et al., 2018). LM22 gene signature files provided by CIBERSORT were used to estimate the abundances of immunocytes accompanying 1,000 permutations. In addition, the Wilcoxon test was applied to establish the differentially infiltrated immune cells in asthma compared to healthy control. The correlation between hub genes and immune infiltrating cells was analyzed by Spearman's rank correlation analysis. The results were visualized by the lollipop chart using the "ggplot2" and "ggpubr" packages.

2.8 Validation in the GEO dataset

Considering that the asthma group in this study was including patients with mild to moderate asthma and severe asthma, we validated the results of this study in mild to moderate asthma and severe asthma separately to avoid our findings being the main effect of a particular phenotype of mild to moderate asthma or severe asthma. The characteristics of participants in the GSE147878 were shown in Table S1. Furthermore, to validate the robustness of the results, we validated the results in the GSE143303 and GSE27066 datasets. The GSE143303 included endobronchial biopsies of adults with severe asthma ($n = 47$), and healthy controls ($n = 13$). The characteristics of participants in the GSE143303 were shown in Table S2. In addition, we also validated our results in animal models of asthma in the GSE27066. The mice model of asthma was constructed as follows ($n = 4$ per group): Mice were immunized with 3 intraperitoneal injections of 50 μg OVA (Sigma-Aldrich) in 0.1 mL PBS on days 1, 4, and 7. Starting on day 12, mice have challenged with 20 μg OVA in 30 μL PBS weekly for 9 weeks; control mice received intraperitoneal injections and were challenged with PBS at the same time (Yu et al., 2011).

2.9 Validation in the OVA models

2.9.1 Animals and treatments

We have also constructed OVA models to validate the bioinformatic results. The OVA model was constructed based on the study by Shen et al. (2003). C57BL/6J male mice were purchased from Vital River Laboratories (Beijing, China). Mice were allowed tap water and rodent chow and were maintained at 22°C with a 12 h light-12 h dark cycle. All mice were acclimatized for 1 week before experimentation. The C57BL/6 mice were randomly divided into 2 groups ($n = 4$ per group). The OVA group was immunized intraperitoneally with OVA and challenged with inhaled OVA. Briefly, mice were injected with 100 μL of 20 μg chicken OVA (Sigma,United States) emulsified in Imject alum (Pierce, United States) on days 0 and 14, and subsequently challenged for 40 min with an aerosol generated by ultrasonic nebulization of 2% OVA in saline from 24 to 41 days. The control group was replaced with saline in both the sensitization and excitation phases. All experimental procedures used in this study were approved and conducted according to the guidelines of the laboratory Animal Management Committee of Shandong University.

2.9.2 Real-time quantitative PCR

The gene expression was tested by real-time quantitative PCR (RT-qPCR). Briefly, TRIzol reagent (Cwbio, Jiangsu, China) was used for total RNA extraction of lung tissues. RNA was reverse transcribed using a HiFiScript cDNA Synthesis Kit (Cwbio), and cDNA was synthesized by reverse transcription using the HiFiScript cDNA Synthesis Kit (Cwbio). RT-qPCR was carried out using an UltraSYBR Mixture (Cwbio) and real-time PCR detection equipment (Bio-Rad, Hercules, CA, United States). Primers used as follows: mouse CAMKK2 (Forward: GGAGGACGAGAACTGCAC AC, Reverse: TTCGCTGCCTTGCTTCGTGA) mouse CISD1(Forward: GCTGTGCGAGTTGA-GTGGAT, Reverse: TGG TGCGATT-CTCTTTAGCGTA), and mouse GAPDH (Forward: GGCCCCTCTGGAAAGCTGTGG, Reverse: CCCGGCATCGAA GGT-GGAAGA) were purchased from Sangon Biotech (Shanghai, China). The *t*-test (two-tailed) was used to compare the expression differences between the groups in GraphPad Prism 9. $p < 0.05$ was considered statistically significant.

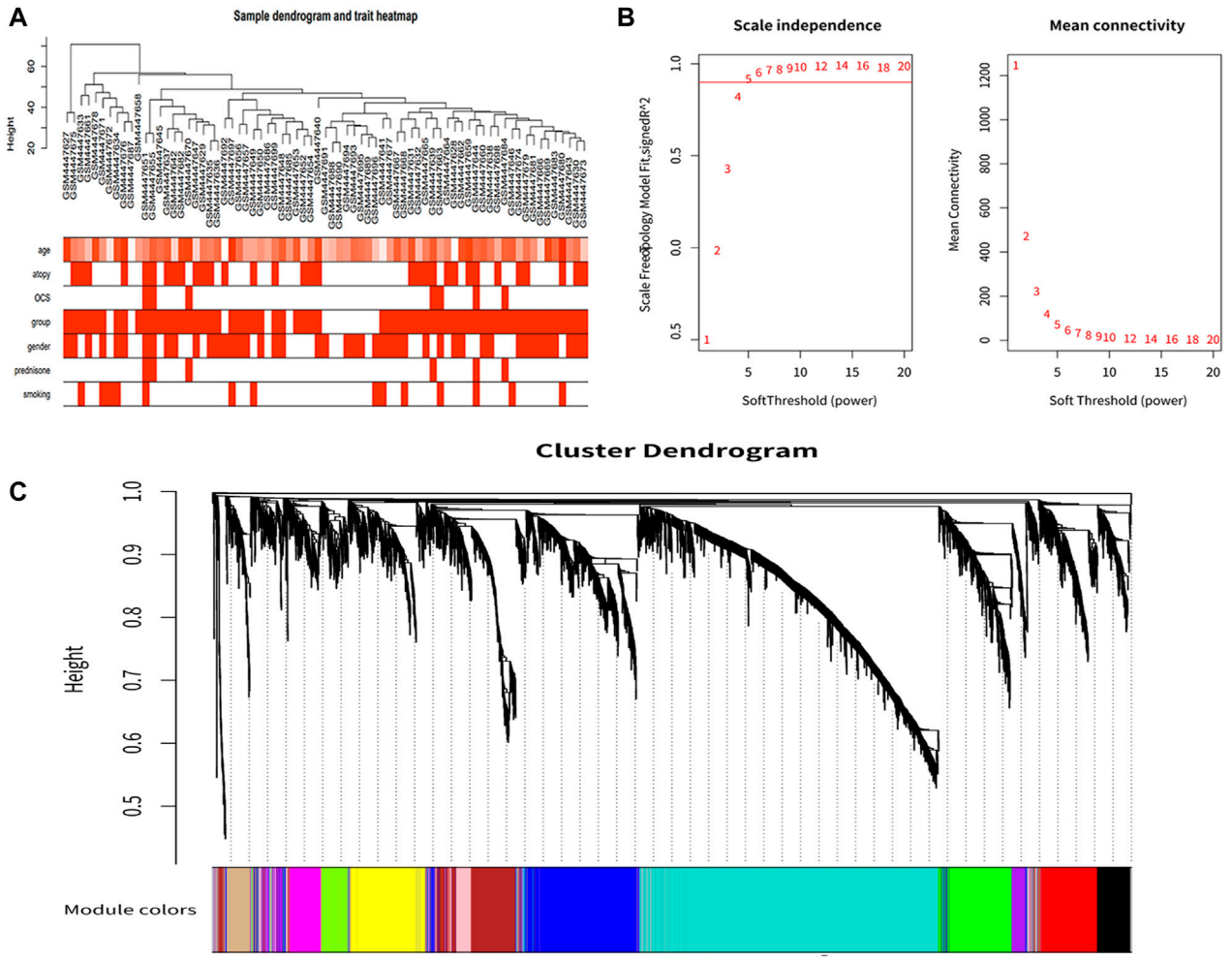

FIGURE 1
Co-expression network construction. **(A)** Sample clustering dendrogram based on Euclidean distance. **(B)** Analysis of network topology for various soft-thresholding powers. With a scale-free topological criterion >0.9, 5 was chosen as the fittest power value. **(C)** Clustering dendrogram of genes, with dissimilarity based on the topological overlap, together with assigned module colors.

2.9.3 Immunofluorescent staining

For immunofluorescent (IF) staining, frozen myocardial tissues were fixed with 4% paraformaldehyde for 20 min Primary antibodies, anti-CISD1 antibody at dilution of 1:25, and anti-CAMKK2 antibody at dilution of 1:200 (Proteintech, Chicago, United States) were used, respectively. The secondary antibody was coralite 594-conjugated goat anti-rabbit Ig G (H + L) (1:200, Proteintech, Chicago, United States). DAPI was applied to stain nuclei (blue). All the above staining was conducted according to the manufacturer's instructions. Staining results were observed and photographed by the fluorescence microscope (Nikon, Tokyo, Japan) and calculated by ImageJ software.

3 Results

3.1 Co-expression network construction

After clustering all samples, we did not discover any outliers in Figure 1A. The soft thresholding power β was set at 5 when the scale independence reached 0.9 in Figure 1B. Finally, 12 gene co-expression modules were constructed after using the one-step network construction function of the WGCNA R package (Figure 1C).

3.2 Identification of the clinically significant module and hub genes

The correlation between module eigengene and clinical features was used to identify module-trait associations (Figure 2A). The black module was shown to be adversely associated with asthma, with correlations of 0.47 ($p < 0.05$). This indicated that genes in the black module were predominantly downregulated in asthmatics. The magenta module was recognized as the positive module with a correlation of 0.51($p< 0.05$). Figures 2B, C, showed that the black, magenta modules had the GS-MM correlation ($p < 0.05$). Finally, we found 26 and 17 key genes in the black and magenta modules (Figures 2D, E).

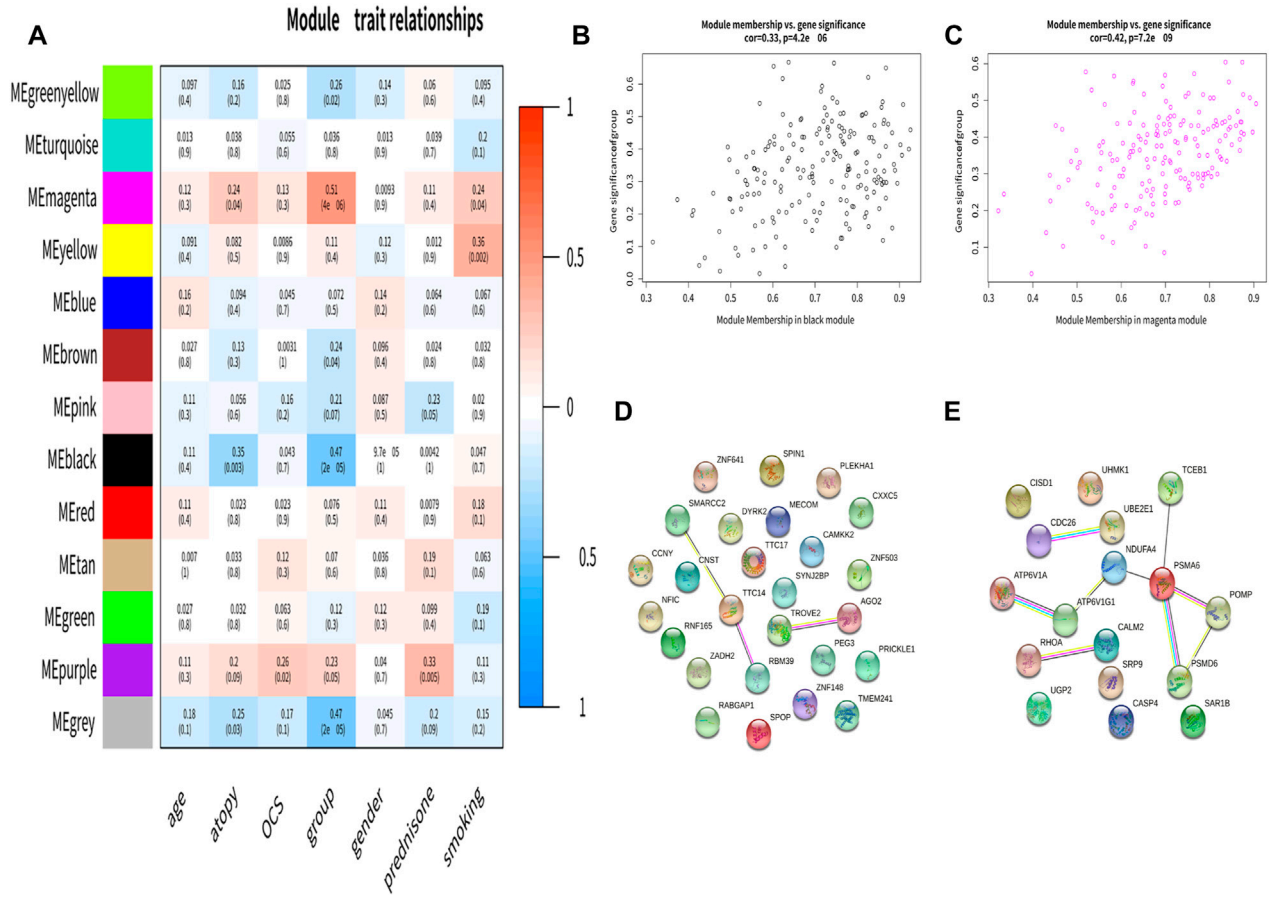

FIGURE 2
Identification of the clinically significant module and hub genes. **(A)** Module-trait associations. Each row corresponds to a module eigengene, column to a clinical trait. **(B,C)** A scatterplot of Gene Significance (GS) for asthma vs. Module Membership (MM) in the black and magenta module. **(D,E)** The PPI network in the black and magenta modules.

3.3 Identification of differentially expressed genes related to ferroptosis

The ferroptosis-related genes including 369 drivers, 348 suppressors, 11 markers, and 116 unclassified were downloaded from the FerrDb. After removing duplicate genes, we obtained 563 genes related to ferroptosis. After overlapping the hub genes in the black module with genes in the FerrDb database, we found that CAMKK2 was associated with ferroptosis in the black module. And only CISD1 in the magenta module was associated with ferroptosis (Figure 3A). We further identified CAMKK2 and CISD1 as suppressors of ferroptosis by FerrDb.

3.4 Enrichment analysis

GO analysis showed that CISD1 was mainly located in the cytoplasmic side of the mitochondrial outer membrane, meanwhile, it was involved in the metal cluster binding, iron-sulfur cluster binding, 2 iron, 2 sulfur cluster binding, and regulation of cellular respiration. We found that CAMKK2 was associated with CAMKK-AMPK signaling cascade, calmodulin-dependent kinase signaling pathway, autophagy of mitochondrion, positive regulation of mitochondrion organization, mitochondrion disassembly and regulation of autophagy of mitochondrion in the GO analysis. KEGG pathway analysis showed that CAMKK2 was mainly involved in the Adipocytokine signaling pathway (Figure 3B).

3.5 Construction of ceRNA network

We discovered that lncRNA such as BLACAT1, CASC15, and CASC2 acted as the miRNA sponge and thus cause the upregulation of CISD1 and CAMKK2 (Figure 3C).

3.6 Immune infiltrating

The top 5 immune cell subtypes with the highest infiltration proportion in the asthma group were macrophages M2, mast cells resting, T-cell CD8, plasma cells, and T-cell CD4 memory resting (Figure 4A). Compared with the healthy control group, the infiltration proportion of Regulatory T-cell (Tregs) ($p < 0.05$) decreased significantly in the asthma group, and macrophages M2 ($p < 0.01$) increased significantly in the asthma group (Figure 4B). In addition, we found a negative correlation between CISD1 and Tregs or plasma

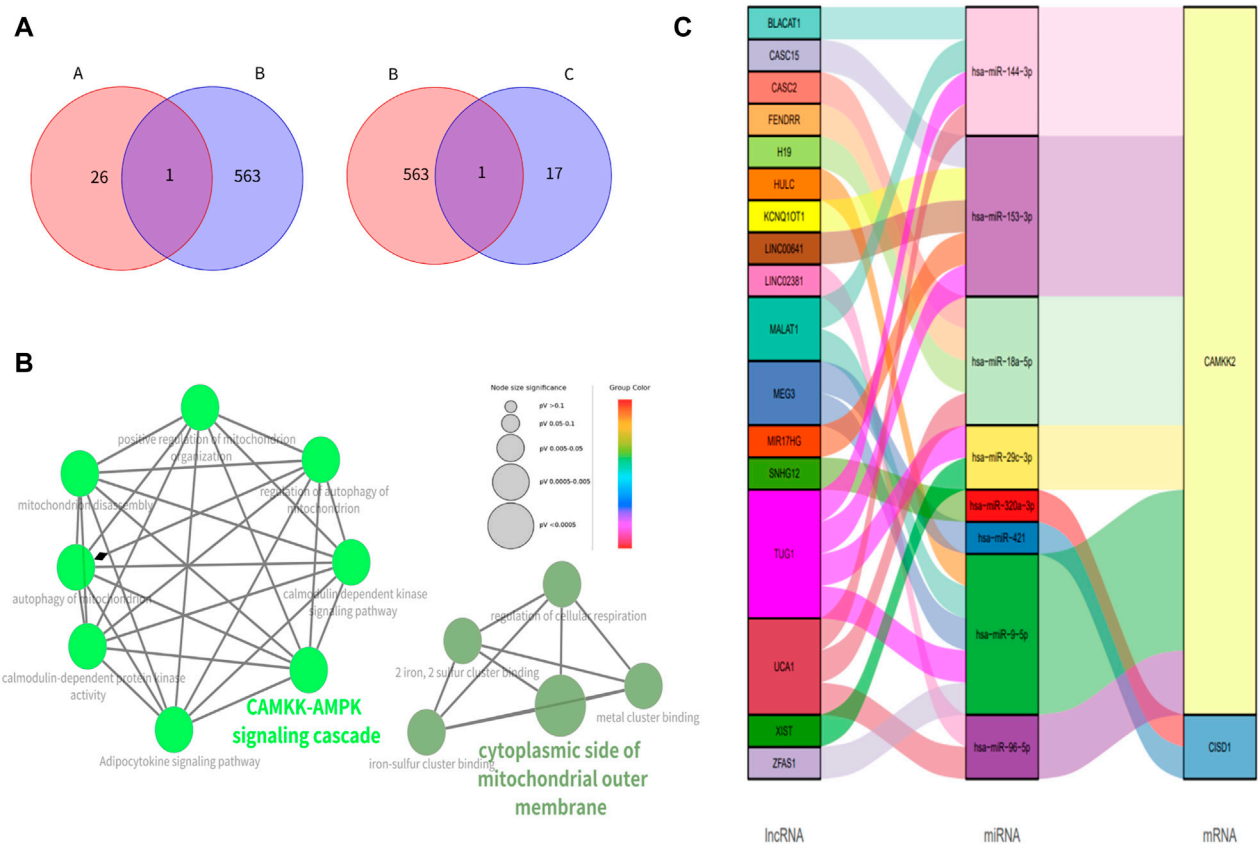

FIGURE 3
Identification of genes related to ferroptosis, enrichment analysis of ferroptosis-associated genes and construction of ceRNA networks **(A)** The Venn figure for intersected genes in FerrBD and different modules (A: black module; B: FerrBD; C: magenta module) **(B)** Functional enrichment of CISD1 AND CAMKK2. The signal pathways were discovered by enrichment analysis into groups based on functional connection, the same group was colored the same color, and the labels of each group of the most essential terms were color-coded. **(C)** The lncRNA-miRNA-mRNA ceRNA network of CISD1 and CAMKK2.

cells in Figure 4C ($p < 0.05$). In contrast, CAMKK2 was not involved in immune cell infiltration in Figure 4D ($p > 0.05$).

3.7 Validation

CISD1 was significantly upregulated and CAMKK2 was downregulated in both mild to moderate asthma and severe asthma compared to healthy controls in the GSE147878 dataset (Figures 5A–D) ($p < 0.05$), which was consistent with the results of this study. Similar results were also obtained in the GSE143303 dataset, CAMKK2 was significantly downregulated in the asthma group, and CISD1 was significantly upregulated in the asthma group (Figures 5E, F) ($p < 0.05$). In addition, we found that CISD1 was also upregulated in the OVA group with no statistically significant difference ($p > 0.05$) in the GSE27066. Interestingly, CAMKK2 was also significantly upregulated in the OVA group (Figures 5G, H) ($p < 0.05$).

IF staining was performed to verify the expression of CISD1 and CAMKK2 between the OVA group and the control group. CISD1 was highly expressed mainly in the airway epithelium of OVA mice, while CAMKK2 was widely expressed around the airway in Figure 6A. The results after fluorescence quantification showed that CISD1 and CAMKK2 were overexpressed in the OVA group compared to the control group in Figures 6B, C ($p < 0.05$). The RT-PCR results were also consistent with the staining results (Figures 6D, E) ($p < 0.05$).

4 Discussion

This study was the first to use WGCNA to investigate the role of genes associated with ferroptosis in asthma. We discovered that CAMKK2 and CISD1 were crucial ferroptosis suppressors in asthma. It was interesting that there was a negative correlation between the gene expression of CISD1 and Tregs, suggesting that CISD1 might be tied to the immunological microenvironment. This result suggested that ferroptosis might play important function in asthma.

Ferroptosis, a novel form of non-apoptotic cell death, was regulated by multiple cellular metabolic pathways, including redox homeostasis, iron handling, mitochondrial activity, and metabolism of amino acids, lipids, and sugars (Li and Li, 2020; Jiang et al., 2021). According to recent studies, various illnesses' pathogenic processes and ferroptosis were related (Liang et al., 2019; Chen et al., 2021; Wu et al., 2021). Cell death-related disorders might benefit from ferroptosis therapy, according to certain research (Tang et al.,

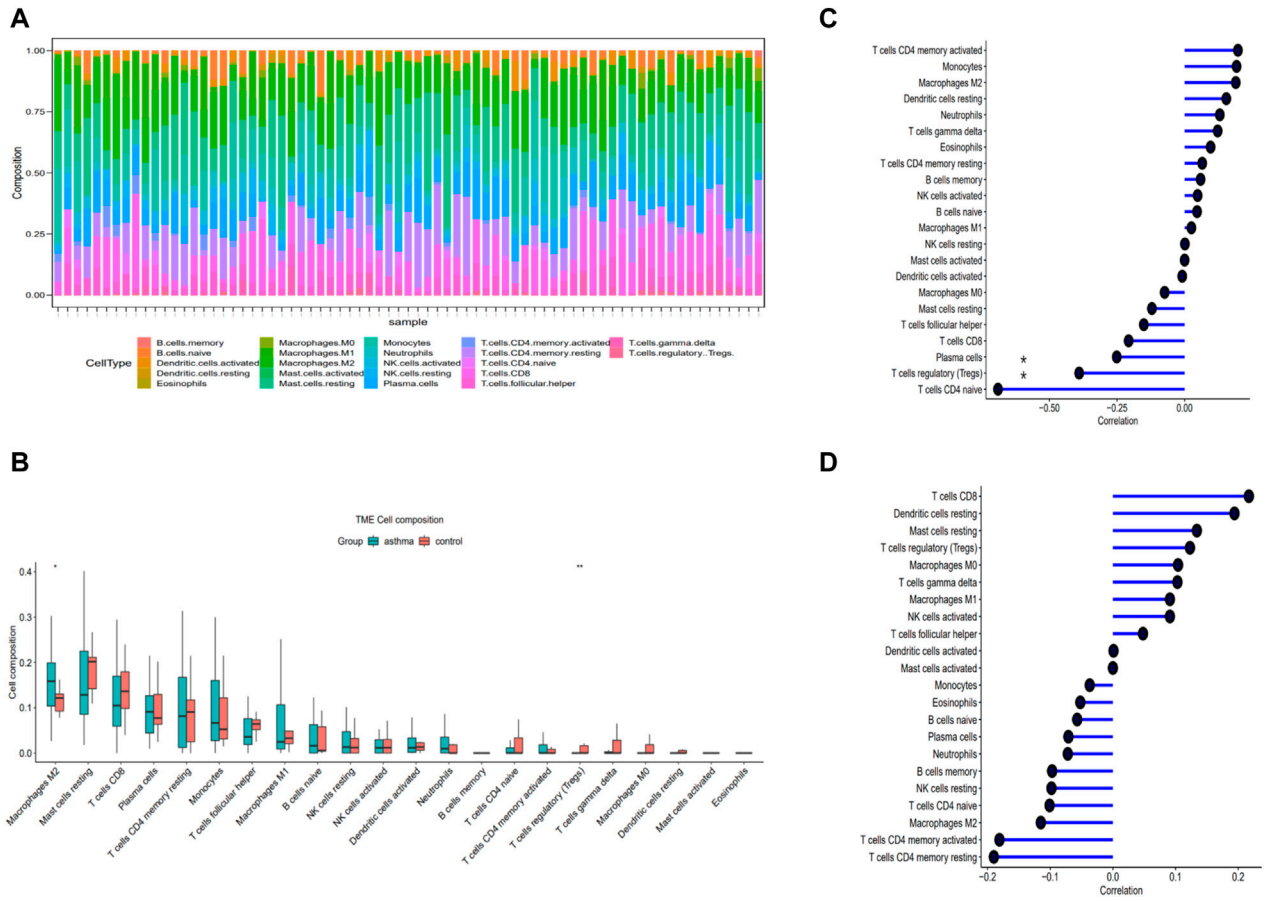

FIGURE 4
Evaluation of immune cell infiltration and correlational analysis. **(A)** Barplot shows the proportion of 22 types of immune cells in asthma. **(B)** The identification of differentially infiltrating immune cells **(C)** The correlation analysis of CISD1 and immune cells. **(D)** The correlation analysis of CAMKK2 and immune cells.

2021). Numerous studies conducted recently have discovered that ferroptosis was crucial to asthma. According to some studies, the malfunctioning of airway epithelial cells caused by ferroptosis might be the cause of asthma control loss. In contrast, inhibiting ferroptosis might reduce inflammation associated with asthma (Wenzel et al., 2017; Zeng et al., 2022). And Wu et al. (2020) have found that ferroptosis inducers could relieve allergic airway inflammation. It was still debatable whether ferroptosis and asthma were related. As we all know, asthma was characterized by the infiltration and activation of immune cells such as eosinophils, neutrophils, lymphocytes, and mast cells (Hammad and Lambrecht, 2021). The investigation of immune cells and ferroptosis together might result in a discussion of possible therapeutic applications.

CISD1, a mitochondrial protein mitoNEET was an iron-containing outer mitochondrial membrane protein with 13 kDa. Additionally, it was crucial for iron and reactive oxygen species (ROS) homeostasis detection and regulation (Geldenhuys et al., 2014; Lipper et al., 2019). The results of the enrichment analysis in this study also showed that CISD1 was mainly located in the cytoplasmic side of mitochondrial outer membrane, meanwhile, it was involved in the iron-sulfur cluster binding, 2 iron, and 2 sulfur cluster binding. These biological processes were highly associated with ferroptosis. However, no studies were conducted to explore the role CISD1 plays in asthma. In the present study, we found that CISD1 was significantly upregulated in the asthma group compared to healthy controls in asthmatic or OVA mice. Previous findings have consistently shown that CISD1 negatively regulated ferroptosis by protection against mitochondrial lipid peroxidation in Cancer (Yuan et al., 2016; Wang et al., 2021a).

Interestingly, we discovered a negative correlation between CISD1 and Tregs, pointing to the potential role of CISD1 in immune cell infiltration. Tregs were viable target against airway allergic inflammatory responses, and played an indispensable role in the maintenance of immune tolerance in asthma (Li et al., 2021; Zhang et al., 2022). By upregulating immunosuppressive molecules and suppressing genes, the Tregs fraction of $CD4^+$ T-cell prevented the development of proinflammatory activities and reduced inflammation (Burzyn et al., 2013; van der Veeken et al., 2016). One intriguing study suggested that generating highly suppressive allergen-specific Tregs could alleviate the inflammatory and allergic aspects of asthma (Burzyn et al., 2013; Dembele et al., 2021). Tregs undoubtedly contributed significantly to asthma. A correlation between ferroptosis and immune infiltration has been found in cancer disease (Wang et al., 2021b; Hu et al., 2021). No studies, however, have found a connection between ferroptosis and immune infiltration in asthma. Ye et al. discovered in gliomas that CYP2E1 was engaged in

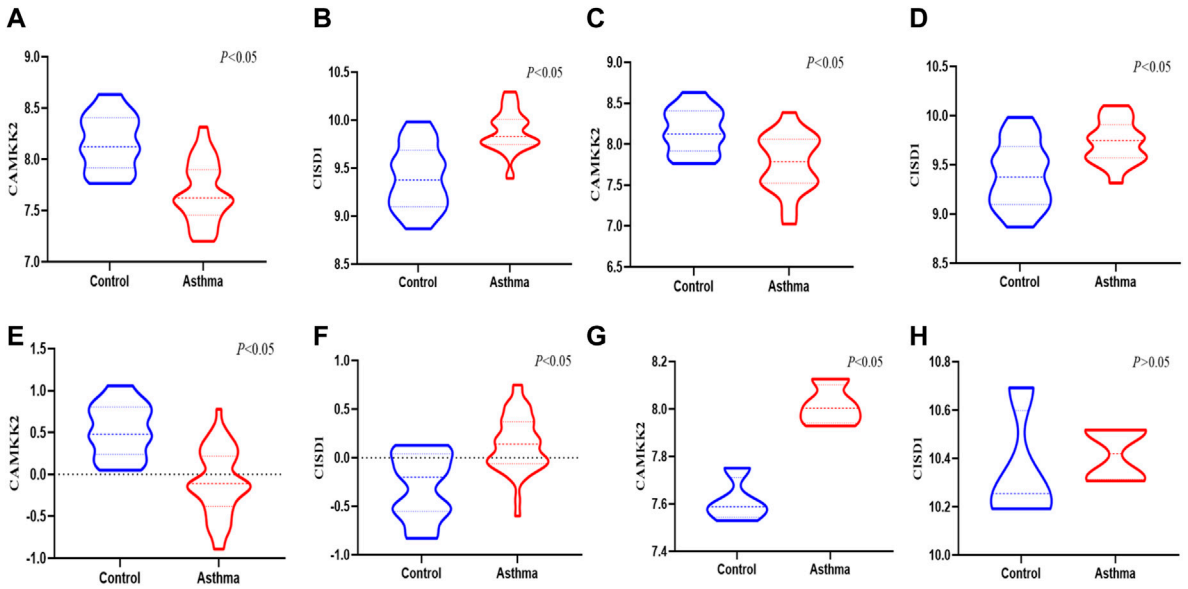

FIGURE 5
The validation of CAMKK2 and CISD1 in the GEO datasets **(A,B)** the expression of CAMKK2 and CISD1 in the severe asthma were verified in GSE 147878 ($p < 0.05$) **(C,D)** The expression of CAMKK2 and CISD1 in the mild/moderate asthma were verified in GSE 147878 ($p < 0.05$) **(E,F)** The expression of CAMKK2 and CISD1 in the severe asthma were verified in GSE 143303($p<0.05$) **(G,H)** The expression of CAMKK2 and CISD1 were verified in GSE 27066 ($p < 0.05$)

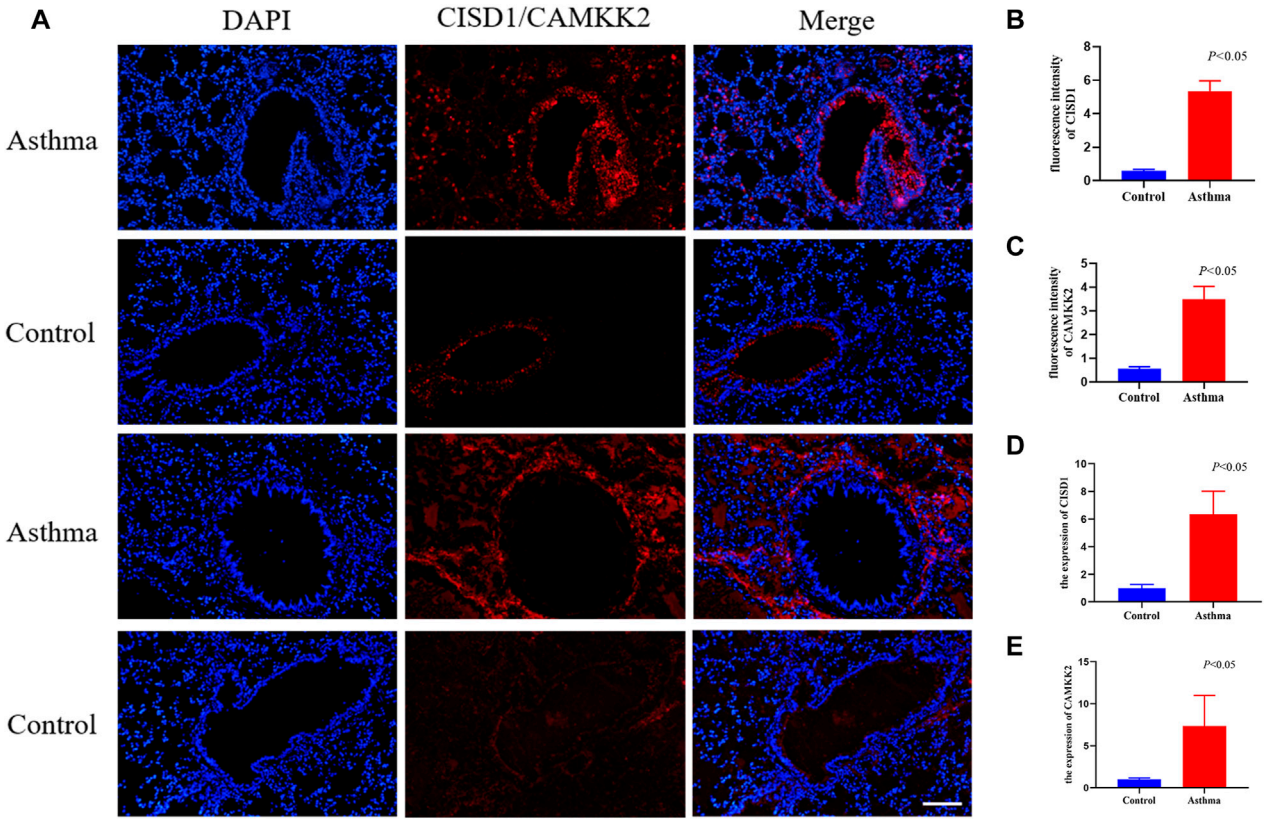

FIGURE 6
The result of validation by immunofluorescent staining and RT-qPCR in mouse models **(A–C)** immunofluorescent staining images of lung tissues and quantification of fluorescence intensity, Nucleus (blue), CISD1/CAMKK2 (red), scale bar, 500 um, (n = 4 per group) **(D–E)** The expression of CISD1 and CAMKK2 verified by RT-PCR in the OVA model (n = 4 per group).

lipid metabolism, ferroptosis, and associated to the tumor immune microenvironment, due to its significant link with Treg levels (Ye et al., 2021). Further investigation on the precise mechanisms governing ferroptosis and immune infiltration in asthma was anticipated in future studies.

CAMKK2 was a member of the serine/threonine-specific protein kinase family (Marcelo et al., 2016). It was a key regulator of glucose metabolism, insulin production, adipogenesis, and inflammation (Williams and Sankar, 2019). We found that CAMKK2 was downregulated in asthmatics and upregulated in animal models of asthma. The inconsistent results were mainly due to the 99% of the asthmatics in this study inhaled glucocorticoids (Shaw et al., 2015) and that glucocorticoids might downregulate CAMKK2. Our previous studies have also found that glucocorticoids downregulated several genes (Wang H. et al., 2022). Although this hypothesis has not been verified in other studies, we look forward to future studies to explore it. We, therefore, believe that CAMKK2 was upregulated in asthma, which in turn inhibited ferroptosis. CAMKK2 was considered to be an inhibitor of ferroptosis. Wang et al. showed that the suppression of CAMKK2 increased the efficacy of the ferroptosis inducer and inhibited the AMPK–NRF2 pathway and promoted ferroptosis (Wang S. et al., 2022). In addition, we found that CAMKK2 was mainly involved in the CAMKK-AMPK signaling cascade, and the Adipocytokine signaling pathway, which was strongly correlated with the development of ferroptosis. Furthermore, our enrichment analysis revealed that CAMKK2 was involved in the autophagy of mitochondrion. Autophagy and ferroptosis were distinct patterns of cell death, and several studies have shown that CAMKK2 did activate mitochondrial autophagy (Lin et al., 2021; Xie et al., 2021), while a study has also found that the activation of autophagy protected cells from ferroptosis and the release of mitochondrial DNA (Zhao et al., 2020). We hypothesize that upregulated CISD1 might activate autophagy, whereas it would inhibit ferroptosis.

Our study was the first to find that upregulated CISD1 and CAMKK2 inhibited ferroptosis and played an important regulatory role in asthma. However, there were some weaknesses in this study. Firstly, we did not obtain consistent results for CAMKK2, which was downregulated in asthma patients and upregulated in the OVA mouse model. We speculated that the inconsistent results were mainly due to the use of inhaled glucocorticoids in asthma patients. However, there was no evidence that glucocorticoids downregulated CAMKK2, so future studies are urgently needed to investigate this problem. Furthermore, the asthma group in this study included patients with different severity of asthma (mild/moderate and severe), and severe asthma accounted for 70% of the patients, our results might only be an effect of severe asthma. Therefore, we verified the expression of CISD1 and CAMKK2 in mild/moderate asthma and severe asthma. We found CISD1 was significantly upregulated and CAMKK2 was downregulated in both mild to moderate asthma and severe asthma compared to healthy controls.

5 Conclusion

We discovered CAMKK2 and CISD1 were ferroptosis-related key genes for asthma patients, which could provide a reference for immunotherapies and targeted therapies.

Further investigation of the role and mechanism of the ferroptosis-related genes in the progression of asthma is still needed.

Data availability statement

The datasets presented in this study can be found in online repositories. The names of the repository/repositories and accession number(s) can be found in the article/Supplementary Material.

Ethics statement

The studies involving human participants were reviewed and approved by GEO DATESETS. The patients/participants provided their written informed consent to participate in this study. The animal study was reviewed and approved by all experimental procedures used in this study were approved and conducted according to the guidelines by the laboratory Animal Management Committee of Shandong University. Written informed consent was obtained from the owners for the participation of their animals in this study. Written informed consent was obtained from the individual(s) for the publication of any potentially identifiable images or data included in this article.

Author contributions

HW, YJ, SY, and OC designed the study; HW, and JG analyzed the data, HW wrote this article. All the authors read and approved the final manuscript.

Funding

This work was supported by the National Natural Science Foundation of China (82172535 and 82172543), the Major Scientific and Technological Innovation Project in Shandong Province (2019JZZY011112), the Natural Science Foundation of Shandong Province (ZR2020MH006), and the Key Research and Development Program of Shandong Province (2019GSF108198).

Conflict of interest

The authors declare that the research was conducted in the absence of any commercial or financial relationships that could be construed as a potential conflict of interest.

Publisher's note

Supplementary material

The Supplementary Material for this article can be found online at: https://www.frontiersin.org/articles/10.3389/fphar.2023.1087557/full#supplementary-material

References

Bao, C., Liu, C., Liu, Q., Hua, L., Hu, J., Li, Z., et al. (2022). Liproxstatin-1 alleviates LPS/IL-13-induced bronchial epithelial cell injury and neutrophilic asthma in mice by inhibiting ferroptosis. *Int. Immunopharmacol.* 109, 108770. doi:10.1016/j.intimp.2022.108770

Bolstad, B. M., Irizarry, R. A., Astrand, M., and Speed, T. P. (2003). A comparison of normalization methods for high density oligonucleotide array data based on variance and bias. *Bioinformatics* 19, 185–193. doi:10.1093/bioinformatics/19.2.185

Burzyn, D., Benoist, C., and Mathis, D. (2013). Regulatory T cells in nonlymphoid tissues. *Nat. Immunol.* 14 (10), 1007–1013. doi:10.1038/ni.2683

Chen, B., Khodadoust, M. S., Liu, C. L., Newman, A. M., and Alizadeh, A. A. (2018). Profiling tumor infiltrating immune cells with CIBERSORT. *Methods Mol. Biol. Clift. N.J.)* 1711, 243–259. doi:10.1007/978-1-4939-7493-1_12

Chen, X., Kang, R., Kroemer, G., and Tang, D. (2021). Ferroptosis in infection, inflammation, and immunity. *J. Exp. Med.* 218 (6), e20210518. doi:10.1084/jem.20210518

Dembele, M., Tao, S., Massoud, A. H., Miah, S. M. S., Lelias, S., De Groot, A. S., et al. (2021). Tregitopes improve asthma by promoting highly suppressive and antigen-specific Tregs. *Front. Immunol.* 12, 634509. doi:10.3389/fimmu.2021.634509

Dixon, S. J., Lemberg, K. M., Lamprecht, M. R., Skouta, R., Zaitsev, E. M., Gleason, C. E., et al. (2012). Ferroptosis: An iron-dependent form of nonapoptotic cell death. *Cell* 149 (5), 1060–1072. doi:10.1016/j.cell.2012.03.042

El-Husseini, Z. W., Gosens, R., Dekker, F., and Koppelman, G. H. (2020). The genetics of asthma and the promise of genomics-guided drug target discovery. *Lancet. Respir. Med.* 8 (10), 1045–1056. doi:10.1016/S2213-2600(20)30363-5

Geldenhuys, W. J., Leeper, T. C., and Carroll, R. T. (2014). mitoNEET as a novel drug target for mitochondrial dysfunction. *Drug Discov. today* 19 (10), 1601–1606. doi:10.1016/j.drudis.2014.05.001

Hammad, H., and Lambrecht, B. N. (2021). The basic immunology of asthma. *Cell* 184 (6), 1469–1485. doi:10.1016/j.cell.2021.02.016

Hassannia, B., Vandenabeele, P., and Vanden Berghe, T. (2019). Targeting ferroptosis to iron out cancer. *Cancer Cell* 35 (6), 830–849. doi:10.1016/j.ccell.2019.04.002

Hu, S., Ma, J., Su, C., Chen, Y., Shu, Y., Qi, Z., et al. (2021). Engineered exosome-like nanovesicles suppress tumor growth by reprogramming tumor microenvironment and promoting tumor ferroptosis. *Acta biomater.* 135, 567–581. doi:10.1016/j.actbio.2021.09.003

Jiang, X., Stockwell, B. R., and Conrad, M. (2021). Ferroptosis: Mechanisms, biology and role in disease. *Nat. Rev. Mol. Cell Biol.* 22 (4), 266–282. doi:10.1038/s41580-020-00324-8

Kaur, R., and Chupp, G. (2019). Phenotypes and endotypes of adult asthma: Moving toward precision medicine. *J. allergy Clin. Immunol.* 144 (1), 1–12. doi:10.1016/j.jaci.2019.05.031

Langfelder, P., and Horvath, S. (2008). Wgcna: an R package for weighted correlation network analysis. *BMC Bioinforma.* 9, 559. doi:10.1186/1471-2105-9-559

Li, D., and Li, Y. (2020). The interaction between ferroptosis and lipid metabolism in cancer. *Signal Transduct. Target. Ther.* 5 (1), 108. doi:10.1038/s41392-020-00216-5

Li, J., Sha, J., Sun, L., Zhu, D., and Meng, C. (2021). Contribution of regulatory T cell methylation modifications to the pathogenesis of allergic airway diseases. *J. Immunol. Res.* 2021, 5590217. doi:10.1155/2021/5590217

Liang, C., Zhang, X., Yang, M., and Dong, X. (2019). Recent progress in ferroptosis inducers for cancer therapy. *Adv. Mater.* 31 (51), e1904197. doi:10.1002/adma.201904197

Lin, C., Blessing, A. M., Pulliam, T. L., Shi, Y., Wilkenfeld, S. R., Han, J. J., et al. (2021). Inhibition of CAMKK2 impairs autophagy and castration-resistant prostate cancer via suppression of AMPK-ULK1 signaling. *Oncogene* 40 (9), 1690–1705. doi:10.1038/s41388-021-01658-z

Lin, Y., Liu, T., Cui, T., Wang, Z., Zhang, Y., Tan, P., et al. (2020). RNAInter in 2020: RNA interactome repository with increased coverage and annotation. *Nucleic acids Res.* 48 (1), D189–D197. doi:10.1093/nar/gkz804

Lipper, C. H., Stofleth, J. T., Bai, F., Sohn, Y., Roy, S., Mittler, R., et al. (2019). Redox-dependent gating of VDAC by mitoNEET. *Proc. Natl. Acad. Sci. U. S. A.* 116 (40), 19924–19929. doi:10.1073/pnas.1908271116

Ma, T., Zhou, Y., Wang, C., Wang, L., Chen, J., Yang, H., et al. (2021). Targeting ferroptosis for lung diseases: Exploring novel strategies in ferroptosis-associated mechanisms. *Oxidative Med. Cell. Longev.* 2021, 1098970. doi:10.1155/2021/1098970

Marcelo, K. L., Means, A. R., and York, B. (2016). The Ca(2+)/calmodulin/CaMKK2 Axis: Nature's metabolic CaMshaft. *Trends Endocrinol. metabolism TEM* 27 (10), 706–718. doi:10.1016/j.tem.2016.06.001

Nagasaki, T., Schuyler, A. J., Zhao, J., Samovich, S. N., Yamada, K., Deng, Y., et al. (2022). 15LO1 dictates glutathione redox changes in asthmatic airway epithelium to worsen type 2 inflammation. *J. Clin. investigation* 132 (1), e151685. doi:10.1172/JCI151685

Newman, A. M., Liu, C. L., Green, M. R., Gentles, A. J., Feng, W., Xu, Y., et al. (2015). Robust enumeration of cell subsets from tissue expression profiles. *Nat. methods* 12 (5), 453–457. doi:10.1038/nmeth.3337

Papi, A., Brightling, C., Pedersen, S. E., and Reddel, H. K. (2018). Asthma. *Lancet (London, Engl.* 391 (10122), 783–800. doi:10.1016/S0140-6736(17)33311-1

Qiu, Y., Cao, Y., Cao, W., Jia, Y., and Lu, N. (2020). The application of ferroptosis in diseases. *Pharmacol. Res.* 159, 104919. doi:10.1016/j.phrs.2020.104919

Shaw, D. E., Sousa, A. R., Fowler, S. J., Fleming, L. J., Roberts, G., Corfield, J., et al. (2015). Clinical and inflammatory characteristics of the European U-BIOPRED adult severe asthma cohort. *Eur. Respir. J.* 46 (5), 1308–1321. doi:10.1183/13993003.00779-2015

Shen, H. H., Ochkur, S. I., McGarry, M. P., Crosby, J. R., Hines, E. M., Borchers, M. T., et al. (2003). A causative relationship exists between eosinophils and the development of allergic pulmonary pathologies in the mouse. *J. Immunol. Baltim. Md* 170 (6), 3296–3305. doi:10.4049/jimmunol.170.6.3296

Tang, D., Chen, X., Kang, R., and Kroemer, G. (2021). Ferroptosis: Molecular mechanisms and health implications. *Cell Res.* 31 (2), 107–125. doi:10.1038/s41422-020-00441-1

van der Veeken, J., Gonzalez, A. J., Cho, H., Arvey, A., Hemmers, S., Leslie, C. S., et al. (2016). Memory of inflammation in regulatory T cells. *Cell* 166 (4), 977–990. doi:10.1016/j.cell.2016.07.006

Vos, T., Flaxman, A. D., Naghavi, M., Lozano, R., Michaud, C., Ezzati, M., et al. (2012). Years lived with disability (YLDs) for 1160 sequelae of 289 diseases and injuries 1990-2010: A systematic analysis for the global burden of disease study 2010. *Lancet (London, Engl.* 380 (9859), 2163–2196. doi:10.1016/S0140-6736(12)61729-2

Wang, D., Chen, S., Ying, Y., Ma, X., Shen, H., Li, J., et al. (2021b). Comprehensive analysis of ferroptosis regulators with regard to PD-L1 and immune infiltration in clear cell renal cell carcinoma. *Front. Cell Dev. Biol.* 9, 676142. doi:10.3389/fcell.2021.676142

Wang, D., Wei, G., Ma, J., Cheng, S., Jia, L., Song, X., et al. (2021a). Identification of the prognostic value of ferroptosis-related gene signature in breast cancer patients. *BMC cancer* 21 (1), 645. doi:10.1186/s12885-021-08341-2

Wang, H., Zhang, Z., Ma, Y., Jia, Y., Ma, B., Gu, J., et al. (2022). Construction of severe eosinophilic asthma related competing endogenous RNA network by weighted gene Co-expression network analysis. *Front. Pharmacol.* 13, 852536. doi:10.3389/fphar.2022.852536

Wang, S., Yi, X., Wu, Z., Guo, S., Dai, W., Wang, H., et al. (2022). CAMKK2 defines ferroptosis sensitivity of melanoma cells by regulating AMPK–NRF2 pathway. *J. investigative dermatology* 142 (1), 189–200.e8. doi:10.1016/j.jid.2021.05.025

Wenzel, S. E., Tyurina, Y. Y., Zhao, J., St Croix, C. M., Dar, H. H., Mao, G., et al. (2017). PEBP1 wardens ferroptosis by enabling lipoxygenase generation of lipid death signals. *Cell* 171 (3), 628–641. doi:10.1016/j.cell.2017.09.044

Williams, J. N., and Sankar, U. (2019). CaMKK2 signaling in metabolism and skeletal disease: A new Axis with therapeutic potential. *Curr. Osteoporos. Rep.* 17 (4), 169–177. doi:10.1007/s11914-019-00518-w

Wu, X., Li, Y., Zhang, S., and Zhou, X. (2021). Ferroptosis as a novel therapeutic target for cardiovascular disease. *Theranostics* 11 (7), 3052–3059. doi:10.7150/thno.54113

Wu, Y., Chen, H., Xuan, N., Zhou, L., Wu, Y., Zhu, C., et al. (2020). Induction of ferroptosis-like cell death of eosinophils exerts synergistic effects with glucocorticoids in allergic airway inflammation. *Thorax* 75 (11), 918–927. doi:10.1136/thoraxjnl-2020-214764

Xie, B., Zhao, M., Song, D., Wu, K., Yi, L., Li, W., et al. (2021). Induction of autophagy and suppression of type I IFN secretion by CSFV. *Autophagy* 17 (4), 925–947. doi:10.1080/15548627.2020.1739445

Xu, W., Deng, H., Hu, S., Zhang, Y., Zheng, L., Liu, M., et al. (2021). Role of ferroptosis in lung diseases. *J. Inflamm. Res.* 14, 2079–2090. doi:10.2147/JIR.S307081

Ye, L., Xu, Y., Wang, L., Zhang, C., Hu, P., Tong, S., et al. (2021). Downregulation of CYP2E1 is associated with poor prognosis and tumor progression of gliomas. *Cancer Med.* 10 (22), 8100–8113. doi:10.1002/cam4.4320

Yu, M., Eckart, M. R., Morgan, A. A., Mukai, K., Butte, A. J., Tsai, M., et al. (2011). Identification of an IFN-γ/mast cell axis in a mouse model of chronic asthma. *J. Clin. investigation* 121 (8), 3133–3143. doi:10.1172/JCI43598

Yuan, H., Li, X., Zhang, X., Kang, R., and Tang, D. (2016). CISD1 inhibits ferroptosis by protection against mitochondrial lipid peroxidation. *Biochem. biophysical Res. Commun.* 478 (2), 838–844. doi:10.1016/j.bbrc.2016.08.034

Zeng, Z., Huang, H., Zhang, J., Liu, Y., Zhong, W., Chen, W., et al. (2022). HDM induce airway epithelial cell ferroptosis and promote inflammation by activating ferritinophagy in asthma. *Fed. Am. Soc. Exp. Biol.* 36 (6), e22359. doi:10.1096/fj.202101977RR

Zhang, J., Zou, Y., Chen, L., Xu, Q., Wang, Y., Xie, M., et al. (2022). Regulatory T cells, a viable target against airway allergic inflammatory responses in asthma. *Front. Immunol.* 13, 902318. doi:10.3389/fimmu.2022.902318

Zhao, H., Tang, X., Wu, M., Li, Q., Yi, X., Liu, S., et al. (2021). Transcriptome characterization of short distance transport stress in beef cattle blood. *Front. Genet.* 12, 616388. doi:10.3389/fgene.2021.616388

Zhao, J., Dar, H. H., Deng, Y., St Croix, C. M., Li, Z., Minami, Y., et al. (2020). PEBP1 acts as a rheostat between prosurvival autophagy and ferroptotic death in asthmatic epithelial cells. *Proc. Natl. Acad. Sci. U. S. A.* 117 (25), 14376–14385. doi:10.1073/pnas.1921618117

Zhou, N., and Bao, J. (2020). FerrDb: A manually curated resource for regulators and markers of ferroptosis and ferroptosis-disease associations. *Database J. Biol. databases curation* 2020, baaa021. doi:10.1093/database/baaa021

frontiers | Frontiers in Pharmacology

TYPE Review
PUBLISHED 16 March 2023
DOI 10.3389/fphar.2023.1129817

OPEN ACCESS

EDITED BY
Poonam Arora,
Shree Guru Gobind Singh Tricentenary University, India

REVIEWED BY
Zhenhua Jia,
Hebei Yiling Hospital, China
An Kang,
Nanjing University of Chinese Medicine, China

*CORRESPONDENCE
Xiangyan Li,
xiangyan_li1981@163.com
Zeyu Wang,
zeyu781022@163.com

†These authors have contributed equally to this work

SPECIALTY SECTION
This article was submitted to Respiratory Pharmacology, a section of the journal Frontiers in Pharmacology

RECEIVED 22 December 2022
ACCEPTED 13 February 2023
PUBLISHED 16 March 2023

CITATION
Song S, Ding L, Liu G, Chen T, Zhao M, Li X, Li M, Qi H, Chen J, Wang Z, Wang Y, Ma J, Wang Q, Li X and Wang Z (2023), The protective effects of baicalin for respiratory diseases: an update and future perspectives.
Front. Pharmacol. 14:1129817.
doi: 10.3389/fphar.2023.1129817

The protective effects of baicalin for respiratory diseases: an update and future perspectives

Siyu Song[1†], Lu Ding[1†], Guangwen Liu[2], Tian Chen[3], Meiru Zhao[3], Xueyan Li[3], Min Li[3], Hongyu Qi[1], Jinjin Chen[1], Ziyuan Wang[4], Ying Wang[4], Jing Ma[4], Qi Wang[3], Xiangyan Li[1*] and Zeyu Wang[1*]

[1]Key Laboratory of Active Substances and Biological Mechanisms of Ginseng Efficacy, Jilin Provincial Key Laboratory of Bio-Macromolecules of Chinese Medicine, Ministry of Education, Northeast Asia Research Institute of Traditional Chinese Medicine, Changchun University of Chinese Medicine, Changchun, Jilin, China, [2]GCP Department, Affiliated Hospital of Changchun University of Chinese Medicine, Changchun, China, [3]College of Integrated Traditional Chinese and Western Medicine, Changchun University of Chinese Medicine, Changchun, China, [4]College of Traditional Chinese Medicine, Changchun University of Chinese Medicine, Changchun, China

Background: Respiratory diseases are common and frequent diseases. Due to the high pathogenicity and side effects of respiratory diseases, the discovery of new strategies for drug treatment is a hot area of research. *Scutellaria baicalensis* Georgi (SBG) has been used as a medicinal herb in China for over 2000 years. Baicalin (BA) is a flavonoid active ingredient extracted from SBG that BA has been found to exert various pharmacological effects against respiratory diseases. However, there is no comprehensive review of the mechanism of the effects of BA in treating respiratory diseases. This review aims to summarize the current pharmacokinetics of BA, baicalin-loaded nano-delivery system, and its molecular mechanisms and therapeutical effects for treating respiratory diseases.

Method: This review reviewed databases such as PubMed, NCBI, and Web of Science from their inception to 13 December 2022, in which literature was related to "baicalin", "*Scutellaria baicalensis* Georgi", "COVID-19", "acute lung injury", "pulmonary arterial hypertension", "asthma", "chronic obstructive pulmonary disease", "pulmonary fibrosis", "lung cancer", "pharmacokinetics", "liposomes", "nano-emulsions", "micelles", "phospholipid complexes", "solid dispersions", "inclusion complexes", and other terms.

Result: The pharmacokinetics of BA involves mainly gastrointestinal hydrolysis, the enteroglycoside cycle, multiple metabolic pathways, and excretion in bile and urine. Due to the poor bioavailability and solubility of BA, liposomes, nano-emulsions, micelles, phospholipid complexes, solid dispersions, and inclusion complexes of BA have been developed to improve its bioavailability, lung targeting, and solubility. BA exerts potent effects mainly by mediating upstream oxidative stress, inflammation, apoptosis, and immune response pathways. It regulates are the NF-κB, PI3K/AKT, TGF-β/Smad, Nrf2/HO-1, and ERK/GSK3β pathways.

Conclusion: This review presents comprehensive information on BA about pharmacokinetics, baicalin-loaded nano-delivery system, and its therapeutic effects and potential pharmacological mechanisms in respiratory diseases. The available studies suggest that BA has excellent possible treatment of respiratory diseases and is worthy of further investigation and development.

KEYWORDS

baicalin, respiratory diseases, molecular mechanisms, pharmacological action, pharmacokinetics, baicalin-loaded nano-delivery system

1 Introduction

Respiratory diseases are a significant worldwide health problem with high morbidity and mortality rates. Smoking, radiation, dust, bacteria, viruses, *mycoplasma*, and obesity can all cause pulmonary diseases, which are coronary viral disease-2019 (COVID-19), acute lung injury (ALI), asthma, chronic obstructive pulmonary disease (COPD), pulmonary arterial hypertension (PAH), pulmonary fibrosis (PF), and lung cancer (LC) (Venkatesan et al., 2007; Kumar et al., 2018). Due to its susceptibility and poor prognosis, drug development in this field has been of great interest.

Chinese herbal medicine, as one of the natural products, has been a rich source of discovery compounds (Hu et al., 2021). *Scutellaria baicalensis* Georgi (SBG) is a *Lamiaceae* family herb widely used in East Asian countries to treat diseases (Shang et al., 2010). Baicalin (BA), baicalein (BE), wogonin, and wogonoside are the main flavonoid compounds found in SBG (Pan et al., 2021). As the main effective constituent, BA has been found to have therapeutic effects on cardiovascular, hepatobiliary, brain, nervous system, and intestinal diseases (Jin et al., 2019; Song et al., 2020; Xin et al., 2020; Ganguly et al., 2022). BA has been extensively reported to treat respiratory diseases (Deng et al., 2022; Ju et al., 2022; Li et al., 2022). However, the widespread use of BA is still a challenge due to its low solubility and poor bioavailability (Haider et al., 2018; Pramual et al., 2022). And the molecular mechanism of BA in treating respiratory diseases has yet to be reported based on a summary of reliable evidence.

Herein, we discuss a comprehensive report of BA on pharmacokinetics and baicalin-loaded nano-delivery system. In addition, we have summarized studies related to BA for the treatment of COVID-19, ALI, asthma, PAH, COPD, PF, and LC. And the main therapeutic targets and the critical signal pathways of BA against respiratory diseases were summarized. This review could provide a theoretical basis for further pharmacological studies and clinical applications of BA for the prevention and treatment of respiratory diseases.

2 Literature survey databases

This review reviewed databases such as PubMed, NCBI, and Web of Science from their inception to 13 December 2022, using terms including “baicalin”, “*Scutellaria baicalensis* Georgi”, “COVID-19”, “acute lung injury”, “pulmonary arterial hypertension”, “asthma”, “chronic obstructive pulmonary disease”, “pulmonary fibrosis”, “lung cancer”, “pharmacokinetics”, “liposomes”, “nano-emulsions”, “micelles”, “phospholipid complexes”, “solid dispersions”, “inclusion complexes”, and other terms. The pharmacokinetics of BA, strategies to improve bioavailability, therapeutic effects, and potential pharmacological mechanisms were summarized. Further research in this area is informed and recommended.

3 Pharmacokinetics of BA

As a glycoside flavonoid, BA has low aqueous solubility and poor membrane permeability, reducing its oral bioavailability and limiting its clinical application (Taiming and Xuehua, 2006; Ju et al., 2022). *In vivo*, BA is rapidly hydrolyzed to its glycosidic ligand BE, which shows excellent permeability and lipophilicity (Wang et al., 2020a). Liu *et al.* investigated the absorption mechanisms of BA and BE in rats and discovered that BA was moderately absorbed in the stomach and poorly absorbed in the small intestine and colon. While BE was well absorbed in the stomach and small intestine and relatively little in the colon (Taiming and Xuehua, 2006). After intravenous BA administration, the drug concentration decreases from high to low in the major organ tissues in the following order: kidney, lung, liver, and spleen (Wei et al., 2016). Notably, BA is the main metabolite in the blood, whether an oral BA or BE (Akao et al., 2013).

The metabolism of BA is a crucial factor in determining its efficacy and toxicity. The first step in the metabolism of BA is the hydrolysis of the glycoside into its ligand BE by the enzyme β-glucuronidase produced by intestinal microbiota (Xing et al., 2005). The type and abundance of intestinal microbes can impact the metabolic processes of BA in the intestine, making the intestinal microbiota an important factor in the metabolic processes of BA (Xie et al., 2020). This was confirmed by conducting studies in a rat model of antibiotic-pretreated rats, which showed that the maximum serum concentration (C_{max}), terminal half-life, elimination rate constant, and plasma drug concentration-time curve (AUC) values were significantly altered compared to normal rats. Moreover, gut microbiota, such as *Escherichia coli* and *Streptococcus* spp., can produce β-glucuronidase which enhances the metabolism of BA (Ishihara et al., 2002).

After metabolism in the intestine, BA undergoes glucuronidation (Zeng et al., 2022). Extensive hepatic and intestinal first-pass glucuronidation of BA has been found in both humans and rats (Akao et al., 2000; Zhang et al., 2007). BA and its glycosidic ligand exhibit inhibitory effects in the liver on UDP-glucuronosyltransferase (UGT) isoforms, including UGT1A1, 1A6, 1A9, and 2B7 (Teng et al., 2013). As one of the essential phase II mechanisms, those UGT isoforms might affect the bioavailability of BA.

Following glucuronidation, the hepatic-intestinal circulation of BA is comprised of several key steps, including uptake by the liver from the blood, excretion from the liver into the bile, transport of the bile to the duodenum for reabsorption, and finally return to the liver *via* the portal circulation (Xing et al., 2005). During this process, BA has two potential two sites of absorption. The first site is the upper intestine, which may directly absorb BA, and the second site is located in the colon in the form of glycosylated ligands (Lu et al., 2007).

As with the intestine, extensive metabolism of BA occurs in the liver. After oral administration of BA to rats, 32 metabolites were detected in blood and urine. During this process, various reactions

TABLE 1 Baicalin delivery systems and improved properties.

Delivery system	Improved properties	Refs.
Liposomes	Sustained drug release; increased oral availability, the peak concentration, and the drug concentrations in the liver, kidney, and lung	Wei et al. (2014)
Liposomes	Prolonged the duration time *in vivo*; increased the drug concentration of lung; inhibited LPS-induced inflammation in mice	Long et al. (2020)
Liposomes	Inhibited the growth rate of nude mice bearing orthotopic human lung cancer; improved lung targeting; sustained drug release; increased drug concentration in the lungs	Wei et al. (2017)
Liposomes	Improved cytotoxicity and cellular uptake; sustained drug release	Chen et al. (2016)
Nano-emulsions	Enhanced drug solubility and stability; prolonged the duration time *in vivo*	Wu et al. (2018)
Nano-emulsions	Improved oral bioavailability; sustained drug release	Zhao et al. (2013)
Micelles	Sustained drug release; improved solubility	Zhang et al. (2014)
Micelles	Improved cellular uptake and cytotoxicity; improved targeting of tumors; reduced side effects and growth of tumor volume in A549 tumor-bearing nude mice	Wang et al. (2019)
Phospholipid complexes	Improved the solubility, biomembrane permeation, and bioavailability	Wu et al. (2014)
Solid dispersions	Improved the dissolution and bioavailability	Li et al. (2013)
Solid dispersions	Enhanced the dissolution rate and bioavailability	Cui et al. (2016)
Inclusion complex	Improved aqueous solubility, dissolution rate, and oral bioavailability	Li et al. (2017)
Inclusion complex	Increased solubility, stability, and antioxidant activity	Li et al. (2009a)

Refs., references; LPS, lipopolysaccharide.

were found in rats, including methylation, hydrolysis, hydroxylation, methoxylation, glucuronide conjugation, sulfate conjugation, and complex reactions. The liver and kidney are the most important organs for metabolite distribution (Zhang et al., 2015). Finally, BA is excreted mainly as gluconate in the bile, accompanied by a small amount of urine (Xing et al., 2005).

In the intestine, β-glucuronidase, which is produced by the intestinal flora, hydrolyzes BA to BE. Glucuronidation is a significant metabolic pathway for BA, which undergoes various reactions in the liver and kidneys, the main metabolic organs. The elimination of metabolites occurs primarily through bile and urine. The biotransformation of BA requires the metabolic enzymes UGT and β-glucuronidase. The pharmacokinetics of BA can also be affected by various factors, including the administration route. The study by (Xing et al., 2005) found that the AUC values for BA administered intravenously (37 μmol/kg) and orally (224 μmol/kg) were 33.57 ± 1.8 (nmol·h/mL) and 4.43 ± 0.4 (nmol·h/mL), respectively. This indicates that the intravenous administration of BA was 6.05 times lower in dose but 7.57 times higher in AUC compared to the oral administration. However, BA's low bioavailability limits its clinical application, leading to the development of various formulations to enhance its solubility, bioavailability, and lung targeting potential.

4 Baicalin-loaded nano-delivery system

In recent years, the combination of nanoscience and biologically active natural compounds has been frequently investigated to create safe, biodegradable, and biocompatible drug delivery systems. Poor bioavailability is the main problem limiting BA in treating respiratory diseases (Xu et al., 2022a). In recent years, the development of new formulations for BA has been of increasing interest to the pharmaceutical field. Various nano-sized delivery systems have been explored, including liposomes, nano-emulsions, micelles, phospholipid complexes, solid dispersions, and inclusion complexes (Li J. et al., 2009; Li et al., 2013; Yue et al., 2013; Zhao et al., 2013; Wu et al., 2014; Zhang et al., 2014) (Tables 1, 2).

4.1 Liposomes

Liposomes are the most widely studied nano drug delivery system due to their synergistic delivery system that increases drug solubility (Huang et al., 2022; Ramedani et al., 2022). It has been demonstrated that the advantage of BA-loaded nanoliposomes for treating respiratory diseases is lung targeting (Wei et al., 2016; Wei et al., 2017). Research has shown that the BA liposome (L-BA) improves oral availability and tissue distribution (Wei et al., 2014). Compared to the same dose of BA, L-BA (100 mg/kg, tail-vein injection) more significantly reduced the W/D ratio, lung injury score, pro-inflammatory factors, and protein in total bronchoalveolar lavage fluid in a mouse model of lipopolysaccharide (LPS)-induced ALI (Long et al., 2020). In particular, the daily increase in tumor weight of BALB/c nude mice injected with A549 human lung cancer tumor cells was significantly reduced by L-BA (100 mg/kg) after intravenous injection of the drug, resulting in increased the survival rate of mice (Wei et al., 2017). L-BA was modified with folic acid and polyethylene glycol to improve further tumor targeting, which exhibited higher cellular uptake than non-targeted liposomes (Chen et al., 2016).

TABLE 2 Drug delivery systems for baicalin studied in preclinical acute lung injury and lung cancer models.

Disease	DDSs	Carrier	Experimental model	Loading efficiency	Encapsulation efficiency	Main results	Refs.
ALI	Liposome	Cholesterol/soy lecithin	Mice	NA	NA	*In vivo*: BA liposome had a better effect on reducing the wet/dry ratio, alleviating the lung injury score, and decreasing the proinflammatory factors (TNF-α and IL-1β) and total proteins in BALF	Long et al. (2020)
LC	Liposome	HSPC/Tween-80/ citric acid/BA	A549 cells/mice/rats	NA	82.8% ± 1.24%	*In vivo*: BA-loaded nanoliposomes showed better antitumor therapeutic efficacy in the nude mice bearing orthotopic human lung cancer	Wei et al. (2017)
LC	Micelles	Que/S-S/oHA/ Man/FA	A549 cells/ RAW264.7 cells/mice	3.50 ± 0.34%	72.63% ± 7.1%	*In vivo*: effective antitumor activity and reduced side effects of micelles were confirmed through antitumor experiments in A549 tumor-bearing nude mice	Wang et al. (2019)
						In vitro: good cellular penetration and tumor cytotoxicity of micelles were demonstrated through cellular studies	

DDSs, drug delivery systems; HSPC, phosopholipon 90H; BA, baicalin; NA, not applicable; BALF, bronchoalveolar lavage fluids; Que/S-S/oHA/Man/FA, quercetin/dithiodipropionic acid/ oligomeric hyaluronic acid/mannose/ferulic acid; TNF-α, tumor necrosis factor-alpha; IL, interleukin; Refs., references; ALI, acute lung injury; LC, lung cancer.

4.2 Nano-emulsions

Nano-emulsions offer unique advantages and properties that increase water solubility and dynamic stability, improve therapeutic efficacy, and reduce adverse effects and toxic reactions (Pangeni et al., 2018). Due to the sustained-release characteristics of the nano-emulsions containing BA, it is very effective in increasing oral availability. A novel nano-emulsion has been proven to improve systemic exposure to BA by promoting intestinal absorption and lymphatic transport (Wu et al., 2018). Zhao et al. (2013) prepared BA-loaded nano-emulsions by internal and external drug addition. And they found that both were superior to BA suspensions in terms of C_{max} and $AUC_{0-\infty}$.

4.3 Micelles

Micelles are synthesized from amphiphilic surfactants in the aqueous phase, which provides hydrophobic cores as reservoirs to increase the solubility of water-insoluble drugs (Gaucher et al., 2005). The carrier material containing a mixture of Pluronic P123 copolymer and sodium taurocholate in bundle gum increased the C_{max} and AUC in rats by 1.77 and 1.54 times more than the BA suspension, respectively (Zhang et al., 2016). The therapeutic effects of BA in micelles have been investigated in preclinical LC models. Novel carrier materials have been screened for structures targeting nano-micelles (named "nano-dandelion") for the simultaneous delivery of curcumin and BA. The nano-dandelion improved cellular uptake and cytotoxicity in the A549 cells, exhibiting better anti-cancer effects. In addition, by aggregating more readily at the tumor site, tail vein injection nano-dandelion exerts a more effective tumor suppression effect than free drug (Wang et al., 2019).

4.4 Phospholipid complexes

As with liposomes, phospholipid complexes can improve the affinity of BA to solubility and cell membranes (Qin et al., 2018). It has been shown that orally administered SBG extract-phospholipid complex improves solubility and bioavailability *in vivo* (Chen S. et al., 2022). Although phospholipid complexes can improve bioavailability, the increased lipophilicity leads to poor solubility and dispersion of the drug in the aqueous phase (Huang et al., 2019; Wang et al., 2020b). Self-emulsifying drug delivery systems (SEDDS) are isotropic mixtures of drugs, lipids, and surfactants, which are well-suited for lipophilic drugs with limited solubility (Salawi, 2022). A preparation for improving the oral availability of BA has been developed by combining a phospholipid complex with a SEDDS, which has been shown to enhance BA transport and relative bioavailability (Wu et al., 2014).

4.5 Solid dispersions

Solid dispersions improve the bioavailability of drugs by reducing the particle size to an absolute minimum, thereby increasing the wettability of the drug (Vasconcelos et al., 2007). Li et al. (2013) have developed that the BA-polyvinylpyrrolidone coprecipitate was prepared by the solid phase dispersion technique solvent method. Compared to the BA raw material capsules, the relative bioavailability of the coprecipitate capsules was 338.2% ± 93.2%. BA mesoporous carbon nanopowder (MCN) solid dispersions offer more advantages over pure BA as an oral delivery system, including shorter time to peak concentration and higher C_{max} and AUC. Significantly, it improves solubility and oral bioavailability without gastrointestinal and renal toxicity (Cui et al., 2016).

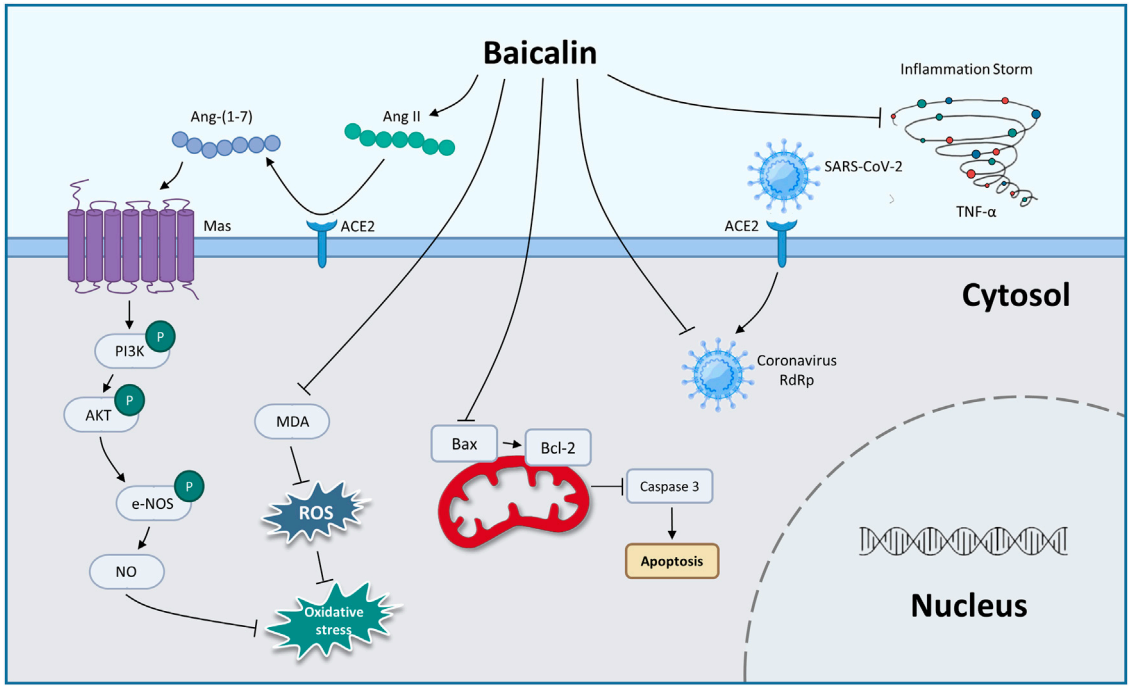

FIGURE 1
The therapeutic mechanism of baicalin on coronary viral disease-2019 (graphics courtesy of freepik.com).

4.6 Inclusion complexes

Cyclodextrins have been widely used as functional excipients in inclusion formulations (Gandhi et al., 2020). Li et al. (2017) synthesized β-cyclodextrin (β-CD) and BA host-guest inclusion complexes to exert better therapeutic effects. And the inclusion complex found that the $AUC_{0\text{-}t}$, $AUC_{0\text{-}\infty}$, and the relative oral bioavailability increased by 2.65, 2.53, and 2 times compared with free BA. To further improve the solubility and stability of the complexation of BA with β-CD, researchers structurally modified the BA complex to synthesize hydroxypropyl-β-CD to enhance antioxidant capacity, which is the most reactive form (Li et al., 2009a).

Due to the low bioavailability of BA, researchers have synthesized various novel formulations of BA to increase its solubility, bioavailability, targeting, cellular uptake, and retention time *in vivo*, increasing the therapeutic effect of BA. However, studies of these novel formulation forms are still in the pre-clinical stage, and further evaluation is needed to determine whether they can be used in the clinic.

5 The protection of BA against respiratory diseases

5.1 COVID-19 prevention

In 2019, the unprecedented COVID-19 was caused by the new coronavirus severe acute respiratory syndrome coronavirus 2 (SARS-CoV-2), which has become a global public health concern (Kciuk et al., 2022; Murali et al., 2022). BA has been shown to inhibit SARS-CoV-2 RNA-dependent RNA polymerase activity and exhibited significant antiviral activity against SARS-CoV-2 *in vitro* (Zandi et al., 2021). Evidence shows that cytokine storm (CS) was a pivotal stage in the advancement of COVID-19 (Hach et al., 2022; Jing et al., 2022; Shevtsova et al., 2022). You et al. (2022) used the method of network pharmacology to analyze the possible pathway of BA inhibiting CS. The enrichment analysis results showed that the tumor necrosis factor-α (TNF-α) pathway and IL (interleukin)-17 pathway might be potentially significant pathways for BA to inhibit CS. Furthermore, BA (200 mg/kg, gavage) exerts an anti-inflammatory effect by decreasing the expression of TNF-α, which alleviates CS against lung injury *in vivo*. As is well known, SARS-CoV-2 uses the ACE2 to enter cells, and ACE2 cleaves angiotensin (Ang) II into Ang 1–7, which is thought to exert a cellular response primarily through the receptor Mas to counteract RAS activation in several organs (Letko et al., 2020; South et al., 2020). A study by Wei reported that BA inhibits Ang II-induced oxidative damage and dysfunction in endothelial cells through activation of the ACE2/Ang-(1–7)/Mas axis and upregulation of the PI3K/AKT/eNOS pathway, thereby exerting a protective effect on endothelial cells (Wei et al., 2015).

From the above summary, we found that BA prevented COVID-19 through antiviral activity, inhibiting CS and protecting against endothelial cell dysfunction and oxidative damage (Figure 1; Table 3). In the future, clinical evaluation of BA for the treatment of COVID-19 needs to be performed.

TABLE 3 Summary of the targets/pathways/mechanisms and effects of baicalin on coronary viral disease 2019 and acute lung injury.

Disease	Inducer	Experimental model	Dose	Targets/pathways/mechanisms	Effects	Refs.
COVID-19	*In vitro*: SARS-CoV-2 (0.1 MOI)	*In vitro*: the Vero CCL-81 cells	*In vitro*: 1.1–30 μM	*In vitro*: SARS-CoV-2 RdRp↓	Inhibits SARS-CoV-2 RdRp	Zandi et al. (2021)
		Human Calu-3 cells				
COVID-19	*In vivo*: LPS (5 mg/kg)	*In vivo*: male C57BL/6J mice	*In vivo*: 200 mg/kg (gavage)	*In vivo*: TNF-α, total cells in BALF↓	Inhibits cytokine storm *via* TNF-α and IL-17 pathway	You et al. (2022)
	In vitro: LPS (100 ng/mL)	*In vitro*: MH-S cells	*In vitro*: 12.5–100 μg/mL	*In vitro*: TNF-α↓		
COVID-19	*In vitro*: Ang II (1×10^{-6} mol/L)	*In vitro*: HUVECs cells	*In vitro*: 12.5–50 μmol/L	*In vitro*: Bcl-2, Ang-(1–7), ACE2 activity, NO, T-AOC, PI3K, p-AKT, p-eNOS/eNOS↑	Protects endothelial dysfunction and oxidative stress *via* modulating the expression of Bax, Bcl-2, and cleaved caspase-3, activating ACE2/Ang-(1–7)/Mas axis and up-regulating PI3K/AKT/eNOS pathway	Wei et al. (2015)
				Bax, cleaved caspase-3, Ang II, MDA, ROS↓		
				mRNA and protein expression of ACE2 and Mas↑		
ALI	*In vivo*: LPS (3 mg/kg, i.t. administration)	*In vivo*: SPF male mice	*In vivo*: 200 mg/kg (orally administration)	*In vivo*: MDA, TNF-α, IL-1β, IL-6, total leukocyte counts, neutrophil counts, macrophage counts, lymphocyte counts↓	Enhances antioxidant systems and significantly and reduces both inflammatory cells and mediators *via* the Nrf2-mediated HO-1 signaling pathway	Meng et al. (2019)
				Nrf2, HO-1, CAT, SOD↑		
ALI	*In vivo*: LPS 10 mg/mL (100 μl) by airway instillation	*In vivo*: male Wistar rats	*In vivo*: 50 and 100 mg/kg (gavage)	*In vivo*: protein concentration in BALF, number of neutrophils, TNF-α, IL-1β, IL-6, CXCL1, MPO, TLR4, MyD88, NLRP3, p-NF-κB/NF-κB, p-ERK/ERK, p-p38 MAPK/p38 MAPK↓	Reduces the permeability of the alveolocapillary membrane, alleviates tissue injury and inflammatory infiltration, and inhibits the secretion of inflammatory factors and the infiltration of neutrophils *via* TLR4/MyD88/NF-κB/NLRP3 and MAPK pathway	Changle et al. (2022)
	In vitro: LPS 50 μg/mL	*In vitro*: BEAS-2B cells	*In vitro*: 5 and 10 μg/mL	*In vitro*: IL-8, IFN-γ, TNF-α, IL-1β, IL-6, GM-CSF, p-NF-κB/NF-κB, NLRP3↓		
				mRNA and protein expression of TLR4 and MyD88↓		
				mRNA and protein expression of NF-κB↑		
ALI	*In vivo*: APEC-O78 strain (2×10^{9} CFU) by i.t. inoculation	*In vivo*: male Hyline Brown healthy chickens	*In vivo*: 50, 100, and 200 mg/kg by oral gavage	*In vivo*: TNF-α, IL-1β, IL-6, MPO, p-IκB, p-p65↓	Reduces the W/D ratio, MPO activity, and production of IL-1β, TNF-α, and IL-6 of lung tissues by regulating NF-κB signaling pathway	Peng et al. (2019)
ALI	*In situ*: infusion of air (0.25 mL/min for 1 min)	*In situ*: isolates and perfuses lungs *in situ* of male SD rats	*In situ*: 1, 2, and 4 mg/kg	*In situ*: protein concentration in BALF, CINC-1, TNF-α, NF-κB, MPO, MDA↓	Reduce the production of proinflammatory cytokines, oxygen radicals, and NF-κB activity	Li et al. (2009b)
				IκB-α↑		

COVID-19, coronary viral disease-2019; TNF-α, tumor necrosis factor-alpha; BALF, bronchoalveolar lavage fluid; IL, interleukin; SARS-CoV-2, Severe Acute Respiratory Syndrome Coronavirus 2; RdRp, RNA-Dependent-RNA, polymerase; Ang, angiogenin; Bcl-2, B-cell lymphoma-2; ACE2, Angiotensin-converting enzyme 2; NO, nitric oxide; T-AOC, total antioxidant capacity; PI3K, Phosphatidylinositol3-kinase; AKT, protein kinase B; NOS, nitric oxide synthase; Bax, Bcl-2-associated X protein; MDA, malondialdehyde; ROS, reactive oxygen species; Nrf2, nuclear factor erythroid 2-related factor 2; HO-1, heme oxygenase-1; CAT, catalase; SOD, superoxide dismutase; CXCL1, chemokine 1; MPO, myeloperoxidase; TLR4, Toll-like receptor 4; MyD88, myeloid differentiation factor 88; NLRP3, NOD-like receptor family pyrin domain containing 3; NF-κB, nuclear factor-kappaB; ERK, extracellular signal-regulated kinase; MAPK, Mitogen-activated protein kinase; IFN-γ, interferon-gamma; GM-CSF, granulocyte-macrophage colony-stimulating factor; CINC-1, cytokine-induced neutrophil chemoattractant-1; IκB-α, Inhibitor of kappaB-α; SD, Sprague-Dawley; LPS, lipopolysaccharide; i.g., intragastric gavage; SPF, specific pathogen-free; APEC, avian pathogenic *Escherichia coli*; i.n., intranasal; i.t., intratracheal; HUVECs, Human umbilical vein endothelial cells; Refs., references; ALI, acute lung injury.

5.2 Acute lung injury

ALI is a life-threatening disease with a high fatality rate in a clinical setting (Guo et al., 2022). Severe lung infection, pulmonary contusion, and pulmonary embolism are the direct causes of ALI (He et al., 2021). The main pathological features are acute inflammation and apoptosis of alveolar epithelial cells (Allen and Kurdowska, 2014; Liu et al., 2020; Gao et al., 2021).

Using the LPS-induced ALI model, BA might be a novel strategy for lung protection, mainly due to BA (200 mg/kg, orally administration) inhibited the expression of TNF-α, IL-1β, IL-6, and malondialdehyde (MDA) and restored antioxidative enzyme activities, including superoxide dismutase (SOD) and catalase (CAT). The suppression of inflammatory and oxidant responses was mediated by activation of the nuclear erythroid factor 2 (Nrf2)-mediated heme oxygenase-1 (HO-1) pathway (Meng et al., 2019). In addition, another similar model study conducted by Zhu *et al.* demonstrated that 50 mg/kg and 100 mg/kg of BA (gavage) significantly alleviated the permeability of the alveolocapillary membrane and tissue injury through the toll-like receptor 4 (TLR4)/myeloid differentiation factor 88 (MyD88)/nuclear factor-kappa B (NF-κB)/nod-like receptor pyrin containing 3 (NLRP3) pathway and the mitogen-activated protein kinase (MAPK) pathway (Changle et al., 2022). The BA-induced attenuation of lung injury *via* the NF-κB anti-inflammatory pathway was confirmed in another lung injury model. Peng showed that BA (80 mg/kg, oral gavage) might alleviate lung injury in an avian pathogenic *E. coli*-induced model by inhibiting the phosphorylation of NF-κB (Peng et al., 2019). The findings demonstrated that BA modulated the NF-κB anti-inflammatory pathway, suggesting that it may contribute to reversing pulmonary injury. In a study of the air embolism-induced ALI model, BA (1, 2, and 4 mg/kg) was added into the lung perfusate, alleviating lung injury in isolated lungs by suppressing the proinflammatory cytokines, oxygen radicals, and NF-κB activity (Li et al., 2009b).

From the above summary, BA exerts anti-oxidative stress and anti-inflammatory effects through the Nrf2-mediated HO-1 pathway. CAT antioxidant enzyme, transforming growth factor-β (TGF-β), and granulocyte-macrophage colony-stimulating factor (GM-CSF) are involved in relieving ALI regulated by BA. And the inhibition of lung inflammation *via* the NF-κB pathway might play a pivotal role in attenuating pulmonary damage by BA (Table 3).

5.3 Asthma

Bronchial asthma is a chronic airway disease predominantly characterized by chronic inflammation and hyperresponsiveness, leading to cough, wheezing, shortness of breath, and chest tightness (Olin and Wechsler, 2014; Banno et al., 2020; Yasuda et al., 2020). It is widely believed that cytokines and inflammatory cells such as eosinophils, neutrophils, lymphocytes, and mast cells are involved in asthma (Yasuda et al., 2020; Zhang et al., 2020).

Ma et al. (2014) confirmed that BA (10–40 mg/kg, gavage) alleviated ovalbumin (OVA)-induced allergic asthma by inhibiting airway resistance, eosinophil count, and IL-4 level, recovering lung compliance, and increasing the expression of IFN-γ. And the study of molecular mechanisms might be associated with the decrease of IL-17A. Another similar model also confirmed the importance of immune regulation in asthma. Xu et al. (2017a) demonstrated that intragastric gavage (i.g.) administration of BA at a dose of 10, 25, and 65 mg/kg protected OVA and LPS-induced allergic asthma in mice models by maintaining Th17/Treg balance. In the study of Sun, researchers administered BA (gavage) dosages ranging from 25 to 100 mg/kg/day to mice with OVA-induced allergic asthma. The result demonstrated that BA reduced the expression of TGF-β1, IL-13, and vascular endothelial growth factor in tissue remodeling by suppressing the activation of the extracellular signal-regulated kinase (ERK) pathway and RAS expressions (Sun et al., 2013). Liu et al. (2016) found BA (10, 25, and 50 mg/kg, i.g. administration) could reduce the expression of immunoglobulin E (IgE), IL-6, TNF-α, CC-chemokine receptor (CCR) 7, C-C chemokine ligand (CCL)19/CCL21 in the OVA-induced mice model, inhibiting airway inflammation *via* the NF-κB pathway.

According to above research, immune modulation and inhibition of inflammatory responses appear to be important mechanisms for BA to treat asthma. It is critical for BA to relieve asthma by inhibiting the ERK pathway and inhibiting CCR7, CCL19/CCL21, and NF-κB pathway (Table 4).

5.4 Chronic obstructive pulmonary disease

COPD is characterized by airway remodeling and progressive lung inflammation, which are the main features of an increase in the number of alveolar macrophages, neutrophils, and T lymphocytes (Barnes, 2014; Chang et al., 2014). Cigarette smoking is one of the primary causes of COPD, resulting in 5 million deaths annually (Jones et al., 2017; Labaki and Rosenberg, 2020).

Hao et al. (2021) utilized cigarette smoke extract-induced mouse lung epithelial cell model and cigarette smoke and LPS-induced mouse model to investigate the anti-inflammatory effect of BA in COPD. They found that BA (25, 50, and 100 mg/kg, i.g. administration) inhibited inflammatory cell infiltration and the secretion of pro-inflammatory factors by regulating the heat shock protein 72 (HSP72)-mediated c-Jun N-terminal kinases (JNK) pathway. In addition, Zhang *et al.* showed that BA (i.g. administration) dosages ranging from 40 to 160 mg/kg suppressed the expression of inflammatory factors in cigarette smoke (extract)-induced human bronchial epithelial cells and airway tissues through suppressing the inflammatory response, enhancing histone deacetylase 2 protein expression, and inhibiting the activation of NF-κB and its downstream target of PAI-1 (Zhang et al., 2021). Using the same model, a study by Zeng *et al.* indicated that BA (20, 40, and 80 mg/kg, i.g. administration) reduced cigarette smoke-induced inflammation in human type II pneumocytes and rats by suppressing IL-6, IL-8, and TNF-α *via* the inhibition of NF-κB activation (Lixuan et al., 2010).

According to recent advances, the mechanism of COPD mitigation by BA revolves around inhibition of the inflammatory response, mainly through tight regulation of the HSP72-mediated JNK pathway, HDAC2/NF-κB/PAI-1 pathway, and NF-κB pathway (Table 4).

TABLE 4 Summary of the targets/pathways/mechanisms and effects of baicalin on asthma, chronic obstructive pulmonary disease, and pulmonary arterial hypertension.

Disease	Inducer	Experimental model	Dose	Targets/pathways/mechanisms	Effects	Refs.
Asthma	*In vivo*: OVA (i.p. injection with 10 μg chicken OVA and 2 mg aluminum hydroxide and then inhalation of 1% OVA solution)	*In vivo*: SPF female BALB/c mice	*In vivo*: 10, 20, and 40 mg/kg (gavage)	*In vivo*: WBC, eosinophils, IL-4, IL-17A, IgE↓	Suppresses IL-4, IL-17A, and Th17 cells, improves IFN-γ, and inhibits both the recruitment of eosinophils and mucus overproduction, leading to attenuated airway inflammation and bronchial hyperresponsiveness	Ma et al. (2014)
				Neutrophil, monocytes, lymphocytes→		
				IFN-γ↑		
Asthma	*In vivo*: OVA (100 μg) mixed with LPS (0.1 μg), then 50 μg OVA alone by i.n. instillations	*In vivo*: SPF female BALB/c mice	*In vivo*: 10, 25 and 65 mg/kg (i.g. administration)	*In vivo*: IgE, IL-17A, IL-6, STAT3↓	Protects against allergic asthma by regulating the immunological imbalance of Th17/Treg responses	Xu et al. (2017a)
				IL-10, FOXP3↑		
Asthma	*In vivo*: OVA (100 μg i.p. injection, then inhaled 1% OVA)	*In vivo*: female BALB/c mice	*In vivo*: 25, 50, and 100 mg/kg (gavage)	*In vivo*: TGF-β1, VEGF, IL-13, ERK, p21ras↓	Exerts anti-remodeling effect on asthmatic airway remodeling by decreasing expression of TGF-β1, IL-13, and VEGF and inhibiting the activation of the ERK pathway	Sun et al. (2013)
Asthma	*In vivo*: OVA (20 μg i.p. injection, and then 3% OVA nebulization)	*In vivo*: female BALB/c mice	*In vivo*: 10, 25, and 50 mg/kg (i.g. administration)	*In vivo*: WBC, eosinophils, IgE, CCL19, CCL21, IL-6, TNF-α, p-IκB, p-p65↓	Exerts an inhibitory effect on airway inflammation by inhibiting CCR7 and CCL19/CCL21	Liu et al. (2016)
				mRNA and protein expression of CCR7↓		
COPD	*In vivo*: cigarette smoke (inhalation) and LPS (10 μg, nasal instillation)	*In vivo*: C57BL/6 SPF male mice	*In vivo*: 25, 50, and 100 mg/kg (i.g. administration)	*In vivo*: HSP72↑	Alleviates COPD by upregulating the expression of HSP72 and resulting in the inhibition of JNK signaling activation	Hao et al. (2021)
				Muc5AC, IL-6, IL-8, and TNF-α, cell number, p-JNK/JNK↓		
	In vitro: cigarette smoke extract	*In vitro*: MLE-12 cells	*In vitro*: 5, 10, and 20 μmol/L	*In vitro*: HSP72↑, IL-6		
				IL-8, TNF-α, p-JNK/JNK↓		
COPD	*In vivo*: cigarette smoke (inhalation)	*In vivo*: male SD rats	*In vivo*: 40, 80, and 160 mg/kg (i.g. administration)	*In vivo*: IL-1β, TNF-α, p-IκB-α/IκB-α, p-p65/p65↓	Ameliorates airway inflammation by modulating of HDAC2/NF-κB/PAI-1 pathway	Zhang et al. (2021)
				mRNA and protein expression of PAI-1↓		
				HDAC2↑		
	In vitro: cigarette smoke extract	*In vitro*: HBE cells	*In vitro*: 10, 20, and 40 μM	*In vitro*: p-IκB-α/IκB-α, p-p65/p65↓		
				HDAC2↑		
				mRNA and protein expression of PAI-1 and TNF-α↓		
COPD	*In vivo*: cigarette smoke (inhalation)	*In vivo*: male SD rats	*In vivo*: 20, 40, and 80 mg/kg (i.g. administration)	*In vivo*: total leukocyte counting, the percentage of neutrophils, nuclear p65, IL-6, IL-8 and TNF-α↓	Exerts anti-inflammatory effect by inhibiting the NF-κB pathway	Lixuan et al. (2010)
				The percentage of mononuclear macrophages and lymphocytes→		
	In vitro: cigarette smoke extract	*In vitro*: human type II pneumocytes	*In vitro*: 5, 10, and 20 μmoL			

(Continued on following page)

TABLE 4 (*Continued*) Summary of the targets/pathways/mechanisms and effects of baicalin on asthma, chronic obstructive pulmonary disease, and pulmonary arterial hypertension.

Disease	Inducer	Experimental model	Dose	Targets/pathways/mechanisms	Effects	Refs.
				In vitro: p-p65, IL-6, IL-8 and TNF-α↓		
				IκB-α↑		
PAH	*In vivo*: MCT (60 mg/kg, subcutaneous injection)	*In vivo*: Wistar rats	*In vivo*: 100 mg/kg (i.g. administration)	*In vivo*: mRNA expression of TNF-α, IL-1β, IL-6, and ET-1↓	Exerts protective effects against the lung and heart damage in experimental PAH maybe through inhibiting vascular endothelial inflammatory response	Luan et al. (2015)
				TGF-β1, ICAM-1, NF-κB↓		
				IκB↑		
PAH	*In vivo*: MCT (50 mg/kg, i.p. injection)	*In vivo*: male Wistar rats	*In vivo*: 20, 50, and 200 mg/kg (i.g. administration)	*In vivo*: α-SMA, P/T NF-κB-p65, VCAM, ICAM↓	Protects against experimental PAH *via* regulating the TNF-α/BMPR2 signaling pathway	Xue et al. (2021)
				BMPR2, Smad1/5/8, p-Smad1/5/8, ID1↑		
				mRNA expression of IL-1β and IL-6↓		
				mRNA and protein expression of TNF-α↓		
	In vitro: TNF-α (5 ng/mL)	*In vitro*: rat pulmonary artery smooth muscle cells	*In vitro*: 100 μg/mL	*In vitro*: Cyclin D1↓		
				p27, BMPR2, ID1, Smad1/5/8, p-Smad1/5/8↑		
PAH	*In vivo*: MCT (50 mg/kg, i.p. injection)	*In vivo*: male SPF SD rats	*In vivo*: 20, 100, and 200 mg/kg (i.p. injection)	*In vivo*: p-p65/total p65, p-ERK/total ERK↓	Interferes with pulmonary vascular remodeling and PAH development through the AKT/eNOS, ERK, and NF-κB signaling pathways	Yan et al. (2019)
				p-AKT/total AKT, p-eNOS/total eNOS↑		
PAH	*In vivo*: hypoxia	*In vivo*: $A_{2A}R$-deficient Balb/c mice and Balb/c wild-type mice	*In vivo*: 60 mg/kg (i.p. injection)	*In vivo*: CXCR4, SDF-1, P-PI3K/PI3K, P-AKT/AKT↓	Enhances $A_{2A}R$ activity and downregulates SDF-1/CXCR4-induced PI3K/AKT pathway	Huang et al. (2017)
				$A_{2A}R$↑		
PAH	*In vivo*: hypoxia	*In vivo*: male SPF SD rats	*In vivo*: 30 mg/kg (i.p. injection)	*In vivo*: mRNA and protein expression of MMP-9↓	Attenuates pulmonary hypertension and cor pulmonale by downregulating the p38 MAPK/MMP-9 pathway	Yan et al. (2016)
				p-p38↓		

OVA, ovalbumin; SPF, specific pathogen free; WBC, white blood cell; IL, interleukin; IgE, Immunoglobulin E; STAT3, Signal transducer and activator of transcription 3; FOXP3, Forkhead Box Protein P3; TGF-β1, transforming growth factor-β1; VEGF, vascular endothelial growth factor; ERK, extracellular signal-regulated kinase; CCL, c-c motif chemokine ligand; TNF-α, tumor necrosis factor-alpha; IκB, Inhibitor of kappaB; CCR, C-C-Motif Receptor; LPS, lipopolysaccharide; HSP72, heat shock protein 72; JNK, c-Jun N-terminal kinase; COPD, chronic obstructive pulmonary disease; SD, sprague dawley; NF-κB, nuclear factor-kappaB; PAI-1, Plasminogen activator inhibitor-1; HDAC2, histone deacetylase 2; PAH, pulmonary arterial hypertension; MCT, monocrotaline; AKT, protein kinase B; NOS, nitric oxide synthase; ET-1, Endothelin-1; ICAM-1, intercellular cell adhesion molecule-1; α-SMA, alpha-smooth muscle actin; VCAM, vascular cell adhesion molecule; Smad, small mothers against decapentaplegic; MLE-12, mouse lung epithelial-12; ADAMTS, A Disintegrin and Metalloproteinase with Thrombospondin Motifs; ID1, inhibitor of DNA, binding 1; BMPR2, bone morphogenetic protein receptor 2; $A_{2A}R$, A2A adenosine receptor; CXCR4, C-X-C chemokine receptor 4; SDF-1, stromal derived factor-1; MMP-9, matrix metalloproteinase-9; Hyp, hydroxyproline; MDA, malondialdehyde; TGF-β1, transforming growth factor-β1; i.p., intraperitoneal; i.n., intranasal; Treg, regulatory T-cell; i.g., intragastric; IκB-α, Inhibitor of kappaB-α; MAPK, Mitogen-activated protein kinase; Refs., reference.

5.5 Pulmonary arterial hypertension

PAH is a progressive and fatal disease with rapid onset and mortality in 7 people for every 100 person-years in Asian countries (Chung et al., 2015). Pulmonary endothelial cell dysfunction, pulmonary artery smooth muscle proliferation, and right ventricular hypertrophy are all involved in the development and formation of PAH (Xu et al., 2022b).

In a study by Luan et al. (2015), the rats with monocrotaline (MCT)-induced PAH were administered BA (i.g. administration) at a daily dose of 100 mg/kg. The results showed that BA downregulated the mRNA levels of TNF-α, IL-13, IL-6, and ET-1 in pulmonary tissues *via* blocking the activation of the NF-κB signaling pathway to attenuate PAH. Utilizing the same model, Xue et al. (2021) found that BA (20, 50, and 200 mg/kg, i.g. administration) profoundly reduced the mRNA and protein levels of inflammatory factors, excessive proliferation, migration of pulmonary artery smooth muscle cells, and vascular remodeling *via* the TNF-α/bone morphogenetic protein receptor 2 (BMPR2) signaling pathway. In an MCT-induced rat model, BA (20, 100, and 200 mg/kg, i.p. injection) protected the rats from the severity

TABLE 5 Summary of the targets/pathways/mechanisms and effects of baicalin on pulmonary fibrosis and lung cancer.

Disease	Inducer	Experimental model	Dose	Targets/pathways/mechanisms	Effects	Refs.
PF	*In vivo*: BLM (5 mg/kg, i.t. instillation)	*In vivo*: adult female Wistar rats	*In vivo*: 50 mg/kg (i.p. administration)	*In vivo*: Hyp, collagen I, collagen III, TGF-β, TNF-α, MDA, caspase-3, Bax, cells in the BALF↓	Inhibits pulmonary fibrosis, inflammation, tissue apoptosis, collagen deposition, oxidative stress-associated damage, and proliferation and arrests cell cycle *via* the inhibition of the CaMKII and AKT signaling pathways	Zhao et al. (2020)
				GSH-px, T-SOD, GSH, Bcl-2↑		
	In vitro: BLM (20 μg/mL)	*In vitro*: rat primary lung fibroblasts	*In vitro*: 80 μg/mL	*In vitro*: cyclin A, cyclin D, cyclin E, PCNA, p-AKT/t-AKT, p-CaMKII/t-CaMKII↓		
PF	*In vivo*: BLM (5 U/kg, i.t. injection)	*In vivo*: wild type Balb/c mice and A2aR homozygous knockout mice	*In vivo*: 120 mg/kg (i.p. injection)	*In vivo*: Hyp, TGF-β1, p-ERK/t-ERK, p-ERK1/2↓	Attenuates pulmonary fibrosis *via* adenosine A2aR-related TGF-β1-induced ERK1/2 signaling pathway	Huang et al. (2016)
				A2aR↑		
				ERK1/2→		
PF	*In vivo*: BLM (5 mg/kg, i.t. instillation)	*In vivo*: male SD rats	*In vivo*: 25 and 100 mg/kg (gavage)	*In vivo*: Hyp, MDA↓	Improves pulmonary fibrosis by the regulation of four key biomarkers involving taurine and hypotaurine metabolism, glutathione metabolism and glycerophospholipid metabolism	Chang et al. (2021)
				SOD↑		
				Regulates taurine and hypotaurine metabolism, glutathione metabolism, and glycerophospholipid metabolism		
PF	*In vitro*: radiation (8 Gy of ^{60}Co γ-rays at a dose rate of 3.64 Gy/min)	*In vitro*: primary rat type II AEC	*In vitro*: 2, 10, and 50 μM	*In vitro*: vimentin, snail, α-SMA, TGF-β, p-ERK/ERK, p-GSK3β/GSK3β, p-Smad2/Smad2, p-Smad3/Smad3↓	Alleviates EMT transition *via* TGF-β and ERK/GSK3β signaling pathways	Lu et al. (2017)
				E-cadherin↑		
PF	*In vivo*: silicosis (2.5 per mouse, oral-tracheal instillation)	*In vivo*: female C57BL/6 mice	*In vivo*: 2 mg per mouse (i.p. administration)	*In vivo*: total cells in BALF, neutrophils number, lymphocytes number, macrophages number, the percentage of CD4+IL-17A+T cells, TNF-α, IL-4↓	Inhibits the Th17 response and reduces inflammation and fibrosis	Liu et al. (2015)
				The percentage of CD4+Foxp3+T-cell↑		
				The percentage of CD4+T-cell co-expressed IFN-γ↓		
				mRNA and protein expression of IL-6↓		
				mRNA expression of Th17A, RORγt, GATA-3, TGF-β, IFN-γ, and IL-23↓		
				mRNA expression of IL-10 and Foxp3↑		
LC	*In vivo*: implants 5 × 10^6/mL tumor cell	*In vivo*: female BALB/c-nu mice	*In vivo*: 20 mg/kg	*In vivo*: p-Akt, p-mTOR, CDK4, and cyclin E2↓	Exerts antitumor activity *via* inducing Akt-dependent cell cycle arrest and promoting apoptosis	Sui et al. (2020)
	In vitro: NA	*In vitro*: H1650 and H1299 cells	*In vitro*: 0–150 μg/mL	*In vitro*: Bax, cleaved caspase-9↑		
				Bcl-2, CDK2, CDK4, cyclin E2, p- Akt, p- mTOR↓		

(Continued on following page)

TABLE 5 (*Continued*) Summary of the targets/pathways/mechanisms and effects of baicalin on pulmonary fibrosis and lung cancer.

Disease	Inducer	Experimental model	Dose	Targets/pathways/mechanisms	Effects	Refs.
LC	*In vivo*: infects with 1 × 10^6 NCI-H460 cells	*In vivo*: BALB/c nude mice	*In vivo*: 40 and 60 mg/kg (oral gavage)	*In vivo*: vimentin, p-PDK1, p-AKT↓	Impedes EMT by inhibiting the PDK1/AKT pathway	Chen et al. (2021)
				E-cadherin↑		
	In vitro: NA	*In vitro*: A549, NCI-H460, and BEAS-2B cells	*In vitro*: 0, 15, and 30 μM	*In vitro*: vimentin, p-PDK1, p-AKT↓		
				E-cadherin↑		
LC	*In vitro*: NA	*In vitro*: A549 and H1299 cells	*In vitro*: 60 μg/mL	*In vitro*: miR-340-5p↑	Elicits antitumor activities by affecting the miR-340-5p/NET1 axis	Zhao et al. (2021)
				mRNA and protein expression of NET1↓		
LC	*In vitro*: NA	*In vitro*: A549 and H1299 cells	*In vitro*: 0–80 μmol/L	*In vitro*: SIRT1, p-AMPK/AMPK, c-caspase-3↑	Inhibits the proliferation and migration by activating the SIRT1/AMPK signaling pathway	You et al. (2018)
				p-mTOR/mTOR, active MMP-2, active MMP-9↓		
LC	*In vivo*: athymic nude mice injected with H441 lung cancer cell (4 ×10^6/0.1 mL)	*In vivo*: athymic nude mice	*In vivo*: 20 and 50 mg/kg (i.p. injection)	*In vivo*: p-Histones H3, p-ERKs, PBK/TOPK↓	Inhibits the proliferation of lung cancer *via* decreasing the PBK/TOPK downstream signaling molecules Histone H3 and ERK2	Diao et al. (2019)
	In vitro: NA	*In vitro*: JB6 Cl41 cells, H441, H1975, H1299, and A549 cells	*In vitro*: 25, 50, and 100 μM	*In vitro*: p-Histones H3/Histones H3, p-EKRs, p-ERKs/ERKs, PBK/TOPK↓		
LC	*In vitro*: NA	*In vitro*: A549 cells and A549/DDP cells (DDP-resistant human lung cancer cells)	*In vitro*: 1–8 μg/mL	*In vitro*: MAPK2 mRNA and protein↓	Inhibits proliferation and invasion and attenuates DDP resistance by decreasing protein expression of MAPK2 and p-Akt	Xu et al. (2017b)
				p-AKT↓		
				AKT→		
LC	*In vitro*: NA	*In vitro*: A549 and H2009 cells	*In vitro*: 75 μM	*In vitro*: p-p38/p38, ROS, cleaved-PARP↑	Enhances the anticancer activity of TRAIL *via* p38 activation and ROS accumulation	Zhang et al. (2017)

Hyp, hydroxyproline; TGF-β1, transforming growth factor-β1; TNF-α, tumor necrosis factor-α; MDA, malondialdehyde; Bax, Bcl-2-associated X protein; BALF, bronchoalveolar lavage fluid; GSH, glutathione; GSH-px, glutathione peroxidase; SOD, superoxide dismutase; Bcl-2, B-cell lymphoma-2; AKT, protein kinase B; CaMKII, calmodulin-dependent kinase II; ERK, extracellular signal-regulated kinase; α-SMA, alpha-smooth muscle actin; GSK3β, glycogen synthase kinase-3, beta; Smad, small mothers against decapentaplegic; EMT, epithelial-mesenchymal transition; AEC, alveolar type epithelial cell; Foxp3, Forkhead Box P3; IFN-γ, interferon-γ; RORγt, retinoid-related orphan nuclear receptor γt; GATA-3, GATA-binding protein 3; mTOR, mechanistic target of rapamycin; CDK, cyclin-dependent kinase; PDK1, phosphoinositide-dependent protein kinase 1; NET1, neuroepithelial cell transforming 1; SIRT1, sirtuin 1; AMPK, adenosine monophosphate-activated protein kinase; SD, Sprague–Dawley; MMP, matrix metalloproteinase; MAPK, Mitogen-activated protein kinase; DDP, cisplatin; ROS, reactive oxygen species; PARP, poly ADP-ribose polymerase; BLM, bleomycin; i.t., intratracheal; PCNA, proliferating cell nuclear antigen; IL, interleukin; MMP, matrix metalloprotein; PBK/TOPK: PDZ-binding kinase/T-LAK, cell-originated protein kinase; A2aR: adenosine A2a receptor; Refs., reference; PF, pulmonary fibrosis; TRAIL, tumor necrosis factor-related apoptosis-inducing ligand; NA, not applicable.

of pulmonary vascular remodeling and cardiorespiratory injury *via* AKT/ERK/NF-κB signaling pathways and p-eNOS protein (Yan et al., 2019). In another PAH model, the relief of chronic hypoxia-induced PAH by BA (60 mg/kg, i.p. injection) through the AKT pathway was confirmed. In addition, the results of *in vivo* studies suggested that BA performed a therapeutic role *via* the attenuation of the adenosine A_{2A} receptor-induced SDF-1/CXCR4/PI3K/AKT pathway (Huang et al., 2017). Yan et al. (2016) demonstrated that 30 mg/kg of BA (i.p. injection) relieved the hypoxia-induced PAH model by mitigating pulmonary hypertension, pulmonary arteriole, and right ventricular remodeling and ameliorating hypoxic cor pulmonale by suppressing the p38 MAPK pathway and the expression of matrix metalloprotein (MMP)-9.

In conclusion, the suppression of inflammatory factors, the TNF-α/BMPR2 pathway, the SDF-1/CXCR4/PI3K/AKT pathway, and the p38 MAPK pathway seem to be essential to the regulation of PAH by BA (Table 4).

5.6 Pulmonary fibrosis

PF is a chronic, progressive, and deadly lung disease primarily affecting middle-aged and older people (Sharif, 2017). It is generally accepted that the occurrence of PF is abnormal wound healing after repeated alveolar injury in genetically susceptible individuals, leading to the destruction of the lung parenchyma, and deposition of extracellular matrix in fibroblasts and alveolar epithelium. In addition, improperly

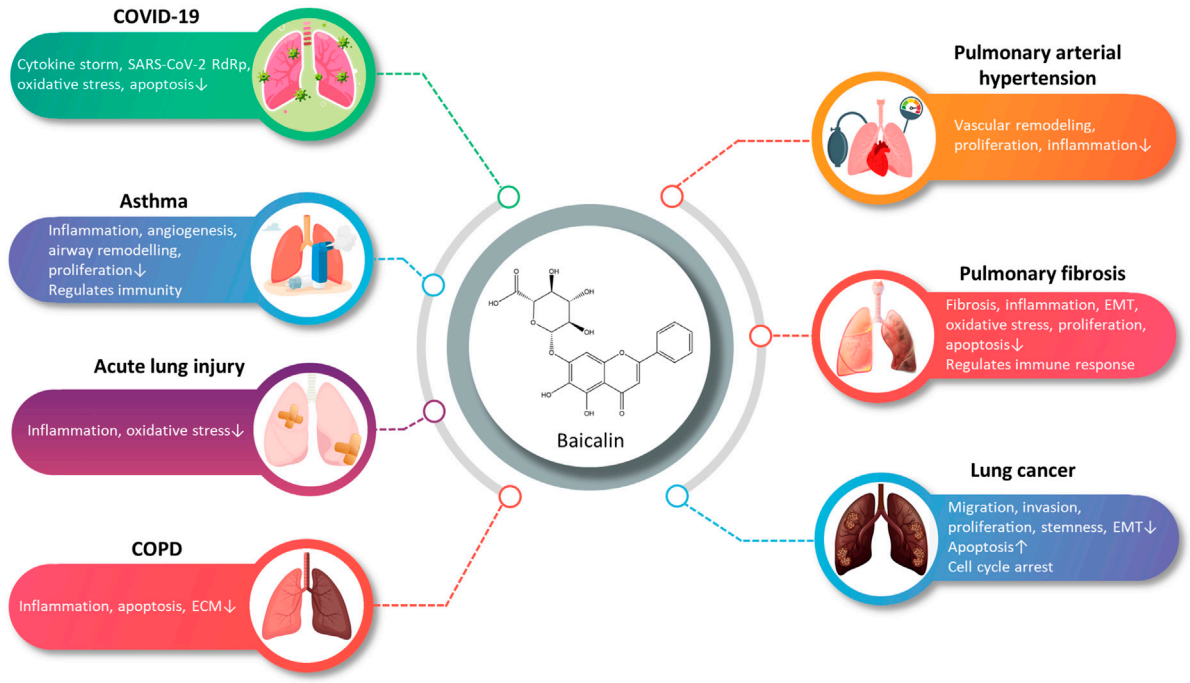

FIGURE 2
A summary of the main pharmacological effects of baicalin and its mechanisms involved in respiratory diseases (graphics courtesy of freepik.com).

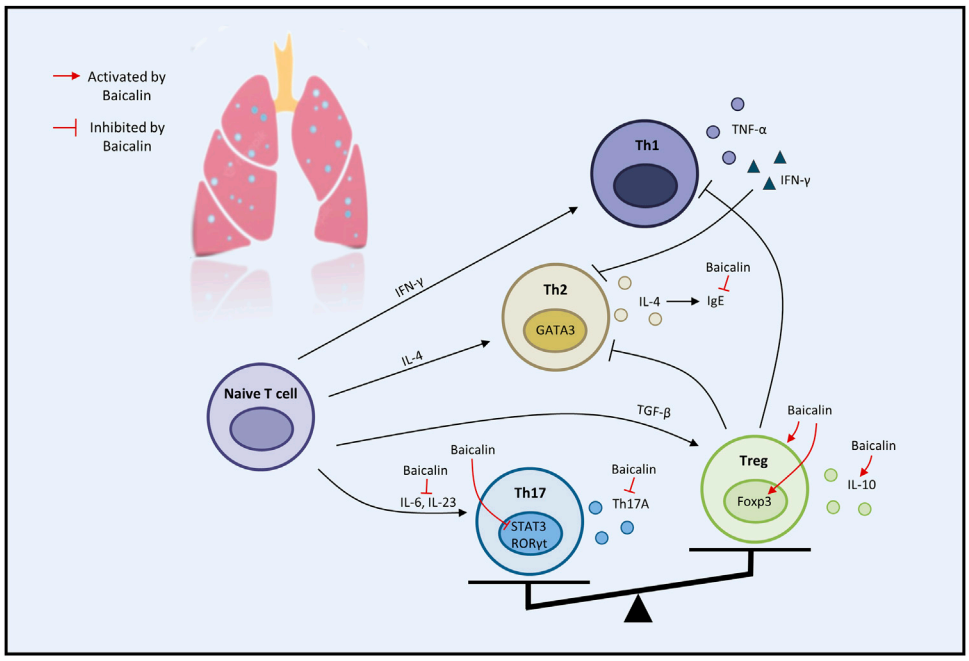

FIGURE 3
The therapeutic effects of baicalin on immune modulation on respiratory disease (graphics courtesy of freepik.com).

activated alveolar epithelial cells (AECs) and fibroblasts cause the fibrotic response (King et al., 2011; Ptasinski et al., 2021).

A recent study indicated that 50 mg/kg BA (i.p. administration) effectively suppresses bleomycin (BLM)-induced PF in rats by decreasing the expression of hydroxyproline, TGF-β, collagen I, collagen III, and TNF-α, enhancing the function of anti-oxidative stress, and inhibiting apoptotic protein expression. Moreover, this study also showed that 80 μg/mL BA reverses BLM-induced fibroblast proliferation, regulating the

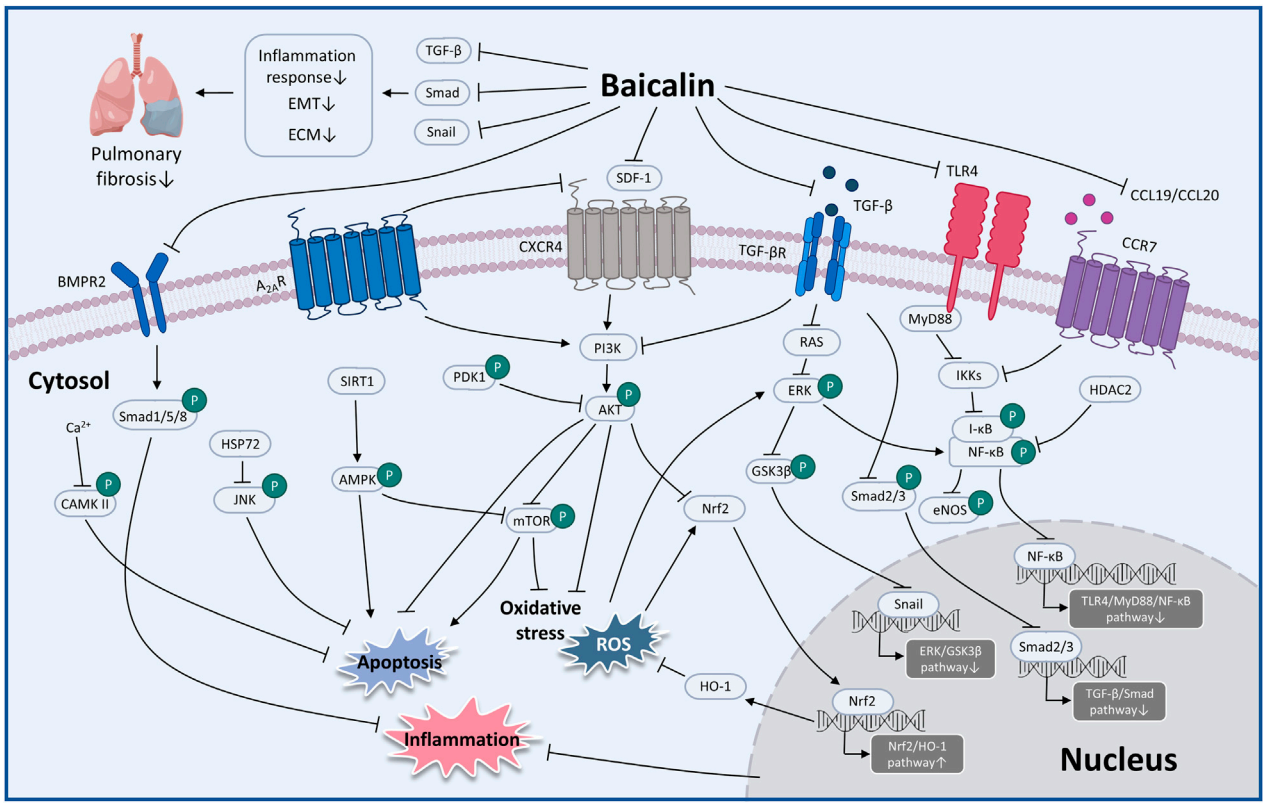

FIGURE 4
The therapeutic mechanism and critical pathways of baicalin against respiratory diseases (graphics courtesy of figdraw.com/static/index.html#/ and freepik.com).

expression of phosphoinositide 3-kinase (PI3K)/AKT and calcium/calmodulin-dependent kinase II *in vitro* (Zhao et al., 2020). Another *in vivo* study revealed that 120 mg/kg BA (i.p. administration) was found to block the TGF-β1-induced ERK1/2 signaling pathway *via* the adenosine A_{2A} receptor, leading to the alleviation of fibrosis caused by BLM (Huang et al., 2016). In recent years, the targeted omics approach for biomarkers discovery has been an effective approach for evaluating the effectiveness and mechanisms of BA (Ullah et al., 2022). In the study of Chang et al. (2021), the researchers administered 25–100 mg/kg BA to rat models with PF caused by BLM. The results demonstrated that BA ameliorated the levels of MDA and SOD to relieve oxidative stress. Furthermore, BA was identified to potentially alleviate PF by regulating four vital metabolic markers, including taurine, hypotaurine, glutathione, and glycerophospholipid metabolism.

TGF-β acts as a potent driver of PF progression by induction of epithelial-mesenchymal transition (EMT) (Qian et al., 2018). At doses of 2–50 μM, BA appears to be implicated in the radiation-induced EMT of AECs by inhibiting TGF-β and ERK/GSK signaling pathways mediated fibrosis (Lu et al., 2017). In terms of immunoregulatory mechanisms, i.p. injection of 100 mg/kg BA decreased PF in mouse models caused by silica by altering the Th17/Treg responses by lowering Th17 cells, activating Treg cells, and inhibiting IL-6 and IL-23 (Liu et al., 2015).

In summary, BA alleviates PF through a variety of mechanisms, including inhibition of the inflammatory response, oxidative stress, EMT, apoptosis and immune modulation (Table 5).

5.7 Lung cancer

LC remains the primary cause of cancer deaths in the world (Wei et al., 2015; Saman et al., 2022). As the most common subtype of LC, non-small cell lung cancer (NSCLC) accounts for around 85% of LC cases (Fiero et al., 2019). Currently, surgery, chemotherapy, radiation, and targeted molecular treatment are the main treatment options for LC patients (South et al., 2020). However, the side effects and toxicity of these techniques have become limiting factors in the clinical treatment of lung cancer (Luan et al., 2015; Yamamoto et al., 2022).

Sui et al. (2020) found that 20 mg/kg of BA can trigger apoptosis and block cell cycle G1/S transition in carcinoma of the lung cells *via* the AKT/mechanistic target of rapamycin (mTOR) pathway. NSCLC is highly prone to invasion and metastasis, which are closely associated with the occurrence of EMT (Xia et al., 2014). In this regard, Chen reported that BA inhibited the EMT of NSCLC through the PDK1/AKT pathway (Chen et al., 2021). Recently, the importance of miRNAs in cancer progression has been reported (He et al., 2005; Lee and Dutta, 2007). Zhao et al. (2021) discovered that

BA (60 μg/mL) restrained cell proliferation and invasion, promoted apoptosis, and arrested the G1/S phase *via* the miR-340-5p/NET1 axis, exerting anti-lung cancer effects. In an *in vitro* study, BA (20–80 μmol/L) inhibited cell viability, triggered apoptosis, and decreased cell migration and invasion by inhibiting the activation of the sirtuin 1 (SIRT1)/adenosine monophosphate-activated protein kinase (AMPK) signaling pathway (You et al., 2018). In several studies, overexpression of PDZ-binding kinase/T-LAK cell-originated protein kinase (PBK/TOPK) has been related to a poor prognosis and is a crucial target for anticancer drugs (Lei et al., 2013; Han et al., 2021). Diao et al. (2019) found that BA inhibited PBK/TOPK activities by directly binding with PBK/TOPK *in vitro* and *in vivo*.

Despite the successful efficacy of chemotherapy, there is growing concerned about chemotherapeutic agents developing resistance (Siddik, 2003; Apps et al., 2015; Pan et al., 2019). Considering this, researchers found that combining BA and DDP (cisplatin) inhibited tumor cells significantly more than DDP or BA alone in A549 and A549/DDP cells (DDP-resistant cells). The attenuation of the resistance of DDP was connected with downregulating MARK2 and p-Akt proteins (Xu et al., 2017b). In addition, tumor necrosis factor-related apoptosis-inducing ligand (TRAIL) is a promising target for overcoming cancer cell resistance (von Karstedt et al., 2017). BA (75 μM) can increase TRAIL-induced apoptosis and intracellular reactive oxygen species generation in cancer cells *via* activating p38 MAPK, enhancing the antitumor effectiveness of TRAIL (Zhang et al., 2017). The findings of the current investigations suggested that targeting MAPK is a significant pathway to reduce drug resistance in cancer. The AKT/mTOR, the PDK1/AKT, the SIRT1/AMPK pathways, and the regulation of active MMP-2, active MMP-9, vimentin, and E-cadherin are connected with the relief of LC (Table 5).

6 Discussion and outlook

Through this review, we have attempted to summarize a comprehensive review of research advances for BA in pharmacokinetics, strategies to improve bioavailability, and the treatment of disorders related to the respiratory system. Despite the poor bioavailability and solubility of BA, the development of DDSs for BA has improved the bioavailability, pulmonary targeting, and solubility, thereby improving the efficacy. The multiple pharmacological activities of BA suggest a broad prospect for the prevention and treatment of ALI, PF, COVID-19, LC, PAH, COPD, and asthma (Figure 2). At present, studies on BA are still in the preclinical stage. This review provides a valuable reference for subsequent pharmacological studies and clinical applications of BA.

Considerable preclinical studies have shown that BA has excellent therapeutic potential to treat respiratory diseases in both *in vivo* and *in vitro* settings. BA exerts therapeutic effects mainly through mediating upstream oxidative stress, inflammation, apoptosis, and immune response pathways. In the regulation of oxidative stress, the PI3K/AKT/eNOS pathway and the Nrf2-mediated HO-1 pathway are critical factors associated with the protective effects of BA on COVID-19 and ALI. Regarding the inflammatory response, TNF-α, IL-1β, IL-6, GM-CSF, IL-8, IL-4, and IL-10 are involved in BA to alleviate COVID-19, ALI, PF, COPD, PAH, and asthma. Regarding the regulation of apoptosis molecules, caspase-3, caspase-9, Bcl-2, and Bax are essential factors in alleviating LC, PF, and COVID-19. Immune modulation therapy has sparked the interest of researchers. The underlying mechanisms of BA in the treatment of immune modulation on PF and asthma manifest as the regulation of Th17/Treg responses by promoting Treg cell differentiation, inhibiting the expression of Th17A, and reducing the levels of IL-6, IFN-γ, IL-4, and IL-23 (Figure 3). Although the target of BA for the treatment of respiratory diseases is still inconclusive. Phosphodiesterase 4 (PDE4) might be a potential therapeutic target for treating respiratory diseases. And PDE4 already has targeted inhibitors approved for treating severe COPD, such as roflumilast (Crocetti et al., 2022; Herrmann et al., 2022). In addition, GSK-256066, a highly selective inhaled PDE4 inhibitor, has been in phase II clinical trials for asthma and COPD (Pagès et al., 2009). BA was found to selectively inhibit the enzymatic activity of PDE4A and 4B to relieve allergic asthma (Park et al., 2016). Thus, it indicates that PDE4 may be a candidate target for BA to target respiratory diseases, which requires further experimental proof. Importantly, we discovered that BA exhibits anti-cancer effects *via* inducing apoptosis and oxidative stress, which is the opposite of BA for the treatment of PF. It suggests that BA exerts a bidirectional regulatory effect to protect the lung. The multiple pharmacological activities suggest that BA is a promising compound for the prevention and treatment of ALI, PF, COVID-19, LC, PAH, COPD, and asthma (Figure 4).

This review identifies a plausible mechanism for the therapeutic efficacy of BA in treating respiratory diseases. However, the experiments have almost always verified the conclusion *in vivo* and *in vitro*. More clinical evidence is needed to verify efficacy. Several aspects of BA need to be investigated before its clinical application. Firstly, the poor water solubility of BA leads to low oral bioavailability. Researchers have developed strategies to improve the bioavailability of BA, including liposomes, nano-emulsions, micelles, phospholipid complexes, solid dispersions, and inclusion complexes (Li J. et al., 2009; Li et al., 2013; Yue et al., 2013; Zhao et al., 2013; Wu et al., 2014; Zhang et al., 2014). Modified versions of these different formulations of BA would be carried out in animal experiments to find their optimal effective dose. And there is also the issue of acute and long-term toxicity of BA in animal models of different respiratory diseases. Secondly, therapeutic doses of BA varied widely across studies. This may be due to disease type, disease state, route of administration, time point of administration (prophylactic or therapeutic administration), number of days of treatment, age, weight, sex of the animals, and environmental factors, etc. Thus, when BA is used as a treatment for respiratory diseases, it needs to be tailored to the specific situation. In addition, as a common dosage form for the treatment of respiratory diseases, inhalation of BA has not been studied. BA is reported to be insoluble in water that may be the main reason for limiting its candidate for the development of inhalation preparation. A number of new formulations have been developed to improve water solubility, including inclusion complexes and phospholipid complexes, etc. BA has shown improved properties as an inhalant component of chinese herbal compound. Transnasal aerosol inhalation of Tanreqing (containing BA) increased the drug concentration of BA in the lungs and showed better anti-inflammatory effects on LPS-induced ALI in mice, compared to intravenous administration (Chen T. F. et al., 2022). This indicates the potential of BA as an

inhalation. Finally, with the advancement of multi-omics studies, those approaches can be used to explore the mechanism of the effects of BA in the treatment of respiratory diseases and to gain a clearer understanding of the multi-target regulatory network of BA. In general, this review presents novel perspectives on the pharmacological effects of BA on respiratory diseases. It must be acknowledged that this review also has some limitations, including the source of BA, the experimental method, and the choice of dose.

Author contributions

SS and LD collected, analyzed, and reviewed the literature, and wrote the main manuscript; GL, TC, MZ, XuL, ML, HQ, and JC assembled figures/tables; ZiW, JM, YW, and QW added and checked references; ZeW and XiL designed and supervised the manuscript; ZeW and XiL revised the final version of the manuscript. All authors have read and agreed to the published version of the manuscript.

Funding

This work was supported by the Key Research and Development Project of Jilin Province (No. 20200404057YY), Jilin Administration of Traditional Chinese Medicine (2022221), and the Science and Technology Development Plan Project of Jilin Province (YDZJ202301ZYTS136, YDZJ202202CXJD049).

Acknowledgments

We thank FIGDRAW (figdraw.com/static/index.html) and freepik (freepik.com) for their graphics courtesy assistance during the preparation of this manuscript.

Conflicts of interest

The authors declare that the research was conducted in the absence of any commercial or financial relationships that could be construed as a potential conflict of interest.

Publisher's note

References

Akao, T., Kawabata, K., Yanagisawa, E., Ishihara, K., Mizuhara, Y., Wakui, Y., et al. (2000). Baicalin, the predominant flavone glucuronide of scutellariae radix, is absorbed from the rat gastrointestinal tract as the aglycone and restored to its original form. *J. Pharm. Pharmacol.* 52 (12), 1563–1568. doi:10.1211/0022357001777621

Akao, T., Sato, K., He, J. X., Ma, C. M., and Hattori, M. (2013). Baicalein 6-O-β-D-glucopyranuronoside is a main metabolite in the plasma after oral administration of baicalin, a flavone glucuronide of scutellariae radix, to rats. *Biol. Pharm. Bull.* 36 (5), 748–753. doi:10.1248/bpb.b12-00850

Allen, T. C., and Kurdowska, A. (2014). Interleukin 8 and acute lung injury. *Arch. Pathol. Lab. Med.* 138 (2), 266–269. doi:10.5858/arpa.2013-0182-RA

Apps, M. G., Choi, E. H., and Wheate, N. J. (2015). The state-of-play and future of platinum drugs. *Endocr. Relat. Cancer* 22 (4), R219–R233. doi:10.1530/ERC-15-0237

Banno, A., Reddy, A. T., Lakshmi, S. P., and Reddy, R. C. (2020). Bidirectional interaction of airway epithelial remodeling and inflammation in asthma. *Clin. Sci. (Lond)* 134 (9), 1063–1079. doi:10.1042/CS20191309

Barnes, P. J. (2014). Cellular and molecular mechanisms of chronic obstructive pulmonary disease. *Clin. Chest Med.* 35 (1), 71–86. doi:10.1016/j.ccm.2013.10.004

Chang, H., Meng, H. Y., Bai, W. F., and Meng, Q. G. (2021). A metabolomic approach to elucidate the inhibitory effects of baicalin in pulmonary fibrosis. *Pharm. Biol.* 59 (1), 1016–1025. doi:10.1080/13880209.2021.1950192

Chang, Y., Al-Alwan, L., Alshakfa, S., Audusseau, S., Mogas, A. K., Chouiali, F., et al. (2014). Upregulation of IL-17a/F from human lung tissue explants with cigarette smoke exposure: Implications for COPD. *Respir. Res.* 15 (1), 145. doi:10.1186/s12931-014-0145-7

Changle, Z., Cuiling, F., Feng, F., Xiaoqin, Y., Guishu, W., Liangtian, S., et al. (2022). Baicalin inhibits inflammation of lipopolysaccharide-induced acute lung injury toll like receptor-4/myeloid differentiation primary response 88/nuclear factor-kappa B signaling pathway. *J. Tradit. Chin. Med.* 42 (2), 200–212. doi:10.19852/j.cnki.jtcm.20211214.004

Chen, J., Yuan, C. B., Yang, B., and Zhou, X. (2021). Baicalin inhibits EMT through PDK1/AKT signaling in human nonsmall cell lung cancer. *J. Oncol.* 2021, 4391581. doi:10.1155/2021/4391581

Chen, S., Xie, Q., Yang, M., Shi, Y., Shi, J., and Zeng, X. (2022). Scutellaria baicalensis extract-phospholipid complex: Preparation and initial pharmacodynamics research in rats. *Curr. Pharm. Biotechnol.* 23 (6), 847–860. doi:10.2174/1389201022666210729142257

Chen, T. F., Song, L., Gao, Y. H., Li, H., Li, J. L., Hou, H. P., et al. (2022). Pharmacokinetics of baicalin and oroxyloside in plasma and different tissues of rats after transnasal aerosol inhalation and intravenous injection of Tanreqing. *Front. Pharmacol.* 13, 951613. doi:10.3389/fphar.2022.951613

Chen, Y., Minh, L. V., Liu, J., Angelov, B., Drechsler, M., Garamus, V. M., et al. (2016). Baicalin loaded in folate-PEG modified liposomes for enhanced stability and tumor targeting. *Colloids Surf. B Biointerfaces* 140, 74–82. doi:10.1016/j.colsurfb.2015.11.018

Chung, W. J., Park, Y. B., Jeon, C. H., Jung, J. W., Ko, K. P., Choi, S. J., et al. (2015). Baseline characteristics of the Korean registry of pulmonary arterial hypertension. *J. Korean Med. Sci.* 30 (10), 1429–1438. doi:10.3346/jkms.2015.30.10.1429

Crocetti, L., Floresta, G., Cilibrizzi, A., and Giovannoni, M. P. (2022). An overview of PDE4 inhibitors in clinical trials: 2010 to early 2022. *Molecules* 27 (15), 4964. doi:10.3390/molecules27154964

Cui, L., Sune, E., Song, J., Wang, J., Jia, X. B., and Zhang, Z. H. (2016). Characterization and bioavailability study of baicalin-mesoporous carbon nanopowder solid dispersion. *Pharmacogn. Mag.* 12 (48), 326–332. doi:10.4103/0973-1296.192199

Deng, L., Li, S., Zhou, L., Ye, S., and Wang, J., (2022). Protective effect and mechanism of baicalin on lung inflammatory injury in BALB/cJ mice induced by PM2.5. *Ecotoxicol. Environ. Saf.* 248, 114329. doi:10.1016/j.ecoenv.2022.114329

Diao, X., Yang, D., Chen, Y., and Liu, W. (2019). Baicalin suppresses lung cancer growth by targeting PDZ-binding kinase/T-LAK cell-originated protein kinase. *Biosci. Rep.* 39 (4). doi:10.1042/BSR20181692

Fiero, M. H., Roydhouse, J. K., Vallejo, J., King-Kallimanis, B. L., Kluetz, P. G., and Sridhara, R. (2019). US Food and Drug Administration review of statistical analysis of patient-reported outcomes in lung cancer clinical trials approved between January, 2008, and December, 2017. *Lancet Oncol.* 20 (10), e582–e589. doi:10.1016/S1470-2045(19)30335-3

Gandhi, S. R., Quintans, J. D. S. S., Gandhi, G. R., Araujo, A. A. D. S., and Quintans Junior, L. J. (2020). The use of cyclodextrin inclusion complexes to improve anticancer drug profiles: A systematic review. *Expert Opin. Drug Deliv.* 17 (8), 1069–1080. doi:10.1080/17425247.2020.1776261

Ganguly, R., Gupta, A., and Pandey, A. K. (2022). Role of baicalin as a potential therapeutic agent in hepatobiliary and gastrointestinal disorders: A review. *World J. Gastroenterol.* 28 (26), 3047–3062. doi:10.3748/wjg.v28.i26.3047

Gao, J., Teng, L., Yang, S., Huang, S., Li, L., Zhou, L., et al. (2021). MNK as a potential pharmacological target for suppressing LPS-induced acute lung injury in mice. *Biochem. Pharmacol.* 186, 114499. doi:10.1016/j.bcp.2021.114499

Gaucher, G., Dufresne, M. H., Sant, V. P., Kang, N., Maysinger, D., and Leroux, J. C. (2005). Block copolymer micelles: Preparation, characterization and application in drug delivery. *J. Control Release* 109 (1-3), 169–188. doi:10.1016/j.jconrel.2005.09.034

Guo, B., Zuo, Z., Di, X., Huang, Y., Gong, G., Xu, B., et al. (2022). Salidroside attenuates HALI via IL-17A-mediated ferroptosis of alveolar epithelial cells by regulating Act1-TRAF6-p38 MAPK pathway. *Cell Commun. Signal* 20 (1), 183. doi:10.1186/s12964-022-00994-1

Hach, T., Shakeri-Nejad, K., Bigaud, M., Dahlke, F., de Micco, M., Petricoul, O., et al. (2022). Rationale for use of sphingosine-1-phosphate receptor modulators in COVID-19 patients: Overview of scientific evidence. *J. Interferon Cytokine Res.* 2022, 0078. doi:10.1089/jir.2022.0078

Haider, M., Hassan, M. A., Ahmed, I. S., and Shamma, R. (2018). Thermogelling platform for baicalin delivery for versatile biomedical applications. *Mol. Pharm.* 15 (8), 3478–3488. doi:10.1021/acs.molpharmaceut.8b00480

Han, Z., Li, L., Huang, Y., Zhao, H., and Luo, Y. (2021). PBK/TOPK: A therapeutic target worthy of attention. *Cells* 10 (2), 371. doi:10.3390/cells10020371

Hao, D., Li, Y., Shi, J., and Jiang, J. (2021). Baicalin alleviates chronic obstructive pulmonary disease through regulation of HSP72-mediated JNK pathway. *Mol. Med.* 27 (1), 53. doi:10.1186/s10020-021-00309-z

He, L., Thomson, J. M., Hemann, M. T., Hernando-Monge, E., Mu, D., Goodson, S., et al. (2005). A microRNA polycistron as a potential human oncogene. *Nature* 435 (7043), 828–833. doi:10.1038/nature03552

He, Y. Q., Zhou, C. C., Yu, L. Y., Wang, L., Deng, J. L., Tao, Y. L., et al. (2021). Natural product derived phytochemicals in managing acute lung injury by multiple mechanisms. *Pharmacol. Res.* 163, 105224. doi:10.1016/j.phrs.2020.105224

Herrmann, F. E., Wollin, L., and Nickolaus, P. (2022). BI 1015550 is a PDE4B inhibitor and a clinical drug candidate for the oral treatment of idiopathic pulmonary fibrosis. *Front. Pharmacol.* 13, 838449. doi:10.3389/fphar.2022.838449

Hu, Q., Zhang, W., Wu, Z., Tian, X., Xiang, J., Li, L., et al. (2021). Baicalin and the liver-gut system: Pharmacological bases explaining its therapeutic effects. *Pharmacol. Res.* 165, 105444. doi:10.1016/j.phrs.2021.105444

Huang, J., Chen, P. X., Rogers, M. A., and Wettig, S. D. (2019). Investigating the phospholipid effect on the bioaccessibility of rosmarinic acid-phospholipid complex through a dynamic gastrointestinal *in vitro* model. *Pharmaceutics* 11 (4), 156. doi:10.3390/pharmaceutics11040156

Huang, S., Zhai, B., Fan, Y., Sun, J., Cheng, J., Zou, J., et al. (2022). Development of paeonol liposomes: Design, optimization, *in vitro* and *in vivo* evaluation. *Int. J. Nanomedicine* 17, 5027–5046. doi:10.2147/IJN.S363135

Huang, X., He, Y., Chen, Y., Wu, P., Gui, D., Cai, H., et al. (2016). Baicalin attenuates bleomycin-induced pulmonary fibrosis via adenosine A2a receptor related TGF-β1-induced ERK1/2 signaling pathway. *BMC Pulm. Med.* 16 (1), 132. doi:10.1186/s12890-016-0294-1

Huang, X., Wu, P., Huang, F., Xu, M., Chen, M., Huang, K., et al. (2017). Baicalin attenuates chronic hypoxia-induced pulmonary hypertension via adenosine A(2A) receptor-induced SDF-1/CXCR4/PI3K/AKT signaling. *J. Biomed. Sci.* 24 (1), 52. doi:10.1186/s12929-017-0359-3

Ishihara, M., Homma, M., Kuno, E., Watanabe, M., and Kohda, Y. (2002). [Combination use of kampo-medicines and drugs affecting intestinal bacterial flora]. *Yakugaku Zasshi* 122 (9), 695–701. doi:10.1248/yakushi.122.695

Jin, X., Liu, M. Y., Zhang, D. F., Zhong, X., Du, K., Qian, P., et al. (2019). Baicalin mitigates cognitive impairment and protects neurons from microglia-mediated neuroinflammation via suppressing NLRP3 inflammasomes and TLR4/NF-κB signaling pathway. *CNS Neurosci. Ther.* 25 (5), 575–590. doi:10.1111/cns.13086

Jing, H., Wu, X., Xiang, M., Liu, L., Novakovic, V. A., and Shi, J. (2022). Pathophysiological mechanisms of thrombosis in acute and long COVID-19. *Front. Immunol.* 13, 992384. doi:10.3389/fimmu.2022.992384

Jones, B., Donovan, C., Liu, G., Gomez, H. M., Chimankar, V., Harrison, C. L., et al. (2017). Animal models of COPD: What do they tell us? *Respirology* 22 (1), 21–32. doi:10.1111/resp.12908

Ju, J., Li, Z., and Shi, Q. (2022). Baicalin inhibits inflammation in rats with chronic obstructive pulmonary disease by the TLR2/MYD88/NF-κBp65 signaling pathway. *Evid. Based Complement. Altern. Med.* 2022, 7273387. doi:10.1155/2022/7273387

Kciuk, M., Mujwar, S., Rani, I., Munjal, K., Gielecińska, A., Kontek, R., et al. (2022). Computational bioprospecting guggulsterone against ADP ribose phosphatase of SARS-CoV-2. *Molecules* 27 (23), 8287. doi:10.3390/molecules27238287

King, T. E., Jr., Pardo, A., and Selman, M. (2011). Idiopathic pulmonary fibrosis. *Lancet* 378 (9807), 1949–1961. doi:10.1016/S0140-6736(11)60052-4

Kumar, A., Cherian, S. V., Vassallo, R., Yi, E. S., and Ryu, J. H. (2018). Current concepts in pathogenesis, diagnosis, and management of smoking-related interstitial lung diseases. *Chest* 154 (2), 394–408. doi:10.1016/j.chest.2017.11.023

Labaki, W. W., and Rosenberg, S. R. (2020). Chronic obstructive pulmonary disease. *Ann. Intern Med.* 173 (3), Itc17–itc32. doi:10.7326/AITC202008040

Lee, Y. S., and Dutta, A. (2007). The tumor suppressor microRNA let-7 represses the HMGA2 oncogene. *Genes Dev.* 21 (9), 1025–1030. doi:10.1101/gad.1540407

Lei, B., Liu, S., Qi, W., Zhao, Y., Li, Y., Lin, N., et al. (2013). PBK/TOPK expression in non-small-cell lung cancer: Its correlation and prognostic significance with Ki67 and p53 expression. *Histopathology* 63 (5), 696–703. doi:10.1111/his.12215

Letko, M., Marzi, A., and Munster, V. (2020). Functional assessment of cell entry and receptor usage for SARS-CoV-2 and other lineage B betacoronaviruses. *Nat. Microbiol.* 5 (4), 562–569. doi:10.1038/s41564-020-0688-y

Li, B., He, M., Li, W., Luo, Z., Guo, Y., Li, Y., et al. (2013). Dissolution and pharmacokinetics of baicalin-polyvinylpyrrolidone coprecipitate. *J. Pharm. Pharmacol.* 65 (11), 1670–1678. doi:10.1111/jphp.12146

Li, J., Jiang, Q., Deng, P., Chen, Q., Yu, M., Shang, J., et al. (2017). The formation of a host-guest inclusion complex system between β-cyclodextrin and baicalin and its dissolution characteristics. *J. Pharm. Pharmacol.* 69 (6), 663–674. doi:10.1111/jphp.12708

Li, J., Zhang, M., Chao, J., and Shuang, S. (2009). Preparation and characterization of the inclusion complex of baicalin (BG) with beta-CD and HP-beta-CD in solution: An antioxidant ability study. *Spectrochim. Acta A Mol. Biomol. Spectrosc.* 73 (4), 752–756. doi:10.1016/j.saa.2009.03.025

Li, L., Liu, Q., Shi, L., Zhou, X., Wu, W., Wang, X., et al. (2022). Baicalin prevents fibrosis of human trabecular meshwork cells via inhibiting the MyD88/NF-κB pathway. *Eur. J. Pharmacol.* 938, 175425. doi:10.1016/j.ejphar.2022.175425

Li, M. H., Huang, K. L., Wu, S. Y., Chen, C. W., Yan, H. C., Hsu, K., et al. (2009). Baicalin attenuates air embolism-induced acute lung injury in rat isolated lungs. *Br. J. Pharmacol.* 157 (2), 244–251. doi:10.1111/j.1476-5381.2009.00139.x

Liu, J., Wei, Y., Luo, Q., Xu, F., Zhao, Z., Zhang, H., et al. (2016). Baicalin attenuates inflammation in mice with OVA-induced asthma by inhibiting NF-κB and suppressing CCR7/CCL19/CCL21. *Int. J. Mol. Med.* 38 (5), 1541–1548. doi:10.3892/ijmm.2016.2743

Liu, T., Dai, W., Liu, F., Chen, Y., and Weng, D., (2015). Baicalin alleviates silica-induced lung inflammation and fibrosis by inhibiting the Th17 response in C57bl/6 mice. *J. Nat. Prod.* 78 (12), 3049–3057. doi:10.1021/acs.jnatprod.5b00868

Liu, Y., Xiang, D., Zhang, H., Yao, H., and Wang, Y. (2020). Hypoxia-inducible factor-1: A potential target to treat acute lung injury. *Oxid. Med. Cell Longev.* 2020, 8871476. doi:10.1155/2020/8871476

Lixuan, Z., Jingcheng, D., Wenqin, Y., Jianhua, H., Baojun, L., and Xiaotao, F. (2010). Baicalin attenuates inflammation by inhibiting NF-kappaB activation in cigarette smoke induced inflammatory models. *Pulm. Pharmacol. Ther.* 23 (5), 411–419. doi:10.1016/j.pupt.2010.05.004

Long, Y., Xiang, Y., Liu, S., Zhang, Y., Wan, J., Yang, Q., et al. (2020). Baicalin liposome alleviates lipopolysaccharide-induced acute lung injury in mice via inhibiting TLR4/JNK/ERK/NF-κB pathway. *Mediat. Inflamm.* 2020, 8414062. doi:10.1155/2020/8414062

Lu, J., Zhong, Y., Lin, Z., Lin, X., Chen, Z., Wu, X., et al. (2017). Baicalin alleviates radiation-induced epithelial-mesenchymal transition of primary type II alveolar epithelial cells via TGF-β and ERK/GSK3β signaling pathways. *Biomed. Pharmacother.* 95, 1219–1224. doi:10.1016/j.biopha.2017.09.037

Lu, T., Song, J., Huang, F., Deng, Y., Xie, L., Wang, G., et al. (2007). Comparative pharmacokinetics of baicalin after oral administration of pure baicalin, Radix scutellariae extract and Huang-Lian-Jie-Du-Tang to rats. *J. Ethnopharmacol.* 110 (3), 412–418. doi:10.1016/j.jep.2006.09.036

Luan, Y., Chao, S., Ju, Z. Y., Wang, J., Xue, X., Qi, T. G., et al. (2015). Therapeutic effects of baicalin on monocrotaline-induced pulmonary arterial hypertension by inhibiting inflammatory response. *Int. Immunopharmacol.* 26 (1), 188–193. doi:10.1016/j.intimp.2015.01.009

Ma, C., Ma, Z., and Fu, Q. (2014). Anti-asthmatic effects of baicalin in a mouse model of allergic asthma. *Phytother. Res.* 28 (2), 231–237. doi:10.1002/ptr.4983

Meng, X., Hu, L., and Li, W. (2019). Baicalin ameliorates lipopolysaccharide-induced acute lung injury in mice by suppressing oxidative stress and inflammation via the activation of the Nrf2-mediated HO-1 signaling pathway. *Naunyn Schmiedeb. Arch. Pharmacol.* 392 (11), 1421–1433. doi:10.1007/s00210-019-01680-9

Murali, M., Gowtham, H. G., Shilpa, N., Krishnappa, H. K. N., Ledesma, A. E., Jain, A. S., et al. (2022). Exploration of anti-HIV phytocompounds against SARS-CoV-2 main protease: Structure-based screening, molecular simulation, ADME analysis and conceptual DFT studies. *Molecules* 27 (23), 8288. doi:10.3390/molecules27238288

Olin, J. T., and Wechsler, M. E. (2014). Asthma: Pathogenesis and novel drugs for treatment. *Bmj* 349, g5517. doi:10.1136/bmj.g5517

Pagès, L., Gavaldà, A., and Lehner, M. D. (2009). PDE4 inhibitors: A review of current developments (2005 - 2009). *Expert Opin. Ther. Pat.* 19 (11), 1501–1519. doi:10.1517/13543770903313753

Pan, L., Cho, K. S., Yi, I., To, C. H., Chen, D. F., and Do, C. W. (2021). Baicalein, baicalin, and wogonin: Protective effects against ischemia-induced neurodegeneration in the brain and retina. *Oxid. Med. Cell Longev.* 2021, 8377362. doi:10.1155/2021/8377362

Pan, X., Chen, Y., Shen, Y., and Tantai, J. (2019). Knockdown of TRIM65 inhibits autophagy and cisplatin resistance in A549/DDP cells by regulating miR-138-5p/ATG7. *Cell Death Dis.* 10 (6), 429. doi:10.1038/s41419-019-1660-8

Pangeni, R., Panthi, V. K., Yoon, I. S., and Park, J. W. (2018). Preparation, characterization, and *in vivo* evaluation of an oral multiple nanoemulsive system for Co-delivery of pemetrexed and quercetin. *Pharmaceutics* 10 (3), 158. doi:10.3390/pharmaceutics10030158

Park, K., Lee, J. S., Choi, J. S., Nam, Y. J., Han, J. H., Byun, H. D., et al. (2016). Identification and characterization of baicalin as a phosphodiesterase 4 inhibitor. *Phytother. Res.* 30 (1), 144–151. doi:10.1002/ptr.5515

Peng, L. Y., Yuan, M., Song, K., Yu, J. L., Li, J. H., Huang, J. N., et al. (2019). Baicalin alleviated APEC-induced acute lung injury in chicken by inhibiting NF-κB pathway activation. *Int. Immunopharmacol.* 72, 467–472. doi:10.1016/j.intimp.2019.04.046

Pramual, S., Lirdprapamongkol, K., Atjanasuppat, K., Chaisuriya, P., Niamsiri, N., and Svasti, J. (2022). PLGA-lipid hybrid nanoparticles for overcoming paclitaxel tolerance in anoikis-resistant lung cancer cells. *Molecules* 27 (23), 8295. doi:10.3390/molecules27238295

Ptasinski, V. A., Stegmayr, J., Belvisi, M. G., Wagner, D. E., and Murray, L. A. (2021). Targeting alveolar repair in idiopathic pulmonary fibrosis. *Am. J. Respir. Cell Mol. Biol.* 65 (4), 347–365. doi:10.1165/rcmb.2020-0476TR

Qian, W., Cai, X., Qian, Q., Zhang, W., and Wang, D. (2018). Astragaloside IV modulates TGF-β1-dependent epithelial-mesenchymal transition in bleomycin-induced pulmonary fibrosis. *J. Cell Mol. Med.* 22 (9), 4354–4365. doi:10.1111/jcmm.13725

Qin, L., Niu, Y., Wang, Y., and Chen, X. (2018). Combination of phospholipid complex and submicron emulsion techniques for improving oral bioavailability and therapeutic efficacy of water-insoluble drug. *Mol. Pharm.* 15 (3), 1238–1247. doi:10.1021/acs.molpharmaceut.7b01061

Ramedani, A., Sabzevari, O., and Simchi, A. (2022). Hybrid ultrasound-activated nanoparticles based on graphene quantum dots for cancer treatment. *Int. J. Pharm.* 629, 122373. doi:10.1016/j.ijpharm.2022.122373

Salawi, A. (2022). Self-emulsifying drug delivery systems: A novel approach to deliver drugs. *Drug Deliv.* 29 (1), 1811–1823. doi:10.1080/10717544.2022.2083724

Saman, H., Raza, A., Patil, K., Uddin, S., and Crnogorac-Jurcevic, T. (2022). Non-invasive biomarkers for early lung cancer detection. *Cancers (Basel)* 14 (23), 5782. doi:10.3390/cancers14235782

Shang, X., He, X., He, X., Li, M., Zhang, R., Fan, P., et al. (2010). The genus Scutellaria an ethnopharmacological and phytochemical review. *J. Ethnopharmacol.* 128 (2), 279–313. doi:10.1016/j.jep.2010.01.006

Sharif, R. (2017). Overview of idiopathic pulmonary fibrosis (IPF) and evidence-based guidelines. *Am. J. Manag. Care* 23, S176–s182.

Shevtsova, Y. A., Goryunov, K. V., Babenko, V. A., Pevzner, I. B., Vtorushina, V. V., Inviyaeva, E. V., et al. (2022). Development of an *in vitro* model of SARS-CoV-induced acute lung injury for studying new therapeutic approaches. *Antioxidants (Basel)* 11 (10), 1910. doi:10.3390/antiox11101910

Siddik, Z. H. (2003). Cisplatin: Mode of cytotoxic action and molecular basis of resistance. *Oncogene* 22 (47), 7265–7279. doi:10.1038/sj.onc.1206933

Song, X., Gong, Z., Liu, K., Kou, J., Liu, B., and Liu, K. (2020). Baicalin combats glutamate excitotoxicity via protecting glutamine synthetase from ROS-induced 20S proteasomal degradation. *Redox Biol.* 34, 101559. doi:10.1016/j.redox.2020.101559

South, A. M., Brady, T. M., and Flynn, J. T. (2020). ACE2 (Angiotensin-Converting enzyme 2), COVID-19, and ACE inhibitor and Ang II (angiotensin II) receptor blocker use during the pandemic: The pediatric perspective. *Hypertension* 76 (1), 16–22. doi:10.1161/HYPERTENSIONAHA.120.15291

Sui, X., Han, X., Chen, P., Wu, Q., Feng, J., Duan, T., et al. (2020). Baicalin induces apoptosis and suppresses the cell cycle progression of lung cancer cells through downregulating akt/mTOR signaling pathway. *Front. Mol. Biosci.* 7, 602282. doi:10.3389/fmolb.2020.602282

Sun, J., Li, L., Wu, J., Liu, B., Gong, W., Lv, Y., et al. (2013). Effects of baicalin on airway remodeling in asthmatic mice. *Planta Med.* 79 (3-4), 199–206. doi:10.1055/s-0032-1328197

Taiming, L., and Xuehua, J. (2006). Investigation of the absorption mechanisms of baicalin and baicalein in rats. *J. Pharm. Sci.* 95 (6), 1326–1333. doi:10.1002/jps.20593

Teng, Y., Nian, H., Zhao, H., Chen, P., and Wang, G. (2013). Biotransformation of baicalin to baicalein significantly strengthens the inhibition potential towards UDP-glucuronosyltransferases (UGTs) isoforms. *Pharmazie* 68 (9), 763–767.

Ullah, I., Yang, L., Yin, F. T., Sun, Y., Li, X. H., Li, J., et al. (2022). Multi-omics approaches in colorectal cancer screening and diagnosis, recent updates and future perspectives. *Cancers (Basel)* 14 (22), 5545. doi:10.3390/cancers14225545

Vasconcelos, T., Sarmento, B., and Costa, P. (2007). Solid dispersions as strategy to improve oral bioavailability of poor water soluble drugs. *Drug Discov. Today* 12 (23-24), 1068–1075. doi:10.1016/j.drudis.2007.09.005

Venkatesan, N., Punithavathi, D., and Babu, M. (2007). Protection from acute and chronic lung diseases by curcumin. *Adv. Exp. Med. Biol.* 595, 379–405. doi:10.1007/978-0-387-46401-5_17

von Karstedt, S., Montinaro, A., and Walczak, H. (2017). Exploring the TRAILs less travelled: TRAIL in cancer biology and therapy. *Nat. Rev. Cancer* 17 (6), 352–366. doi:10.1038/nrc.2017.28

Wang, B., Zhang, W., Zhou, X., Liu, M., Hou, X., Cheng, Z., et al. (2019). Development of dual-targeted nano-dandelion based on an oligomeric hyaluronic acid polymer targeting tumor-associated macrophages for combination therapy of non-small cell lung cancer. *Drug Deliv.* 26 (1), 1265–1279. doi:10.1080/10717544.2019.1693707

Wang, C. Z., Zhang, C. F., Luo, Y., Yao, H., Yu, C., Chen, L., et al. (2020). Baicalein, an enteric microbial metabolite, suppresses gut inflammation and cancer progression in Apc(Min/+) mice. *Clin. Transl. Oncol.* 22 (7), 1013–1022. doi:10.1007/s12094-019-02225-5

Wang, M., You, S. K., Lee, H. K., Han, M. G., Lee, H. M., Pham, T. M. A., et al. (2020). Development and evaluation of docetaxel-phospholipid complex loaded self-microemulsifying drug delivery system: Optimization and *in vitro*/*ex vivo* studies. *Pharmaceutics* 12 (6), 544. doi:10.3390/pharmaceutics12060544

Wei, X., Zhu, X., Hu, N., Zhang, X., Sun, T., Xu, J., et al. (2015). Baicalin attenuates angiotensin II-induced endothelial dysfunction. *Biochem. Biophys. Res. Commun.* 465 (1), 101–107. doi:10.1016/j.bbrc.2015.07.138

Wei, Y., Guo, J., Zheng, X., Wu, J., Zhou, Y., Yu, Y., et al. (2014). Preparation, pharmacokinetics and biodistribution of baicalin-loaded liposomes. *Int. J. Nanomedicine* 9, 3623–3630. doi:10.2147/IJN.S66312

Wei, Y., Liang, J., Zheng, X., Liu, H., and Yang, H., (2017). Lung-targeting drug delivery system of baicalin-loaded nanoliposomes: Development, biodistribution in rabbits, and pharmacodynamics in nude mice bearing orthotopic human lung cancer. *Int. J. Nanomedicine* 12, 251–261. doi:10.2147/IJN.S119895

Wei, Y., Pi, C., Yang, G., Xiong, X., Lan, Y., Yang, H., et al. (2016). LC-UV determination of baicalin in rabbit plasma and tissues for application in pharmacokinetics and tissue distribution studies of baicalin after intravenous administration of liposomal and injectable formulations. *Molecules* 21 (4), 444. doi:10.3390/molecules21040444

Wu, H., Long, X., Yuan, F., Chen, L., Pan, S., Liu, Y., et al. (2014). Combined use of phospholipid complexes and self-emulsifying microemulsions for improving the oral absorption of a BCS class IV compound, baicalin. *Acta Pharm. Sin. B* 4 (3), 217–226. doi:10.1016/j.apsb.2014.03.002

Wu, L., Bi, Y., and Wu, H. (2018). Formulation optimization and the absorption mechanisms of nanoemulsion in improving baicalin oral exposure. *Drug Dev. Ind. Pharm.* 44 (2), 266–275. doi:10.1080/03639045.2017.1391831

Xia, Y., Wu, Y., Liu, B., Wang, P., and Chen, Y. (2014). Downregulation of miR-638 promotes invasion and proliferation by regulating SOX2 and induces EMT in NSCLC. *FEBS Lett.* 588 (14), 2238–2245. doi:10.1016/j.febslet.2014.05.002

Xie, Y., Hu, F., Xiang, D., Lu, H., Li, W., Zhao, A., et al. (2020). The metabolic effect of gut microbiota on drugs. *Drug Metab. Rev.* 52 (1), 139–156. doi:10.1080/03602532.2020.1718691

Xin, L., Gao, J., Lin, H., Qu, Y., Shang, C., Wang, Y., et al. (2020). Regulatory mechanisms of baicalin in cardiovascular diseases: A review. *Front. Pharmacol.* 11, 583200. doi:10.3389/fphar.2020.583200

Xing, J., Chen, X., and Zhong, D. (2005). Absorption and enterohepatic circulation of baicalin in rats. *Life Sci.* 78 (2), 140–146. doi:10.1016/j.lfs.2005.04.072

Xu, D., Hu, Y. H., Gou, X., Li, F. Y., Yang, X. Y. C., Li, Y. M., et al. (2022). Oxidative stress and antioxidative therapy in pulmonary arterial hypertension. *Molecules* 27 (12), 3724. doi:10.3390/molecules27123724

Xu, L., Li, J., Zhang, Y., Zhao, P., and Zhang, X. (2017). Regulatory effect of baicalin on the imbalance of Th17/Treg responses in mice with allergic asthma. *J. Ethnopharmacol.* 208, 199–206. doi:10.1016/j.jep.2017.07.013

Xu, W., Niu, Y., Ai, X., Xia, C., Geng, P., Zhu, H., et al. (2022). Liver-targeted nanoparticles facilitate the bioavailability and anti-HBV efficacy of baicalin *in vitro* and *in vivo*. *Biomedicines* 10 (4), 900. doi:10.3390/biomedicines10040900

Xu, Z., Mei, J., and Tan, Y. (2017). Baicalin attenuates DDP (cisplatin) resistance in lung cancer by downregulating MARK2 and p-Akt. *Int. J. Oncol.* 50 (1), 93–100. doi:10.3892/ijo.2016.3768

Xue, X., Zhang, S., Jiang, W., Wang, J., Xin, Q., Sun, C., et al. (2021). Protective effect of baicalin against pulmonary arterial hypertension vascular remodeling through regulation of TNF-α signaling pathway. *Pharmacol. Res. Perspect.* 9 (1), e00703. doi:10.1002/prp2.703

Yamamoto, T., Katsuta, Y., Sato, K., Tsukita, Y., Umezawa, R., Takahashi, N., et al. (2022). Longitudinal analyses and predictive factors of radiation-induced lung toxicity-related parameters after stereotactic radiotherapy for lung cancer. *PLoS One* 17 (12), e0278707. doi:10.1371/journal.pone.0278707

Yan, G., Wang, J., Yi, T., Cheng, J., Guo, H., He, Y., et al. (2019). Baicalin prevents pulmonary arterial remodeling *in vivo* via the AKT/ERK/NF-κB signaling pathways. *Pulm. Circ.* 9 (4), 2045894019878599. doi:10.1177/2045894019878599

Yan, S., Wang, Y., Liu, P., Chen, A., Chen, M., Yao, D., et al. (2016). Baicalin attenuates hypoxia-induced pulmonary arterial hypertension to improve hypoxic cor pulmonale by reducing the activity of the p38 MAPK signaling pathway and MMP-9. *Evid. Based Complement. Altern. Med.* 2016, 2546402. doi:10.1155/2016/2546402

Yasuda, Y., Nagano, T., Kobayashi, K., and Nishimura, Y. (2020). Group 2 innate lymphoid cells and the house dust mite-induced asthma mouse model. *Cells* 9 (5), 1178. doi:10.3390/cells9051178

You, J., Cheng, J., Yu, B., Duan, C., and Peng, J. (2018). Baicalin, a Chinese herbal medicine, inhibits the proliferation and migration of human non-small cell lung

carcinoma (NSCLC) cells, A549 and H1299, by activating the SIRT1/AMPK signaling pathway. *Med. Sci. Monit.* 24, 2126–2133. doi:10.12659/msm.909627

You, J., Li, H., Fan, P., Yang, X., Wei, Y., Zheng, L., et al. (2022). Inspiration for COVID-19 treatment: Network analysis and experimental validation of baicalin for cytokine storm. *Front. Pharmacol.* 13, 853496. doi:10.3389/fphar.2022.853496

Yue, P. F., Li, Y., Wan, J., Wang, Y., Yang, M., Zhu, W. F., et al. (2013). Process optimization and evaluation of novel baicalin solid nanocrystals. *Int. J. Nanomedicine* 8, 2961–2973. doi:10.2147/IJN.S44924

Zandi, K., Musall, K., Oo, A., Cao, D., Liang, B., Hassandarvish, P., et al. (2021). Baicalein and baicalin inhibit SARS-CoV-2 RNA-dependent-RNA polymerase. *Microorganisms* 9 (5), 893. doi:10.3390/microorganisms9050893

Zeng, W., Liu, X., Wu, Y., Cai, Y., Li, Z., Ye, F., et al. (2022). Dysregulated hepatic UDP-glucuronosyltransferases and flavonoids glucuronidation in experimental colitis. *Front. Pharmacol.* 13, 1053610. doi:10.3389/fphar.2022.1053610

Zhang, H., Liu, B., Jiang, S., Wu, J. F., Qi, C. H., Mohammadtursun, N., et al. (2021). Baicalin ameliorates cigarette smoke-induced airway inflammation in rats by modulating HDAC2/NF-κB/PAI-1 signalling. *Pulm. Pharmacol. Ther.* 70, 102061. doi:10.1016/j.pupt.2021.102061

Zhang, H., Yang, X., Zhao, L., Jiao, Y., Liu, J., and Zhai, G. (2016). In vitro and in vivo study of Baicalin-loaded mixed micelles for oral delivery. *Drug Deliv.* 23 (6), 1933–1939. doi:10.3109/10717544.2015.100870

Zhang, H., Zhao, L., Chu, L., Han, X., and Zhai, G. (2014). Preparation, optimization, characterization and cytotoxicity *in vitro* of Baicalin-loaded mixed micelles. *J. Colloid Interface Sci.* 434, 40–47. doi:10.1016/j.jcis.2014.07.045

Zhang, J., Cai, W., Zhou, Y., Liu, Y., Wu, X., Li, Y., et al. (2015). Profiling and identification of the metabolites of baicalin and study on their tissue distribution in rats by ultra-high-performance liquid chromatography with linear ion trap-Orbitrap mass spectrometer. *J. Chromatogr. B Anal. Technol. Biomed. Life Sci.* 985, 91–102. doi:10.1016/j.jchromb.2015.01.018

Zhang, J., Zhou, Y., Gu, H., Tang, H., and Rong, Q., (2020). LncRNA-AK149641 associated with airway inflammation in an OVA-induced asthma mouse model. *J. Bioenerg. Biomembr.* 52 (5), 355–365. doi:10.1007/s10863-020-09844-6

Zhang, L., Lin, G., and Zuo, Z. (2007). Involvement of UDP-glucuronosyltransferases in the extensive liver and intestinal first-pass metabolism of flavonoid baicalein. *Pharm. Res.* 24 (1), 81–89. doi:10.1007/s11095-006-9126-y

Zhang, L., Wang, X., Wang, R., Zheng, X., and Li, H., (2017). Baicalin potentiates TRAIL-induced apoptosis through p38 MAPK activation and intracellular reactive oxygen species production. *Mol. Med. Rep.* 16 (6), 8549–8555. doi:10.3892/mmr.2017.7633

Zhao, F., Zhao, Z., Han, Y., Li, S., Liu, C., and Jia, K. (2021). Baicalin suppresses lung cancer growth phenotypes via miR-340-5p/NET1 axis. *Bioengineered* 12 (1), 1699–1707. doi:10.1080/21655979.2021.1922052

Zhao, H., Li, L., Liu, J., Gao, Y., and Mu, K., (2020). Baicalin alleviates bleomycin-induced pulmonary fibrosis and fibroblast proliferation in rats via the PI3K/AKT signaling pathway. *Mol. Med. Rep.* 21 (6), 2321–2334. doi:10.3892/mmr.2020.11046

Zhao, L., Wei, Y., Huang, Y., He, B., Zhou, Y., and Fu, J. (2013). Nanoemulsion improves the oral bioavailability of baicalin in rats: *In vitro* and *in vivo* evaluation. *Int. J. Nanomedicine* 8, 3769–3779. doi:10.2147/IJN.S51578

Glossary

ACE2 angiotensin-converting enzyme-2
AECs alveolar epithelial cells
ALI acute lung injury
AMPK adenosine monophosphate-activated protein kinase
Ang II angiotensin II
AUC plasma drug concentration-time curve
BA Baicalin
BE Baicalein
BLM bleomycin
BMPR2 bone morphogenetic protein receptor 2
CAT catalase
CCR CC-chemokine receptor
CCL C-C chemokine ligand
C_{max} maximum serum concentration
COPD chronic obstructive pulmonary disease
COVID-19 coronary viral disease-2019
CS cytokine storm
DDP cisplatin
DDSs drug delivery systems
EMT Epithelial-mesenchymal transition
ERK extracellular signal-regulated kinase
GM-CSF Granulocyte-macrophage colony stimulating factor
HO-1 heme oxygenase-1
HSP72 heat shock protein 72
i.g. intragastric gavage
i.p. intraperitoneal
IgE immunoglobulin E
IL interleukin
JNK c-Jun N-terminal kinases
L-BA BA liposome
LC lung cancer
LPS lipopolysaccharide
MAPK mitogen-activated protein kinase
MCN mesoporous carbon nanopowder
MCT monocrotaline
MDA malondialdehyde
MMP matrix metalloprotein
mTOR mechanistic target of rapamycin
MyD88 myeloid differentiation factor 88
NF-κB nuclear factor-kappa B
NLRP3 nod-like receptor pyrin containing 3
Nrf2 nuclear erythroid factor 2
NSCLC Non-small cell lung cancer
OVA ovalbumin
PAH pulmonary arterial hypertension
PAI-1 plasminogen activator inhibitor-1
PBK/TOPK PDZ-binding kinase/T-LAK cell-originated protein kinase
PDE4 phosphodiesterase 4
PF pulmonary fibrosis
PI3K Phosphoinositide 3-kinase
SARS-CoV-2 severe acute respiratory syndrome coronavirus 2
SBG Scutellaria baicalensis Georgi
SEDDS self-emulsifying drug delivery systems
SIRT1 sirtuin 1
SOD superoxide dismutase
TCM traditional Chinese medicine
TGF-β transforming growth factor-β
TLR4 Toll Like Receptor 4
TNF-α tumor necrosis factor-α
TRAIL Tumor necrosis factor-related apoptosis-inducing ligand
UGT UDP-glucuronosyltransferase
VEGF vascular endothelial growth factor
β-CD β-cyclodextrin

frontiers | Frontiers in Pharmacology

TYPE Original Research
PUBLISHED 24 April 2023
DOI 10.3389/fphar.2023.1145994

OPEN ACCESS

EDITED BY
Poonam Arora,
Shree Guru Gobind Singh Tricentenary University, India

REVIEWED BY
Krishna C. Penumatsa,
Tufts University, United States
Ramon Jose Ayon,
University of Virginia, United States

*CORRESPONDENCE
Isabel Blanco,
iblanco2@clinic.cat

†PRESENT ADDRESS
Maribel Marquina,
Faculty of Health Sciences, Valencian International University (VIU), Valencia, Spain

RECEIVED 16 January 2023
ACCEPTED 11 April 2023
PUBLISHED 24 April 2023

CITATION
Blanco I, Marquina M, Tura-Ceide O, Ferrer E, Ramírez AM, Lopez-Meseguer M, Callejo M, Perez-Vizcaino F, Peinado VI and Barberà JA (2023), Survivin inhibition with YM155 ameliorates experimental pulmonary arterial hypertension. *Front. Pharmacol.* 14:1145994. doi: 10.3389/fphar.2023.1145994

Survivin inhibition with YM155 ameliorates experimental pulmonary arterial hypertension

Isabel Blanco[1,2,3]*, Maribel Marquina[3†], Olga Tura-Ceide[1,2,3,4], Elisabet Ferrer[1,2,5], Ana M. Ramírez[1], Manuel Lopez-Meseguer[6], Maria Callejo[3,7], Francisco Perez-Vizcaino[3,7], Victor Ivo Peinado[1,2,3,8] and Joan Albert Barberà[1,2,3]

[1]Department of Pulmonary Medicine, Hospital Clínic-University of Barcelona, Barcelona, Spain, [2]Institut d'Investigacions Biomèdiques August Pi i Sunyer (IDIBAPS), Barcelona, Spain, [3]Biomedical Research Networking Center on Respiratory Diseases (CIBERES), Madrid, Spain, [4]Biomedical Research Institute-IDIBGI, Girona, Spain, [5]Department of Medicine, Addenbrooke's Hospital, University of Cambridge, Cambridge, United Kingdom, [6]Department of Pulmonary Medicine, Hospital Vall d'Hebron, Barcelona, Spain, [7]Departament of Pharmacology and Toxicology, School of Medicine, Instituto de Investigación Sanitaria Gregorio Marañón (IISGM), Universidad Complutense de Madrid, Madrid, Spain, [8]Department of Experimental Pathology, Institut d'Investigacions Biomèdiques de Barcelona (IIBB-CSIC), Barcelona, Spain

Background: Imbalance between cell proliferation and apoptosis underlies the development of pulmonary arterial hypertension (PAH). Current vasodilator treatment of PAH does not target the uncontrolled proliferative process in pulmonary arteries. Proteins involved in the apoptosis pathway may play a role in PAH and their inhibition might represent a potential therapeutic target. Survivin is a member of the apoptosis inhibitor protein family involved in cell proliferation.

Objectives: This study aimed to explore the potential role of survivin in the pathogenesis of PAH and the effects of its inhibition.

Methods: In SU5416/hypoxia-induced PAH mice we assessed the expression of survivin by immunohistochemistry, western-blot analysis, and RT-PCR; the expression of proliferation-related genes (Bcl2 and Mki67); and the effects of the survivin inhibitor YM155. In explanted lungs from patients with PAH we assessed the expression of survivin, BCL2 and MKI67.

Results: SU5416/hypoxia mice showed increased expression of survivin in pulmonary arteries and lung tissue extract, and upregulation of survivin, Bcl2 and Mki67 genes. Treatment with YM155 reduced right ventricle (RV) systolic pressure, RV thickness, pulmonary vascular remodeling, and the expression of survivin, Bcl2, and Mki67 to values similar to those in control animals. Lungs of patients with PAH also showed increased expression of survivin in pulmonary arteries and lung extract, and also that of BCL2 and MKI67 genes, compared with control lungs.

Abbreviations: Akt, protein kinase B; EC, endothelial cells; ERK, extracellular signal-regulated kinases; LV, left ventricle; MCT-PAH, monocrotaline-induced PAH model; PAH, pulmonary arterial hypertension; PASMC, pulmonary artery smooth muscle cells; PI3-K, phosphoinositide 3-kinase; RV, right ventricle; RVSP, right ventricle systolic pressure; SMA, smooth muscle α-actin; SU-Hx, SU5416, hypoxia; SU-Hx-YM155, SU5416, hypoxia and YM155; VEGF, vascular endothelial growth factor; Veh-Nx, vehicle, normoxia; YM155, sepantronium bromide; YM155-Nx, vehicle, normoxia and YM155.

Conclusion: We conclude that survivin might be involved in the pathogenesis of PAH and that its inhibition with YM155 might represent a novel therapeutic approach that warrants further evaluation.

KEYWORDS

pulmonary circulation, animal model, hypoxia, SU5416, YM155, pathway

Introduction

Pulmonary arterial hypertension (PAH) is a rare form of pulmonary hypertension that affects small pulmonary arteries. It is characterized by thickened vessel walls that gradually obliterate the arterial lumen and increase pulmonary vascular resistance, which may evolve to right ventricular failure and eventually death (Galiè et al., 2009; Humbert et al., 2010; Galiè et al., 2016).

Vascular remodeling in PAH is mainly characterized by a pro-proliferative and anti-apoptotic phenotype with some similarities to cancer, with sustained increase in proliferation of pulmonary artery smooth muscle cells (PASMC) and endothelial cells (EC), and resistance to apoptosis in vascular cells (Morrell et al., 2001). Since the imbalance between cell proliferation and apoptosis underlie the development of PAH, proteins involved in the apoptosis pathway may play a role in PAH. Survivin (encoded by BIRC5 gene) is a 16.5-kDa member of the inhibitor of apoptosis protein family. It is highly expressed in cancer cells and its expression is associated with tumor progression, proliferation, induction of anticancer drug resistance and poor prognosis (Duffy et al., 2007). Survivin is also expressed in pulmonary arteries of patients with PAH, but not in subjects without PAH (McMurtry et al., 2005), as well as in PASM cells of the monocrotaline-induced PAH model (MCT-PAH) in rats (McMurtry et al., 2005; Lao et al., 2016).

Considering that the survivin signaling pathway plays a fundamental role in cell proliferation and division, it has been proposed that it could contribute to the development of PAH (Blanc-Brude et al., 2002; McMurtry et al., 2005). *In vitro* studies have demonstrated that the inhibition of survivin induces apoptosis and reduces the proliferation of PASM cells (Ai et al., 2006; Ye et al., 2022). McMurtry *et. al.* (McMurtry et al., 2005) also reported that gene therapy with a phosphorylation deficient survivin mutant lowered pulmonary vascular resistance, right ventricular hypertrophy and pulmonary artery medial hypertrophy, and prolonged the survival time in MCT-induced PAH rats. Importantly, serum levels of survivin have been used as biomarkers to assess the operability in patients with congenital heart disease with severe PAH (Li et al., 2019). Overall, these observations suggest that the survivin pathway is disturbed in PAH and could constitute a potential new therapeutic target for the disease.

Survivin expression can be inhibited by administering pro-apoptotic agents such as YM155 (Iwasa et al., 2008; Nakahara et al., 2011). YM155 (sepantronium bromide) is a small, imidazolium-based compound that specifically interacts with the survivin core promoter, inhibiting its gene expression and phosphorylation (Nakahara et al., 2011; Chang et al., 2015). In fact, it has been shown that abrogation of survivin by targeting its transcription with a histone deacetylase inhibitor or directly using a small synthetic inhibitor of survivin was sufficient to promote the apoptosis of arterial smooth muscle cells and to reverse pulmonary hypertension, in both *in vitro* and *in vivo* models of high blood flow-induced PAH and chronic hypoxia (Fan et al., 2015; Lao et al., 2016).

A number of preclinical studies in cancer have reported that YM155 effectively inhibits survivin expression and consequently reduces cell proliferation, increases apoptosis, and sensitizes cells to cytotoxic genes and radiotherapy (Nakahara et al., 2007; Tao et al., 2012). Interestingly, YM155 does not affect normal tissues (Cheng et al., 2016). Phase I and II studies have confirmed the tolerability of YM155 and the achievement of plasma concentrations that induced antitumor activity in patients with advanced cancers (Satoh et al., 2009; Lewis et al., 2011; Tolcher et al., 2012).

The present study aims to further understand the role of survivin in PAH and to assess the effects of treatment with its inhibitor YM155 in the SU5416/hypoxia mouse and in the MCT rat, which are well validated animal models of PAH. We assessed survivin expression in both the SU5416/hypoxia mouse and the MCT rat models (Blanco et al., 2017). In the SU5416/hypoxia mouse model (Bueno-Beti et al., 2018) we additionally assessed the effects of its inhibition with YM155 on pulmonary hemodynamics, pulmonary vascular remodeling, RV hypertrophy, and cell apoptosis and proliferation. The expression of survivin and its relationship with apoptosis/proliferation pathways was further assessed in explanted lungs from patients with PAH.

Materials and methods (more details are provided in the online supplemental material)

In vivo models of pulmonary hypertension

In the SU5416/hypoxia model, thirty-two male C57BL/6J mice (Netherlands, Envigo) were divided into four groups: vehicle, normoxia (Veh-Nx); vehicle, normoxia and YM155 (YM155-Nx); SU5416, hypoxia (SU-Hx); and SU5416, hypoxia and YM155 (SU-Hx-YM155). PAH was induced in the SU5416-hypoxia groups by exposure to 10% O_2 in a normobaric hypoxic chamber (ProOx P360 senses oxygen, Biospherix, NY) plus weekly subcutaneous injections of SU5416 (20 mg/kg in DMSO, Tocris Bioscience, Bristol, United Kingdom) for 3 weeks. Control groups were housed in room air and vehicle (DMSO) was administered each week for 3 weeks. In the groups treated with the survivin inhibitor, 5 mg/kg of YM155 (CAS 781661-94-7, Calbiochem), resuspended in saline solution, was administrated subcutaneously every day during the last week of SU5416/hypoxia exposure (Figure 1). The dose of YM155 used in our study was selected based on the findings of Nakahara et al. (Nakahara et al., 2011).

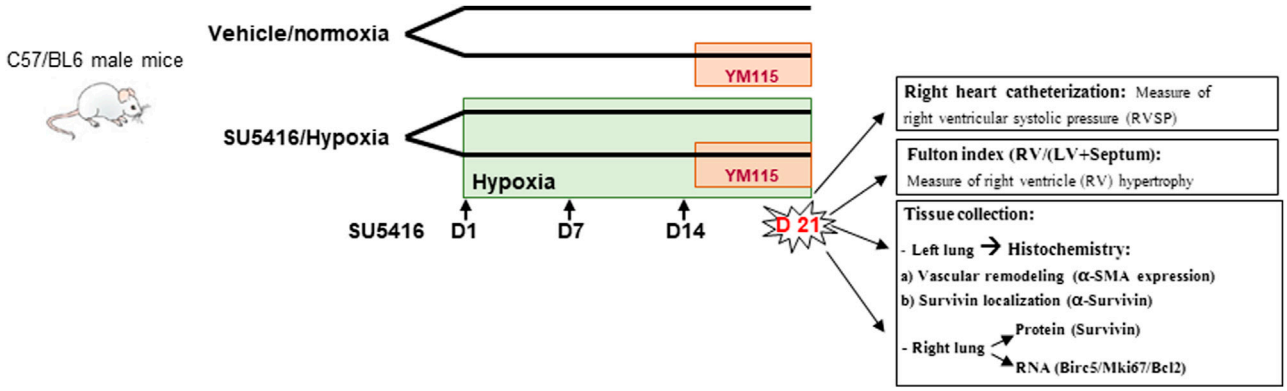

FIGURE 1
Schematic of the experimental design. Vehicle: DMSO; SU5416: Sugen; YM155: Survivin inhibitor.

All animal procedures were approved by the ethics review board on animal research of the University of Barcelona (CEEA 377/13) and complied with national and international guidelines.

We measured right ventricle systolic pressure (RVSP) with a 1F 20 cm catheter inserted through the jugular vein. Afterwards, mice were mechanically ventilated, and a midline sternotomy was performed to expose the heart and lungs. The right lung was excised for gene and protein expression analysis. The left lung was distended until full inflation and fixed by perfusion with 4% phosphate-buffered formaldehyde through the tracheal tube at a constant pressure of 25 cm H_2O for 24 h. In the excised heart, we calculated the Fulton index (weight of right ventricle (RV)/ weight of left ventricle (LV) + septum) to assess right ventricular hypertrophy. Phosphate-buffered formaldehyde-fixed paraffin sections obtained from the midsection of the left lung were used for morphometric analysis. Standard hematoxylin-and-eosin, Von Willebrand Factor and smooth muscle *a*-actin (SMA) stains were performed. More than 100 small vessels (diameter <50 μm) per lung sections were assessed in all the slides. Vessels immunostained for smooth muscle α-actin (SMA) were further classified semi-quantitatively, depending on the proportion of the vessel wall positive for SMA, as: non-muscularized, ≤1/4 of the vessel wall; partially muscularized, >1/4 to 3/4 of the vessel wall; or fully muscularized, >3/4 of the muscle wall. Vascular remodeling was expressed as a percentage of positive immunostaining for SMA (partially muscularized or fully muscularized of the vessel wall) per number of small pulmonary vessels (positive staining for Von Willebrand Factor) in the whole section.

In lung homogenates, we assessed the expression of the BIRC5 gene, which encodes the protein baculoviral inhibitor of apoptosis repeat-containing-5, commonly known as survivin. Survivin inhibits apoptosis and also induces proliferation by increasing mRNA levels of Bcl2, a family of proteins that regulate cell death, by inhibiting apoptosis, and inducing the proliferation marker Mki67. Accordingly, to further characterize the mechanisms of apoptosis and proliferation related to survivin, we examined mRNA expression of *Bcl2*, the founding member of the Bcl2 family, and Mki*67* in the lungs of experimental animals by quantitative RT-PCR.

In the MCT rat model, only survivin and the relationship to MCT-induced changes were assessed. Male Sprague–Dawley rats (n = 19) received a single subcutaneous injection of monocrotaline (MCT; 40 mg/kg, Sigma Aldrich) at day 0 to induce PAH. Control group (n = 16) received a subcutaneous injection of PBS. RVSP, right ventricular hypertrophy (Fulton Index) and survivin expression protein were measured in groups of control and MCT-treated rats.

Patients with PAH

Survivin, BCL2 and MKI67 expression were also evaluated in lung samples from patients with PAH and control lungs. Samples of patients with PAH were obtained from explanted lungs provided by the lung transplant unit of Hospital Vall d'Hebron, Barcelona and the Pulmonary Biobank Consortium of the Biomedical Research Networking Center on Respiratory Diseases (CIBERES). Ten lungs from non-smoker, no-cancer donors, discarded to transplant, also provided by the CIBERES Pulmonary Biobank Consortium, were used as controls. The protocol was approved by the institutional review board of Hospital Clínic of Barcelona (CEIm 2013/8571) and that of the Pulmonary Biobank Consortium.

Statistical analysis

Parametric data are presented as mean ± SD and non-parametric data as median (interquartile range). Groups were compared using, as appropriate, unpaired Student's t tests, non-parametric Mann-Whitney U test or Kruskal Wallis, or one-way ANOVA with Bonferroni *post hoc* tests using Prism 9 software (GraphPad Prism Software, San Diego, CA). A p-value < 0.05 was considered significant in all cases.

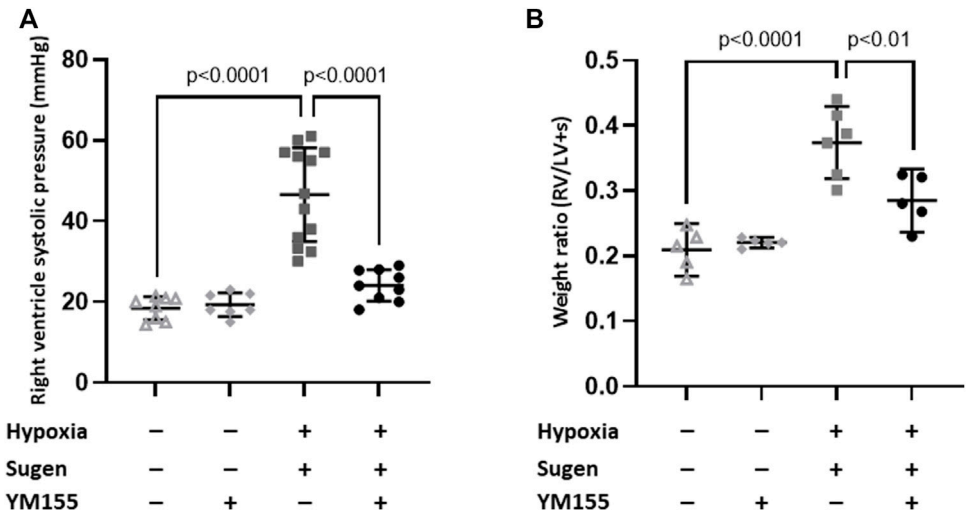

FIGURE 2
Effect of YM155 on right ventricle systolic pressure and hypertrophy in SU5416/hypoxia-induced PAH mice. Values of right ventricle systolic pressure (RVSP) **(A)** and right ventricular hypertrophy as measured by the Fulton's index **(B)** in the different study groups. Values are expressed as mean ± SD. Statistical significance was assessed by the one-way ANOVA. Drugs doses used were: SU5416, 20 mg/kg, s. c.i; YM155, 5 mg/kg, s. c.i.

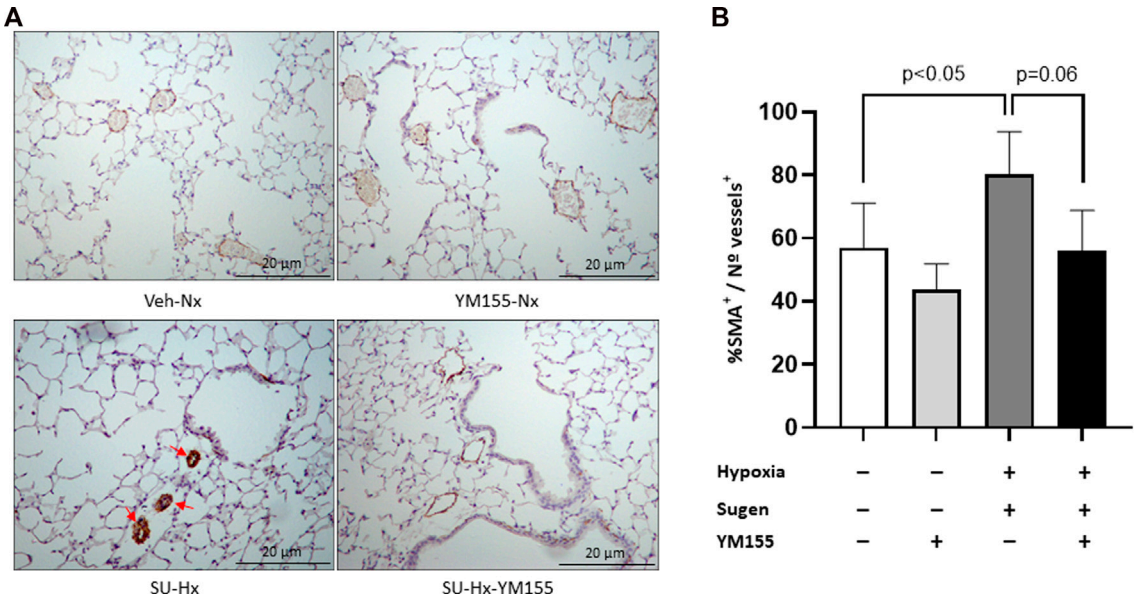

FIGURE 3
Effect of YM155 on pulmonary vascular remodeling in SU5416/hypoxia-induced PAH mice. **(A)** Representative α-smooth muscle actin (α-SMA) stained pulmonary arterioles in the different experimental groups (Veh-Nx = vehicle and normoxia; YM155-Nx = vehicle, normoxia and YM155; SU-Hx = SU5416 and hypoxia; SU-Hx-YM155 = SU5416, hypoxia and YM155). **(B)** Percent of α-SMA positive arteries with respect to the total number of vessels in each experimental group. Values are expressed as median (IQR) and statistical significance was assessed by the *Kruskal–Wallis* test. Arrows indicate muscularised small pulmonary arteries strongly immunostained with alpha α-SMA antibody.

Results

Survivin expression in experimental PAH

In the SU5416/hypoxia mouse model, SU-Hx mice showed a significant increase in RVSP (46.6 ± 11.6 mmHg), compared with control animals (18.4 ± 2.9 mmHg, $p < 0.0001$) (Figure 2A). These hemodynamic differences were consistent with differences in right ventricular hypertrophy, assessed by the Fulton index (RV/LV + S). RV weight was increased in SU-Hx mice (0.37 ± 0.05) compared with control mice (0.21 ± 0.03; $p < 0.0001$) (Figure 2B).

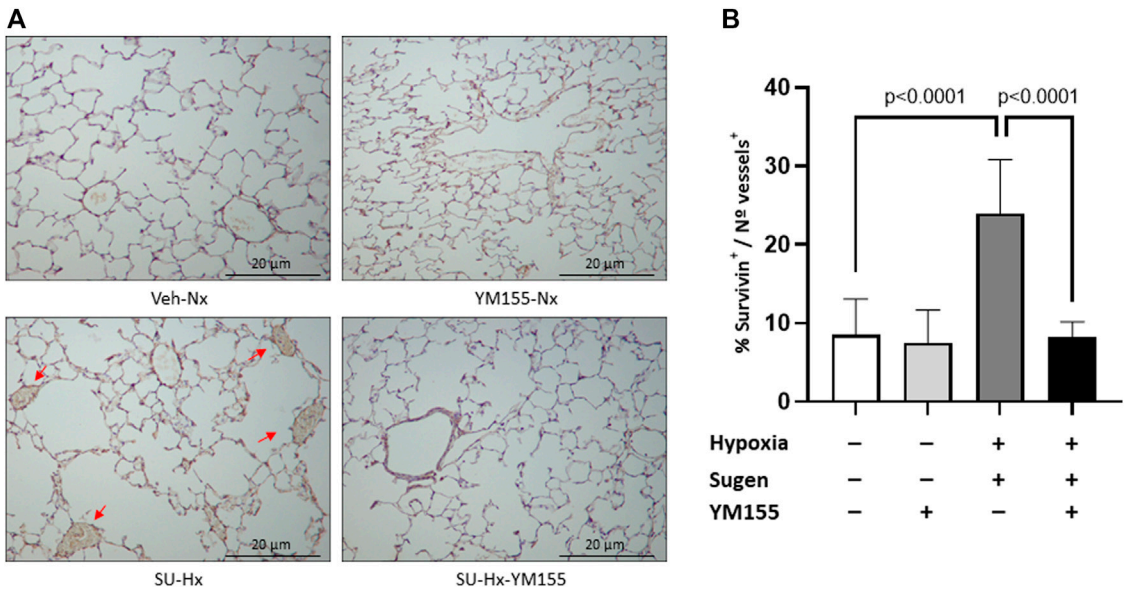

FIGURE 4
Effect of YM155 on survivin protein expression in small pulmonary arteries in SU5416/hypoxia-induced PAH mice. **(A)** Photomicrographs showing the immunostaining for survivin in small pulmonary vessels in the different experimental groups (Veh-Nx = vehicle and normoxia; YM155-Nx = vehicle, normoxia and YM155; SU-Hx = SU5416 and hypoxia; SU-Hx-YM155 = SU5416, hypoxia and YM155). **(B)** Percent of survivin positive vessels with respect to the total number of vessels in each experimental group. Values are expressed as mean ± SD. Statistical significance was assessed by the one-way ANOVA. Arrows indicate the localization of survivin in small pulmonary arteries.

The SU-Hx group exhibited a higher proportion of muscularized vessels (80.2% ± 6.2% SMA$^+$/total number of vessels) compared with controls (Veh-Nx) (57.0% ± 6.6% SMA$^+$/total number of vessels; p = 0.05) (Figure 3).

The immunohistochemical analysis showed an increased expression of survivin in pulmonary vessels of SU-Hx mice (23.9% ± 2.6% survivin$^+$ vessels/total number of vessels) compared with the Veh-Nx group (8.5% ± 1.5% survivin$^+$ vessels/total number of vessels; p = 0.0001) (Figure 4).

The expression of survivin protein in whole lung extracts, assessed by western blot analysis, was numerically higher in the SU-Hx group (1.33 ± 0.30) compared with the Veh-Nx group (1.09 ± 0.32) (p = 0.07) (Figure 5A).

Quantitative RT-PCR assessment of mRNA survivin levels showed similar results. Survivin gene (BIRC 5) expression was twofold higher in the SU-Hx group than in the Veh-Nx group (p = 0.01) (Figure 5B).

mRNA expression in lung homogenates of the apoptosis regulator Bcl2 and the proliferation marker Mki67 were increased in the SU-Hx group, compared with the control Veh-Nx group (p < 0.05) (Figure 6).

In the rat model, after MCT administration, RVSP was measured in groups of control and MCT-treated rats (n = 2/3/group/week). RVSP was significantly increased in MCT-challenged rats by 2 weeks, rising to a level of 71.5 (±5.6 mmHg), compared to 26.1 (±0.6 mmHg) in controls, by week 4 (Supplementary Figure S1A). Furthermore, a significant elevation in right ventricular hypertrophy (Fulton Index) was observed after 3-week MCT treatment (Supplementary Figure S1B). We assessed the expression of survivin protein in the rat lung, survivin gene expression was also twofold higher in MCT rats (p < 0.001) compared to controls (Supplementary Figure S2).

Effects of treatment with YM155 in the SU5416/hypoxia mouse model

In the mice model, treatment with YM155 significantly reduced RVSP (24.1 ± 3.9 mmHg) (p < 0.0001 compared with SU-Hx) (Figure 2A) and attenuated RV hypertrophy in SU-Hx mice (0.28 ± 0.04, p = 0.01) compared with untreated SU-Hx mice) (Figure 2B).

The proportion of vessels with muscularized walls trended to be lower in the SU-Hx-YM155 group (55.9% ± 3.2% SMA$^+$/total number of vessels) compared with the SU-Hx group (p = 0.06), with values similar to those of the Veh-Nx group (Figure 3).

Additionally, treatment with YM155 significantly decreased survivin expression in SU-Hx mice (8.3% ± 0.7% survivin$^+$ vessels/total number of vessels; p = 0.0001 compared with untreated SU-Hx mice) (Figure 4) and also reduced survivin protein expression in SU-Hx mice (0.57 ± 0.21) (p = 0.0012, compared with the SU-Hx untreated group) (Figure 5A). Additionally, treatment with YM155, reduced survivin mRNA expression in SU-Hx mice (p = 0.01, compared with the untreated SU-Hx group) to levels equivalent to those in the Veh-Nx group (Figure 5B).

In terms of apoptosis/proliferation markers, treatment with YM155 significantly also decreased the expression of both Bcl2 and Mki67 genes in SU-Hx mice (p < 0.05, compared with the SU-Hx untreated group) (Figure 6).

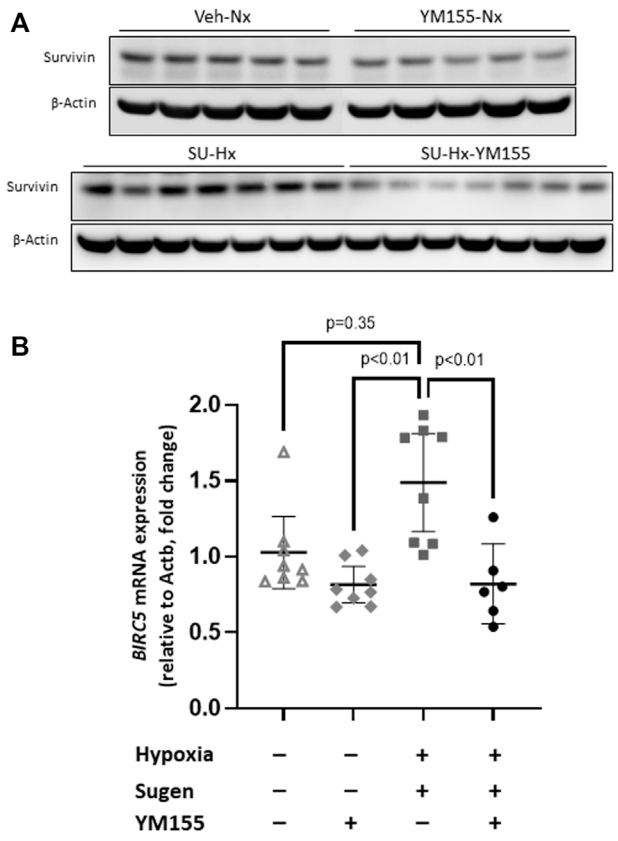

FIGURE 5
Effect of YM155 on survivin protein and mRNA expression in whole lung extracts of SU5416/hypoxia-induced PAH mice. **(A)** Immunoblots of the expression of survivin and the constitutive protein ß-actin in the different experimental groups (Veh-Nx = vehicle and normoxia; YM155-Nx = vehicle, normoxia and YM155; SU-Hx = SU5416 and hypoxia; SU-Hx-YM155 = SU5416, hypoxia and YM155). **(B)** Quantitative mRNA expression of BIRC5, the gene encoding survivin, related to Actb expression using RT-PCR in the different experimental groups. Values are expressed as median (IQR) and statistical significance was assessed by the *Kruskal–Wallis* test.

Survivin and apoptosis/proliferation axis-related genes expression in patients with PAH

Immunohistochemical analysis of explanted lungs showed prominent expression of survivin in the intimal layer of pulmonary arteries of patients with PAH, whereas it was not expressed in pulmonary arteries of control lungs (Figure 7).

Quantitative RT-PCR analysis confirmed increased mRNA expression of BIRC5, the gene encoding survivin, in lungs of patients with PAH, compared with control subjects ($p < 0.05$) (Figure 8A). Patients with PAH also showed increased lung expression of BCL2 and MKI67 genes compared with control lungs ($p < 0.0001$) (Figures 8B, C).

Discussion

Results of the present study show that the expression of the anti-apoptotic protein survivin is increased in pulmonary arteries of patients with PAH and in the lungs of two experimental models of PAH, the SU5416/hypoxia mouse and the MCT rat. In the SU5416/hypoxia model, treatment with the survivin inhibitor YM155 prevented the development of PH, reduced the transcriptional and post-transcriptional expression of survivin and also that of genes related with apoptosis/proliferation pathways, which can be understand as a positive attribute with a consistent translational relevance.

In our study we show increased transcriptional and post-transcriptional expression of survivin in pulmonary arteries and lungs of patients with PAH and also in two validated experimental models of PAH (Blanco et al., 2017; Bueno-Beti et al., 2018). The increased expression of survivin was associated with a disbalanced expression of genes related with apoptosis and cell proliferation, suggesting a mechanistic role of survivin, an anti-apoptotic molecule, in the development of PAH and their consequences on the right ventricle. Our findings concur with

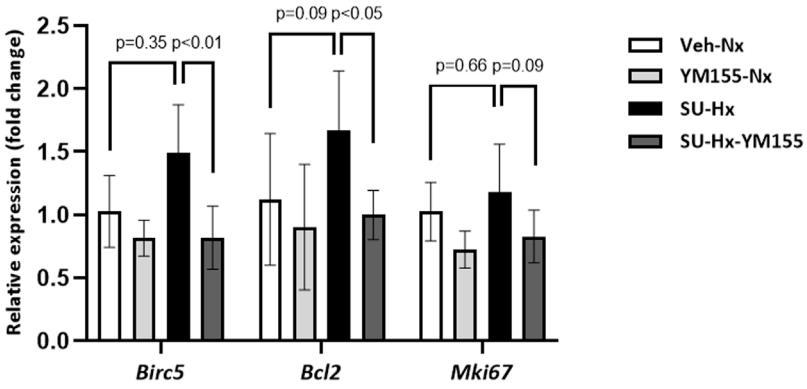

FIGURE 6
Effect of YM155 on apoptosis/proliferation related genes in whole lung extracts of SU5416/hypoxia-induced PAH mice. Quantitative mRNA expression of *Birc5*, *Bcl2*, and *Mki67*, related to Actb expression, using RT-PCR in the different experimental groups. Bcl2 and Mki67 values are expressed as mean ± SD and statistical significance was assessed by the one-way ANOVA. Birc5 values are expressed as median (IQR) and statistical significance was assessed by the *Kruskal–Wallis* test.

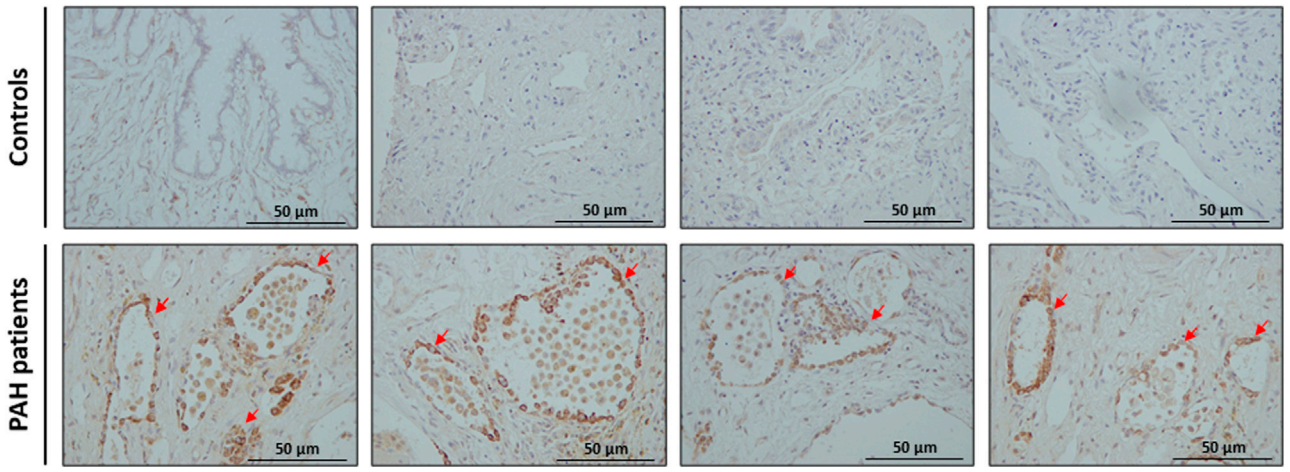

FIGURE 7
Expression of survivin in pulmonary arteries of patients with PAH. Representative photomicrographs showing immunohistochemical staining and labelling with anti-survivin antibody in pulmonary arteries of patients with PAH but not in lungs of control individuals. Arrows indicate survivin positive cells in pulmonary arteries.

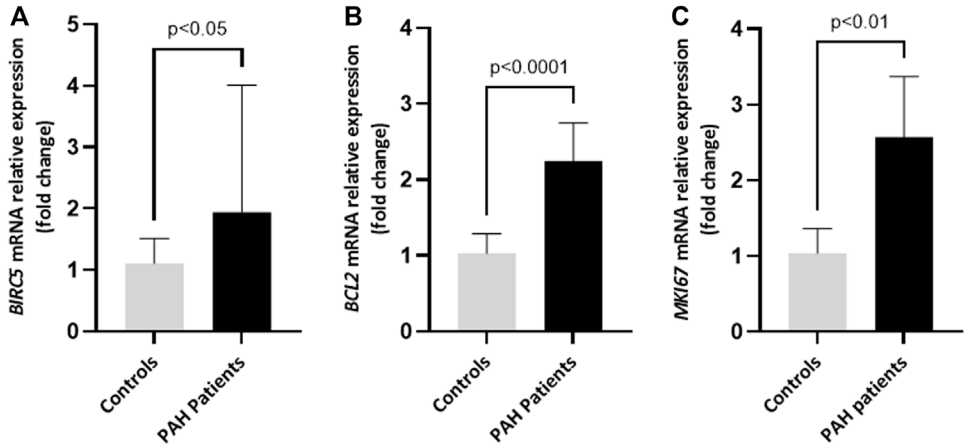

FIGURE 8
mRNA expression of survivin and genes involved in apoptosis and proliferation in whole lung extracts of patients with PAH. Quantitative RT-PCR assay of the mRNA expression of *BIRC5*, the gene encoding survivin **(A)**, *BCL2* **(B)** and *MKI67* **(C)** in lung explants from patients with PAH compared with control lungs. *BIRC5* values are expressed as median (IQR) and statistical significance was assessed by the U-Mann Whitney test. *BCL2* and *MKI67* values are expressed as mean ± SD and statistical significance was assessed by the two-tailed Student´s t-test.

those of McMurtry et al. (McMurtry et al., 2005), who showed increased survivin expression in pulmonary arteries of 6 patients with PAH and in the MCT-induced PH rat model, and with those of other models *in vitro* and *in vivo* exposed to hypoxia (Fan et al., 2015; Zhang et al., 2015; Zhang et al., 2016; Ye et al., 2022). We also extend these results to the SU5416-hypoxia mouse model and show the interaction between survivin expression and genes related with apoptosis/proliferation pathways. Overall, these findings suggest that survivin may contribute to the antiapoptotic, proproliferative cell phenotype that characterizes PAH (Humbert et al., 2019).

Treatment of SU5416/hypoxia mice with the survivin inhibitor YM155 (sepantronium bromide) reduced the expression of survivin, both at the transcriptional and post-transcriptional levels, in the whole lung and in the pulmonary artery wall. Importantly, SU5416/hypoxia mice treated with YM155 did not develop pulmonary vascular remodeling, increase of RVSP or right ventricular hypertrophy. Similar findings were observed in high blood flow-induced PAH and chronic hypoxia models (Fan et al., 2015; Zhang et al., 2015; Zhang et al., 2016; Ye et al., 2022) and also using gene therapy,

inhalation of an adenovirus carrying a phosphorylation-deficient survivin mutant with dominant-negative properties, in the monocrotaline-induced PH rat model by McMurtry et al. (McMurtry et al., 2005). That said, our study adds information to a model that is closer to the HAP. That said, our study shows that treatment with YM155 leads to reduced expression of survivin in a model that closely mimics HAP. All in all, these observations suggest that survivin inhibition might conform a novel potential therapeutic approach to PAH, which is currently feasible with the use of YM155.

The balance between apoptosis and cell proliferation related genes was altered in the lungs of PAH patients and also in the SU5416/hypoxia mouse model, with an increased expression of pro-proliferative genes, such BCL2 and MKI67. The vascular endothelial growth factor (VEGF) is an important angiogenic mediator and a key factor for endothelial cell survival, due to its anti-apoptotic effect (Voelkel and Gomez-Arroyo, 2014). VEGF expression levels are increased in some types of tumors and in patients with PAH (Tuder et al., 2013). We also observed an increased expression of VEGF in endothelial and smooth muscle cells and in fibroblasts of mice with SU5416/hypoxia-induced PH (data not shown). VEGF enhances endothelial cell survival by inducing the expression of Bcl2 through the activation of extracellular signal-regulated kinases (ERK) 1/2 and phosphoinositide 3-kinase (PI3-K)/protein kinase B (Akt) signaling pathways (Zhao et al., 2011). Both ERK and Akt play an important role in the proliferation, differentiation and survival of different cell types and have been related to a wide variety of anti-apoptotic functions (Kumar et al., 2004; Kovacs et al., 2019). Furthermore, BCL2 inhibits cell death signals in endothelial cells through the upregulation of survivin (Kumar et al., 2004; Li et al., 2008). Interestingly, treatment with YM155 not only reduced the expression of survivin but also that of Bcl2 and the proliferation of SMA + cells in pulmonary arteries of SU5416/hypoxia-exposed mice, suggesting that it restored the proliferation/apoptosis balance and prevented pulmonary vascular remodeling.

The therapeutic efficacy and safety of the survivin inhibitor YM155 has been evaluated in phase I and II clinical trials in different types of cancers (Giaccone et al., 2009; Miura et al., 2011) and in ongoing trials registered in clinicaltrials.gov. Trials reported so far have shown adequate tolerability of YM155 and antitumoral activity in different types of tumors (Tolcher et al., 2012; Kelly et al., 2013). Therefore, if there are no adverse safety signals in the ongoing clinical studies, the effect of YM155 could be evaluated in patients with PAH to assess its potential usefulness.

Our study has strengths and limitations. The robust effect of the inhibitor on hemodynamic and histologic parameters of experimental PAH *in vivo* and the inclusion of lung explant samples are strengths of the study. There are also some limitations; first, the assessment of the effects of YM155 in the experimental model used a "preventive" design. That is, YM155 was administered during the last week of the development of the experimental model. Therefore, we cannot assert that YM155 will have the same effect when lung lesions are already developed, which is what happens in patients with PAH.

Second, YM155 was used only in an animal model, but the results are similar to those of McMurtry *et al.* (McMurtry et al., 2005) using gene therapy and other recent studies (Fan et al., 2015; Zhang et al., 2015; Zhang et al., 2016; Ye et al., 2022). Therefore, the concept of the beneficial effect of inhibition of survivin in experimental PAH is well demonstrated, and now in this study in a more robust experimental model than that of rat exposed to monocrotaline or hypoxia. Third, mice were treated with the half maximum tolerated dose of YM155 but dose optimization was not performed in the animal model and no drug concentrations were assessed.

Finally, the increased expression of survivin in pulmonary arteries was shown in patients with end-stage PAH, undergoing lung transplantation. Therefore, we cannot conclude that the same will occur in patients with less severe PAH.

In conclusion, survivin expression is increased in pulmonary arteries of patients with PAH and in a robust experimental model of PAH, suggesting that it might be involved in the pathogenesis of PAH by disturbing apoptosis/proliferation signaling pathways. In experimental PAH, treatment with the survivin inhibitor YM155 prevented the development of pulmonary vascular remodeling and hence that of PH and its consequences on the right ventricle by restoring the balance between genes related to apoptosis and cell proliferation. Accordingly, survivin inhibition with YM155 might represent a novel therapeutic target for this devasting disease that deserves further evaluation.

Data availability statement

The original contributions presented in the study are included in the article/Supplementary Material, further inquiries can be directed to the corresponding author.

Ethics statement

The animal study was reviewed and approved by Ethics review board on animal research of the University of Barcelona (CEEA 377/13).

Author contributions

Conceptualization, IB, MM, OT-C, EF, AR, ML-M, MC, FP-V, VP, and JB; Data curation, IB, MM, and EF; Formal analysis, IB, MM, EF, AR, MM, and FP-V; Investigation, IB, MM, OT-C, EF, AR, ML-M, MC, FP-V, VP, and JB; Methodology, IB, MM, OT-C, EF, AR, ML-M, MC, FP-V, VP, and JB; Resources, IB; Supervision, IB, MM, OT-C, EF, AR, ML-M, MC, FP-V, VP, and JB; Visualization, IB, MM, OT-C, EF, AR, ML-M, MC, FP-V, VP, and JB; Writing—original draft, IB, MM, VP, and JB; Writing—review and editing, IB, MM, OT-C, EF, AR, ML-M, MC, FP-V, VP, and JB. All authors read and approved the final manuscript.

Funding

The study was supported by grants PI14/0782 and PI17/1515 from the *Instituto de Salud Carlos III* (ISCiii), co-funded

by the European Union (ERDF/ESF, "A way to make Europe"/"Investing in your future"), *Sociedad Española de Neumología y Cirugía Torácica* (SEPAR), *Societat Catalana de Pneumologia* (SOCAP) and *Fundación contra la Hipertensión Pulmonar* (FCHP). O. Tura-Ceide is the recipient of a Miguel Servet contract from the ISCiii (CP17/00114). F. Perez-Vizcaino is funded by Ministerio de Ciencia e innovación (PID2019-105847rb-i00), Comunidad de Madrid (CARDIOBOOST/P2022/BMD-7245).

Acknowledgments

The authors wish to acknowledge the invaluable contribution of the CIBERES Biobank for the samples provided, and would also like to thank Susana Maqueda, Neus Luque, Victoria Pisano, Cristina Bonjoch and Angela Vea for their technical support, Nick W Morrell for his support providing the funding and facilities for the MCT model and to Fernanda Hernández-González and Rodrigo Torres-Castro for helping in the final editing of the manuscript.

Conflict of interest

The authors declare that the research was conducted in the absence of any commercial or financial relationships that could be construed as a potential conflict of interest.

Publisher's note

All claims expressed in this article are solely those of the authors and do not necessarily represent those of their affiliated organizations, or those of the publisher, the editors and the reviewers. Any product that may be evaluated in this article, or claim that may be made by its manufacturer, is not guaranteed or endorsed by the publisher.

Supplementary material

The Supplementary Material for this article can be found online at: https://www.frontiersin.org/articles/10.3389/fphar.2023.1145994/full#supplementary-material

References

Ai, Z., Yin, L., Zhou, X., Zhu, Y., Zhu, D., Yu, Y., et al. (2006). Inhibition of survivin reduces cell proliferation and induces apoptosis in human endometrial cancer. *Cancer* 107 (4), 746–756. doi:10.1002/cncr.22044

Blanc-Brude, O. P., Yu, J., Simosa, H., Conte, M. S., Sessa, W. C., and Altieri, D. C. (2002). Inhibitor of apoptosis protein survivin regulates vascular injury. *Nat. Med.* 8 (9), 987–994. doi:10.1038/nm750

Blanco, I., Ferrer, E., Paul, T., Tura-Ceide, O., Peinado, V. I., and Barberà, J. A. (2017). New potential pathways of pulmonary arterial hypertension (PAH) in rodent models: Survivin pathway. *Am. J. Respir. Crit. Care* 195, A4195.

Bueno-Beti, C., Hadri, L., Hajjar, R. J., and Sassi, Y. (2018). The sugen 5416/hypoxia mouse model of pulmonary arterial hypertension. *Methods Mol. Biol.* 1816, 243–252. doi:10.1007/978-1-4939-8597-5_19

Chang, B. H., Johnson, K., LaTocha, D., Rowley, J. S. J., Bryant, J., Burke, R., et al. (2015). YM155 potently kills acute lymphoblastic leukemia cells through activation of the DNA damage pathway. *J. Hematol. Oncol.* 8 (1), 39–12. doi:10.1186/s13045-015-0132-6

Cheng, X. J., Lin, J. C., Ding, Y. F., Zhu, L., Ye, J., and Tu, S. P. (2016). Survivin inhibitor YM155 suppresses gastric cancer xenograft growth in mice without affecting normal tissues. *Oncotarget* 7 (6), 7096–7109. doi:10.18632/oncotarget.6898

Duffy, M. J., O'Donovan, N., Brennan, D. J., Gallagher, W. M., and Ryan, B. M. (2007). Survivin: A promising tumor biomarker. *Cancer Lett.* 249 (1), 49–60. doi:10.1016/j.canlet.2006.12.020

Fan, Z., Liu, B., Zhang, S., Liu, H., Li, Y., Wang, D., et al. (2015). YM155, a selective survivin inhibitor, reverses chronic hypoxic pulmonary hypertension in rats via upregulating voltage-gated potassium channels. *Clin. Exp. Hypertens.* 37 (5), 381–387. doi:10.3109/10641963.2014.987390

Galiè, N., Humbert, M., Vachiery, J. L., Gibbs, S., Lang, I., Torbicki, A., et al. (2016). 2015 ESC/ERS guidelines for the diagnosis and treatment of pulmonary hypertension: The joint task force for the diagnosis and treatment of pulmonary hypertension of the European society of cardiology (ESC) and the European respiratory society (ERS): Endorsed by: Association for European paediatric and congenital cardiology (AEPC), international society for heart and lung transplantation (ISHLT). *Eur. Heart J.* 37 (1), 67–119. doi:10.1093/eurheartj/ehv317

Galiè, N., Manes, A., Negro, L., Palazzini, M., Bacchi-Reggiani, M. L., and Branzi, A. (2009). A meta-analysis of randomized controlled trials in pulmonary arterial hypertension. *Eur. Heart J.* 30 (4), 394–403. doi:10.1093/eurheartj/ehp022

Giaccone, G., Zatloukal, P., Roubec, J., Floor, K., Musil, J., Kuta, M., et al. (2009). Multicenter phase II trial of YM155, a small-molecule suppressor of survivin, in patients with advanced, refractory, non-small-cell lung cancer. *J. Clin. Oncol.* 27 (27), 4481–4486. doi:10.1200/JCO.2008.21.1862

Humbert, M., Guignabert, C., Bonnet, S., Dorfmüller, P., Klinger, J. R., Nicolls, M. R., et al. (2019). Pathology and pathobiology of pulmonary hypertension: State of the art and research perspectives. *Eur. Respir. J.* 53 (1), 1801887. doi:10.1183/13993003.01887-2018

Humbert, M., Sitbon, O., Chaouat, A., Bertocchi, M., Habib, G., Gressin, V., et al. (2010). Survival in patients with idiopathic, familial, and anorexigen-associated pulmonary arterial hypertension in the modern management era. *Circulation* 122 (2), 156–163. doi:10.1161/CIRCULATIONAHA.109.911818

Iwasa, T., Okamoto, I., Suzuki, M., Nakahara, T., Yamanaka, K., Hatashita, E., et al. (2008). Radiosensitizing effect of YM155, a novel small-molecule survivin suppressant, in non-small cell lung cancer cell lines. *Clin. Cancer Res.* 14 (20), 6496–6504. doi:10.1158/1078-0432.CCR-08-0468

Kelly, R. J., Thomas, A., Rajan, A., Chun, G., Lopez-Chavez, A., Szabo, E., et al. (2013). A phase I/II study of sepantronium bromide (YM155, survivin suppressor) with paclitaxel and carboplatin in patients with advanced non-small-cell lung cancer. *Ann. Oncol.* 24 (10), 2601–2606. doi:10.1093/annonc/mdt249

Kovacs, L., Cao, Y., Han, W., Meadows, L., Kovacs-Kasa, A., Kondrikov, D., et al. (2019). PFKFB3 in smooth muscle promotes vascular remodeling in pulmonary arterial hypertension. *Am. J. Respir. Crit. Care Med.* 200 (5), 617–627. doi:10.1164/rccm.201812-2290OC

Kumar, P., Miller, A. I., and Polverini, P. J. (2004). p38 MAPK mediates γ-irradiation-induced endothelial cell apoptosis, and vascular endothelial growth factor protects endothelial cells through the phosphoinositide 3-kinase-Akt-Bcl-2 pathway. *J. Biol. Chem.* 279 (41), 43352–43360. doi:10.1074/jbc.M405777200

Lao, J., Pang, Y., Wang, K., Liu, D., Su, D., Zhang, F., et al. (2016). Inhibition of survivin promotes pulmonary arterial smooth muscle cell apoptosis in high blood flow-induced pulmonary arterial hypertension in rats. *Int. J. Clin. Exp. Pathol.* 9 (7), 6821–6834.

Lewis, K. D., Samlowski, W., Ward, J., Catlett, J., Cranmer, L., Kirkwood, J., et al. (2011). A multi-center phase II evaluation of the small molecule survivin suppressor YM155 in patients with unresectable stage III or IV melanoma. *Invest. New Drugs* 29 (1), 161–166. doi:10.1007/s10637-009-9333-6

Li, G., Zhang, H., Zhao, L., Zhang, Y., Yan, D., Liu, Y., et al. (2019). The expression of survivin in irreversible pulmonary arterial hypertension rats and its value in evaluating the reversibility of pulmonary arterial hypertension secondary to congenital heart disease. *Pulm. Circ.* 9 (3), 2045894019859480. doi:10.1177/2045894019859480

Li, L., Gao, Y., Zhang, L., Zeng, J., He, D., and Sun, Y. (2008). Silibinin inhibits cell growth and induces apoptosis by caspase activation, down-regulating survivin and blocking EGFR-ERK activation in renal cell carcinoma. *Cancer Lett.* 272 (1), 61–69. doi:10.1016/j.canlet.2008.06.033

McMurtry, M. S., Archer, S. L., Altieri, D. C., Bonnet, S., Haromy, A., Harry, G., et al. (2005). Gene therapy targeting survivin selectively induces pulmonary vascular apoptosis and reverses pulmonary arterial hypertension. *J. Clin. Invest.* 115 (6), 1479–1491. doi:10.1172/JCI23203

Miura, K., Fujibuchi, W., Ishida, K., Naitoh, T., Ogawa, H., Ando, T., et al. (2011). Inhibitor of apoptosis protein family as diagnostic markers and therapeutic targets of colorectal cancer. *Surg. Today* 41 (2), 175–182. doi:10.1007/s00595-010-4390-1

Morrell, N. W., Yang, X., Upton, P. D., Jourdan, K. B., Morgan, N., Sheares, K. K., et al. (2001). Altered growth responses of pulmonary artery smooth muscle cells from patients with primary pulmonary hypertension to transforming growth factor-beta(1) and bone morphogenetic proteins. *Circulation* 104 (7), 790–795. doi:10.1161/hc3201.094152

Nakahara, T., Kita, A., Yamanaka, K., Mori, M., Amino, N., Takeuchi, M., et al. (2011). Broad spectrum and potent antitumor activities of YM155, a novel small-molecule survivin suppressant, in a wide variety of human cancer cell lines and xenograft models. *Cancer Sci.* 102 (3), 614–621. doi:10.1111/j.1349-7006.2010.01834.x

Nakahara, T., Takeuchi, M., Kinoyama, I., Minematsu, T., Shirasuna, K., Matsuhisa, A., et al. (2007). YM155, a novel small-molecule survivin suppressant, induces regression of established human hormone-refractory prostate tumor xenografts. *Cancer Res.* 67 (17), 8014–8021. doi:10.1158/0008-5472.CAN-07-1343

Satoh, T., Okamoto, I., Miyazaki, M., Morinaga, R., Tsuya, A., Hasegawa, Y., et al. (2009). Phase I study of YM155, a novel survivin suppressant, in patients with advanced solid tumors. *Clin. Cancer Res.* 15 (11), 3872–3880. doi:10.1158/1078-0432.CCR-08-1946

Tao, Y. F., Lu, J., Du, X. J., Sun, L. C., Zhao, X., Peng, L., et al. (2012). Survivin selective inhibitor YM155 induce apoptosis in SK-NEP-1 Wilms tumor cells. *BMC Cancer* 12, 619. doi:10.1186/1471-2407-12-619

Tolcher, A. W., Quinn, D. I., Ferrari, A., Ahmann, F., Giaccone, G., Drake, T., et al. (2012). A phase II study of YM155, a novel small-molecule suppressor of survivin, in castration-resistant taxane-pretreated prostate cancer. *Ann. Oncol.* 23 (4), 968–973. doi:10.1093/annonc/mdr353

Tuder, R. M., Archer, S. L., Dorfmüller, P., Erzurum, S. C., Guignabert, C., Michelakis, E., et al. (2013). Relevant issues in the pathology and pathobiology of pulmonary hypertension. *J. Am. Coll. Cardiol.* 62 (25 Suppl. L), D4–D12. doi:10.1016/j.jacc.2013.10.025

Voelkel, N. F., and Gomez-Arroyo, J. (2014). The role of vascular endothelial growth factor in pulmonary arterial hypertension: The angiogenesis paradox. *Am. J. Respir. Cell Mol. Biol.* 51 (4), 474–484. doi:10.1165/rcmb.2014-0045TR

Ye, B., Peng, X., Su, D., Liu, D., Huang, Y., Huang, Y., et al. (2022). Effects of YM155 on the proliferation and apoptosis of pulmonary artery smooth muscle cells in a rat model of high pulmonary blood flow-induced pulmonary arterial hypertension. *Clin. Exp. Hypertens.* 44 (5), 470–479. doi:10.1080/10641963.2022.2071919

Zhang, S., Liu, B., Fan, Z., Wang, D., Liu, Y., Li, J., et al. (2016). Targeted inhibition of survivin with YM155 promotes apoptosis of hypoxic human pulmonary arterial smooth muscle cells via the upregulation of voltage-dependent K^+ channels. *Mol. Med. Rep.* 13 (4), 3415–3422. doi:10.3892/mmr.2016.4977

Zhang, S., Liu, B., Zhang, B., and Fan, Z. (2015). The effect of survivin expression on the apoptosis and proliferation of hypoxic human pulmonary arterial smooth muscle cells. *Zhonghua jie he he hu xi za zhi = Zhonghua jiehe he huxi zazhi = Chin. J. Tuberc. Respir. Dis.* 38 (1), 45–49.

Zhao, X., Ogunwobi, O. O., and Liu, C. (2011). Survivin inhibition is critical for Bcl-2 inhibitor-induced apoptosis in hepatocellular carcinoma cells. *PLoS One* 6 (8), e21980. doi:10.1371/journal.pone.0021980

frontiers | Frontiers in Pharmacology

TYPE Review
PUBLISHED 11 May 2023
DOI 10.3389/fphar.2023.1186060

OPEN ACCESS

EDITED BY
Lalit Mohan Nainwal,
GD Goenka University, India

REVIEWED BY
Manoj Kumar Sharma,
Apeejay Stya University, India
Neelkant Prasad,
Shree Guru Gobind Singh Tricentenary University, India

*CORRESPONDENCE
Aparoop Das,
aparoopdas@dibru.ac.in

†These authors have contributed equally to this work and share first authorship

RECEIVED 14 March 2023
ACCEPTED 25 April 2023
PUBLISHED 11 May 2023

CITATION
Das A, Pathak MP, Pathak K, Saikia R and Gogoi U (2023), Herbal medicine for the treatment of obesity-associated asthma: a comprehensive review.
Front. Pharmacol. 14:1186060.
doi: 10.3389/fphar.2023.1186060

Herbal medicine for the treatment of obesity-associated asthma: a comprehensive review

Aparoop Das[1*†], Manash Pratim Pathak[2†], Kalyani Pathak[1], Riya Saikia[1] and Urvashee Gogoi[1]

[1]Department of Pharmaceutical Sciences, Dibrugarh University, Dibrugarh, Assam, India, [2]Faculty of Pharmaceutical Science, Assam Down Town University, Guwahati, Assam, India

Obesity is fast growing as a global pandemic and is associated with numerous comorbidities like cardiovascular disease, hypertension, diabetes, gastroesophageal reflux disease, sleep disorders, nephropathy, neuropathy, as well as asthma**.** Studies stated that obese asthmatic subjects suffer from an increased risk of asthma, and encounter severe symptoms due to a number of pathophysiology. It is very vital to understand the copious relationship between obesity and asthma, however, a clear and pinpoint pathogenesis underlying the association between obesity and asthma is scarce. There is a plethora of obesity-asthma etiologies reported viz., increased circulating pro-inflammatory adipokines like leptin, resistin, and decreased anti-inflammatory adipokines like adiponectin, depletion of ROS controller Nrf2/HO-1 axis, nucleotide-binding domain, leucine-rich-containing family, pyrin domain-containing-3 (NLRP3) associated macrophage polarization, hypertrophy of WAT, activation of Notch signaling pathway, and dysregulated melanocortin pathway reported, however, there is a very limited number of reports that interrelates these pathophysiologies. Due to the underlying complex pathophysiologies exaggerated by obese conditions, obese asthmatics respond poorly to anti-asthmatic drugs. The poor response towards anti-asthmatic drugs may be due to the anti-asthmatics approach only that ignores the anti-obesity target. So, aiming only at the conventional anti-asthmatic targets in obese-asthmatics may prove to be futile until and unless treatment is directed towards ameliorating obesity pathogenesis for a holistic approach towards amelioration of obesity-associated asthma. Herbal medicines for obesity as well as obesity-associated comorbidities are fast becoming safer and more effective alternatives to conventional drugs due to their multitargeted approach with fewer adverse effects. Although, herbal medicines are widely used for obesity-associated comorbidities, however, a limited number of herbal medicines have been scientifically validated and reported against obesity-associated asthma. Notable among them are quercetin, curcumin, geraniol, resveratrol, β-Caryophyllene, celastrol, tomatidine to name a few. In view of this, there is a dire need for a comprehensive review that may summarize the role of bioactive phytoconstituents from different sources like plants, marine as well as essential oils in terms of their therapeutic mechanisms. So, this review aims to critically discuss the therapeutic role of herbal medicine in the form of bioactive phytoconstituents against obesity-associated asthma available in the scientific literature to date.

KEYWORDS

obesity-associated asthma, herbal medicine, bioactive phytoconstituents, adiponectin, macrophage polarization, NLRP3, NOTCH1

1 Introduction

Obesity affects more than one billion people worldwide, including 650 million adults, 340 million adolescents, and 39 million children, and the number is alarmingly rising (World Health Organization, 2022). Hippocrates, the Greek Physician in the classical Greek era quoted that "Corpulence is not only a disease itself but the harbinger of others," which holds true in today's modern world. Obesity is associated with numerous comorbidities like cardiovascular disease, hypertension, diabetes, gastroesophageal reflux disease, sleep disorders, nephropathy, neuropathy, as well as asthma. As per the latest World Health Organization statistics, ischemic heart disease (IHC) tops the leading causes of death globally, however, reports stated that obesity is one of the prominent causes of IHC (World Health Organization, 2021). Studies stated that obese asthmatic subjects suffer from an increased risk of asthma, and encounter severe symptoms that result in the excessive release of white adipose-derived pro-inflammatory adipokines producing severe oxidative stress in the respiratory system (Global Initiative for Asthma, 2020; Pathak et al., 2021). Obesity and asthma have both increased in the United States over the last several decades with nearly 60% of adults with severe asthma being obese. Asthma prevalence is prominent in obese adult women and children. Obesity has a copious effect on the risk of asthma, the higher the body mass index (BMI), the higher the risk of asthma (Peters et al., 2018; Koebnick et al., 2016). There is a plethora of reported obesity-asthma pathophysiologies, namely, modulation of adipose tissue (Lumeng and Saltiel, 2011), increased circulating pro-inflammatory adipokines like leptin, and resistin, and decreased anti-inflammatory adipokines like adiponectin (Fu et al., 2017; Salvator et al., 2021; Palma et al., 2022), depletion of ROS controller Nrf2/HO-1 axis (Yuan et al., 2018; Pathak et al., 2021), NLRP3 associated macrophage polarization (Russo and Lumeng, 2018), activation of the Notch signaling pathway (Zeng et al., 2019), downregulation of Ucp1 in BAT (Cannon and Nedergaard, 2004) followed by downregulated AMPKα (Yamauchi et al., 2003) and melanocortin pathway (Raap et al., 2003) are reported (Figure 1). Asthma is worsened in obese patients and they become less responsive to conventional anti-asthmatic drugs. Inhaled corticosteroids (ICTs) are the common and most-effective drugs that provide fast relief by acting on the airways. Although effective in non-obese asthmatics, ICT does not provide relief to obese asthmatics, and in fact, increased ICT doses lead to poorer asthma control in the absence of eosinophilic inflammation in the sputum or presence of bronchial neutrophilia (Peerboom et al., 2020). Humankind is bestowed with the greatest gift of nature in the form of herbal medicine which comes with a multi-targeted pathway and fewer side effects. There has been an increase in scientific studies evaluating the value of compounds acquired from herbal medicine, which has traditionally been used in folk medicine. Plant-based compounds such as flavonoids, alkaloids, and

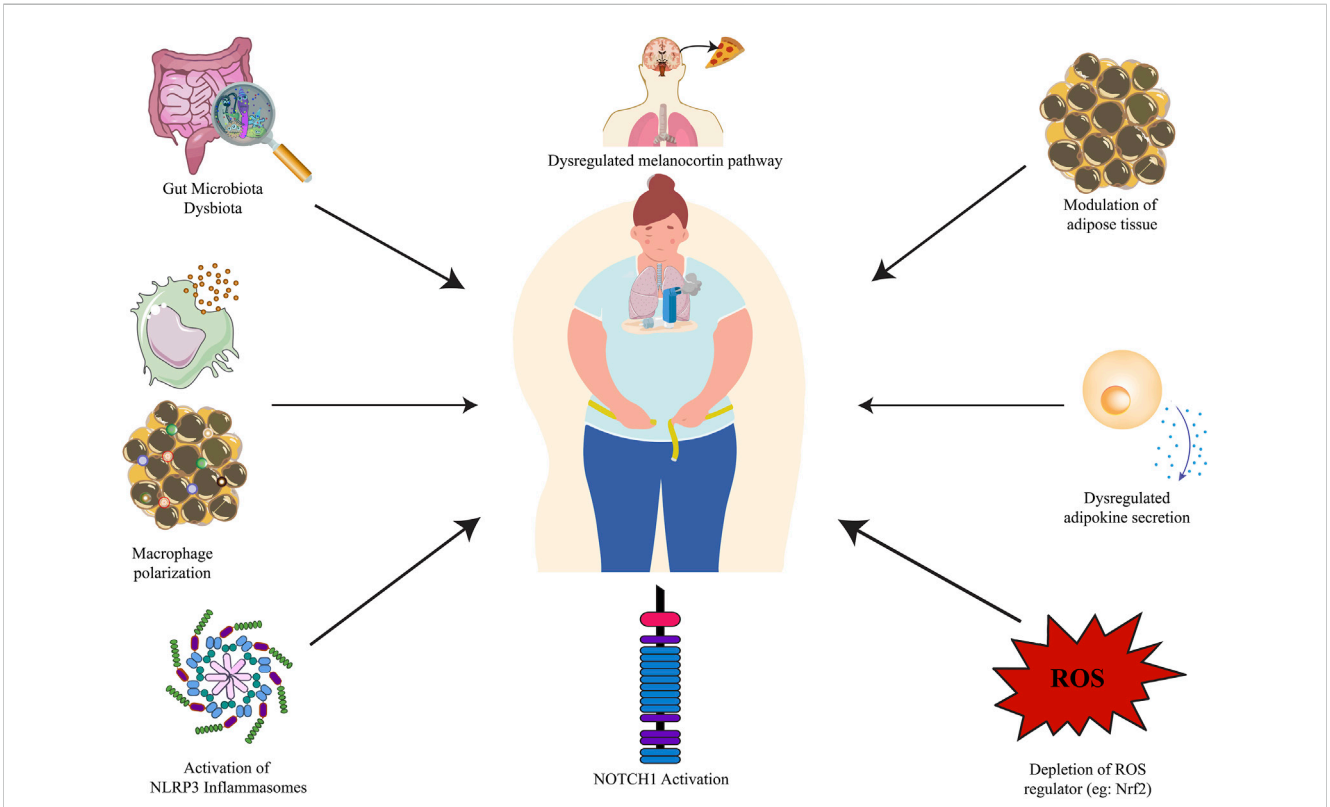

FIGURE 1
Obesity-asthma pathophysiology. NLRP3: nucleotide-binding domain, leucine-rich-containing family, pyrin domain-containing-3; NOTCH1: Neurogenic locus notch homolog protein 1.

terpenoids have been reported to show promising *in-vitro* and *in-vivo* anti-obesity effects through a repertoire of mechanisms, namely, appetite suppression, triglyceride reduction, metabolic rate increase, pancreatic lipase inhibition, etc. Recently piperine, found in Piper species, has been reported to ameliorate obesity via the alteration of the gut microbiota (He et al., 2022a) as well as found to combat pancreatic β-Cell apoptosis in obese diabetic mice (He et al., 2022b). Similarly, there have been reports of the therapeutic role of plant extract and their bioactive phytoconstituents in allergic asthma. Solasodine, found in Solanaceae family, is reported to suppress ovalbumin (OVA) induced allergic asthma through modulation of different inflammatory markers (Arora et al., 2022a); piperine is also reported to suppress inflammatory markers and oxidative stress in cigarette smoke-exposed experimental mice (Arora et al., 2022b). Likewise, stamen extract of *Mesua ferrea* L. (Calophyllaceae) from the Calophyllaceae family and root extract of *Clerodendrum serratum* of the genus *Clerodendrum* is reported to ameliorate allergic asthma through the modulation of few asthma-associated cytokines like TNF-α, IL-5, and IL-4. The authors speculated that the ameliorative effect of *M. ferrea* L. may be due to the presence of bioactive phytoconstituents like rhusflavanone, mesuaferrone B, α-Amyrin or β-Amyrin (Arora et al., 2021) and of *C. serratum* due to compounds like scutellarein, icosahydropicenic acid, oleanolic acid, ursolic acid, and queretaroic acid (Arora et al., 2022a). Similarly, the root extract of *Withania somnifera* demonstrated potential anti-asthmatic properties. The study reported that treatment with root extract of *W. somnifera* downregulated pro-inflammatory cytokines like immunoglobulin E (IgE), IL-4), and TNF-α as well as Histone deacetylase 2 (HDAC2) in the blood and bronchoalveolar lavage fluid (BALF) of the treated animals (Ali et al., 2023). From the above published reports, it is observed that bioactive phytoconstituents like piperine possess both the anti-asthmatic as well as anti-obesity properties separately, however, very few studies are undertaken to study both the properties in the same animal model. Although, herbal medicines are widely used for obesity-associated comorbidities nowadays, however, a very smaller number of herbal medicines in the form of bioactive phytoconstituents have been scientifically validated and reported against obesity-associated asthma. Notable among them are resveratrol, β-Caryophyllene, celastrol, and tomatidine. In view of this, there is a dire need for a comprehensive review that may summarize the role of herbal medicines targeting obesity-associated asthma in terms of their therapeutic mechanisms. So, this review aims to critically discuss the therapeutic role of herbal medicine in the form of bioactive phytoconstituents against obesity-associated asthma available in the scientific literature to date.

2 Obesity-asthma pathophysiology

2.1 Modulation of adipose tissue

The adipose tissue produces cytokines and hormones that regulate metabolism and immunity (Sideleva et al., 2012). Adipose tissue can be divided into 2 major types: white adipose tissue (WAT) and brown adipose tissue (BAT). The largest portion of adipose tissue in most organisms is WAT, which is used for energy storage, whereas BAT plays a major role in thermogenesis in small mammals and neonates (Curat et al., 2004; Fantuzzi, 2005). Lean adipose tissue secretes low levels of proinflammatory cytokines [e.g., IL-6, IL-8, tumor necrosis factor (TNF)-α] and adipokines (e.g., leptin), while producing high levels of the anti-inflammatory adipokine adiponectin. Adipose tissue hypertrophies in obese individuals and becomes infiltrated with macrophages that promote inflammation (Lumeng and Saltiel, 2011) and may exaggerate asthmatic conditions in obese individuals (Shim et al., 2023). Consequently, proinflammatory adipokines are speculated to enhance asthmatic airway inflammation in obesity. A recent report suggests that two significant depots of white adipose tissue, i.e., visceral fat are responsible for the narrowing of bronchial lumina and subcutaneous fat for bronchial wall thickening (Yang et al., 2018).

In metabolic syndrome, mitochondrial dysfunction and defective mitochondrial biogenesis are observed in various organs such as adipose tissue, muscle, liver, and beta islet cells in the pancreas (Kim et al., 2008; Luptak et al., 2019). Factors affecting mitochondrial function include hereditary, environmental, and lifestyle influences. Overeating and high-fat consumption are two of the most common causes of obesity, resulting in nutritional overload, excess electron flux, increased oxidative stress, accumulated partially oxidized substrates, and eventually, damage to the body (Koves et al., 2008). Researchers have found that mitochondrial dysfunction in the airway epithelium was a major contributor to allergic asthma models in mice (Mabalirajan et al., 2008). In a similar model, Aguilera-Aguirre et al. (2009) found that pre-existing mitochondrial dysfunction increased asthma severity. Pattnaik et al. (2016) showed that the levels of asymmetric dimethylarginine (ADMA) in allergically inflamed lungs were extremely high, and IL-4 increased ADMA synthesis via protein arginine methyl transferases and inhibited its degradation by dimethylarginine dimethylaminohydrolase 2. In airway epithelial cells, IL-4 and ADMA worked together to fragment mitochondria, increase mitochondrial ROS release, and reduce mitochondrial mass. As a result of this, obesity and asthma, both of which have high ADMA and IL-4 levels, could potentiate each other by causing mitochondrial dysfunction to become more severe (Bhatraju and Agrawal, 2017). There is increasing evidence that energy metabolism plays a significant role in the development and maintenance of inflammatory conditions such as asthma. Energy metabolism depends heavily on adipose tissue. White adipocytes store energy in the form of triglycerides, and beige/brown adipocytes are involved in heat metabolism (Wu et al., 2012; Harms and Seale, 2013). Several studies have indicated that brown adipose tissue (BAT) can be used as an obesity therapeutic target. BATs are specialized for metabolic thermogenesis mediated by mitochondrial uncoupling protein 1 (UCP1), which uncouples respiration from ATP synthesis (Cannon and Nedergaard, 2004). UCP1 is an inner mitochondrial membrane protein that uncouples oxidative phosphorylation from ATP synthesis through FA/H+ symports (Chouchani et al., 2019). UCP1 expression is mainly driven through β3-adrenoreceptors (β3-AR) stimulation by sympathetically and non-sympathetically produced norepinephrine in thermogenically active adipocytes

(Alzaim et al., 2020). Thermogenesis in BAT is due to UCP1, also called thermogenin or SLC25A7 (Dalgaard and Pedersen, 2001). Brown adipose tissue-induced thermogenesis is reported to activate the AMPK pathway which is responsible for the amelioration of asthma in obese subjects (Liu et al., 2023). In cold environments and during the postpartum period, UCP1-mediated thermogenesis is critical for thermoregulation (Tsubota et al., 2019) as well as in regulating adiposity. In both rodents and humans, the activation of UCP1-mediated thermogenesis raises total body energy expenditure and reduces fat mass (Okamatsu-Ogura et al., 2020; Saito et al., 2020). In BAT, UCP1 is highly expressed and oversees adaptive thermogenesis. When UCP1 is stimulated, the respiratory chain is activated. The combustion of readily available substrates produces heat, which the circulatory system then transfers to the other parts of the body (Ricquier, 2011; Jorge et al., 2017). The UCP1 protein helps the body burn energy and lose weight through a process called thermogenesis. It is also involved in maintaining healthy levels of glucose and lipids in the body (Kozak and Anunciado-Koza, 2008; Stanford et al., 2013).

2.2 Dysregulated adipokine secretion

Adipokines are substances produced by fat cells that play a crucial role in the relationship between metabolism and immune system function. However, when they are not regulated properly, as is often the case in obesity, they can cause persistent, low-level inflammation that can lead to various health problems (Taylor, 2021). Adipose tissue has functions beyond just storing energy. It also produces and releases various substances called adipokines, which can act on the fat tissue itself as well as other organs like the heart and lungs to regulate their function. Adipokines act in both local and systemic ways (McGillis, 2005). In addition, adipokines can influence the production of cytokines, which are signaling molecules that can have either pro-inflammatory or anti-inflammatory effects, depending on the specific circumstances (Fu et al., 2017; Salvator et al., 2021; Palma et al., 2022). In general, the production of most adipokines increases in obesity, and the pro-inflammatory ones tend to contribute to the development of health problems associated with obesity as well as in lean subjects, such as asthma where adipokines play an important role in the pathogenesis (Sood and Shore, 2013).

2.2.1 Proinflammatory adipokines

2.2.1.1 Leptin

Leptin is the most well-known proinflammatory adipokine, and it was originally described as a satiation hormone (Friedman and Halaas, 1998). Leptin stimulates the production of chemokine (C-C motif) ligand 2 (CCL2) and vascular endothelial growth factor in human hepatic stellate cells and activates monocytes and macrophages to produce pro-inflammatory interleukin-6 (IL-6), tumor necrosis factor-alpha (TNF-α), and interleukin-12 (IL-12) (Gainsford et al., 1996; Aleffi et al., 2005). Other inflammation signals, such as TNF-α and lipopolysaccharides (LPS), increase leptin and leptin receptor expression (Grunfeld et al., 1996; Gan et al., 2012). In $CD4^+$ T cells, leptin also increases the production of pro-inflammatory Th1 cytokines while suppressing the release of anti-inflammatory Th2 cytokines such as interleukin-4 (IL-4) (Lord et al., 1998). Increased expression of leptin is reported to be associated with obesity-asthma phenotype through the activation of the STAT3 signaling pathway (Chong et al., 2019). Several clinical studies reported an increased level of leptin in obese asthmatics as compared to the non-obese population (Sánchez-Ortega et al., 2022). As reported in human normal BEAS-2 bronchial epithelial cells, leptin promotes exacerbation in obese asthmatic patients by upregulating the mitochondrial reactive oxygen species/NOD-, LRR-, and pyrin domain-containing protein 3 (mostly known as mtROS/NLRP3) inflammasome signaling pathways (Chong et al., 2021). A recent systematic review and meta-analysis also confirmed the pathological role of leptin in obesity-associated asthma where leptin was reported to hold responsible for activating the signaling pathways of inflammation and parasympathetic system that lead to the disease severity (Sánchez-Ortega et al., 2022).

2.2.1.2 Interleukin-6

In adult adipose tissue, IL-6 is highly expressed and favorably linked with obesity (Kwon and Pessin, 2013). One of the most researched factors linked to poor adipogenesis and insulin resistance is IL-6, a pro-inflammatory and immunomodulatory cytokine. IL-6 suppresses the synthesis of adiponectin and impairs insulin signaling, which together contribute to inflammation in obesity (Tzanavari et al., 2010). C-reactive protein (CRP) is also produced as a result, which intensifies the inflammatory response (Bahceci et al., 2007). Additionally, IL-6 participates in the early and late phases of the asthma response and is correlated with the severity of the condition (Sideleva et al., 2012). Plasma IL-6 exerts its pathological aspects in obese-asthmatics by targeting several lung cells, i.e., endothelial cells, epithelial cells, and other airway cells as well as immune cells like regulatory T cells and Th17 cells. The same study reveals that IL-6 high subset of obese asthmatics suffering from other metabolic dysfunctions like hypertension has the highest incidence of asthma as compared with obese asthmatics without any metabolic dysfunctions. This finding reveals a contentious relationship between high plasma IL-6 and obese asthmatics with other metabolic dysfunctions that warrant further studies (Peters et al., 2016).

2.2.1.3 Tumor necrosis factor

Tumour necrosis factor-alpha (TNF-α) is a multi-functional cytokine that can regulate many cellular and biological processes such as immune function, cell differentiation, proliferation, apoptosis, and energy metabolism. It is synthesized as a 26-kDa transmembrane monomer (mTNF-α). In the pulmonary environment, alveolar macrophages can create significant levels of TNF-α, which plays an important role in the pathogenesis of asthma (Kim et al., 2012). The TNF-α receptor 1 (TNFR1) mediates the anti-adipogenic effects of TNF-α (Cawthorn and Sethi, 2008). The number of preadipocytes undergoing differentiation in the abdomen subcutaneous tissue is decreased due to elevated levels of mitogen-activated protein kinase kinase 4 (MAP4K4), which is engaged in the TNF-signaling pathway, leading to hypertrophic fat cells in conjunction with obesity. This implies that fat accumulation and proinflammatory capability are inversely correlated (Cawthorn et al., 2007; Isakson et al., 2009; Al-Mansoori et al., 2022). A study conducted on diet-induced obese (DIO)-mice revealed that

controlling obesity through exercise and diet control was found to be an effective means decrease the pulmonary TNF-α levels which result in decreased asthma severity in obesity-associated asthma (Kim et al., 2015). Extracellular matrix (ECM) protects the airways by preventing them from collapsing during expiration, and metalloproteinase (MMPs) enzymes are responsible for ECM renewal, making them important in pulmonary biology. In obese mice, intraperitoneal administration of anti-TNF- monoclonal antibody significantly decreased lung matrix metallopeptidase 9 (MMP-9) activity, demonstrating a link between TNF- and increased asthma severity in obese subjects (Vieira et al., 2020).

2.2.1.4 Resistin

Resistin, a 10 kDa polypeptide of 114 amino acids in rodents, is known to produce pulmonary inflammation and insulin resistance (Holcomb et al., 2000; Steppan et al., 2001). Peripheral blood inflammatory cells, monocytes, and macrophages are the principal producers of resistin. Resistin has also been found in the cells of the bone marrow, lungs, placenta, pancreatic islet tissue, and adipose tissue (Le and Pang, 2006). Resistin expression in human macrophages is induced by inflammatory cytokines such IL-1, IL-6, TNF-α, and LPS. Through the NF-κB signalling pathway, resistin induces human peripheral mononuclear cells to release IL-6 and TNF-α, whereas rosiglitazone, a peroxisome proliferator-activated receptor (PPAR) agonist, inhibits resistin expression in adipose tissues, reducing inflammatory responses (Bokarewa et al., 2005). As per a recent study, serum resistin levels were found to be elevated in obese asthmatics especially in females as compared to males which further confirms the role of resistin in the exaggeration of asthma in obese (Hosny et al., 2021). The hResistin:adiponectin ratio is found to be much higher in obese asthmatics, supporting the idea that hResistin may make a significant contribution to increased severity in the obese population which encourages the idea that this ratio could be a possible therapeutic avenue for managing the obese asthma phenotype (Lin and Johns, 2020).

There are several other proinflammatory adipokines that have been suggested to contribute to the inflammation associated with obesity, although they have not been studied as much as others. These include chemerin, retinol binding protein 4 (RBP4), CC-Chemokine Ligand 2 and CC-Chemokine Receptor Type 5, Angiopoietin-Like Protein 2, and lipocalin 2 (LCN2).

2.2.2 Anti-inflammatory adipokines

2.2.2.1 Adiponectin

Adipocytes strongly express the potent anti-inflammatory molecule adiponectin. A complex molecule, adiponectin can aggregate into complexes with low, intermediate, and high molecular weights in the blood. The AdipoR1 and AdipoR2 receptors, which are involved in immune cells and tissues, activate AMP-activated protein kinase (AMPK) to produce its effects (Yamauchi et al., 2003). The high-molecular-weight complex possesses anti-inflammatory effects that are known to suppress inflammation by preventing NF-κB activation and decreasing cytokines including TNFα, IL-6, and IL-18 (Yokota et al., 2000; Ouchi et al., 2011). Increased inflammatory responses are seen in adiponectin-knockout mice, pointing to the crucial role of adiponectin in reducing tissue and systemic inflammation (Summer et al., 2008; Yoshida et al., 2014). Many clinical investigations have discovered lower serum adiponectin levels in adult obese-asthmatic patients when compared to non-obese asthmatics or controls, with a statistically significant connection between BMI and adiponectin (Bianco et al., 2017). Low adiponectin level is especially found in female obese asthmatics as compared to men which imply that adiponectin responds differently in both sexes having a common type of asthma in obese phenotype (Sood et al., 2008). It has recently been revealed that a high BMI and a low level of adiponectin in children may suggest severe asthma (Machado et al., 2022). Although there have been reports of the protective effect of adiponectin on obese asthmatics, however, there are also reports of the negative impacts of adiponectin in the same condition. As per reports, an elevated level of serum adiponectin is linked to adverse clinical outcomes of asthma in men but not in women, however, the study ruled out the association of BMI with the change in absolute forced expiratory volume in 1 s (FEV1) (Sood et al., 2011). The controversies surrounding adiponectin may be due to polymorphisms in the ADIPOQ gene, where rs822396 and the T allele of rs1063537 have been linked to an increased risk of asthma, whereas variants of rs11760956, rs11763517, and rs2167270 have been linked to a protective nature in obese-asthmatics. There is an urgent need to clarify the diverse role played by adiponectin in different asthma and obese phenotypes before targeting adiponectin for therapeutic implications.

2.2.2.2 C1q/TNF-related protein (CTRP) family

A highly conserved family of adiponectin paralogs known as the C1q/TNF-related proteins (CTRP3) is reported to play an important role in obesity-associated comorbidities (Wong et al., 2004). Similarly, to adiponectin, some CTRPs such as CTRP6, CTRP9, and CTRP12 are mainly expressed in adipose tissue (Wong et al., 2008). CTRP3 is reported to inhibit PS-induced expression of macrophage migration inhibitory factor (MIF), MCP-1, and C-C motif chemokine ligand4 (CCL4) in human monocyte-derived macrophages (Weigert et al., 2005). CTRP6 is reported to increase the expression of anti-inflammatory cytokine IL-10 in human monocyte-derived macrophages through the p42/44 mitogen-activated protein kinase (MAPK)-dependent pathway (Kim et al., 2010). Plasma CTRP9 levels are reported to decrease in mouse models of obesity. Additionally, CTRP9 forms heterotrimers with adiponectin and shares the receptor Adipo R1 with adiponectin in vascular endothelial cells and cardiac myocytes (Kim et al., 2010; Kambara et al., 2012; Ohashi et al., 2014). CTRP12 or adipolin is an insulin-sensitizing adipokine that is abundantly produced by AT and whose expression levels decrease in rodent models of obesity (Enomoto et al., 2011). Additionally, adipolin treatment reduced macrophage infiltration and the expression of pro-inflammatory genes in the adipose tissue of obese mice (Alzaim et al., 2020). In a clinical study involving chronic obstructive pulmonary disease (COPD) patients with a BMI of 22.88 ± 2.78 kg/m^2, CTRP-3 and CTRP-5 were found to be elevated in COPD patients however only CTRP-5 was inversely related to FEV1/FVC ratio. The study discovered that CTRPs were statistically unrelated to adiponectin levels, however, like CTRPS, adiponectin was found to be elevated in COPD patients (Li et al., 2015). The elevated level of adiponectin might be due to COPD-

induced hyperinflation, necessitating chronic respiratory muscle exercise to restore normal lung function (Pathak et al., 2020) but the reason behind the elevated expressions of the CTRPs is yet to divulge. Although, there are reports of the effect of CTRPs in obese conditions and in pulmonary conditions like COPD, however, there has been a minimal report on the role of CTRPs in modulating obesity-associated asthma.

2.2.2.3 Omentin

Omentin is a type of adipokine whose levels tend to be lower in obese individuals and are negatively correlated with a measure of arterial stiffness (Shibata et al., 2011; Yoo et al., 2011). Additionally, coronary artery disease prevalence and angiographic severity are adversely correlated with omentin expression (Askin et al., 2020). Omentin increases eNOS activity and reduces TNFα-induced endothelial COX2 expression (Zhong et al., 2012). Omentin-1 has been demonstrated to reduce inflammatory responses in endothelial cells in culture by inhibiting JNK activation via the AMPK/eNOS signalling pathway (Yamawaki et al., 2011). Reports on the role played by omentin in respiratory diseases are inconsistent. Omentin was found to be elevated in the airway epithelial sample of asthma as well as in the circulatory sample of obstructive sleep apnea syndrome and decreased in the airway epithelium sample of COPD (Zhou et al., 2017). A significantly reduced level of circulating omentin was found in a group of none-obese (BMI 23.81 ± 3.57 kg/m^2) patients with severe persistent asthma as compared to the control group which revealed the inverse relationship of omentin to asthma (Zhou et al., 2018). There has been reporting on the decreased level of omentin in obese subjects as well as in non-obese asthmatics, however, a study on the level of omentin in obese asthmatics is not missing in the scientific literature which is the need of the hour to ascertain the role of omentin the later condition.

2.3 Activation of NLRP3 inflammasomes and macrophage polarization

Innate immunity depends on pathogen-associated molecular patterns (PAMPs) and danger-associated molecular patterns (DAMPs), which activate a variety of immune cells including dendritic cells and the inflammasome (Lee et al., 2014). Inflammasomes are multi-protein complexes that are essential for innate immunity and play a role in controlling inflammatory responses that are triggered by infection or cellular injury. There are numerous different types of inflammasomes, including NLRC4, NLRP1, NLRP6, AIM2, and IFI16 (Rathinam et al., 2012), NLRP3, however, is the inflammasome that has received the most attention. The NLRP3 inflammasome is a group of proteins found in immune cells such as macrophages and dendritic cells, as well as other types of cells. The activation of NLRP3 has also been linked to various metabolic and inflammatory conditions such as gout, diabetes, insulin resistance, and obesity. The activation of NLRP3 plays a crucial role in various metabolic conditions however, too much activation of the inflammasome can cause excessive inflammation and damage to tissues, contributing to the development of chronic inflammatory diseases such as asthma (Williams et al., 2021). The activation of inflammasome-mediated reactions is necessary for an appropriate immunological reaction; however, excessive activation can lead to elevated inflammation and tissue damage, affecting the pathogenic mechanisms of chronic inflammatory diseases such as asthma. In a recent study, activation of NLRP3 inflammasome gene expression along with other inflammatory markers like TLR4, and IL-1β were found to exaggerate the asthmatic episode in obese asthmatic patients as compared to non-obese asthmatics which confirms the negative role of NLRP3 in obesity-associated asthma (Wood et al., 2019). The relationship between NLRP3 and asthma was further cemented when the activation of NLRP3 was inhibited by some novel NLRP3 inhibitors or by silencing of NLRP3. There have been reports of reduction of airway hyperresponsiveness (AHR) and airway inflammation in murine models of ovalbumin (OVA)-induced respiratory infections model by NLRP3 inhibitors like MCC950 and AC-YVAD-cho (Kim et al., 2017). Similarly, silencing the NLRP3 gene through short hairpin RNA is reported to reduce NLRP3 mediated IL-1β secretions in human bronchial epithelial cells (Theofani et al., 2019). Macrophages are immune cells that play a role in inflammation and the immune response. The activation state of macrophages, or their "polarization," has been found to significantly influence the development of asthma. When macrophages are recruited to a specific area of the body, they can be activated in one of two ways: a "classically activated" or M1 state, or an "alternatively activated" or M2 state, depending on the local environment (Saradna et al., 2018). Weisberg et al. (2003) and Xu et al. (2003) first described the infiltration of a significant number of macrophages into the adipose tissues of obese persons. M1 macrophages typically produce inflammation through the activation of receptors for TNF-α, IL-1β, and CD36, which leads to the activation of NF-κB and the production of NLRP3 and other pro-inflammatory cytokines such as IL-1β and IL-18. This process, which is known as "priming," sets the stage for further inflammation (Russo and Lumeng, 2018). However, the NLRP3 inflammasome requires a second "hit" or stimulus to assemble and become active. This second stimulus is usually provided by substances such as ceramides, fatty acids, oxidized low-density lipoproteins, and cholesterol crystals, which bind to TLR 2/4 receptors (Rajamaki et al., 2010; Camell et al., 2015; Karasawa et al., 2018; Okla et al., 2018). The claim of the second "hit" by substances for NLRP3 activation was further cemented when microarray data demonstrated a significant increase of ceramide accumulation during M1 macrophage polarization in obese asthmatics. In the same study, M1 macrophage polarization as well as an elevated level of airway hyperresponsiveness (AHR) and C18:0 ceramide levels were observed in obese mice which confirms the role of ceramide or similar substances in the deterioration of obesity-associated asthma (Choi et al., 2020). Finally, sustained activation of NLRP3 leads to the formation of GSDMD pores in the membrane of macrophages (Liu et al., 2016). This process, called "pyroptosis," causes the cell to die and release pro-inflammatory molecules into the surrounding area. It does this by disrupting the osmotic potential inside the cell (Evavold et al., 2018; López-Reyes et al., 2020). M1 macrophages are believed to be beneficial in asthma and make a significant contribution to the pathogenesis of obesity, whereas M2 macrophages are responsible for asthma pathology but restrict the obesity comorbidities

(Sharma et al., 2018). T2 cytokines and the NLRP3 inflammasome, which is responsible for obesity-related asthma, were recently discovered to have a link, making them targets for therapeutic applications (Pinkerton et al., 2022).

2.4 Dysregulated melanocortin pathway

Eosinophil infiltration into the airways, a characteristic of bronchial asthma, is crucial to the pathophysiology of the disease (De Monchy et al., 1985; Bousquet et al., 1990). Although there have been significant advancements in our understanding of the aetiology of this disease over the past 20 years, the therapy of choice is still the same as it was 30 years ago: inhaled 2-adrenoceptor agonists and glucocorticoids. As a result, there is still a very real medical need for treating the disease's symptoms and underlying pathology. Melanocortins may be used to suppress airway inflammation, according to one study. In an OVA-challenged model of airway inflammation, α-Melanocyte-stimulating hormone (α-MSH) reduced eosinophil migration and subsequently IgE, IL-4, and IL-13 levels, but had no effect on IL-5. Although it may appear odd that eosinophils are inhibited but not IL-5, α-MSH inhibits VCAM-1, which is regulated by IL-4 and IL-13, which may account for the decrease in migratory cells. α-MSH can also promote the anti-inflammatory cytokine IL-10, as was previously mentioned with the production of the anti-inflammatory protein heme oxygenase-1 (HO-1) (Lam et al., 2005). Given that α-MSH is inactive in IL-10 null animals, this would seem to be a crucial mechanism for the anti-inflammatory effects of the melanocortin. Very few substances can treat the underlying pathophysiology of bronchial hyperresponsiveness, even though many have been demonstrated to block certain components of the inflammatory response associated with asthma. Since α-MSH suppressed the inflammation as well as cellular migration and cytokine production, it had steroid-like effects (Montague and O'Rahilly, 2000). The central melanocortin system is reported to play important role in obesity and diabetes. Aside from its effects on food intake and body weight, α-MSH has anti-inflammatory activities in both immune cells and non-immune cells (e.g., adipocytes) that express melanocortin receptors which may be a potential target for obesity-associated asthma (Goit et al., 2022).

2.5 Depletion of ROS regulator

The rise in free fatty acid levels boosts adipocyte ROS production by activating NADPH oxidase and decreasing the expression of enzymatic antioxidants, which is correlated with fat adipocyte fat storage (Hattori et al., 2005; Johnson et al., 2007; Devaraj et al., 2008). Anti-inflammatory adiponectin levels decrease and the concentration of pro-inflammatory adipocytokines increases in adipocytes with OS (Soares et al., 2005; Chen et al., 2009). Because there are no accurate ways to measure oxidative stress *in vivo*, most of the evidence indicating the action of ROS in asthma is indirect or circumstantial. The analysis of lipid peroxidation based on diene conjugate and thiobarbituric acid (TBA), measurement of increases in nitric oxide (NO), H_2O_2, and pentane in exhaled gas or breath condensates, and evaluation of substrate oxidisability (or spin trapping) of free radical adducts *ex vivo* all have low sensitivity and specificity. However, utilizing these techniques, it was discovered that adults and children with different asthma severity and acute asthma exacerbations had an increased generation of ROS (Jarjour et al., 1992; Dohlman et al., 1993; Antczak et al., 1997; Olopade et al., 1997; Saleh et al., 1998). Nrf2 is a key regulator in the transcriptional activation of antioxidation and biosynthesis of endogenous antioxidants (Kasai et al., 2020). Nrf2 signals the nucleus during oxidative stress to promote the expression of HO-1, which in turn, protects the lung from oxidative stress (Pathak et al., 2021). Both Nrf2 and HO-1 are reported to be downregulated in obese conditions.

2.6 Notch signaling pathway

Currently, Notch signaling pathway has gained considerable attention as a therapeutic target for obesity-associated asthma. Notch signaling activation is reported to inhibit adipocyte differentiation by suppressing the expression of CCAAT/enhancer binding protein alpha (C/EBPα) and peroxisome proliferator-activated receptor gamma (PPARγ) in the 3T3-L1 preadipocytes (Ross et al., 2004). In obese mice, inactivating Notch1 causes the browning of white adipose tissue and increased expression of UCP1, a key regulator of thermogenesis (Bi et al., 2014). Notch signaling pathway having $CD4^+$ T cell (Th17 cell) is reported to express increased interleukin (IL)-17 in obese asthmatic individuals. In a preclinical study, γ-Secretase inhibitor (GSI) is reported to reduce the Notch1, Th17 cell proportion and serum IL-17 in a diet-induced-obesity-ovalbumin (DIO-OVA) C57BL/6 mice model of asthma (Zeng et al., 2019). Pre-clinical and clinical studies involving Notch signaling pathway reveals that targeting Notch signaling pathway therapeutically may open new avenues in the treatment of obesity-associated asthma in recent times.

2.7 Gut microbiota dysbiosis

Investigating how gut microbiota affects asthma has gained popularity in recent years. Children at risk for developing asthma exhibited considerably reduced relative abundances of the taxa *Faecalibacterium*, *Lachnospira*, *Rothia*, and *Veillonella* (FLVR) in their gut microbiomes at 3 months of age. Increased risk of asthma was linked to higher *Veillonella* abundance and lower *Roseburia*, *Alistipes*, and *Flavonifractor* abundances at 1-year-old age for children with asthma at age 5 (n = 60), albeit the association was only significant for kids whose mothers also had asthma (Stokholm et al., 2018). According to various research, people with asthma had higher concentrations of *Streptococcus pneumoniae*, *Haemophilus influenzae*, *Moraxella catarrhalis*, and *Haemophilus* species in their airway microbiomes (Bisgaard et al., 2007; Hilty et al., 2010; Green et al., 2014). Diet can cause fast microbial alterations in the gut microbiome. According to one study, lifetime vitamin D administration increased the number of *Acinetobacter* operational taxonomic units (OTUs) in the lungs of female mice. The lung microbiota was significantly more altered by allergic airway illness that was brought on by ovalbumin, suggesting that vitamin D's ability to modulate the microbiota may be constrained (Roggenbuck

et al., 2016). According to recent studies, food, gut microbiota, and airway inflammation interact via short chain fatty acids (SCFAs) and pro- or anti-inflammatory cytokines. Additionally, because observational human studies are associative, creating possible prebiotic or probiotic treatments might benefit from employing mouse models that focus on the causative relationships between microbiome dysbiosis and airway pathobiology. Obesity is linked to changes in the gut microbiota (Yuan et al., 2018). According to several studies, obesity in humans is linked to a higher *Firmicutes*/*Bacteroidetes* (F/B) ratio at the phylum level (Rahat-Rozenbloom et al., 2014; Serena et al., 2018). Which bacteria are most impacted by obesity has been the subject of widely varying studies. Lachnospiraceae, *Prevotellaceae*, *Megamonas* spp., *Roseburia* sp., *Veillonellaceae*, *Lactobacillus* spp., *Bacteroides fragilis*, *Faecalibacterium* sp., and a *Prevotella* spp. -dominated enterotype are more prevalent in people with obesity who have microbiota dysbiosis. Additionally, obesity was linked to decreased gene richness, decreased microbiota diversity, and decreased levels of Oscillospiraceae, *Succinivibrio* sp., Odoribacteraceae, Clostridaceae, and *Oscillospira* sp. (Murugesan et al., 2015; Liu et al., 2017). Significant correlations between changes in metabolic syndrome markers and gut microbial dysbiosis have been found in several human cohort studies. After adjusting for age and sex, Fu et al. (2015) found a negative correlation between gut bacterial richness and both BMI and serum triglyceride levels and a positive correlation between gut bacterial richness and serum HDL levels. According to this study's estimates, the makeup of the gut microbiota may account for up to 6% of the variation in independent of age, genetic variables, blood lipid levels, and sex. The gut microbiome affects not only obesity and metabolic syndrome, but also airway inflammation mostly through the production of short-chain fatty acid and cytokine levels and triggers asthma (Kim, 2021). The administration of prebiotics and probiotics are reported to play an important role in the amelioration of obesity-associated asthma through modulation of the gut microbiota. In a recent study, dietary fiber pectin, a prebiotic, demonstrated a promising effect on the O_3-exposed db/db mice model of AHR indicating the importance of targeting gut microbiota in the therapeutic strategy of obesity-associated asthma (Tashiro et al., 2019).

3 Bioactive phytoconstituents in obesity-associated asthma

Obese patients with asthma experience poor asthma control for many reasons, but a crucial one appears to be that their reaction to controller medication is impaired. Many studies have indicated that obese individuals do not respond as effectively to conventional control regimens. It appears that inhaled corticosteroids and combination inhalation corticosteroid-long-acting agonists are superior to montelukast for treating asthma in obese persons (Park et al., 2009). All existing approved asthma drugs were developed using lean animal models of asthma and tested on patient populations that were far slimmer than the typical patient population seen today (Halliwell et al., 1992). Herbs have always been a crucial and valuable treatment option for many persistent health problems, including obesity. Herbs generally have fewer side effects than single-compound drugs, except for allergic reactions in those particularly sensitive to them (Park et al., 2009). There has been a rise in scientific studies assessing the value of substances obtained from herbal medicine, which have traditionally been employed in folk medicine. Plant-based compounds, such as flavonoids, alkaloids, and terpenoids, have been shown to have biological effects *in vitro* and *in vivo*. *Tripterygium wilfordii*, *Hibiscus sabdariffa, Ilex paraguariensis, Coffea arabica, Caralluma fimbriata, Panax ginseng,* plants from solanaceae family, and many others have all been shown to have positive effects on obesity through various mechanisms, such as appetite suppression, triglyceride reduction, metabolic rate increase, pancreatic lipase inhibition, and so on. Therefore, they aid in the process of losing weight (MacNee, 2001; Kannaiyan et al., 2011).

Here we have emphasized the effects of some important bioactive compounds like celastrol, tomatidine, resveratrol, quercetin, ascorbic acid, β-Carotene, chrysophanol, etc. (Figure 2), for treatment of obesity-associated asthma in experimental models and in humans and pointing out some possible mechanisms of action are emphasized.

3.1 Celastrol

Celastrol is an effective natural bioactive component isolated from *T. wilfordii*'s roots. It has proven highly beneficial in anti-inflammatory, anti-cancer, anti-rheumatic, and autoimmune illness (Kannaiyan et al., 2011). In addition, it has been shown to have a remarkable effect on body mass reduction in mice (Lee et al., 2006). Celastrol was reported to cause significant weight loss in a hyperleptinemic DIO mice model through the reduction of food intake, increasing energy expenditure, and leptin sensitivity (Liu et al., 2015). Celastrol has also been shown to lower airway inflammation and AHR in allergic asthma, which is interesting. On a model of obesity and asthma, celastrol therapy reduced the frequency of Th17 cell growth and IL-17A production in the lung and serum. The research study's findings suggested that Th17 and its cytokine, as assessed in the spleen and lung, were strongly linked to AHR. In addition, celastrol inhibits Th17 in obese asthmatic mice, which has been demonstrated to decrease AHR. Celastrol reduces AHR and inhibits Th17 responses in obese asthmatic mice (Zhang et al., 1990).

3.2 Tomatidine

Tomatidine is a steroidal alkaloid under the *Solanaceae* family is obtained from leaves of eggplant, potato, and tomato. *Solanaceae* plants release tomatidine and α-Tomatine to combat fungal infections (Norton, 1998). Tomatidine has demonstrated promising anti-obesity in animal models. In male C57BL/6 mice, tomatidine significantly reduces body weight, fat weight, and regulates other metabolic parameters such as total cholesterol, fasting blood glucose, low-density lipoprotein, and triglyceride levels in serum (Wu et al., 2021). Tomatidine suppresses the reproduction of *Staphylococcus aureus*, according to a previous study. Additionally, tomatidine reduces the invasion activity of A549 human lung adenocarcinoma cells and promotes death in

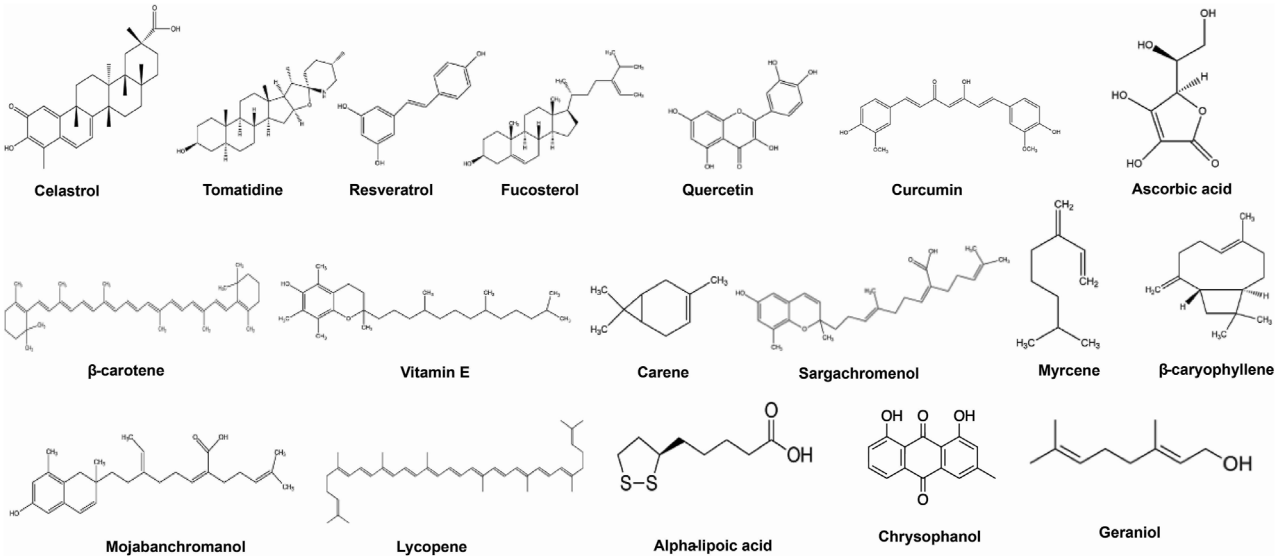

FIGURE 2
Bioactive phytoconstituents targeting obesity-associated asthma.

HL60 human myeloid leukemia cells. Tomatidine inhibits iNOS and COX-2 production by blocking the NF-κB pathway in LPS-stimulated RAW 264.7 cells, according to a study conducted (Steel and Drysdale, 1988). The research found that tomatidine ameliorates the allergic inflammatory response in the airways in asthma by reducing the levels of Th2-associated cytokines, goblet cell hyperplasia, eosinophil infiltration, and AHR. Tomatidine inhibited the generation of Th2 cytokines in bronchoalveolar lavage fluid. In lung tissue, tomatidine inhibited the expression of inflammatory and Th2 cytokine genes. Tomatidine decreased the generation of proinflammatory cytokines and CCL11 in inflammatory BEAS-2B bronchial epithelial cells *in vitro*. These findings suggest that tomatidine ameliorates AHR and eosinophil infiltration in asthmatic mice by inhibiting the inflammatory response and Th2 cell activity (Kuo et al., 2017). The above reports showcase the ameliorative action of tomatidine against both obesity and respiratory diseases like asthma and AHR by targeting various pathways which support the possible therapeutic efficacy of tomatidine against obesity-associated asthma which is yet to explore.

3.3 Curcumin (diferuloylmethane)

Curcumin, the active phytoconstituent in turmeric, is a polyphenol having anti-inflammatory, anti-amyloid, antibacterial, anti-tumor, anti-allergic, and anti-oxidative activities (Kurup and Barrios, 2008). Curcumin has been shown to have potent anti-obesity properties. Curcumin reportedly interacts with white adipose tissue to reduce chronic inflammation, macrophage infiltration, and nuclear factor B (NF-κB) activation. Curcumin also reduces the proinflammatory adipokines tumour necrosis factor (TNF), monocyte chemoattractant protein-1 (MCP-1), and plasminogen activator inhibitor type-1 (PAI-1) and increases adiponectin expression (Bradford, 2013). Curcumin acts as an HDAC activator or inhibits histamine release from mast cells, which reduces the production and level of cytokines like IL-2 and IL-5 in lung tissue (Biswas and Rahman, 2008). Curcumin's ability to regulate asthma phenotypes indicates that it can alleviate asthma symptoms, decrease eosinophil recruitment to the airway, and improve airway hyper-responsiveness, all of which contribute to weight loss. These results suggest curcumin could be an effective adjunct treatment for obesity-related asthma (Brouet and Ohshima, 1995; Mortellini et al., 2000).

3.4 Resveratrol

Resveratrol (3,4,5-trihydroxystilbene) is a phytoalexin present in plant sources, such as grapes, berries, and peanuts as well as known as a component in red wine. Resveratrol is one of the polyphenolic molecules comprised of two phenol rings joined by a 2-carbon methylene bridge with multiple effects on cardiovascular protection, anticancer impact, and as a positive regulator of several areas of metabolism. Resveratrol can eliminate intracellular reactive oxygen species by activating and stabilizing antioxidant enzymes such as catalase, SOD, and glutathione peroxidase hemoxygenase (Das and Das, 2007; Shankar et al., 2007). In addition to its reducing properties, resveratrol has been shown to reduce inflammation by inhibiting prostaglandin production and decreasing the phosphorylation of ERK1/2, cyclooxygenase-2 activity, and the activity of various transcription factors, including NF-B, STAT3, HIF-1α, and β-Catenin (Shankar et al., 2007; Pirola and Fröjdö, 2008). Resveratrol is reported to exert its anti-obesity effect by the browning of WAT as well as by targeting several intracellular components such as sirtuin-1 (SIRT-1), adenosine monophosphate-activated protein kinase (AMPK), and the peroxisome proliferator-activated receptor coactivator-1 (PGC-1)

(Price et al., 2012). Resveratrol can also modulate the innate immune response by inhibiting the expression of costimulatory molecules (CD80 and CD86) and major histocompatibility complex classes I and II in bone marrow-derived dendritic cells and by inhibiting angiogenesis pathway mediated by the expression of MMPs, VEGF, cathepsin D, ICAM-1, and E-selectin. Resveratrol has demonstrated potent ameliorative in obesity-associated asthma effect in experimental animal model. Resveratrol was effective in combating ovalalbumin and obesity-induced oxidative stress in obese asthmatic rat models by inhibiting Keap1 and activating the Nrf2 antioxidant defense system (Li et al., 2018).

3.5 Carotenoids

Carotenoids are a group of pigmented compounds produced by fruits, vegetables, and microorganisms. Carotenoids, which are found as micro-components in fruits and vegetables, are responsible for their yellow, orange, and red colours (Rao and Rao, 2007). β-Carotene, α-Carotene, lycopene, β-Cryptoxanthin and lutein are some of the major dietary carotenoids. In several observational studies, low level of α-Carotene, β-Carotene, and β-Cryptoxanthin has been linked to both asthma as well as obesity (Tobias et al., 2019). Total vitamin A is composed of preformed vitamin A (retinol) and provitamin A molecules, known as carotenoids, with beta-carotene being the most essential. Plants and microbes have carotenoids as pigments (Rao and Rao, 2007). Various studies have revealed that carotenoids may protect or inhibit some types of cancer, atherosclerosis, immunological problems, asthma, and other diseases (Gallicchio et al., 2008; Young et al., 2008). Carotenoids may influence the activation of many transcription factors (Niles 2004). β-Carotene inhibits oxidative stress-induced activation of NF-κB and generation of IL-6, TNF-α, and inflammatory cytokines in cells treated with β-Carotene. Carotenoids may impact the apoptotic process in healthy cells. β-Carotene can boost the expression of the anti-apoptotic protein Bcl-2 in normal cells but the pro-apoptotic protein Bax is downregulated when external stimuli are induced. It has also been demonstrated that lycopene regulates transcription factors. Lycopene inhibits AP-1 binding and reduces the activation of insulin-like growth factor-I in mammary cancer cells (Sharoni et al., 2004). These combined functions of vitamin A and dietary carotenoids make carotenoids an excellent anti-inflammatory agent in the treatment of obesity-associated asthma.

3.6 Vitamin C

Vitamin C (ascorbic acid) is a vital and effective antioxidant in the body's aqueous environment. It exists in two interconvertible biologically active forms, ascorbic acid and its oxidized derivative, dehydro-ascorbic acid (Romieu and Trenga, 2001). As a hydrogen donor, vitamin C reverses oxidation and shields membranes from oxidation (i.e., reducing agent). Vitamin C, also known as ascorbic acid, has been shown to inhibit adipocyte lipolysis, regulate glucocorticoid release from the adrenal glands, inhibit glucose metabolism, modulate glucose metabolism, decrease glycosylation in obese-diabetic models, and reduce the inflammatory response (Garcia-Diaz et al., 2014). A deficiency in vitamin C is related to an increased risk of asthma in obese individuals, who have significantly lower levels of ascorbic acid; conversely, treatment with vitamin C is advantageous for asthmatic adults who smoke, lowering cough and wheezing (Allen et al., 2009). Vitamin C can also regulate factors that affect gene expression, apoptosis, and other cellular processes. It protects against cell death induced by a variety of stressors, and much of the protection is due to its antioxidant capacity (Romieu and Trenga, 2001). Vitamin C controls the AP-1 complex, which consists of the Fos and Jun superfamilies. Vitamin C treatment of cells exposed to UV-B resulted in a 50% decrease in JNK phosphorylation, which activates AP-1 and inhibits the JNK/AP-1 signaling pathways (Catani et al., 2001). Currently, however, the evidence from randomized controlled trials is insufficient to suggest a specific role for vitamin C in the treatment of asthma due to the various study design and typically flawed reporting systems (Kaur et al., 2009).

3.7 Vitamin E

There are eight distinct forms of fat-soluble vitamin E. It consists of a group of chemicals belonging to two closely related families, the tocopherols and tocotrienols, each of which exists in multiple isomeric forms (Riccioni and D'Orazio, 2005). Alpha-tocopherol is the most active form of vitamin E in humans and its primary antioxidant activity is lipid peroxidation prevention (Moriguchi and Muraga, 2000; Devarah et al., 2002). Vitamin E is also reported to ameliorative role in the obese condition. Vitamin E administration reduced oxidative stress, deposition of collagen in the visceral adipose tissue of obese mice, which resulted in a reduction in circulating cytokines and hepatic steatosis, hypertriglyceridemia, and followed by improvement of insulin sensitivity (Alcalá et al., 2015). Vitamin E is well known for playing a potent role in curbing the generation of free radicals which is due to its high concentration in the body among all lipid-soluble vitamins. Vitamin E is associated with a low incidence of asthma in infants as well as in adults. Vitamin E administration during pregnancy is associated with a lower chance of exacerbation of asthma in children (Miyazawa et al., 2019). Vit-E alleviated AHR by lowering Th2 responses, namely, as IL-4, IL-5, IL-13, and OVA-specific IgE, eotaxin, transforming growth factor-1, airway inflammation, lipid peroxidation, and nitric oxide metabolites, and by restoring mitochondrial dysfunction in the lungs (Mabalirajan et al., 2009). Besides, several epidemiological studies have demonstrated the effectiveness of vitamin E supplementation in treating bronchial asthma in obese and non-obese patients (Picado et al., 2001; Troisi et al., 1995; Trenga et al., 2001; Pearson et al., 2004; Pletsityi et al., 1995). However, the exact mechanism underlying the ameliorative role of vitamin E in obese asthmatics is yet to be unearth.

3.8 Alpha-lipoic acid

α-Lipoic acid (ALA), an organosulfur chemical produced from octanoic acid, is also known as thiothic acid. ALA is quickly absorbed from the diet and swiftly transformed into

dihydrolipoic acid (DHLA), its reduced dithiol form. LA and DHLA are both potent antioxidants (Prior and Cao, 2000). Spinach, broccoli, and tomatoes are high in lipoyllysine -containing plant sources. ALA has been demonstrated to drastically lower serum IgE concentration, attenuate Th2 cytokines, IL-4, IL-5, IL-13, and IL-18, and reduce NF-B activation by decreasing intracellular ROS levels in a mouse model of asthma with allergic airway inflammation (Bustamante et al., 1998). In addition, ALA activation connected to VEGF expression, a crucial asthma factor, suppresses the pathogenesis of HIF-1 (Bustamante et al., 1998). These studies demonstrate that ALA is a multifunctional molecule in airway inflammatory illnesses, acting as a potent antioxidant and a regulator of gene expression that induces inflammatory cascades and plasma exudation and promotes the management of obesity (Cao and Phillis, 1995). ALA has demonstrated a marked effect in targeting obesity clinically by reducing body weight and BMI significantly without any effect on waist circumference (Namazi et al., 2018; Vajdi and Abbasalizad Farhangi, 2020). As observed in the animal models, ALA exerted its anti-obesity effect by modulating oxidative stress, and inflammation and by increasing insulin sensitivity in the subcutaneous and visceral adipose tissue of high-fat diet rats (Dajnowicz-Brzezika et al., 2022; Sztolsztener et al., 2022). ALA is reported to play a positive role in the antioxidant level of pulmonary tissue of obese asthmatic mice. The study reported that the administration of ALA combined with L-ascorbic acid to obese C57BL6 mice resulted in the upregulation of the endogenous antioxidant enzymes superoxide dismutase and catalase which demonstrated the antioxidant property of ALA. However, the effect of a single administration of ALA in obese asthmatic animals is reported to date.

3.9 Chrysophanol

Chrysophanol is an anthraquinone reported to found in many plants, insects, and microbes. In plants, chrysophanol was first reported in *Rheum rhabarbarum*, in fungi it was first reported in *Penicillium islandicum* Sopp, however, in insects, chrysophanol was reported to use as a defensive chemical (Yusuf et al., 2019). In animal models, chysophanol has demonstrated potential anti-obesity efficacy. Chrysophenol has been shown to reduce lipid accumulation in HFD rats' primary hepatocytes, reduce inflammation by significantly lowering IL-6 and IL-1 levels, and increase IL-10 levels. Furthermore, the same study found that chrysophanol decreased the expression of lipogenic genes by activating AMP-activated protein kinase (AMPK)/ Sirtuin 1. (SIRT1). Chrysophanol has also demonstrated ameliorative effects in asthma by inhibiting the activation of nuclear factor-kappa B (NF-kB) signaling pathway in animal models (Song et al., 2019). In a recent study involving the systematic pharmacological and bioinformatics analysis, chrysophanol was found to a potential candidate for combating obesity asthma/childhood asthma comorbidities. The study found that chrysophanol It was discovered that chrysophanol regulates inflammation by being involved in the resistance of EGFR tyrosine kinase inhibitor, the HIF-1 signaling pathway, and the trapping of extracellular neutrophils. However, the study emphasized the importance of experimental verification of their claim using *in-vitro*, *in-vivo*, and OMICS technologies (Liu et al., 2023).

3.10 Flavonoids

With more than 8,000 molecules reported, flavonoids are the most important group of low molecular weight polyphenolic secondary plant metabolites. They are found in fruits, vegetables, nuts, seeds, stems, flowers, roots, tea, wine, and coffee, and are prevalent in our diet (Hollman and Katan, 1999). Flavonoids limit the release of histamine and other granule-associated mediators by reducing the activation of basophils and mast cells (Harborne and Williams, 2000). Furthermore, flavonoids suppress the synthesis of IL-4, IL-13, and CD40 ligand, whereas they stimulate the production of novel phospholipid-derived mediators. Quercetin, one of the well-studied flavonoids, inhibits concentration-dependently the eosinophilic secretion of Charcot-Leyden crystal protein and eosinophil cationic protein (Balsano and Alisi, 2009). In addition, quercetin's inhibitory effect on other inflammatory cells appears to be superior to that of any other clinically accessible drug (Middleton et al., 2000). Li et al. (2010) have proven that apigenin displays anti-inflammatory effects in a mouse asthma model and can modify the immune response to allergens toward the T-helper type 1 cell (Th1) profile. These results imply that flavonoids are excellent anti-allergenic and anti-inflammatory medicines for the treatment and prevention of asthma. Vascular alterations are one of the primary factors in the pathophysiology of asthma (Li et al., 2010). The alterations include a rise in vascular permeability, vascular dilation/ engorgement, and vasculogenesis/angiogenesis (Williams and Grayer, 2004). Flavonoids and their related chemicals influence the production of HIF-1, VEGF, matrix metalloproteinases (MMPs), and the epidermal growth factor receptor, but also inhibit the NF-B, PI3K/Akt, and ERK1/2 signaling pathways (Hollman and Katan, 1999). Observations indicate that flavonoids and their related substances block some phases of angiogenesis, including cell migration, microcapillary tube formation, and matrix metallopeptidase (MMP) production.

3.11 Bioactive compounds from marine sources

Fucosterol, a phytosterol derived from the marine brown algae *Padina boryana*, exhibited anti-inflammatory properties via dose-dependently down regulating pro-inflammatory cytokines (IL-1, IL-6, and TNF) and the Nrf2/HO-1 pathway and aid in the process of losing weight in obesity associated asthma (Sohn et al., 2021). Mojabanchromanol (MC), a chromanol isolated from the brown alga *Sargassum horneri*, exhibited anti-oxidant effects via the attenuation of particulate matter-induced oxidative stress, the reduction of the ROS-mediated phosphorylation of MAPK extracellular signal-regulated kinase 1/2 (Erk1/2) and of c-JNK, and the inhibition of the secretion of pro-inflammatory cytokines (The authors proposed that mojabanchromanol be developed as a treatment for airway inflammation caused by particulate matter

(Herath et al., 2020). Sargachromenol, isolated from *S. horneri*, exhibited anti-inflammatory effects in LPS-stimulated RAW 264.7 macrophages, by reducing nitric oxide (NO); and in intracellular reactive oxygen species (ROS), by reducing the mRNA expression levels of inflammatory cytokines (IL-1, IL-6, and TNF-) and by inhibiting the activation of NFκB and MAPK signaling (Herath et al., 2020). Pyrenocine A, which is derived from the marine-derived fungus *Penicillium paxilli*, suppresses pro-inflammatory mediators (TNF- and PGE2) and NFB-related gene expression in LPS-stimulated macrophages (Toledo et al., 2014). Spirulina extract (Immulina®), a high-molecular-weight polysaccharide extract from the Cyanobacterium *Arthrospira platensis* (Spirulina), exhibited anti-inflammatory and inhibitory effects on histamine release from RBL-2H3 mast cells and an induced allergic inflammatory response. Moreover, it has the potential to block the IgE-antigen-complex-induced generation of TNF-, IL-4, leukotrienes, and histamine, and it exhibited promising results in relieving allergic rhinitis symptoms (Appel et al., 2018).

3.12 Bioactive compounds from essential oils

Essential oils from *Citrus paradisi*, *Cymbopogon nardus* L., *Pogostemon cablin* Benth, *Hamelia patens*, *Citrus sinensis* and many more are reported to have promising anti-obesity effects. The anti-obesity effects in those essential oils might be due to the presence of a myriad of bioactive phytoconstituents like α-Pinene, β-Myrcene, geraniol, β-Citronellol, citronellol, α-Patchoulene, β-Patchoulene, carvacrol, linalool, D-limonene (De Blasio et al., 2021; Miya et al., 2021). Along with their anti-obesity potential, these essential oil isolated bioactive phytoconstituents has demonstrated significant efficacy in respiratory diseases like asthma and AHR. Geraniol is reported to ameliorate allergic asthma by reducing eosinophils, Th2 cytokines like IL-4, 5 and 3 and increasing Th1 cytokine like interferon γ, Nrf2 protein expression, and reduced glutathione (Xue et al., 2016). β-Caryophyllene (BCP), a dietary bicyclic sesquiterpene cannabinoid-2 (CB2) receptor-ligand is repoeted to found mainly in the essential oils of *Syzygium aromaticum* (Prashar et al., 2006). BCP suppresses obesity-related AHR by its effects on macrophage polarization (inhibited by activation of AMPK, Nrf2/HO-1 and AdipoR1 and AdipoR2 signaling pathway, upregulation of adiponectin, glucagon-like peptide-1 (GLP-1), interferon-gamma (IFN-γ), superoxide dismutases (SOD), catalase, and downregulation of NF-κ-B, leptin, IL-4, TNF-α, and IL-1). The browning of eWAT through the promotion of thermogenesis and activation of the melanocortin pathway also had a role in the reduction of obesity-related AHR. The findings of the study demonstrated that BCP reduced obesity-related AHR by inhibiting macrophage polarisation, activating AMPK, activating Nrf2/HO-1, increasing AdipoR1 and AdipoR2 expression, and decreasing NFB expression in the lungs of animals (Pathak et al., 2021).

4 Conclusion and prospects

The state of being obese is the reason behind many diseases where obesity is either primarily responsible or exaggerates the ongoing diseased condition. The pathogenesis of asthma in obese individuals is different from the normal weight individuals due to different genotypes and so responds poorly to the conventional asthma treatment. Although several mechanisms have been proposed, however, the exact mechanism behind the exaggeration of asthma in obese asthmatics is yet to unfurl. Studies found that for a better therapeutic outcome in obesity-associated asthma, pathogenesis related to obesity should also be targeted along with the asthma for a better outcome. Herbal medicines are known to possess a myriad of therapeutic approach together with low adverse effects. Although several bioactive phytoconstituents has demonstrated potential efficacy against obesity-associated asthma in pre-clinical models, however their number is less. In depth studies are warranted to decipher the pinpoint mechanisms to design effective therapeutic approach targeting the obesity-associated asthma. Similarly, it is high time to explore promising bioactive phytoconstituents having proven anti-obesity efficacy for amelioration of obesity-associated asthma in clinical setup for better understanding of their mechanism of actions.

Author contributions

MP, KP, and AD: Conception and design. MP, KP, AD, RS, and UG: Writing and revising the manuscript. All authors have contributed to and approved this work.

Acknowledgments

The authors are thankful to Dibrugarh University, Dibrugarh, Assam, India, and Assam Down Town University, Guwahati, Assam, India, for providing all necessary facilities and support to carry out this work.

Conflict of interest

The authors declare that the research was conducted in the absence of any commercial or financial relationships that could be construed as a potential conflict of interest.

Publisher's note

References

Aguilera-Aguirre, L., Bacsi, A., Saavedra-Molina, A., Kurosky, A., Sur, S., and Boldogh, I. (2009). Mitochondrial dysfunction increases allergic airway inflammation. *J. Immunol.* 183 (8), 5379–5387. doi:10.4049/JIMMUNOL.0900228

Al-Mansoori, L., Al-Jaber, H., Prince, M. S., and Elrayess, M. A. (2022). Role of inflammatory cytokines, growth factors and adipokines in adipogenesis and insulin resistance. *Inflammation* 45, 31–44. doi:10.1007/s10753-021-01559-z

Alcalá, M., Sánchez-Vera, I., Sevillano, J., Herrero, L., Serra, D., Ramos, M. P., et al. (2015). Vitamin E reduces adipose tissue fibrosis, inflammation, and oxidative stress and improves metabolic profile in obesity. *Obesity* 23 (8), 1598–1606. doi:10.1002/oby.21135

Aleffi, S., Petrai, I., Bertolani, C., Parola, M., Colombatto, S., Novo, E., et al. (2005). Upregulation of proinflammatory and proangiogenic cytokines by leptin in human hepatic stellate cells. *Hepatology* 42, 1339–1348. doi:10.1002/HEP.20965

Ali, N. H., Rehman, S., Naqvi, M., Reshi, M. R., Gulati, K., and Ray, A. (2023). Withania somnifera extract ameliorates airway inflammation and oxidative stress in ovalbumin-induced bronchial asthma in rats. *S. Afr. J. Bot.* 155, 310–317. doi:10.1016/j.sajb.2023.02.003

Allen, S., Britton, J. R., and Leonardi-Bee, J. A. (2009). Association between antioxidant vitamins and asthma outcome measures: Systematic review and meta-analysis. *Thorax* 64, 610–619. doi:10.1136/thx.2008.101469

Alzaim, I., Hammoud, S. H., Al-Koussa, H., Ghazi, A., Eid, A. H., and El-Yazbi, A. F. (2020). Adipose tissue immunomodulation: A novel therapeutic approach in cardiovascular and metabolic diseases. *Front. Cardiovasc. Med.* 7, 602088. doi:10.3389/fcvm.2020.602088

Antczak, A., Nowak, D., Shariati, B., Król, M., Piasecka, G., and Kurmanowska, Z. (1997). Increased hydrogen peroxide and thiobarbituric acid-reactive products in expired breath condensate of asthmatic patients. *Eur. Respir. J.* 10, 1235–1241. doi:10.1183/09031936.97.10061235

Appel, K., Munoz, E., Navarrete, C., Cruz-Teno, C., Biller, A., and Thiemann, E. (2018). Immunomodulatory and inhibitory effect of Immulina®, and Immunloges® in the ig-E mediated activation of RBL-2H3 cells. A new role in allergic inflammatory responses. *Plants (Basel)* 7 (1), 13. doi:10.3390/plants7010013

Arora, P., Ansari, S. H., and Nainwal, L. M. (2021). Mesua ferrea L. (Calophyllaceae) exerts therapeutic effects in allergic asthma by modulating cytokines production in asthmatic rats. *Turk. J. Bot.* 45 (8), 820–832. doi:10.3906/bot-2111-22

Arora, P., Athari, S. S., and Nainwal, L. M. (2022b). Piperine attenuates production of inflammatory biomarkers, oxidative stress and neutrophils in lungs of cigarette smoke-exposed experimental mice. *Food Biosci.* 49, 101909. doi:10.1016/j.fbio.2022.101909

Arora, P., Nainwal, L. M., Gupta, G., Singh, S. K., Chellappan, D. K., Oliver, B. G., et al. (2022a). Orally administered solasodine, a steroidal glycoalkaloid, suppresses ovalbumin-induced exaggerated Th2-immune response in rat model of bronchial asthma. *Chem. Biol. Interact.* 366, 110138. doi:10.1016/j.cbi.2022.110138

Askin, L., Duman, H., Ozyıldız, A., Tanriverdi, O., and Turkmen, S. (2020). Association between omentin-1 and coronary artery disease: Pathogenesis and clinical research. *Curr. Cardiol. Rev.* 16, 198–201. doi:10.2174/1573403X16666200511085304

Bahceci, M., Gokalp, D., Bahceci, S., Tuzcu, A., Atmaca, S., and Arikan, S. (2007). The correlation between adiposity and adiponectin, tumor necrosis factor α, interleukin-6 and high sensitivity C-reactive protein levels. Is adipocyte size associated with inflammation in adults? *J. Endocrinol. Invest.* 30, 210–214. doi:10.1007/BF03347427

Balsano, C., and Alisi, A. (2009). Antioxidant effects of natural bioactive compounds. *Curr. Pharmaceu. Des.* 15, 3063–3073. doi:10.2174/138161209789058084

Bhatraju, N. K., and Agrawal, A. (2017). Mitochondrial dysfunction linking obesity and asthma. *Ann. Am. Thorac. Soc.* 14 (5), S368–S373. doi:10.1513/ANNALSATS.201701-042AW

Bi, P., Shan, T., Liu, W., Yue, F., Yang, X., Liang, X. R., et al. (2014). Inhibition of Notch signaling promotes browning of white adipose tissue and ameliorates obesity. *Nat. Med.* 20 (8), 911–918. doi:10.1038/nm.3615

Bianco, A., Nigro, E., Monaco, M. L., Matera, M. G., Scudiero, O., Mazzarella, G., et al. (2017). The burden of obesity in asthma and COPD: Role of adiponectin. *Pulm. Pharmacol. Ther.* 43, 20–25. doi:10.1016/j.pupt.2017.01.004

Bisgaard, H., Hermansen, M. N., Buchvald, F., Loland, L., Halkjaer, L. B., Bønnelykke, K., et al. (2007). Childhood asthma after bacterial colonization of the airway in neonates. *N. Engl. J. Med.* 357 (15), 1487–1495. doi:10.1056/NEJMoa052632

Biswas, S., and Rahman, I. (2008). Modulation of steroid activity in chronic inflammation: A novel antiinflammatory role for curcumin. *Mol. Nutr. Food Res.* 52, 987–994. doi:10.1002/mnfr.200700259

Bokarewa, M., Nagaev, I., Dahlberg, L., Smith, U., and Tarkowski, A. (2005). Resistin, an adipokine with potent proinflammatory properties. *J. Immunol.* 174, 5789–5795. doi:10.4049/JIMMUNOL.174.9.5789

Bousquet, J., Chanez, P., Lacoste, J. Y., Barneon, G., Ghavanian, N., Enander, I., et al. (1990). Eosinophilic inflammation in asthma. *N. Engl. J. Med.* 323, 1033–1039. doi:10.1056/NEJM199010113231505

Bradford, P. G. (2013). Curcumin and obesity. *Biofactors* 39 (1), 78–87. doi:10.1002/biof.1074

Brouet, I., and Ohshima, H. (1995). Curcumin, an anti-tumour promoter and anti-inflammatory agent, inhibits induction of nitric oxide synthase in activated macrophages. *Biochem. Biophys. Res. Commun.* 206, 533–540. doi:10.1006/bbrc.1995.1076

Bustamante, J., Lodge, J. K., Marcocci, L., Tritschler, H. J., Packer, L., and Rihn, B. H. (1998). Alpha-lipoic acid in liver metabolism and disease. *Free Radic. Biol. Med.* 24, 1023–1039. doi:10.1016/s0891-5849(97)00371-7

Camell, C. D., Nguyen, K. Y., Jurczak, M. J., Christian, B. E., Shulman, G. I., Shadel, G. S., et al. (2015). Macrophage-specific de Novo synthesis of ceramide is dispensable for inflammasome-driven inflammation and insulin resistance in obesity. *J. Biol. Chem.* 290, 29402–29413. doi:10.1074/jbc.M115.680199

Cannon, B., and Nedergaard, J. (2004). Brown adipose tissue: Function and physiological significance. *Physiol. Rev.* 84, 277–359. doi:10.1152/physrev.00015.2003

Cao, X., and Phillis, J. W. (1995). The free radical scavenger, alpha-lipoic acid, protects against cerebral ischemia-reperfusion injury in gerbils. *Free Radic. Res.* 23, 365–370. doi:10.3109/10715769509065257

Catani, M. V., Rossi, A., Costanzo, A., Sabatini, S., Levrero, M., Melino, G., et al. (2001). Induction of gene expression *via* activator protein-1 in the ascorbate protection against UVinduced damage. *Biochem. J.* 356, 77–85. doi:10.1042/0264-6021:3560077

Cawthorn, W. P., Heyd, F., Hegyi, K., and Sethi, J. K. (2007). Tumour necrosis factor-alpha inhibits adipogenesis via a beta-catenin/TCF4(TCF7L2)-dependent pathway. *Cell Death Differ.* 147, 1361–1373. doi:10.1038/sj.cdd.4402127

Cawthorn, W. P., and Sethi, J. K. (2008). TNF-alpha and adipocyte biology. *FEBS Lett.* 582, 117–131. doi:10.1016/J.FEBSLET.2007.11.051

Chen, B., Wei, J., Wang, W., Cui, G., Zhao, Y., Zhu, X., et al. (2009). Identification of signaling pathways involved in aberrant production of adipokines in adipocytes undergoing oxidative stress. *Arch. Med. Res.* 40, 241–248. doi:10.1016/j.arcmed.2009.03.007

Choi, Y., Kim, M., Kim, S. J., Yoo, H. J., Kim, S. H., and Park, H. S. (2020). Metabolic shift favoring C18: 0 ceramide accumulation in obese asthma. *Allergy* 75 (11), 2858–2866. doi:10.1111/all.14366

Chong, L., Li, H., Zhu, L., and Yu, G. (2021). Regulatory effect of mitoQ on the mtROS-NLRP3 inflammasome pathway in leptin-pretreated BEAS-2 cells. *Exp. Ther. Med.* 21 (5), 466–469. doi:10.3892/etm.2021.9897

Chong, L., Liu, L., Zhu, L., Li, H., Shao, Y., Zhang, H., et al. (2019). Expression levels of predominant adipokines and activations of STAT3, STAT6 in an experimental mice model of obese asthma. *Iran. J. Allergy, Asthma Immunol.* 18, 62–71. doi:10.18502/ijaai.v18i1.631

Chouchani, E. T., Kazak, L., and Spiegelman, B. M. (2019). New advances in adaptive thermogenesis: UCP1 and beyond. *Cell Metab.* 29 (1), 27–37. doi:10.1016/J.CMET.2018.11.002

Curat, C. A., Miranville, A., Sengenes, C., Diehl, M., Tonus, C., Busse, R., et al. (2004). From blood monocytes to adipose tissue-resident macrophages. *Diabetes* 53 (5), 12851292. doi:10.2337/diabetes.53.5.1285

Dajnowicz-Brzezika, P., Żebrowskaa, E., Maciejczykb, M., Zalewskac, A., and Chabowskia, A. (2022). The effect of α-lipoic acid on oxidative stress in adipose tissue of rats with obesity-induced insulin resistance. *Cell Physiol. Biochem.* 56, 239–253. doi:10.33594/000000528

Dalgaard, L. T., and Pedersen, O. (2001). Uncoupling proteins: Functional characteristics and role in the pathogenesis of obesity and Type II diabetes. *Diabetologia* 44, 946–965. doi:10.1007/s001250100596

Das, S., and Das, D. K. (2007). Resveratrol: A therapeutic promise for cardiovascular diseases. *Recent pat.cardiovasc. Drug Discov.* 2, 133–138. doi:10.2174/157489007780832560

De Blasio, A., D'Anneo, A., Lauricella, M., Emanuele, S., Giuliano, M., Pratelli, G., et al. (2021). The beneficial effects of essential oils in anti-obesity treatment. *Int. J. Mol. Sci.* 22 (21), 11832. doi:10.3390/ijms222111832

De Monchy, J. G., Kauffman, H. F., Venge, P., Koeter, G. H., Jansen, H. M., Sluiter, H. J., et al. (1985). Bronchoalveolar eosinophilia during allergeninduced late asthmatic reactions. *Am. Rev. Respir. Dis.* 131, 373–376. doi:10.1164/arrd.1985.131.3.373

Devarah, S., Harris, A., and Jialal, I. (2002). Modulation of monocyte-macrophage function with alpha-tocopherol: Implications for atherosclerosis. *Nutr. Rev.* 60, 8–14. doi:10.1301/002966402760240381

Devaraj, S., Wang-Polagruto, J., Polagruto, J., Keen, C. L., and Jialal, I. (2008). High-fat, energydense, fast-food-style breakfast results in an increase in oxidative stress in metabolic syndrome. *Metab. Clin. Exp.* 57, 867–870. doi:10.1016/j.metabol.2008.02.016

Dohlman, A. W., Black, H. R., and Royall, J. A. (1993). Expired breath hydrogen peroxide is a marker of acute airway inflammation in pediatric patients with asthma. *Am. Rev. Respir.* 148, 955–960. doi:10.1164/ajrccm/148.4_Pt_1.955

Enomoto, T., Ohashi, K., Shibata, R., Higuchi, A., Maruyama, S., Izumiya, Y., et al. (2011). Adipolin/C1qdc2/CTRP12 protein functions as an adipokine that improves glucose metabolism. *J. Biol. Chem.* 286, 34552–34558. doi:10.1074/jbc.M111.277319

Evavold, C. L., Ruan, J., Tan, Y., Xia, S., Wu, H., and Kagan, J. C. (2018). The pore-forming protein gasdermin D regulates interleukin-1 secretion from living macrophages. *Immunity* 48, 35–44. doi:10.1016/J.IMMUNI.2017.11.013

Fantuzzi, G. (2005). Adipose tissue, adipokines, and inflammation. *J. Allergy Clin. Immunol.* 115 (5), 911–919. doi:10.1016/J.JACI.2005.02.023

Friedman, J. M., and Halaas, J. L. (1998). Leptin and the regulation of body weight in mammals. *Nat* 395, 763–770. doi:10.1038/27376

Fu, J., Bonder, M. J., Cenit, M. C., Tigchelaar, E. F., Maatman, A., Dekens, J. A. M., et al. (2015). The gut microbiome contributes to a substantial proportion of the variation in blood lipids. *Circ. Res.* 117 (9), 817–824. doi:10.1161/CIRCRESAHA.115.306807

Fu, S., Liu, L., Han, L., and Yu, Y. (2017). Leptin promotes IL-18 secretion by activating the NLRP3 inflammasome in RAW 264.7 cells. *Mol. Med. Rep.* 16 (6), 9770–9776. doi:10.3892/mmr.2017.7797

Gainsford, T., Willson, T. A., Metcalf, D., Handman, E., Mcfarlane, C., Ng, A., et al. (1996). Leptin can induce proliferation, differentiation, and functional activation of hemopoietic cells. *Proc. Natl. Acad. Sci. U. S. A.* 93, 14564–14568. doi:10.1073/PNAS.93.25.14564

Gallicchio, L., Boyd, K., Matanoski, G., Tao, X. G., Chen, L., Lam, T. K., et al. (2008). Carotenoids and the risk of developing lung cancer: A systematic review. *Am. J. Clin. Nutr.* 88, 372–383. doi:10.1093/ajcn/88.2.372

Gan, L., Guo, K., Cremona, M. L., McGraw, T. E., Leibel, R. L., and Zhang, Y. (2012). TNF-α up-regulates protein level and cell surface expression of the leptin receptor by stimulating its export via a PKC-dependent mechanism. *Endocrinology* 153, 5821–5833. doi:10.1210/EN.2012-1510

Garcia-Diaz, D. F., Lopez-Legarrea, P., Quintero, P., and Martinez, J. A. (2014). Vitamin C in the treatment and/or prevention of obesity. *J. Nutri. Sci. Vitaminol.* 60 (6), 367–379. doi:10.3177/jnsv.60.367

Global Initiative for Asthma (2020). Global strategy for asthma management and prevention. Available at: www.ginasthma.org (Accessed January 27, 2023).

Goit, R. K., Taylor, A. W., and Lo, A. C. Y. (2022). The central melanocortin system as a treatment target for obesity and diabetes: A brief overview. *Eur. J. Pharmacol.* 924, 174956. doi:10.1016/j.ejphar.2022.174956

Green, B. J., Wiriyachaiporn, S., Grainge, C., Rogers, G. B., Kehagia, V., Lau, L., et al. (2014). Potentially pathogenic airway bacteria and neutrophilic inflammation in treatment resistant severe asthma. *PLoS One* 9 (6), e100645. doi:10.1371/journal.pone.0100645

Grunfeld, C., Zhao, C., Fuller, J., Pollock, A., Moser, A., Friedman, J., et al. (1996). Endotoxin and cytokines induce expression of leptin, the ob gene product, in hamsters. *J. Clin. Invest.* 97, 2152–2157. doi:10.1172/JCI118653

Halliwell, B., Gutteridge, J. M., and Cross, C. E. (1992). Free radicals, antioxidants, and human disease: Where are we now? *J. Lab. Clin. Med.* 119, 598–620.

Harborne, J. B., and Williams, C. A. (2000). Advances in flavonoid research since 1992. *Phytochemistry* 55, 481–504. doi:10.1016/s0031-9422(00)00235-1

Harms, M., and Seale, P. (2013). Brown and beige fat: Development, function and therapeutic potential. *Nat. Med.* 19 (10), 1252–1263. doi:10.1038/nm.3361

Hattori, Y., Akimoto, K., Gross, S. S., Hattori, S., and Kasai, K. (2005). Angiotensin-II-induced oxidative stress elicits hypoadiponectinaemia in rats. *Diabetologia* 48, 1066–1074. doi:10.1007/s00125-005-1766-7

He, J., Le, Q., Wei, Y., Yang, L., Cai, B., Liu, Y., et al. (2022a). Effect of piperine on the mitigation of obesity associated with gut microbiota alteration. *Curr. Res. Nutr. Food Sci.* 5, 1422–1432. doi:10.1016/j.crfs.2022.08.018

He, J., Xu, J.-Y., Gu, J., Tong, X., Wan, Z., Gu, Y., et al. (2022b). Piperine is capable of improving pancreatic β-cell apoptosis in high fat diet and streptozotocin induced diabetic mice. *J. Funct. Foods* 88, 104890. doi:10.1016/j.jff.2021.104890

Herath, K., Kim, H. J., Jang, J. H., Kim, H. S., Kim, H. J., Jeon, Y. J., et al. (2020). Mojabanchromanol isolated from Sargassum horneri attenuates particulate matter induced inflammatory responses via suppressing TLR2/4/7-MAPK signaling in MLE-12 cells. *Mar. Drugs* 18 (7), 355. doi:10.3390/md18070355

Hilty, M., Burke, C., Pedro, H., Cardenas, P., Bush, A., Bossley, C., et al. (2010). Disordered microbial communities in asthmatic airways. *PLoS One* 5 (1), e8578. doi:10.1371/journal.pone.0008578

Holcomb, I. N., Kabakoff, R. C., Chan, B., Baker, T. W., Gurney, A., Henzel, W., et al. (2000). FIZZ1, a novel cysteine-rich secreted protein associated with pulmonary inflammation, defines a new gene family. *EMBO J.* 19, 4046–4055. doi:10.1093/EMBOJ/19.15.4046

Hollman, P. C., and Katan, M. B. (1999). Health effects and bioavailability of dietary flavonols. *Free Rad. Res.* 31, S75–S80. doi:10.1080/10715769900301351

Hosny, S. S., Farres, M. N., Melek, N. A., Kamal, S. T., El Najjar, M. R., Abou El Fotoh, R. H., et al. (2021). Assessment of serum levels of adiponectin and resistin in adult patients with asthma: Relation to obesity and disease severity. *Egypt. J. Chest Dis. Tuberc.* 70 (2), 223.

Isakson, P., Hammarstedt, A., Gustafson, B., and Smith, U. (2009). Impaired preadipocyte differentiation in human abdominal obesity: Role of wnt, tumor necrosis factor-alpha, and inflammation. *Diabetes* 58, 1550–1557. doi:10.2337/DB08-1770

Jarjour, N. N., Busse, W. W., and Calhoun, W. J. (1992). Enhanced production of oxygen radicals in nocturnal asthma. *Am. Rev. Respir. Dis.* 146, 905–911. doi:10.1164/ajrccm/146.4.905

Johnson, J. B., Summer, W., Cutler, R. G., Martin, B., Hyun, D-H., Dixit, V. D., et al. (2007). Alternate day calorie restriction improves clinical findings and reduces markers of oxidative stress and inflammation in overweight adults with moderate asthma. *Free Radic. Biol. Med.* 42, 665–674. doi:10.1016/j.freeradbiomed.2006.12.005

Jorge, A. S. B., Jorge, G. C. B., Paraíso, A. F., Franco, R. M. P., Vieira, L. J. T., Hilzenderger, A. M., et al. (2017). Brown and white adipose tissue expression of IL6, UCP1 and SIRT1 are associated with alterations in clinical, metabolic and anthropometric parameters in obese humans. *Exp. Clin. Endocrinol. Diabetes* 125 (3), 163–170. doi:10.1055/s-0042-119525

Kambara, T., Ohashi, K., Shibata, R., Ogura, Y., Maruyama, S., Enomoto, T., et al. (2012). CTRP9 protein protects against myocardial injury following ischemia-reperfusion through AMP-activated protein kinase (AMPK)-dependent mechanism. *J. Biol. Chem.* 287, 18965–18973. doi:10.1074/JBC.M112.357939

Kannaiyan, R., Shanmugam, M. K., and Sethi, G. (2011). Molecular targets of celastrol derived from thunder of god vine: Potential role in the treatment of inflammatory disorders and cancer. *Cancer Lett.* 303 (1), 9–20. doi:10.1016/j.canlet.2010.10.025

Karasawa, T., Kawashima, A., Usui-Kawanishi, F., Watanabe, S., Kimura, H., Kamata, R., et al. (2018). Saturated fatty acids undergo intracellular crystallization and activate the NLRP3 inflammasome in macrophages. *Arterioscler. Thromb. Vasc. Biol.* 38, 744–756. doi:10.1161/ATVBAHA.117.310581

Kasai, S., Shimizu, S., Tatara, Y., Mimura, J., and Itoh, K. (2020). Regulation of Nrf2 by mitochondrial reactive oxygen species in physiology and pathology. *Biomolecules* 10 (2), 320. doi:10.3390/biom10020320

Kaur, B., Rowe, B. H., and Arnold, E. (2009). Vitamin C supplementation for asthma. *Cochrane Database syst.rev.* 1, CD000993. doi:10.1002/14651858.CD000993

Kim, C. H. (2021). Control of lymphocyte functions by gut microbiota-derived short-chain fatty acids. *Cell. Mol. Immunol.* 18 (5), 1161–1171. doi:10.1038/s41423-020-00625-0

Kim, J. A., Wei, Y., and Sowers, J. R. (2008). Role of mitochondrial dysfunction in insulin resistance. *Circ. Res.* 102 (4), 401–414. doi:10.1161/CIRCRESAHA.107.165472

Kim, J. Y., Sohn, J. H., Choi, J. M., Lee, J. H., Hong, C. S., Lee, J. S., et al. (2012). Alveolar macrophages play a key role in cockroach-induced allergic inflammation via TNF-α pathway. *PLoS One* 7, e47971. doi:10.1371/JOURNAL.PONE.0047971

Kim, J. Y., Sohn, J. H., Lee, J. H., and Park, J. W. (2015). Obesity increases airway hyperresponsiveness via the TNF-α pathway and treating obesity induces recovery. *PLoS One* 10 (2), e0116540. doi:10.1371/journal.pone.0116540

Kim, M. J., Lee, W., Park, E. J., and Park, S. Y. (2010). C1qTNF-Related protein-6 increases the expression of interleukin-10 in macrophages. *Mol. Cells* 30, 59–64. doi:10.1007/S10059-010-0088-X

Kim, R. Y., Pinkerton, J. W., Essilfie, A. T., Robertson, A. A., Baines, K. J., Brown, A. C., et al. (2017). Role for NLRP3 inflammasome–mediated, IL-1β–dependent responses in severe, steroid-resistant asthma. *Am. J. Respir. Crit. Care Med.* 196 (3), 283–297. doi:10.1164/rccm.201609-1830OC

Koebnick, C., Fischer, H., Daley, M. F., Ferrara, A., Horberg, M. A., Waitzfelder, B., et al. (2016). Interacting effects of obesity, race, ethnicity and sex on the incidence and control of adult-onset asthma. *Allergy Asthma Clin. Immunol.* 12 (1), 50. doi:10.1186/s13223-016-0155-8

Koves, T. R., Ussher, J. R., Noland, R. C., Slentz, D., Mosedale, M., Ilkayeva, O., et al. (2008). Mitochondrial overload and incomplete fatty acid oxidation contribute to skeletal muscle insulin resistance. *Cell Metab.* 7 (1), 45–56. doi:10.1016/J.CMET.2007.10.013

Kozak, L. P., and Anunciado-Koza, R. (2008). UCP1: Its involvement and utility in obesity. *Int. J. Obes. (Lond).* 32, S32–S38. doi:10.1038/IJO.2008.236

Kuo, C. Y., Huang, W. C., Liou, C. J., Chen, L. C., Shen, J. J., and Kuo, M. L. (2017). Tomatidine attenuates airway hyperresponsiveness and inflammation by suppressing Th2 cytokines in a mouse model of asthma. *Mediat. Inflamm.* 2017, 5261803. doi:10.1155/2017/5261803

Kurup, V. P., and Barrios, C. S. (2008). Immunomodulatory effects of curcumin in allergy. *Mol. Nutr. Food Res.* 52, 1031–1039. doi:10.1002/mnfr.200700293

Kwon, H., and Pessin, J. E. (2013). Adipokines mediate inflammation and insulin resistance. *Front. Endocrinol. (Lausanne).* 4, 71. doi:10.3389/fendo.2013.00071

Lam, C. W., Getting, S. J., and Perretti, M. (2005). *In vitro* and *in vivo* induction of heme oxygenase 1 in mouse macrophages following melanocortin receptor activation. *J. Immunol.* 174, 2297–2304. doi:10.4049/jimmunol.174.4.2297

Le, Y., and Pang, S. (2006). The role of FAM3B in turmorgenesis view project role of resistin in inflammation and inflammation-related diseases. Available at: https://www.researchgate.net/publication/7230027 (Accessed December 29, 2022).

Lee, J. H., Koo, T. H., Yoon, H., Jung, H. S., Jin, H. Z., Lee, K., et al. (2006). Inhibition of NF-kappa B activation through targeting I kappa B kinase by celastrol, a quinone methide triterpenoid. *Biochem. Pharmacol.* 72 (10), 1311–1321. doi:10.1016/j.bcp.2006.08.014

Lee, T.-H., Song, H. J., and Park, C.-S. (2014). Role of inflammasome activation in development and exacerbation of asthma. *Asia Pac. Allergy* 4, 187–196. doi:10.5415/APALLERGY.2014.4.4.187

Li, D., Wu, Y., Tian, P., Zhang, X., Wang, H., Wang, T., et al. (2015). Adipokine CTRP-5 as a potential novel inflammatory biomarker in chronic obstructive pulmonary disease. *Medicine* 94 (36), e1503. doi:10.1097/md.0000000000001503

Li, R. R., Pang, L. L., Du, Q., Shi, Y., Dai, W. J., and Yin, K. S. (2010). Apigenin inhibits allergen-induced airway inflammation and switches immune response in a murine model of asthma.Immunopharmacol. *Immunotoxicology* 32, 364–370. doi:10.3109/08923970903420566

Li, X. N., Ma, L. Y., Ji, H., Qin, Y. H., Jin, S. S., and Xu, L. X. (2018). Resveratrol protects against oxidative stress by activating the Keap-1/Nrf2 antioxidant defense system in obese-asthmatic rats. *Exp. Ther. Med.* 16 (6), 4339–4348. doi:10.3892/etm.2018.6747

Lin, Q., and Johns, R. A. (2020). Resistin family proteins in pulmonary diseases. *Am. J. Physiol. Lung Cell Mol. Physiol.* 319 (3), L422–L434. doi:10.1152/ajplung.00040.2020

Liu, J., Lee, J., Hernandez, M. A. S., Mazitschek, R., and Ozcan, U. (2015). Treatment of obesity with celastrol. *Cell* 161 (5), 999–1011. doi:10.1016/j.cell.2015.05.011

Liu, R., Hong, J., Xu, X., Feng, Q., Zhang, D., Gu, Y., et al. (2017). Gut microbiome and serum metabolome alterations in obesity and after weight-loss intervention. *Nat. Med.* 23 (7), 859–868. doi:10.1038/nm.4358

Liu, X., Bai, L., Li, L., Piao, X., and Yu, J. (2023). *A practical strategy for exploring the pharmacological mechanism of chrysophanol against obesity asthma/childhood asthma comorbidity*. United States: Wiley.

Liu, X., Zhang, Z., Ruan, J., Pan, Y., Magupalli, V. G., Wu, H., et al. (2016). Inflammasome-activated gasdermin D causes pyroptosis by forming membrane pores. *Nat* 535, 153–158. doi:10.1038/nature18629

López-Reyes, A., Martinez-Armenta, C., Espinosa-Velázquez, R., Vázquez-Cárdenas, P., Cruz-Ramos, M., Palacios-Gonzalez, B., et al. (2020). NLRP3 inflammasome: The stormy link between obesity and COVID-19. *Front. Immunol.* 11, 570251. doi:10.3389/fimmu.2020.570251

Lord, G. M., Matarese, G., Howard, J. K., Baker, R. J., Bloom, S. R., and Lechler, R. I. (1998). Leptin modulates the T-cell immune response and reverses starvation-induced immunosuppression. *Nat* 394, 897–901. doi:10.1038/29795

Lumeng, C. N., and Saltiel, A. R. (2011). Inflammatory links between obesity and metabolic disease. *J. Clin. Investig.* 121 (6), 2111–2117. doi:10.1172/jci57132

Luptak, I., Qin, F., Sverdlov, A. L., Pimentel, D. R., Panagia, M., Croteau, D., et al. (2019). Energetic dysfunction is mediated by mitochondrial reactive oxygen species and precedes structural remodeling in metabolic heart disease. *Antioxid. Redox Signal.* 31 (7), 539–549. doi:10.1089/ARS.2018.7707

Mabalirajan, U., Aich, J., Leishangthem, G. D., Sharma, S. K., Dinda, A. K., and Ghosh, B. (2009). Effects of vitamin E on mitochondrial dysfunction and asthma features in an experimental allergic murine model. *J. Appl. Physiology* 107 (4), 1285–1292. doi:10.1152/japplphysiol.00459.2009

Mabalirajan, U., Dinda, A. K., Kumar, S., Roshan, R., Gupta, P., Sharma, S. K., et al. (2008). Mitochondrial structural changes and dysfunction are associated with experimental allergic asthma. *J. Immunol.* 181 (5), 3540–3548. doi:10.4049/JIMMUNOL.181.5.3540

Machado, M. E., Porto, L. C., Alves Galvão, M. G., Sant'Anna, C. C., and Lapa e Silva, J. R. (2022). SNPs, adipokynes and adiposity in children with asthma. *J. Asthma* 60 (3), 446–457. doi:10.1080/02770903.2022.2077218

MacNee, W. (2001). Oxidative stress and lung inflammation in airways disease. *Eur. J. Pharmacol.* 429, 195–207. doi:10.1016/s0014-2999(01)01320-6

McGillis, J. P. (2005). White adipose tissue, inert No more. *Endocrinology* 146, 2154–2156. doi:10.1210/EN.2005-0248

Middleton, E. J., Kandaswami, C., and Theoharides, T. C. (2000). The effects of plant flavonoids on mammalian cells: Implications for inflammation, heart disease, and cancer. *Pharmacol. Rev.* 52, 673–751.

Miya, G., Nyalambisa, M., Oyedeji, O., Gondwe, M., and Oyedeji, A. (2021). Chemical profiling, toxicity and anti-inflammatory activities of essential oils from three grapefruit cultivars from KwaZulu-Natal in South Africa. *Molecules* 26 (11), 3387. doi:10.3390/molecules26113387

Miyazawa, T., Burdeos, G. C., Itaya, M., Nakagawa, K., and Miyazawa, T. (2019). Vitamin E: Regulatory redox interactions. *IUBMB life* 71 (4), 430–441. doi:10.1002/iub.2008

Montague, C. T., and O'Rahilly, S. (2000). The perils of portliness: Causes and consequences of visceral adiposity. *Diabetes* 49, 883–888. doi:10.2337/diabetes.49.6.883

Moriguchi, S., and Muraga, M. (2000). Vitamin E and immunity. *Vitam. Horm.* 59, 305–336. doi:10.1016/s0083-6729(00)59011-6

Mortellini, R., Foresti, R., Bassi, R., and Green, C. J. (2000). Curcumin, an antioxidant and anti-inflammatory agent, induces heme oxygenase-1 and protects endothelial cells against oxidative stress. *Free Radic. Biol. Med.* 28, 1301–1312.

Murugesan, S., Ulloa-Martínez, M., Martínez-Rojano, H., Galván-Rodríguez, F. M., Miranda-Brito, C., Romano, M. C., et al. (2015). Study of the diversity and short-chain fatty acids production by the bacterial community in overweight and obese Mexican children. *Eur. J. Clin. Microbiol. Infect. Dis.* 34 (7), 1337–1346. doi:10.1007/s10096-015-2355-4

Namazi, N., Larijani, B., and Azadbakht, L. (2018). Alpha-lipoic acid supplement in obesity treatment: A systematic review and meta-analysis of clinical trials. *Clin. Nutr.* 37 (2), 419–428. doi:10.1016/j.clnu.2017.06.002

Norton, S. A. (1998). Useful plants of dermatology. III. Corticosteroids, strophanthus, and dioscorea. *J. Am. Acad. Dermatol.* 38, 256–259. doi:10.1016/s0190-9622(98)70245-2

Ohashi, K., Shibata, R., Murohara, T., and Ouchi, N. (2014). Role of anti-inflammatory adipokines in obesity-related diseases. *Trends Endocrinol. Metab.* 25, 348–355. doi:10.1016/j.tem.2014.03.009

Okamatsu-Ogura, Y., Kuroda, M., Tsutsumi, R., Tsubota, A., Saito, M., Kimura, K., et al. (2020). UCP1-dependent and UCP1-independent metabolic changes induced by acute cold exposure in Brown adipose tissue of mice. *Metabolism* 113, 154396. doi:10.1016/j.metabol.2020.154396

Okla, M., Zaher, W., Alfayez, M., and Chung, S. (2018). Inhibitory effects of toll-like receptor 4, NLRP3 inflammasome, and interleukin-1β on white adipocyte browning. *Inflammation* 41, 626–642. doi:10.1007/s10753-017-0718-y

Olopade, C. O., Zakkar, M., Swedler, W. I., and Rubinstein, I. (1997). Exhaled pentane levels in acute asthma. *Chest* 111, 862–865. doi:10.1378/chest.111.4.862

Ouchi, N., Parker, J. L., Lugus, J. J., and Walsh, K. (2011). Adipokines in inflammation and metabolic disease. *Nat. Rev. Immunol.* 112, 85–97. doi:10.1038/nri2921

Palma, G., Sorice, G. P., Genchi, V. A., Giordano, F., Caccioppoli, C., D'Oria, R., et al. (2022). Adipose tissue inflammation and pulmonary dysfunction in obesity. *Int. J. Mol. Sci.* 23 (13), 7349. doi:10.3390/ijms23137349

Park, H. S., Kim, S. R., and Lee, Y. C. (2009). Impact of oxidative stress on lung diseases. *Respirology* 14, 27–38. doi:10.1111/j.1440-1843.2008.01447.x

Pathak, M. P., Das, A., Patowary, P., and Chattopadhyay, P. (2020). Contentious role of 'Good Adiponectin'in pulmonary and cardiovascular diseases: Is adiponectin directed therapy a boon or a bane? *Biochimie* 175, 106–119. doi:10.1016/j.biochi.2020.05.008

Pathak, M. P., Patowary, P., Goyary, D., Das, A., and Chattopadhyay, P. (2021). β-caryophyllene ameliorated obesity-associated airway hyperresponsiveness through some non-conventional targets. *Phytomedicine* 89, 153610. doi:10.1016/j.phymed.2021.153610

Pattnaik, B., Bodas, M., Bhatraju, N. K., Ahmad, T., Pant, R., Guleria, R., et al. (2016). IL-4 promotes asymmetric dimethylarginine accumulation, oxo-nitrative stress, and hypoxic response–induced mitochondrial loss in airway epithelial cells. *J. Allergy Clin. Immunol.* 138 (1), 130–141. doi:10.1016/J.JACI.2015.11.036

Pearson, P. J., Lewis, S. A., Britton, J., and Fogarty, A. (2004). Vitamin E supplements in asthma: A parallel group randomised placebo controlled trial. *Thorax* 59, 652–656. doi:10.1136/thx.2004.022616

Peerboom, S., Graff, S., Seidel, L., Paulus, V., Henket, M., Sanchez, C., et al. (2020). Predictors of a good response to inhaled corticosteroids in obesity-associated asthma. *Biochem. Pharmacol.* 179, 113994. doi:10.1016/j.bcp.2020.113994

Peters, M. C., McGrath, K. W., Hawkins, G. A., Hastie, A. T., Levy, B. D., Israel, E., et al. (2016). Plasma interleukin-6 concentrations, metabolic dysfunction, and asthma severity: A cross-sectional analysis of two cohorts. *Lancet Resp. medi.* 4 (7), 574–584. doi:10.1016/S2213-2600(16)30048-0

Peters, U., Dixon, A. E., and Forno, E. (2018). Obesity and asthma. *J. Allergy Clin. Immunol.* 141 (4), 1169–1179. doi:10.1016/j.jaci.2018.02.004

Picado, C., Deulofeu, R., Lleonart, R., Agusti, M., Mullol, J., Quintó, L., et al. (2001). Dietary.micronutrients/antioxidants and their relationship with bronchial asthma severity. *Allergy* 56, 43–49. doi:10.1034/j.1398-9995.2001.00793.x

Pinkerton, J. W., Kim, R. Y., Brown, A. C., Rae, B. E., Donovan, C., Mayall, J. R., et al. (2022). Relationship between type 2 cytokine and inflammasome responses in obesity-associated asthma. *J. Allergy Clin. Immunol.* 149 (4), 1270–1280. doi:10.1016/j.jaci.2021.10.003

Pirola, L., and Fröjdö, S. (2008). Resveratrol: One molecule, many targets. *IUBMB Life* 60, 323–332. doi:10.1002/iub.47

Pletsityi, K. D., Vasipa, S. B., Daydova, T. V., and Fomina, V. G. (1995). Vitamin E: Immunocorrecting effect in bronchial asthma patients. *Vopr. Med. Khim.* 41, 33–36.

Prashar, A., Locke, I. C., and Evans, C. S. (2006). Cytotoxicity of clove *(Syzygium aromaticum)* oil and its major components to human skin cells. *Cell Prolif.* 39 (4), 241–248. doi:10.1111/j.1365-2184.2006.00384.x

Price, N. L., Gomes, A. P., Ling, A. J., Duarte, F. V., Martin-Montalvo, A., North, B. J., et al. (2012). SIRT1 is required for AMPK activation and the beneficial effects of resveratrol on mitochondrial function. *Cell metab.* 15 (5), 675–690. doi:10.1016/j.cmet.2012.04.003

Prior, R. L., and Cao, G. (2000). Antioxidant phytochemicals in fruits and vegetables: Diet and health implications. *HortScience* 35, 588–592. doi:10.21273/hortsci.35.4.588

Raap, U., Brzoska, T., Sohl, S., Path, G., Emmel, J., Herz, U., et al. (2003). Alpha-melanocyte-stimulating hormone inhibits allergic airway inflammation. *J. Immunol.* 171 (1), 353–359. doi:10.4049/jimmunol.171.1.353

Rahat-Rozenbloom, S., Fernandes, J., Gloor, G. B., and Wolever, T. M. S. (2014). Evidence for greater production of colonic short-chain fatty acids in overweight than lean humans. *Int. J. Obes. (Lond).* 38 (12), 1525–1531. doi:10.1038/ijo.2014.46

Rajamaki, K., Lappalainen, J., Öörni, K., Välimäki, E., Matikainen, S., Kovanen, P. T., et al. (2010). Cholesterol crystals activate the NLRP3 inflammasome in human macrophages: A novel link between cholesterol metabolism and inflammation. *PLoS One* 5, e11765. doi:10.1371/JOURNAL.PONE.0011765

Rao, A. V., and Rao, L. G. (2007). Carotenoids and human health. *Pharmacol. Res.* 55, 207–216. doi:10.1016/j.phrs.2007.01.012

Rathinam, V. A. K., Vanaja, S. K., and Fitzgerald, K. A. (2012). Regulation of inflammasome signaling. *Nat. Immunol.* 134 13, 333–342. doi:10.1038/ni.2237

Riccioni, G., and D'Orazio, N. (2005). The role of selenium, zinc and antioxidant vitamin supplementation in the treatment of bronchial asthma: Adjuvant therapy or not? *Expert Opin. Investig. Drugs* 14, 1145–1155. doi:10.1517/13543784.14.9.1145

Ricquier, D. (2011). Uncoupling protein 1 of Brown adipocytes, the only uncoupler: A historical perspective. *Front. Endocrinol. (Lausanne)* 2, 85. doi:10.3389/fendo.2011.00085

Roggenbuck, M., Anderson, D., Barfod, K. K., Feelisch, M., Geldenhuys, S., Sørensen, S. J., et al. (2016). Vitamin D and allergic airway disease shape the murine lung microbiome in a sex-specific manner. *Respir. Res.* 17 (1), 116. doi:10.1186/s12931-016-0435-3

Romieu, I., and Trenga, C. (2001). Diet and obstructive lung diseases. *Epidemiol. Rev.* 23 (2), 268–287. doi:10.1093/oxfordjournals.epirev.a000806

Ross, D. A., Rao, P. K., and Kadesch, T. (2004). Dual roles for the Notch target gene Hes-1 in the differentiation of 3T3-L1 preadipocytes. *Mol. Cell. Biol.* 24 (8), 3505–3513. doi:10.1128/mcb.24.8.3505-3513.2004

Russo, L., and Lumeng, C. N. (2018). Properties and functions of adipose tissue macrophages in obesity. *Immunology* 155 (4), 407–417. doi:10.1111/imm.13002

Saito, M., Matsushita, M., Yoneshiro, T., and Okamatsu-Ogura, Y. (2020). Brown adipose tissue, diet-induced thermogenesis, and thermogenic food ingredients: From mice to men. *Front. Endocrinol. (Lausanne)* 11, 222. doi:10.3389/fendo.2020.00222

Saleh, D., Ernst, P., Lim, S., Barnes, P. J., and Giaid, A. (1998). Increased formation of the potent oxidant peroxynitrite in the airways of asthmatic patients is associated with induction of nitric oxide synthase: Effect of inhaled glucocorticoid. *FASEB J.* 12, 929–937. doi:10.1096/fasebj.12.11.929

Salvator, H., Grassin-Delyle, S., Brollo, M., Couderc, L.-J., Abrial, C., Victoni, T., et al. (2021). Adiponectin inhibits the production of TNF-α, IL-6 and chemokines by human lung macrophages. *Front. Pharmacol.* 12, 718929. doi:10.3389/fphar.2021.718929

Sánchez-Ortega, H., Jiménez-Cortegana, C., Novalbos-Ruiz, J. P., Gómez-Bastero, A., Soto-Campos, J. G., and Sánchez-Margalet, V. (2022). Role of leptin as a link between asthma and obesity: A systematic review and meta-analysis. *Int. J. Mol. Sci.* 24 (1), 546. doi:10.3390/ijms24010546

Saradna, A., Do, D. C., Kumar, S., Fu, Q. L., and Gao, P. (2018). Macrophage polarization and allergic asthma. *Transl. Res.* 191, 1–14. doi:10.1016/J.TRSL.2017.09.002

Serena, C., Ceperuelo-Mallafré, V., Keiran, N., Queipo-Ortuño, M. I., Bernal, R., Gomez-Huelgas, R., et al. (2018). Elevated circulating levels of succinate in human obesity are linked to specific gut microbiota. *ISME J.* 12 (7), 1642–1657. doi:10.1038/s41396-018-0068-2

Shankar, S., Singh, G., and Srivastava, R. K. (2007). Chemoprevention by resveratrol: Molecular mechanisms and therapeutic potential. *Front. Biosci.* 12, 4839–4854. doi:10.2741/2432

Sharma, N., Akkoyunlu, M., and Rabin, R. L. (2018). Macrophages-common culprit in obesity and asthma. *Allergy* 73 (6), 1196–1205. doi:10.1111/all.13369

Shibata, R., Takahashi, R., Kataoka, Y., Ohashi, K., Ikeda, N., Kihara, S., et al. (2011). Association of a fat-derived plasma protein omentin with carotid artery intima-media thickness in apparently healthy men. *Hypertens. Res.* 34, 1309–1312. doi:10.1038/hr.2011.130

Shim, J.-S., Lee, H.-S., Kwon, H., Kim, M.-H., Cho, Y.-J., and Park, H.-W. (2023). Inhibition of glutaminase 1 activity reverses airway hyperresponsiveness and decreases IL-1β+ M1s and IL-17 producing ILC3s in high-fat diet-fed obese mice. *Am. J. Physiol. Lung Cell Mol. Physiol.* 324 (5), L625–L638. doi:10.1152/ajplung.00181.2022

Sideleva, O., Suratt, B. T., Black, K. E., Tharp, W. G., Pratley, R. E., Forgione, P., et al. (2012). Obesity and asthma: An inflammatory disease of adipose tissue not the airway. *Am. J. Respir. Crit. Care Med.* 186 (7), 598–605. doi:10.1164/rccm.201203-0573oc

Soares, A. F., Guichardant, M., Cozzone, D., Bernoud-Hubac, N., Bouzaidi-Tiali, N., Lagarde, M., et al. (2005). Effects of oxidative stress on adiponectin secretion and lactate production in 3T3-L1 adipocytes. *Free Radic. Biol. Med.* 38, 882–889. doi:10.1016/j.freeradbiomed.2004.12.010

Sohn, S. I., Rathinapriya, P., Balaji, S., Jaya Balan, D., Swetha, T. K., Durgadevi, R., et al. (2021). Phytosterols in seaweeds: An overview on biosynthesis to biomedical applications. *Int. J. Mol. Sci.* 22 (23), 12691. doi:10.3390/ijms222312691

Song, G., Zhang, Y., Yu, S., Lv, W., Guan, Z., Sun, M., et al. (2019). Chrysophanol attenuates airway inflammation and remodeling through nuclear factor-kappa B signaling pathway in asthma. *Phytotherapy Res.* 33 (10), 2702–2713. doi:10.1002/ptr.6444

Sood, A., Cui, X., Qualls, C., Beckett, W. S., Gross, M. D., Steffes, M. W., et al. (2008). Association between asthma and serum adiponectin concentration in women. *Thorax* 63 (10), 877–882. doi:10.1136/thx.2007.090803

Sood, A., Dominic, E., Qualls, C., Steffes, M. W., Thyagarajan, B., Smith, L. J., et al. (2011). Serum adiponectin is associated with adverse outcomes of asthma in men but not in women. *Front. Pharmacol.* 2, 55. doi:10.3389/fphar.2011.00055

Sood, A., and Shore, S. A. (2013). Adiponectin, leptin, and resistin in asthma: Basic mechanisms through population studies. *J. Allergy* 2013. doi:10.1155/2013/785835

Stanford, K. I., Middelbeek, R. J. W., Townsend, K. L., An, D., Nygaard, E. B., Hitchcox, K. M., et al. (2013). Brown adipose tissue regulates glucose homeostasis and insulin sensitivity. *J. Clin. Invest.* 123, 215–223. doi:10.1172/JCI62308

Steel, C. C., and Drysdale, R. B. (1988). Electrolyte leakage from plant and fungal tissues and disruption of liposome membranes by α-tomatine. *Phytochemistry* 27, 1025–1030. doi:10.1016/0031-9422(88)80266-8

Steppan, C. M., Bailey, S. T., Bhat, S., Brown, E. J., Banerjee, R. R., Wright, C. M., et al. (2001). The hormone resistin links obesity to diabetes. *Nat* 409, 307–312. doi:10.1038/35053000

Stokholm, J., Blaser, M. J., Thorsen, J., Rasmussen, M. A., Waage, J., Vinding, R. K., et al. (2018). Maturation of the gut microbiome and risk of asthma in childhood. *Nat. Commun.* 9 (1), 141. doi:10.1038/s41467-017-02573-2

Summer, R., Little, F. F., Ouchi, N., Takemura, Y., Aprahamian, T., Dwyer, D., et al. (2008). Alveolar macrophage activation and an emphysema-like phenotype in adiponectin-deficient mice. *Am. J. Physiol. - Lung Cell. Mol. Physiol.* 294, 1035–1042. doi:10.1152/AJPLUNG.00397.2007

Sztolsztener, K., Hodun, K., and Chabowski, A. (2022). α-lipoic acid ameliorates inflammation state and oxidative stress by reducing the content of bioactive lipid derivatives in the left ventricle of rats fed a high-fat diet. *Biochimica Biophysica Acta (BBA)-Molecular Basis Dis.* 1868 (9), 166440. doi:10.1016/j.bbadis.2022.166440

Tashiro, H., Cho, Y., Kasahara, D. I., Brand, J. D., Bry, L., Yeliseyev, V., et al. (2019). Microbiota contribute to obesity-related increases in the pulmonary response to ozone. *Am. J. Respir. Cell Mol. Biol.* 61(6), 702–712. doi:10.1165/rcmb.2019-0144OC

Taylor, E. B. (2021). The complex role of adipokines in obesity, inflammation, and autoimmunity. *Clin. Sci. (Lond).* 135, 731–752. doi:10.1042/CS20200895

Theofani, E., Semitekolou, M., Morianos, I., Samitas, K., and Xanthou, G. (2019). Targeting NLRP3 inflammasome activation in severe asthma. *J. Clin. Med.* 8 (10), 1615. doi:10.3390/jcm8101615

Tobias, T. A., Wood, L. G., and Rastogi, D. (2019). Carotenoids, fatty acids and disease burden in obese minority adolescents with asthma. *Clin. Exp. Allergy* 49 (6), 838–846. doi:10.1111/cea.13391

Toledo, T. R., Dejani, N. N., Monnazzi, L. G., Kossuga, M. H., Berlinck, R. G., Sette, L. D., et al. (2014). Potent anti-inflammatory activity of pyrenocine A isolated from the marine-derived fungus Penicillium paxilli Ma(G)K. *Mediat. Inflamm.* 2014, 767061. doi:10.1155/2014/767061

Trenga, C., Koenig, J. Q., and Williams, P. V. (2001). Dietary antioxidants and ozone-induced bronchial hyperresponsiveness in adults with asthma. *Arch. Environ. Health.* 56, 242–249. doi:10.1080/00039890109604448

Troisi, R. J., Willett, W. C., Weiss, S. T., Trichopoulos, D., Rosner, B., and Speizer, F. E. (1995). A prospective study of diet and adult-onset asthma. *Am. J. Respir. Crit. Care Med.* 151, 1401–1408. doi:10.1164/ajrccm.151.5.7735592

Tsubota, A., Okamatsu-Ogura, Y., Bariuan, J. V., Mae, J., Matsuoka, S., Nio-Kobayashi, J., et al. (2019). Role of Brown adipose tissue in body temperature control during the early postnatal period in Syrian hamsters and mice. *J. Vet. Med. Sci.* 81 (10), 1461–1467. doi:10.1292/JVMS.19-0371

Tzanavari, T., Giannogonas, P., and Karalis, K. P. (2010). TNF-alpha and obesity. *Curr. Dir. Autoimmun.* 11, 145–156. doi:10.1159/000289203

Vajdi, M., and Abbasalizad Farhangi, M. (2020). Alpha-lipoic acid supplementation significantly reduces the risk of obesity in an updated systematic review and dose response meta-analysis of randomised placebo-controlled clinical trials. *Int. J. Clin. Pract.* 74 (6), e13493. doi:10.1111/ijcp.13493

Vieira, C. P., de Oliveira, L. P., Da Silva, M. B., Andre, D. M., Tavares, E. B. G., Pimentel, E. R., et al. (2020). Role of metalloproteinases and TNF-α in obesity-associated asthma in mice. *Life Sci.* 259, 118191. doi:10.1016/j.lfs.2020.118191

Weigert, J., Neumeier, M., Schäffler, A., Fleck, M., Schölmerich, J., Schütz, C., et al. (2005). The adiponectin paralog CORS-26 has anti-inflammatory properties and is produced by human monocytic cells. *FEBS Lett.* 579, 5565–5570. doi:10.1016/J.FEBSLET.2005.09.022

Weisberg, S. P., McCann, D., Desai, M., Rosenbaum, M., Leibel, R. L., and Ferrante, A. W. (2003). Obesity is associated with macrophage accumulation in adipose tissue. *J. Clin. Invest.* 112, 1796–1808. doi:10.1172/JCI19246

Williams, C. A., and Grayer, R. J. (2004). Anthocyanins and other flavonoids. *Nat. Prod. Rep.* 21, 539–573. doi:10.1039/b311404j

Williams, E. J., Negewo, N. A., and Baines, K. J. (2021). Role of the NLRP3 inflammasome in asthma: Relationship with neutrophilic inflammation, obesity, and therapeutic options. *J. Allergy Clin. Immunol.* 147, 2060–2062. doi:10.1016/j.jaci.2021.04.022

Wong, G. W., Krawczyk, S. A., Kitidis-Mitrokostas, C., Revett, T., Gimeno, R., and Lodish, H. F. (2008). Molecular, biochemical and functional characterizations of C1q/TNF family members: Adipose-tissue-selective expression patterns, regulation by PPAR-γ agonist, cysteine-mediated oligomerizations, combinatorial associations and metabolic functions. *Biochem. J.* 416, 161–177. doi:10.1042/BJ20081240

Wong, G. W., Wang, J., Hug, C., Tsao, T. S., and Lodish, H. F. (2004). A family of Acrp30/adiponectin structural and functional paralogs. *Proc. Natl. Acad. Sci. U. S. A.* 101, 10302–10307. doi:10.1073/PNAS.0403760101

Wood, L. G., Li, Q., Scott, H. A., Rutting, S., Berthon, B. S., Gibson, P. G., et al. (2019). Saturated fatty acids, obesity, and the nucleotide oligomerization domain–like receptor protein 3 (NLRP3) inflammasome in asthmatic patients. *J. Allergy Clin. Immunol.* 143 (1), 305–315. doi:10.1016/j.jaci.2018.04.037

World Health Organization (2021). Cardiovascular diseases (CVDs). Available at: https://www.who.int/news-room/fact-sheets/detail/cardiovascular-diseases (Accessed December 27, 2023).

World Health Organization (2022). World obesity day 2022 – accelerating action to stop obesity. Available at: https://www.who.int/news/item/04-03-2022-world-obesity-day-2022-accelerating-action-to-stop-obesity (Accessed January 3, 2023).

Wu, J., Boström, P., Sparks, L. M., Ye, L., Choi, J. H., Giang, A. H., et al. (2012). Beige adipocytes are a distinct type of thermogenic fat cell in mouse and human. *Cell* 150 (2), 366–376. doi:10.1016/J.CELL.2012.05.016

Wu, S. J., Huang, W. C., Yu, M. C., Chen, Y. L., Shen, S. C., Yeh, K. W., et al. (2021). Tomatidine ameliorates obesity-induced nonalcoholic fatty liver disease in mice. *J. Nutr. Biochem.* 91, 108602. doi:10.1016/j.jnutbio.2021.108602

Xu, H., Barnes, G. T., Yang, Q., Tan, G., Yang, D., Chou, C. J., et al. (2003). Chronic inflammation in fat plays a crucial role in the development of obesity-related insulin resistance. *J. Clin. Invest.* 112, 1821–1830. doi:10.1172/JCI19451

Xue, Z., Zhang, X. G., Wu, J., Xu, W. C., Li, L. Q., Liu, F., et al. (2016). Effect of treatment with geraniol on ovalbumin-induced allergic asthma in mice. *Ann. Allergy, Asthma & Immunol.* 116 (6), 506–513. doi:10.1016/j.anai.2016.03.029

Yamauchi, T., Kamon, J., Ito, Y., Tsuchida, A., Yokomizo, T., Kita, S., et al. (2003). Cloning of adiponectin receptors that mediate antidiabetic metabolic effects. *Nature* 423 (6941), 762–769. doi:10.1038/nature01705

Yamawaki, H., Kuramoto, J., Kameshima, S., Usui, T., Okada, M., and Hara, Y. (2011). Omentin, a novel adipocytokine inhibits TNF-induced vascular inflammation in human endothelial cells. *Biochem. Biophys. Res. Commun.* 408, 339–343. doi:10.1016/J.BBRC.2011.04.039

Yang, M. S., Choi, S., Choi, Y., and Jin, K. N. (2018). Association between airway parameters and abdominal fat measured via computed tomography in asthmatic patients. *Allergy Asthma Immunol. Res.* 10 (5), 503–515. doi:10.4168/aair.2018.10.5.503

Yokota, T., Oritani, K., Takahashi, I., Ishikawa, J., Matsuyama, A., Ouchi, N., et al. (2000). Adiponectin, a new member of the family of soluble defense collagens, negatively regulates the growth of myelomonocytic progenitors and the functions of macrophages. *Blood* 96, 1723–1732. doi:10.1182/BLOOD.V96.5.1723

Yoo, H. J., Hwang, S. Y., Hong, H. C., Choi, H. Y., Yang, S. J., Seo, J. A., et al. (2011). Association of circulating omentin-1 level with arterial stiffness and carotid plaque in type 2 diabetes. *Cardiovasc. Diabetol.* 10, 103–108. doi:10.1186/1475-2840-10-103

Yoshida, S., Fuster, J. J., and Walsh, K. (2014). Adiponectin attenuates abdominal aortic aneurysm formation in hyperlipidemic mice. *Atherosclerosis* 235, 339–346. doi:10.1016/J.ATHEROSCLEROSIS.2014.05.923

Young, C. Y., Yuan, H. Q., He, M. L., and Zhang, J. Y. (2008). Carotenoids and prostate cancer risk. *Mini Rev.Med. Chem.* 8, 529–537. doi:10.2174/138955708784223495

Yuan, Y., Ran, N., Xiong, L., Wang, G., Guan, X., Wang, Z., et al. (2018). Obesity-related asthma: Immune regulation and potential targeted therapies. *J. Immunol. Res.* 2018. doi:10.1155/2018/1943497

Yusuf, M. A., Singh, B. N., Sudheer, S., Kharwar, R. N., Siddiqui, S., Abdel-Azeem, A. M., et al. (2019). Chrysophanol: A natural anthraquinone with multifaceted biotherapeutic potential. *Biomolecules* 9 (2), 68. doi:10.3390/biom9020068

Zeng, Z., Wang, L., Ma, W., Zheng, R., Zhang, H., Zeng, X., et al. (2019). Inhibiting the Notch signaling pathway suppresses Th17-associated airway hyperresponsiveness in obese asthmatic mice. *Lab. Invest.* 99 (12), 1784–1794. doi:10.1038/s41374-019-0294-x

Zhang, L. X., Yu, F. K., Zheng, Q. Y., Fang, Z., and Pan, D. J. (1990). Immunosuppressive and antiinflammatory activities of tripterine. *Yao Xue Xue Bao* 25 (8), 573–577.

Zhong, X., Li, X., Liu, F., Tan, H., and Shang, D. (2012). Omentin inhibits TNF-α-induced expression of adhesion molecules in endothelial cells via ERK/NF-κB pathway. *Biochem. Biophys. Res. Commun.* 425, 401–406. doi:10.1016/J.BBRC.2012.07.110

Zhou, Q., Fu, Y., Hu, L., Li, Q., Jin, M., and Jiang, E. (2018). Relationship of circulating chemerin and omentin levels with Th17 and Th9 cell immune responses in patients with asthma. *J. Asthma* 55 (6), 579–587. doi:10.1080/02770903.2017.1355378

Zhou, Y., Zhang, B., Hao, C., Huang, X., Li, X., Huang, Y., et al. (2017). Omentin-A novel adipokine in respiratory diseases. *Int. J. Mol. Sci.* 19 (1), 73. doi:10.3390/ijms19010073

frontiers | Frontiers in Pharmacology

TYPE Original Research
PUBLISHED 19 May 2023
DOI 10.3389/fphar.2023.1117238

OPEN ACCESS

EDITED BY
Poonam Arora,
Shree Guru Gobind Singh Tricentenary University, India

REVIEWED BY
Abhitinder Kumar,
GD Goenka University, India
Yunsen Zhang,
University of Macau, China
Yahong Chen,
Peking University Third Hospital, China
Lalit Mohan Nainwal,
GD Goenka University, India

*CORRESPONDENCE
Chuanbiao Wen,
wenchuanbiao@cdutcm.edu.cn
Chongcheng Xi,
xichongcheng@bucm.edu.cn
Quansheng Feng,
fengqs118@163.com

RECEIVED 06 December 2022
ACCEPTED 10 May 2023
PUBLISHED 19 May 2023

CITATION
Ye H, He B, Zhang Y, Yu Z, Feng Y, Wen C, Xi C and Feng Q (2023), Herb-symptom analysis of Erchen decoction combined with Xiebai powder formula and its mechanism in the treatment of chronic obstructive pulmonary disease. *Front. Pharmacol.* 14:1117238. doi: 10.3389/fphar.2023.1117238

Herb-symptom analysis of Erchen decoction combined with Xiebai powder formula and its mechanism in the treatment of chronic obstructive pulmonary disease

Hua Ye[1], Beibei He[1], Yujie Zhang[1], Ziwei Yu[2], Yifan Feng[3], Chuanbiao Wen[1]*, Chongcheng Xi[4]* and Quansheng Feng[4]*

[1]School of Intelligent Medicine, Chengdu University of Traditional Chinese Medicine, Chengdu, China, [2]School of Pharmacy, Chengdu University of Traditional Chinese Medicine, Chengdu, China, [3]Pharmaceutics Center, Institute of Medicinal Plant Development, Chinese Academy of Medical Sciences and Peking Union Medical College, Beijing, China, [4]School of Basic Medical Sciences, Chengdu University of Traditional Chinese Medicine, Chengdu, China

Background: In recent years, the incidence and mortality rates of chronic obstructive pulmonary disease (COPD) have increased significantly. Erchen Decoction combined with Xiebai Powder (ECXB) formula is mainly used to treat lung diseases in traditional Chinese medicine (TCM). However, the active ingredients of ECXB formula, COPD treatment-related molecular targets, and the mechanisms are still unclear. To reveal its underlying action of mechanism, network pharmacology, molecular docking, and molecular dynamic (MD) simulation approaches were used to predict the active ingredients and potential targets of ECXB formula in treating COPD. As a result, Herb-Symptom analysis showed that the symptoms treated by both TCM and modern medicine of ECXB formula were similar to the symptoms of COPD. Network pharmacology identified 170 active ingredients with 137 targets, and 7,002 COPD targets was obtained. 120 targets were obtained by intersection mapping, among which the core targets include MAPK8, ESR1, TP53, MAPK3, JUN, RELA, MAPK1, and AKT1. Functional enrichment analysis suggested that ECXB formula might exert its treat COPD pharmacological effects in multiple biological processes, such as cell proliferation, apoptosis, inflammatory response, and synaptic connections, and ECXB formula treated COPD of the KEGG potential pathways might be associated with the TNF signaling pathway, cAMP signaling pathway, and VEGF signaling pathway. Molecular docking showed that ECXB formula treatment COPD core active ingredients can bind well to core targets. MD simulations showed that the RELA-beta-sitosterol complex and ESR1-stigmasterol complex exhibited higher conformational stability and lower interaction energy, further confirming the role of ECXB formula in the treatment of COPD through these core components and core targets. Our study analyzed the medication rule of ECXB formula in the treatment of COPD from a new perspective and found that the symptoms treated by both TCM and modern medicine of ECXB formula were similar to the symptoms of COPD. ECXB formula could treat COPD through multi-component, multi-target, and multi-pathway synergistic effects, providing a scientific basis for further study on the

mechanism of ECXB formula treatment of COPD. It also provides new ideas for drug development.

KEYWORDS

chronic obstructive pulmonary disease, Erchen decoction, Xiebai powder, synergistic mechanism, traditional Chinese medicine, herb-symptom analysis

1 Introduction

Chronic obstructive pulmonary disease (COPD) is a common chronic respiratory disease mainly characterized by incompletely reversible airflow restriction. In Europe and the United States, the prevalence of COPD ranges from 3.4% to 13.4% (Blanco et al., 2018), However, in Asia, its prevalence ranges from 3.5% to 19.1% (Buist et al., 2007). Outpatient visit cost accounts for 15%–41% of the total direct cost in the United States and Europe and 4%–48% of the total direct cost in Asian countries (Rehman et al., 2020), one of the main contributors to the global burden of disease. Hence, an in-depth study on COPD is still an urgent need.

Global Strategy for the Diagnosis, Management, and Prevention of Chronic Obstructive Lung Disease: the GOLD science committee report 2019 Singh et al. (2019) proposed stable COPD treatment methods mainly include smoking cessation, bronchodilator, mucolytic agent, immunomodulator, respiratory function exercise, home oxygen therapy, and nutritional therapy. The above methods can improve the symptoms, respiratory function, and quality of life of patients with stable COPD to a certain extent, but all of them need to be maintained for a long time. Due to the high price of non-invasive ventilators, in addition, some patients believe that the comfort of wearing is not good, poor compliance, lack of knowledge, and other factors limit, little benefit, and increase the economic burden for patients.

COPD belongs to the category of "lung distension" in traditional Chinese medicine (TCM), and TCM has unique advantages in the treatment of COPD. Zhen et al. (2018) confirmed in the systematic evaluation and meta-analysis of TCM tonalizing kidney therapy (Bu shen) in the treatment of stable chronic obstructive pulmonary disease that tonalizing kidney therapy can increase lung capacity and reduce the number of $CD4^+$ and $CD8^+$ lymphocytes in patients with stable chronic obstructive pulmonary disease. Huang et al. (2022) found that the TCM combined with Western medicine (WM) can effectively treat the symptoms related to COPD, the treatment efficiency is significantly improved compared with traditional WM. Therefore, it is very meaningful to study the treatment of COPD with TCM.

Erchen Decoction is composed of Chenpi (*Pericarpium Citri Reticulatae*), Banxia (*Pinellia ternata*), Fulin (*Poria cocos*) and Gancao (*Glycyrrhizae Radix et Rhizome*), Xiebai Powder is composed of Sangbaipi (*Mori cortex*), Digupi (*Lycii Cortex*), Gancao (*Glycyrrhizae radix et rhizome*), Non-glutinous Rice, both TCM formulas have been widely used to treat respiratory diseases (Deng et al., 2020; Zhang et al., 2022). In China, two enduring and effective Chinese classical formulas derived from TCM with a long-standing history spanning centuries, namely, Erchen Decoction combined with Xiebai Powder (ECXB formula), have been extensively employed in treating COPD. Mei and Li (2012) observed the effect of ECXB formula in the treatment of acute exacerbation of COPD and found that the use of this formula can shorten the course of COPD and improve the curative effect. The empirical formula created by famous veteran doctors of TCM is derived from ECXB formula, which can control infection and the accompanied symptoms caused by infection and has good clinical effects in treating COPD (Li and Luo, 2014). So far, the main components, target, and potential synergy mechanism of ECXB formula are not yet clear.

In this study, we aimed to use the SymMap platform to analyze the relationship between the symptoms treated by ECXB formula and the symptoms of COPD. Furthermore, network pharmacology, molecular docking, and molecular dynamic (MD) simulation approaches explore potential targets and mechanisms of ECXB formula for COPD treatment. This study provided a scientific basis for future validation experiments and clinical applications. The detailed flowchart of this study is summarized in Figure 1.

2 Materials and methods

2.1 "Herb-symptom" network construction

SymMap platform (http://www.symmap.org/) (Wu et al., 2019) was utilized to collect related symptoms treated by both TCM and modern medicine of *Pinellia ternata, Pericarpium Citri Reticulatae, Poria cocos, Glycyrrhizae Radix et Rhizome, Lycii cortex*, and *Mori cortex* in the formula of ECXB. Cytoscape 3.9.0 software (Shannon et al., 2003) was used for visual analyses of the network of "Herb-TCM symptoms" and "Herb-modern medicine symptoms." According to the International Clinical Practice Guideline of Chinese Medicine Chronic Obstructive Pulmonary Disease (Li, 2020) and Global Strategy for the Diagnosis, Management, and Prevention of Chronic Obstructive Lung Disease: the GOLD science committee report 2019 (Singh et al., 2019), related COPD symptoms were collected.

2.2 Collection of active ingredients and prediction on targets of ECXB formula

The active ingredients of ECXB formula were searched by the TCM Systems Pharmacology Database and Analysis Platform (TCMSP, https://old.tcmsp-e.com/tcmsp.php) (Ru et al., 2014). Oral bioavailability (OB) (Xu et al., 2012) represents the percentage of an orally administered dose of an unchanged drug that reaches the systemic circulation, which reveals the convergence of the ADME process. High oral bioavailability is often a key indicator to determine the drug-like property of bioactive molecules as therapeutic agents. Drug-likeness (DL) (Tao et al., 2013) is a qualitative concept used in drug design to estimate how "drug-like" a prospective compound is, which helps to optimize

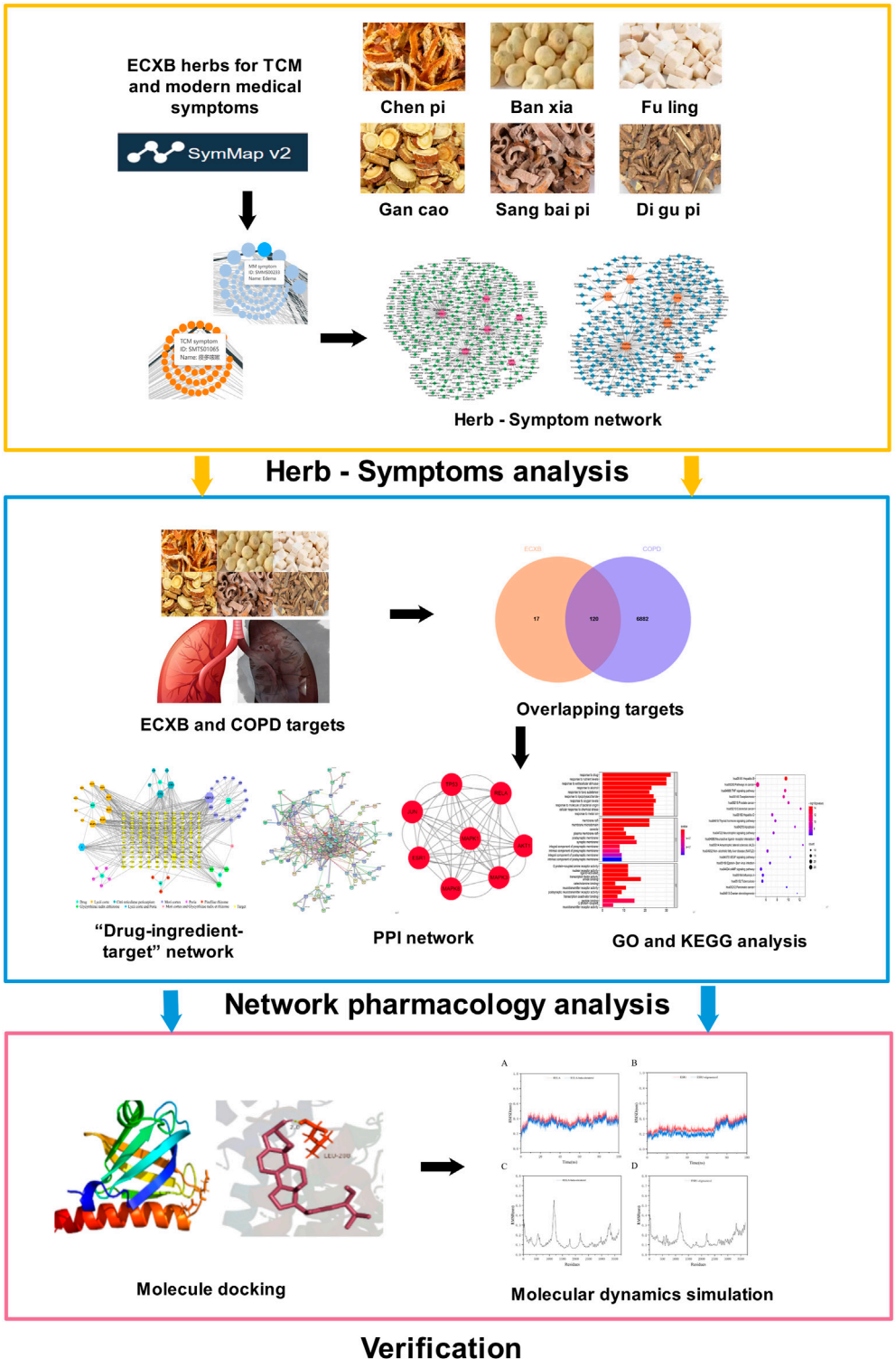

FIGURE 1
The flowchart of this study is based on Herb-Symptom analysis, network pharmacology, molecular docking, and molecular dynamics simulation for deciphering the potential mechanisms of ECXB formula treatment COPD.

pharmacokinetic and pharmaceutical properties, such as solubility and chemical stability. The "drug-like" level of the compounds is 0.18, which is used as a selection criterion for the "drug-like" compounds in traditional Chinese herbs. Therefore, the active ingredients were screened according to the following criteria: OB ≥ 30% and DL ≥ 0.18. Using the PubChem database (https://pubchem.ncbi.nlm.nih.gov/) (Kim et al., 2021), the SMILE number corresponding to the active ingredients screened from the TCMSP

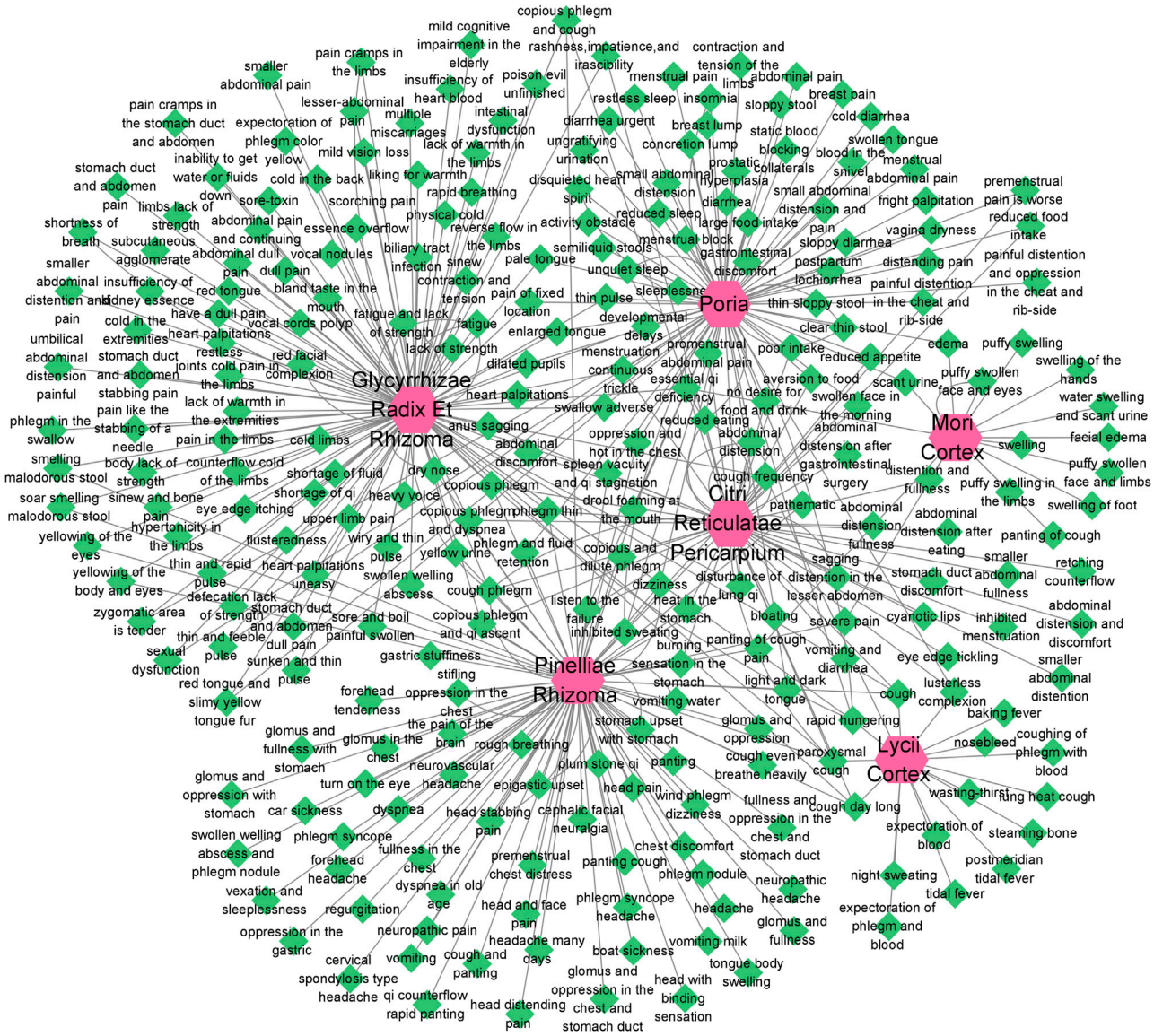

FIGURE 2
"Herb-TCM Symptom" network diagram. The pink node represents herbs, while green nodes show the TCM Symptoms.

database was downloaded. The SMILE structure of active ingredients was uploaded to the Swiss Target Prediction database (http://www.swisstargetprediction.ch/) (Daina et al., 2019) for target prediction. The predicted targets of active ingredients were obtained and integrated. UniProt database (https://www.uniprot.org/) (Bateman et al., 2021) was used for standardized and unified processing of target names, and the species was limited to "HUMAN."

2.3 Collection of disease target and prediction of intersection target

By taking "Chronic obstructive pulmonary diseases" as the keyword, the related targets were searched in the GeneCards® database (https://www.genecards.org) (Safran et al., 2021) and OMIM ® database (https://omim.org/) (Amberger et al., 2015). The predicted targets of ECXB formula were mapped to the related targets of COPD, and the common targets of ECXB formula in the treatment of COPD were obtained and further visualized using a Venn diagram.

2.4 "Drug-ingredient-target" network and core active ingredients screening

The common targets of ECXB formula in the treatment of COPD have imported into Cytoscape 3.9.0 software, the network diagram of "Drug-ingredient-target" was constructed, and the core active ingredients were screened according to the degree value ranking.

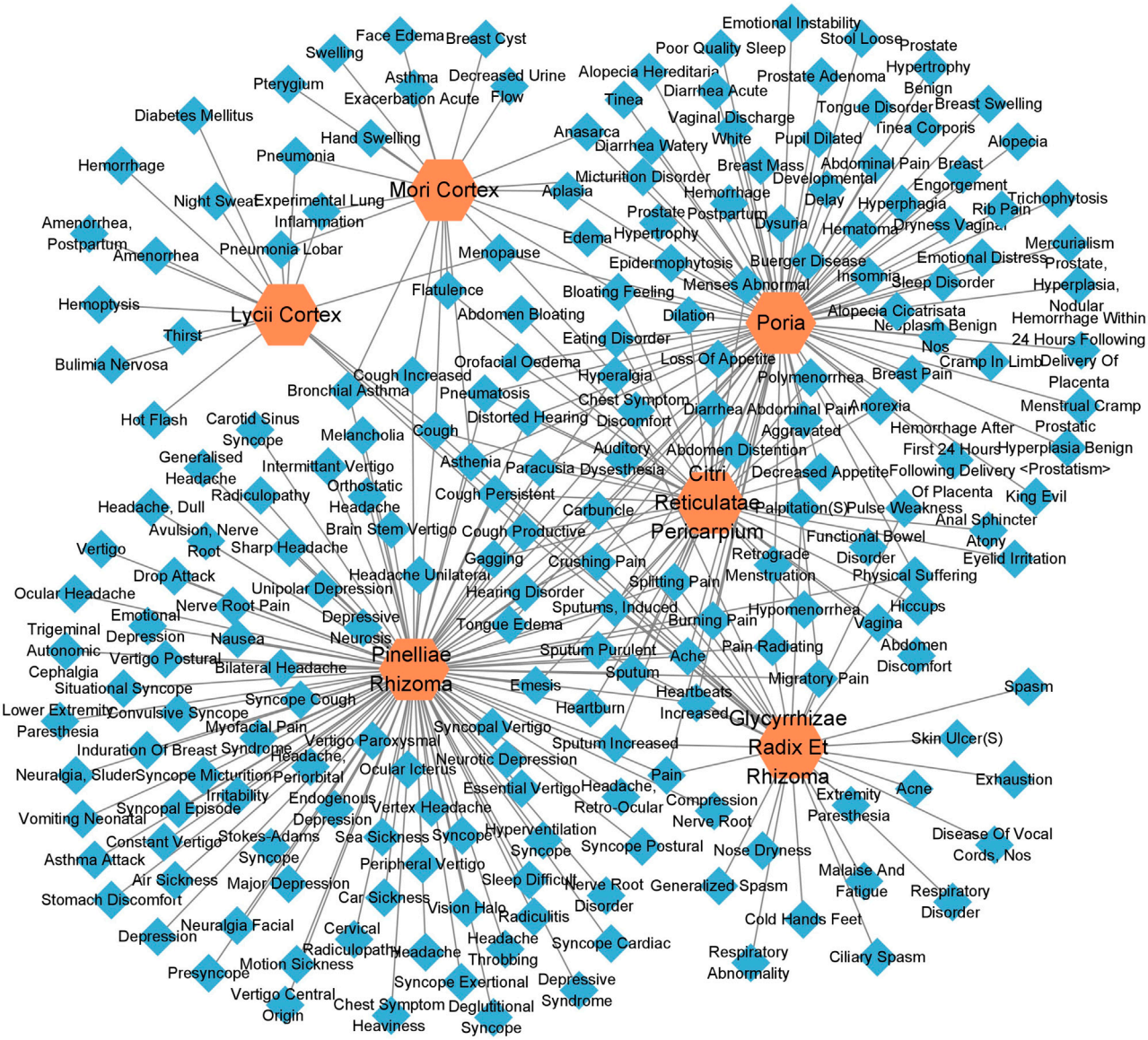

FIGURE 3
"Herb-modern medicine Symptom" network diagram. The orange node represents herbs, while the blue nodes show modern medicine Symptoms.

2.5 PPI network construction and screening of core protein targets

The intersection target of ECXB formula in the treatment of COPD was imported into the STRING online website (https://cn.string-db.org/) (Szklarczyk et al., 2019), and the protein type was set as "*Homo sapiens*", the highest confidence parameter score was greater than 0.7, and other parameters were set as default values (network type: full STRING network, meaning of network edges: evidence). The core network of ECXB formula for the treatment of COPD protein interaction was constructed, and the TSV file was exported. Node1, node2, and the combined score in the TSV file were imported into Cytoscape 3.9.0 software, mapping interaction networks, and screening core protein targets.

2.6 Enrichment analysis of GO and KEGG

Gene Ontology (GO) analysis and Kyoto Encyclopedia of Gene and Genome (KEGG) pathway analysis for ECXB formula in the treatment of COPD targets were conducted by using the DAVID database (https://david.ncifcrf.gov/) (Huang et al., 2009b; Sherman et al., 2022). The results of the two analysis methods were mapped in the form of histograms and bubbles by using Bioinformatics online platform (http://www.bioinformatics.com.cn/) (Huang et al., 2009a).

2.7 Molecular docking verification

In the PDB database (https://www.rcsb.org/) (Berman, 2000), the crystal structure of the core target protein was selected and its "PDB"

TABLE 1 Symptoms targeted by TCM and modern medicine as well as COPD symptoms.

Herb	Symptoms treated by TCM	Symptoms treated by modern medicine	COPD symptoms
Pinelliae rhizome	Cough, panting, stifling oppression in the chest	Cough, Sputum, Hyperventilation Syncope	Dyspnea
Poria	The lusterless complexion, edema, phlegm, and fluid retention	Tongue Edema, Anasarca, Sputum	Coughing up phlegm
Glycyrrhizae radix et rhizome	cough phlegm, fatigue and lack of strength, lack of warmth in the limbs	Cough Persistent, Sputum, Malaise and Fatigue, Respiratory Disorder, Extremity Paresthesia	Chronic cough
Citri reticulatae pericarpium	cough phlegm, reduced eating	Sputum Increased, Loss Of Appetite	Loss of appetite
Mori cortex	panting of cough, puffy swollen face and limbs, scant urine	Asthma Exacerbation Acute, Bronchial Asthma, Face Edema	Chest breathing
Lycii cortex	tidal fever, night sweating, lung heat cough, expectoration of phlegm and blood	Pneumonia, Night Sweat, Hot Flash, Cough Persistent	Other symptoms

TABLE 2 Basic information on some active ingredients of ECXB formula.

Herb	MOL Id	Ingredients	OB (%)	DL
Pinelliae rhizome	MOL001755	24-Ethylcholest-4-en-3-one	36.08	0.76
	MOL002670	Cavidine	35.64	0.81
	MOL002714	baicalein	33.52	0.21
	MOL002776	Baicalin	40.12	0.75
Citri reticulatae	MOL000359	sitosterol	36.91	0.75
pericarpium	MOL004328	naringenin	59.29	0.21
Poria	MOL000290	Poricoic acid A	30.61	0.76
	MOL000291	Poricoic acid B	30.52	0.75
	MOL000276	7,9(11)-dehydropachymic acid	35.11	0.81
	MOL000289	pachymic acid	33.63	0.81
Glycyrrhizae	MOL004835	Glypallichalcone	61.6	0.19
radix et rhizome	MOL004841	Licochalcone B	76.76	0.19
	MOL004996	icos-5-enoic acid	30.7	0.2
Lycii cortex	MOL001552	OIN	45.97	0.19
	MOL001645	Linoleyl acetate	42.1	0.2
	MOL001689	acacetin	34.97	0.24
Mori cortex	MOL012692	kuwanon D	31.09	0.8
	MOL012689	beta-sitosterol	36.79	0.87
	MOL000358	sanggenone H	36.91	0.75
	MOL012755	campest-5-en-3beta-ol	37.5	0.53
	MOL005043	sanguinarine	37.58	0.71
	MOL001474	moracin M-6,3′-di-O-β-D-glucopyranoside	37.81	0.86

(Erchen Decoction is composed of P*inelliae rhizome, Citri reticulatae pericarpium, Poria, and Glycyrrhizae radix et rhizome*. Xiebai Powder is composed of Glycyrrhizae radix et rhizome, Lycii cortex, and Mori cortex.).

format file was downloaded. The core active ingredients in the "2D SDF" structure were downloaded from the PubChem database and imported into Chem3D 18.0 for their optimization. The PDB files of ligand molecules were imported into AutoDock Tools for processing, and saved as a PDBQT format file for later use. AutoDock 4.2 was used to dock the processed active ingredients with the core target protein

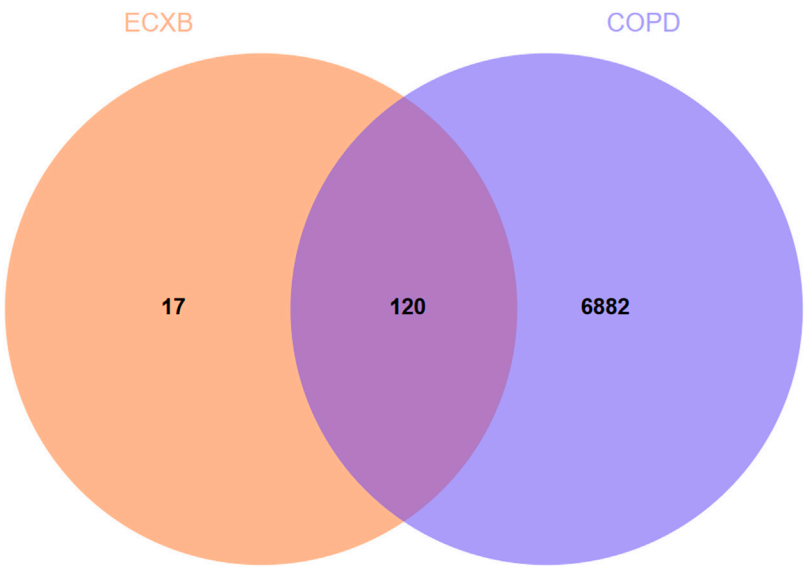

FIGURE 4
Venn diagram of ECXB formula combined with COPD. The Venn map showed that 120 targets were shared between ECXB formula and COPD.

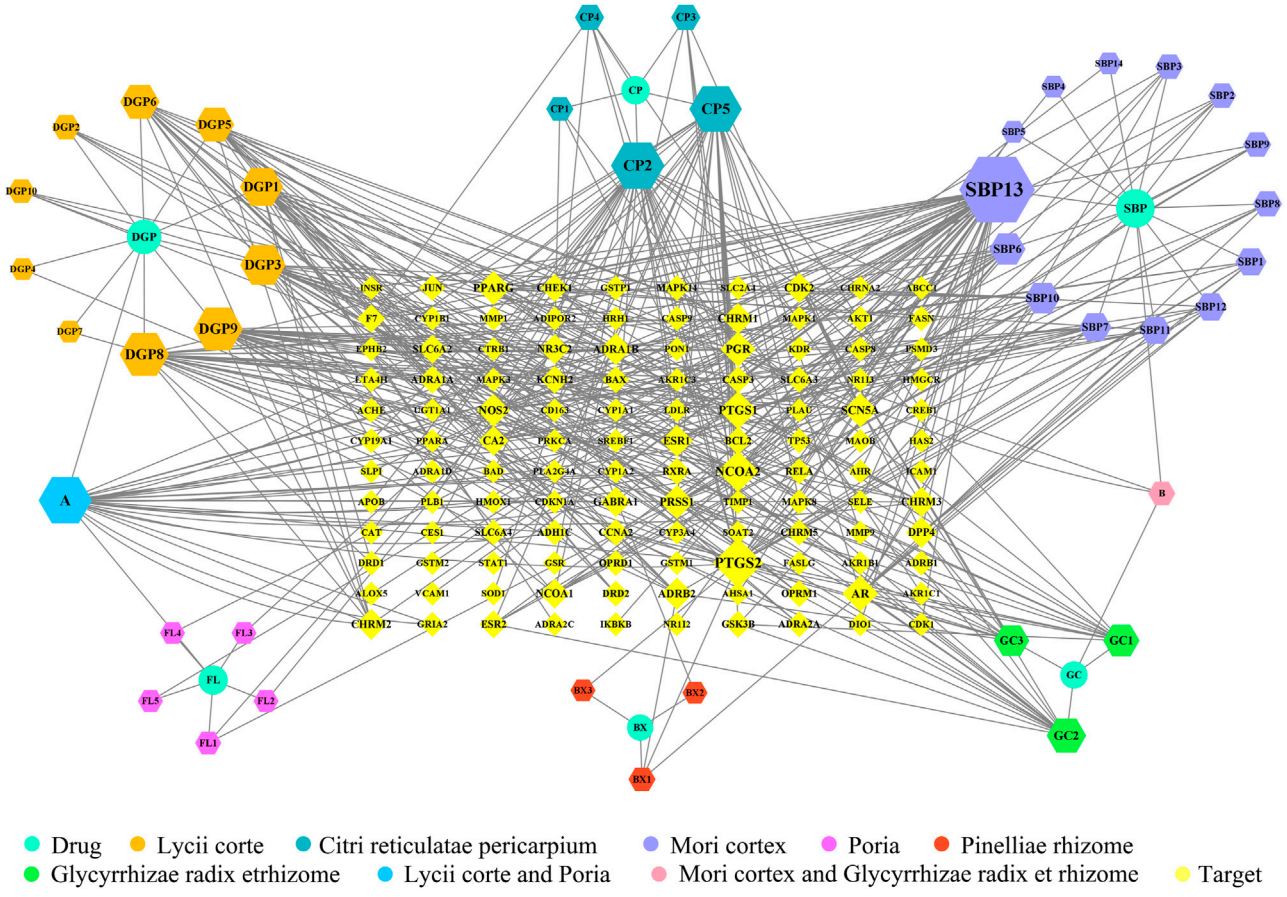

FIGURE 5
"Drug-ingredient-target" network diagram of ECXB formula in the treatment of COPD. The node size and node label size are determined by the node degree value. The higher the degree value, the larger will be the node and label.

TABLE 3 Core Ingredients of ECXB formula.

Molid	Ingredients	Degree	Number	Drug
MOL000422	kaempferol	52	51	*Mori cortex*
MOL000296	hederagenin	30	14	*Poria, Lycii cortex*
MOL004328	naringenin	30	29	*Citri reticulatae pericarpium*
MOL005828	nobiletin	29	28	*Citri reticulatae pericarpium*
MOL000358	beta-sitosterol	26	25	*Lycii cortex*
MOL000449	Stigmasterol	26	25	*Lycii cortex*
MOL001689	acacetin	22	21	*Lycii cortex*
MOL001552	OIN	20	19	*Lycii cortex*
MOL002219	Atropine	16	15	*Lycii cortex*
MOL002222	sugiol	16	15	*Lycii cortex*

(Morris et al., 2009). Using the minimum binding energy as the docking result of the target protein and ligand, the Pymol 2.5.2 software (https://pymol.org/2/) was used for observation and mapping.

2.8 Molecular dynamics simulation

GROMACS (2020.3) (Van Der Spoel et al., 2005) was used to analyze the MD simulation to check the stability of the protein-ligand complexes. The docking models of the complexes on the top two molecular docking results were used as the initial conformation for MD simulations. The root mean square deviation (RMSD) of each complex was analyzed to measure the stability of the complex system according to the degree of the molecular structure change. The root mean square fluctuation (RMSF) of the identified complexes was analyzed to understand the relative fluctuation of proteins. The receptor-ligand binding free energy was calculated using the Molecular Mechanics Poisson–Boltzmann Surface Area (MMPBSA) method in the 25 ns MD simulation trajectory.

3 Results

3.1 Analysis of "herb-symptom" network

According to the information related to symptoms treated by both TCM and modern medicine of diseases treated by herbs in the formula of ECXB collected on the SymMap platform, a total of 258 TCM symptoms were obtained, including 93 symptoms treated by *Pinelliae rhizome*, 54 by *Citri reticulatae pericarpium*, 84 by *Poria*, 116 by *Glycyrrhizae radix et rhizome*, 16 by *Lycii cortex*, and 16 by *Mori cortex*, as shown in Figure 2 (Supplementary Table S1). A total of 207 symptoms were treated by modern medicine, including 104 by *Pinelliae rhizome*, 37 by *Citri reticulatae pericarpium*, 81 by Poria, 33 by *Glycyrrhizae radix et rhizome*, 16 by *Lycii cortex*, and 21 by Mori cortex, as shown in Figure 3 (Supplementary Table S2). Symptoms targeted by TCM and modern medicine as well as COPD symptoms are shown in Table 1. It was found that the symptoms treated by both TCM and modern medicine of ECXB formula were the same as those of COPD patients with dyspnea, coughing up phlegm, chronic cough, and chest breathing, indicated that ECXB formula treatment for COPD is consistent with symptomatic treatment of TCM.

3.2 Acquisition of active ingredients and predicted targets

According to the screening procedure, a total of 1,314 active ingredients of ECXB formula were obtained from TCMSP, including 386 in Pinelliae rhizome, 147 in Citri reticulatae pericarpium, 69 in Poria, 75 in Glycyrrhizae radix et rhizome, 239 in Lycii cortex, and 398 in Mori cortex. Guiding by the ADME and DL standard (OB threshold ≥30% and DL threshold ≥0.18), 170 active ingredients were obtained after removing duplicated compounds. Among them, 13 were extracted from Pinelliae rhizome, 5 in Citri reticulatae pericarpium, 15 in Poria, 92 in Glycyrrhizae radix et rhizome, 13 in Lycii cortex, and 32 in Mori cortex (Supplementary Table S3). Partial results are listed in Table 2. 137 prediction targets of ECXB formula were obtained from the Swiss Target Prediction platform.

3.3 Acquisition of targets for COPD and prediction of intersection target

A total of 7002 COPD-related targets were collected from GeneCards® and OMIM ® databases (Supplementary Table S4). The predicted targets of ECXB formula were intersected with COPD-related targets, then 120 potential targets of ECXB formula for the treatment of COPD were obtained, and Venn diagrams were drawn in Figure 4 (Supplementary Table S5).

3.4 Analysis of the "drug-ingredient-target" network and screening of core active ingredients

The 120 overlapping targets of ECXB formula and COPD as well as these targets corresponding ingredients were imported into

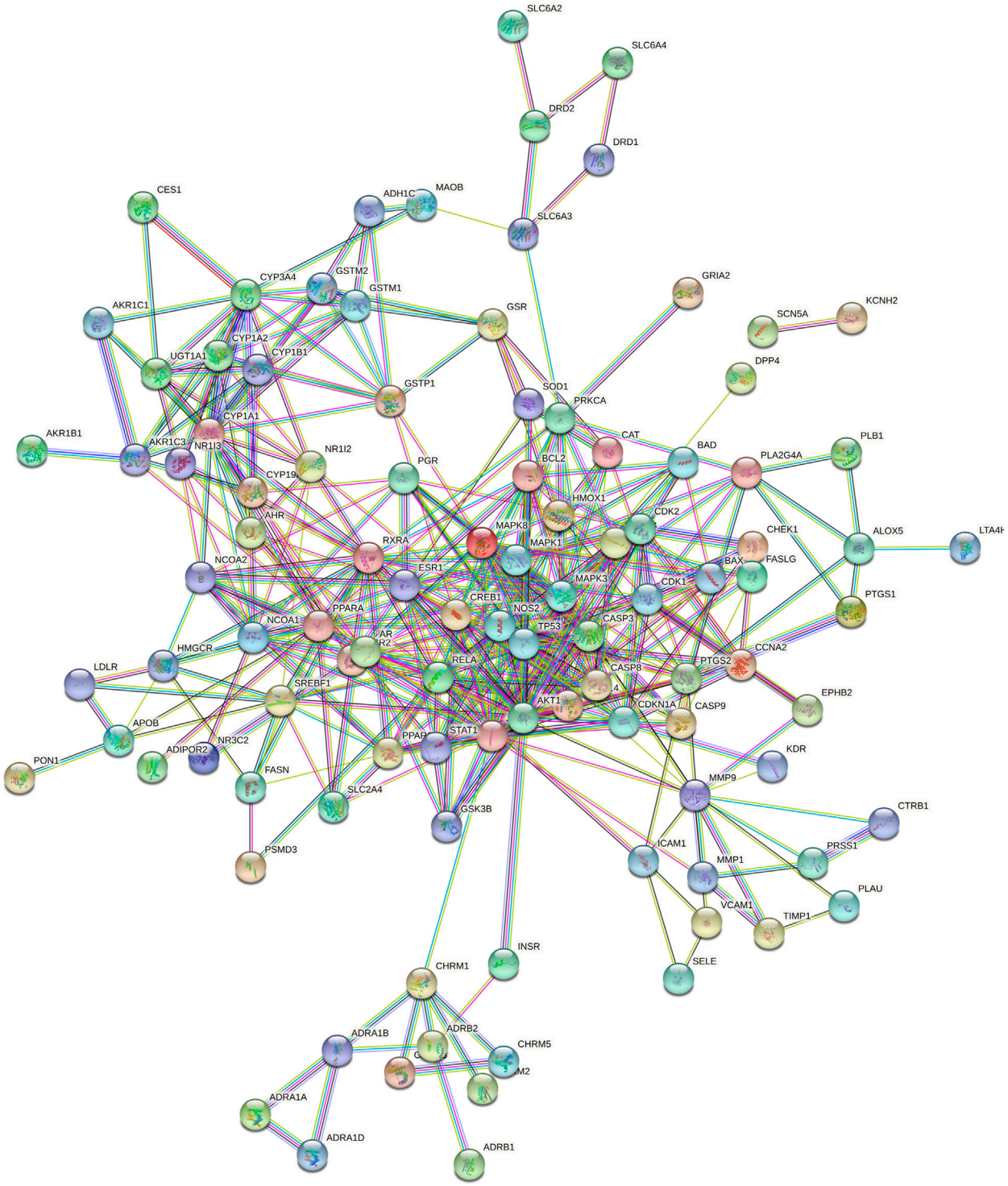

FIGURE 6
Protein interaction network diagram. 120-node and 424-edge PPI network of potential targets of the ECXB formula working on COPD was acquired at the String database.

Cytoscape software to construct a "Drug-ingredient-target" network. As shown in Figure 5, nodes in the network diagram represented drugs, active ingredients, and targets. The edges indicated that the nodes can interact with each other. The top 10 active ingredients of degree value were selected as the core ingredients, including kaempferol, hederagenin, naringenin, nobiletin, beta-sitosterol, stigmasterol, acacetin, OIN, atropine, and sugiolas (Table 3).

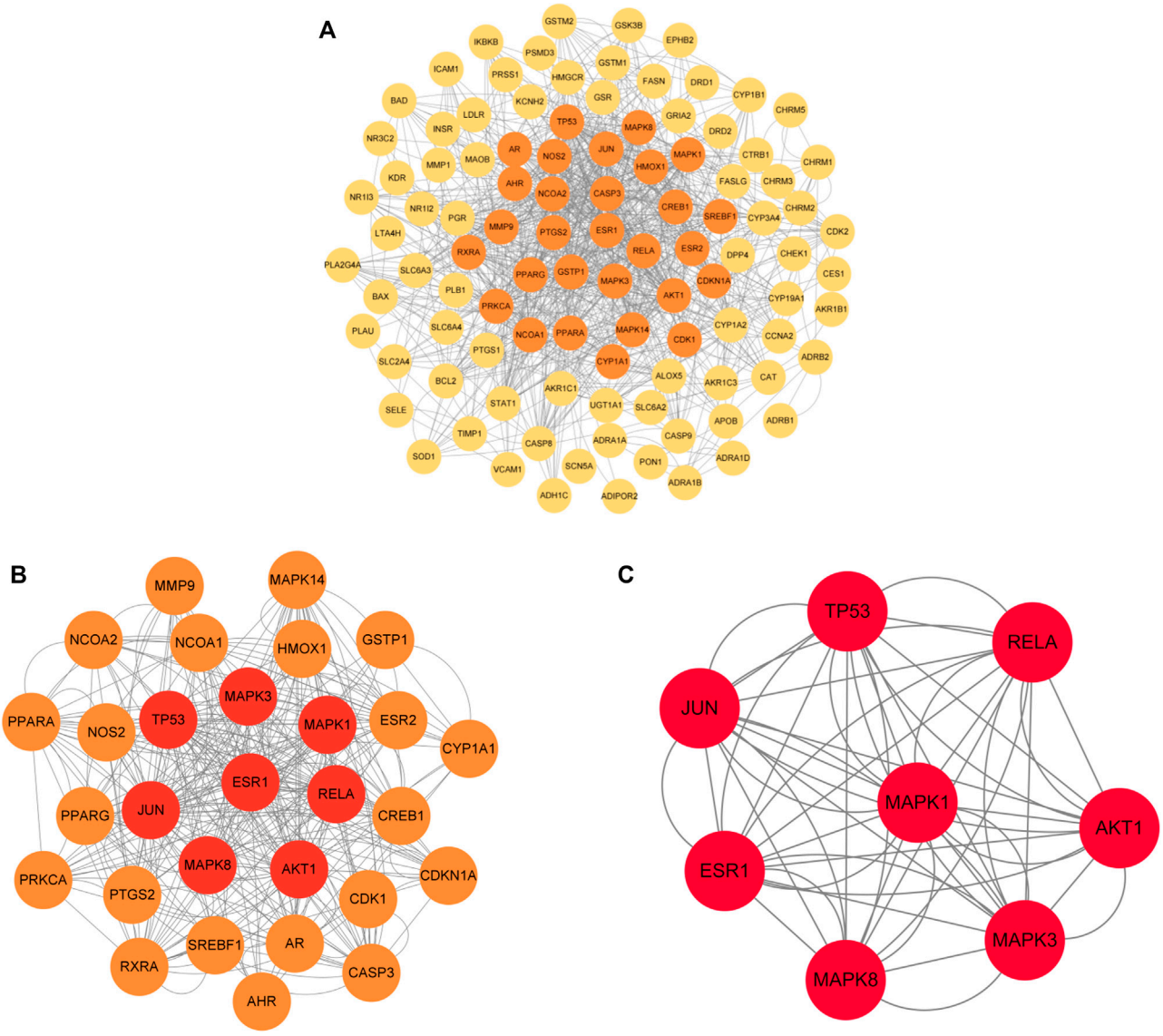

FIGURE 7
Core protein interaction network. **(A)** Interactive PPI network of ECXB formula-related targets and COPD-related targets. **(B)** PPI network of significant proteins extracted from **(A)**. **(C)** PPI network of candidate COPD targets for ECXB formula treatment extracted from **(B)**.

3.5 Analysis of PPI network and screening of core targets

The 120 intersecting targets were imported into the STRING database, and the obtained information was imported into Cytoscape software to construct a PPI network between ECXB formula and the treatment of COPD, as shown in Figure 6. Using Cytoscape CytoNCA, under the condition that the values of DC, BC, CC, EC, LAC, and NC were all greater than their corresponding median values (Supplementary Tables S6–S8). Among them, 8 core targets were screened, including MAPK8, ESR1, TP53, MAPK3, JUN, RELA, MAPK1, and AKT1, as shown in Figure 7.

3.6 Analysis of GO and KEGG pathway

The intersecting targets of ECXB formula for the treatment of COPD were imported into the DAVID database to screen GO entries and KEGG signaling pathways of $p < 0.01$. GO functional enrichment analysis was performed under the conditions of Count ≥ 4, $p \leq 0.01$, FDR (False Discovery Rate) ≤0.01, and a total of 563 results were obtained. There were 403 Biological Processes (BPs), 109 Molecular Functions (MFs), and 51 Cellular Components (CCs) (Supplementary Table S9). The top 10 results of count values were selected to draw a histogram, as shown in Figure 8.

KEGG pathway analysis showed that the intersecting targets mapped 87 KEGG signaling pathways (Supplementary Table S10),

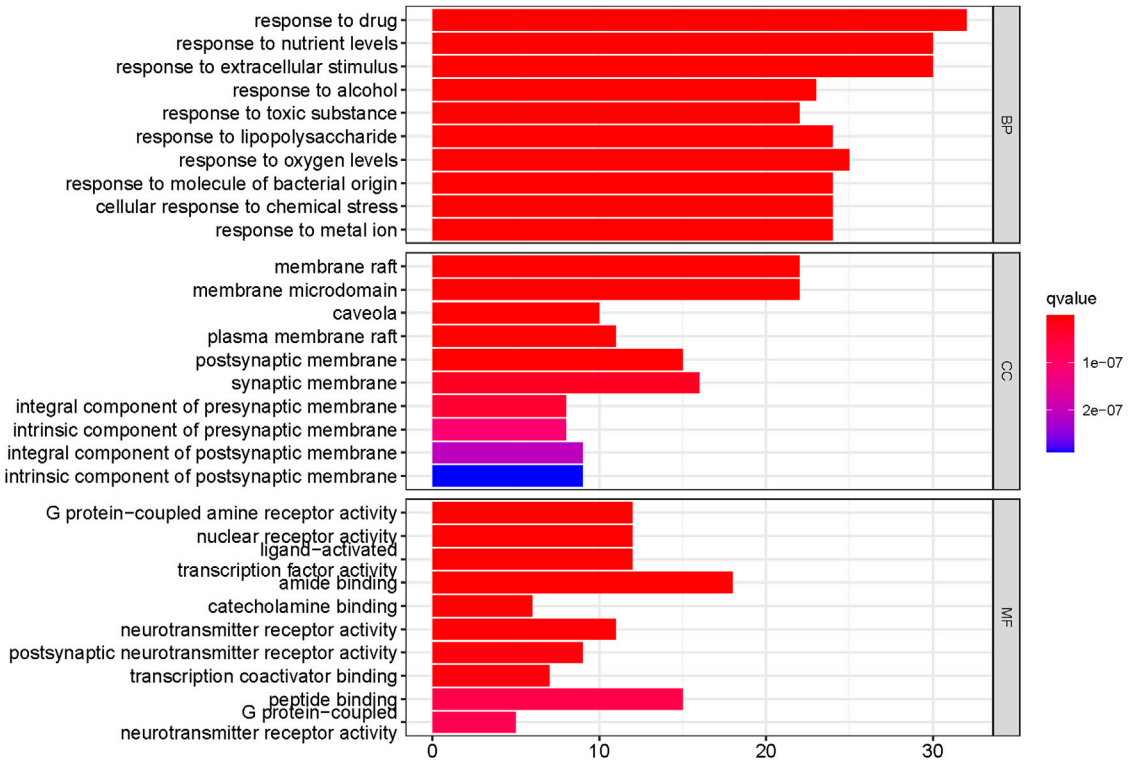

FIGURE 8
Functional enrichment analysis of the top 10 in GO. The Y-axis shows the enriched GO items of target genes. The X-axis shows the gene counts for the items. The color indicates the q value.

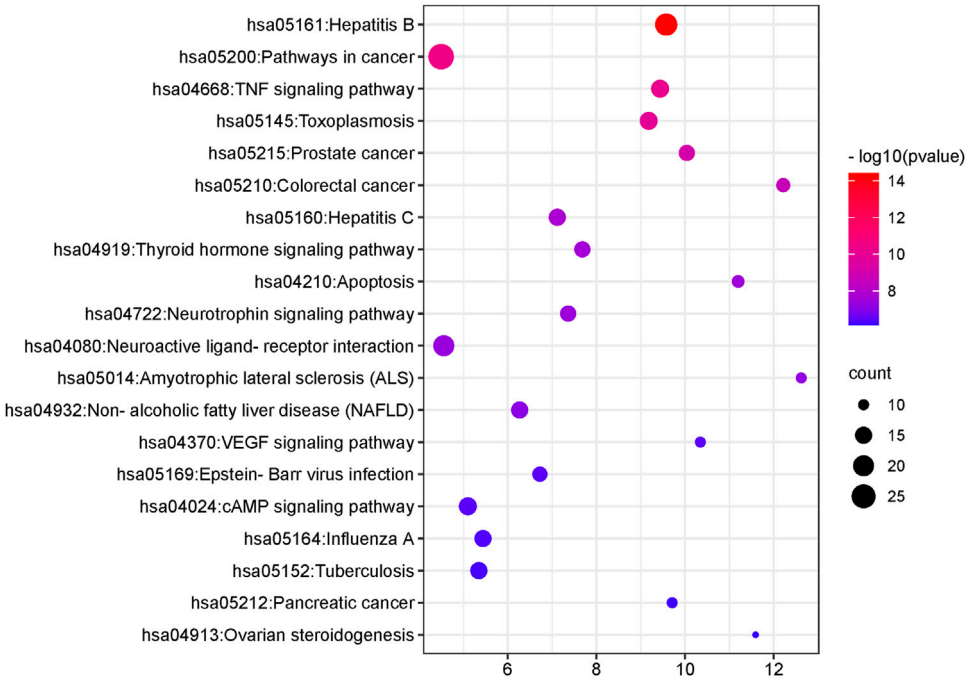

FIGURE 9
The first 20 KEGG pathways. The Y-axis shows the enriched KEGG pathways for target genes. The X-axis shows the gene counts for the items. The color indicates the *p*-value.

TABLE 4 KEGG pathway analysis for the treatment of COPD.

ID	Pathway	*p*-value	Count
hsa05417	Lipid and atherosclerosis	4.70E-20	28
hsa05207	Chemical carcinogenesis - receptor activation	5.73E-18	26
hsa05161	Hepatitis B	2.18E-17	23
hsa05215	Prostate cancer	1.26E-14	17
hsa01524	Platinum drug resistance	4.25E-14	15
hsa05160	Hepatitis C	3.44E-13	19
hsa04668	TNF signaling pathway	2.19E-12	16
hsa05145	Toxoplasmosis	2.19E-12	16
hsa04933	AGE-RAGE signaling pathway in diabetic complications	5.43E-12	15
hsa05418	Fluid shear stress and atherosclerosis	5.67E-12	17
hsa05167	Kaposi sarcoma-associated herpesvirus infection	1.58E-11	19
hsa05208	Chemical carcinogenesis - reactive oxygen species	2.22E-11	20
hsa04932	Non-alcoholic fatty liver disease	3.36E-11	17
hsa01522	Endocrine resistance	5.74E-11	14
hsa05162	Measles	6.40E-11	16
hsa05210	Colorectal cancer	1.40E-10	13
hsa05169	Epstein-Barr virus infection	2.76E-10	18
hsa05222	Small cell lung cancer	3.35E-10	13
hsa04657	IL-17 signaling pathway	4.42E-10	13
hsa05212	Pancreatic cancer	4.43E-10	12
hsa04210	Apoptosis	4.89E-10	15
hsa05170	Human immunodeficiency virus 1 infection	6.10E-10	18
hsa04722	Neurotrophin signaling pathway	8.17E-10	14
hsa04919	Thyroid hormone signaling pathway	1.02E-09	14
hsa04370	VEGF signaling pathway	6.63E-09	10
hsa04936	Alcoholic liver disease	8.48E-09	14
hsa05163	Human cytomegalovirus infection	1.14E-08	17
hsa05152	Tuberculosis	2.41E-08	15
hsa05022	Pathways of neurodegeneration - multiple diseases	2.64E-08	24
hsa04913	Ovarian steroidogenesis	2.71E-08	9

and the top 20 pathways were selected to draw a bubble map, as shown in Figure 9. Detailed data are shown in Table 4. The targets and 20 pathways were imported into Cytoscape to construct a "target-pathway" network (Figure 10). Therefore, the network analysis suggested that ECXB formula may play a therapeutic role in COPD treatment by regulating signaling pathways, including the TNF signaling pathway, cAMP signaling pathway, VEGF signaling pathway, Hepatitis B Pathways, and Hepatitis C Pathways, suggesting that these pathways may mediate the treatment of COPD. Among them, the TNF signaling pathway was the KEGG pathway with a large number of gene enrichment and obvious significance. The visualization analysis of the TNF signaling pathway is shown in Figure 11.

3.7 Analysis of molecular docking

The selected top ten active ingredients included hederagenin (MOL000296), beta-sitosterol (MOL000358), kaempferol (MOL000422), Stigmasterol (MOL000449), OIN (MOL001552), acacetin (MOL001689), Atropine (MOL002219), surgical (MOL002222), naringenin (MOL004328), and nobiletin

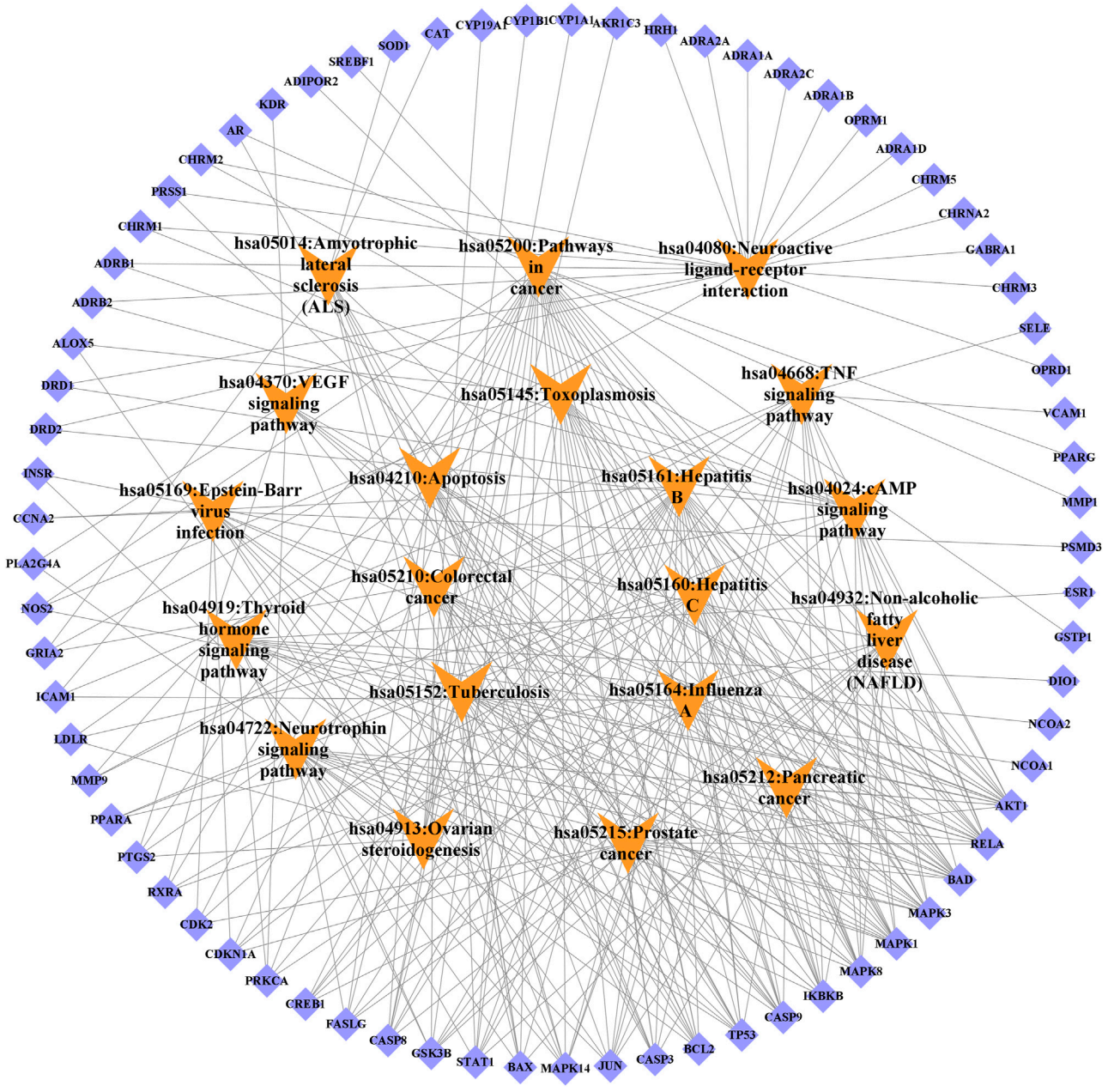

FIGURE 10
Target-signal pathway network diagram. The orange boxes indicate the signal pathways. The blue boxes indicate the gene names.

(MOL005828). The protein structures of core targets were acquired online from RCSB PDB, including MAPK8 (PDB ID: 2XRW), TP53 (PDB ID: 6GGC), MAPK3 (PDB ID: 4QTB), MAPK1 (PDB ID: 4ZZN), AKT1 (PDB ID: 1unq), ESR1 (PDB ID: 7baa), JUN (PDB ID: 6y3v), and RELA (PDB ID: 6nv2). The molecular docking for the top ten active ingredients and the protein structures of core targets were conducted by using AutoDock 4.2. The results of molecular docking indicate that the lower the binding energy, the more stable the active ingredients and targets are (Supplementary Table S11). Processed by PyMOL software, the optimal docking image of the active ingredients and the targets was displayed. It can be seen from Figure 12 that the best affinity modes were RELA-beta-sitosterol and ESR1-stigmasterol. Table 5.

3.8 Results of molecular dynamics simulation

We selected the top two ingredient-target dockings (RELA-beta-sitosterol and ESR1-stigmasterol) to conduct molecular dynamics simulations. After 100 ns of MD simulations, the dynamic evolutions of the RELA-beta-sitosterol and ESR1-stigmasterol complexes could be analyzed. The RMSD curve represents

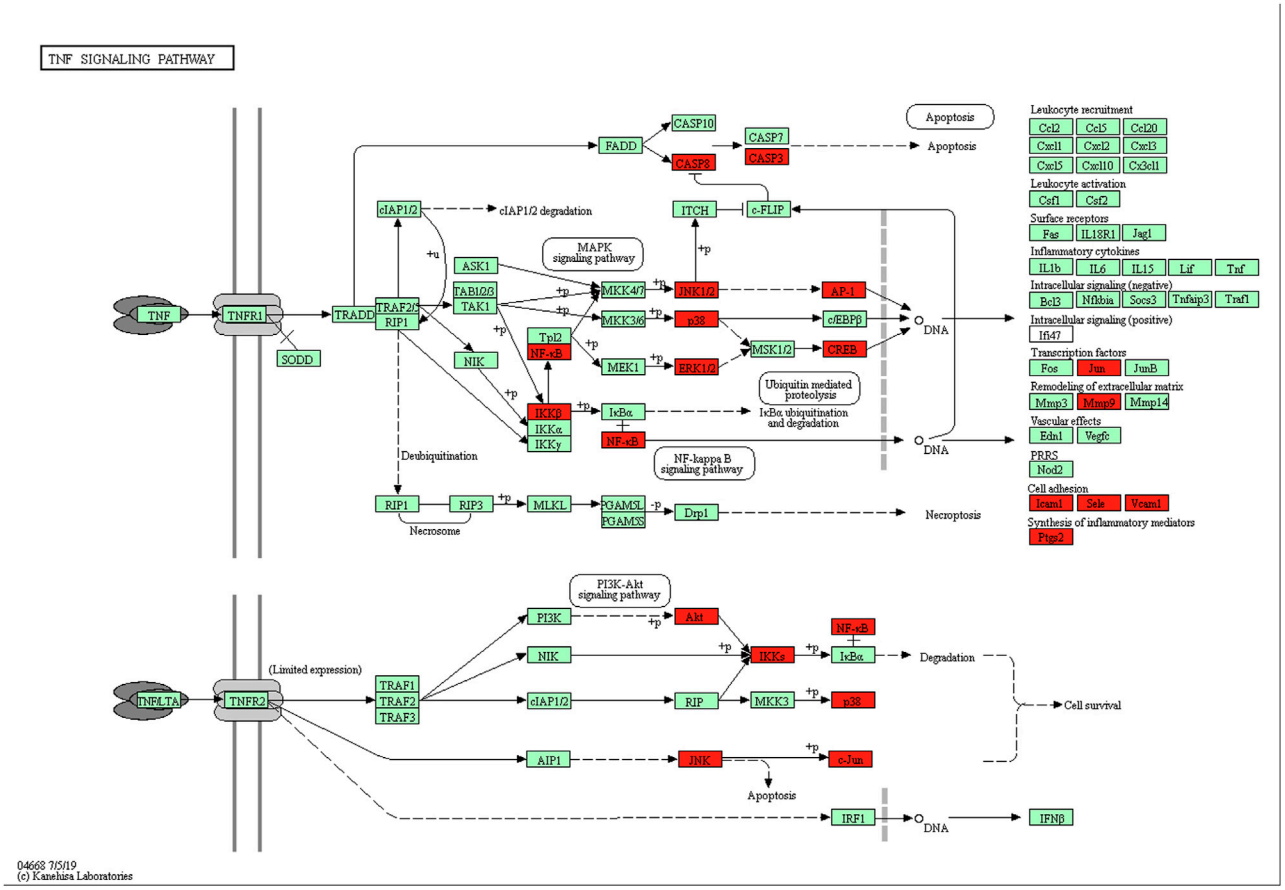

FIGURE 11
The TNF-α signaling pathway of potential target genes of ECXB formula in COPD. Arrows indicate upstream and downstream relationships between genes. The red blocks are ECXB formula target genes in the network.

positional deviations in the protein. As can be seen from Figures 13A, B, the RELA-beta-sitosterol complex was in an equilibrium state and the average RMSD value was 0.34448675 during 80–100 ns. Meanwhile, the ESR1-stigmasterol complex had a rise within 90 ns and tended to balance out the last 10 ns with the average RMSD value was 0.35742059. The low fluctuation of the two complexes indicated that their stability was stronger. The RMSF curve represents the fluctuation of the protein amino acid residues. The fluctuations of the two complexes in the 1,108–1,203 regions were relatively high. Inversely, most of the residues fluctuated at lower values in other regions, suggesting that the binding residues of RELA-beta-sitosterol and ESR1-stigmasterol were stable (Figures 13C, D). In addition, the binding energy of RELA-beta-sitosterol was −129.870 kcal/mol, and the ESR1-stigmasterol complex was −121.686 kcal/mol (Table 4).

4 Discussion

COPD is a chronic inflammatory airway disease that can be prevented and treated. In recent 10 years, the prevalence of COPD in Chinese over 40 years old has increased from 8.2% to 13.7%, and the risk of hospitalization and mortality has also increased (Zhang et al., 2019; Zhang et al., 2019). Notably, TCM treatment can relieve the symptoms of COPD patients and improve their survival rate. As classical formulas of TCM in COPD treatment, ECXB formula has respectively obtained some achievements in clinical efficacy and action of mechanism. However, the study of the combination of the two formulas for COPD is still in the initial stage. In this study, we used the SymMap platform to collect related symptoms treated by both TCM and modern medicine of herbs in the formula of ECXB to conduct Herb-Symptom comparative analysis, and applied the network pharmacology, molecular docking, and MD simulation to explore the potential mechanisms of ECXB formula on COPD in order to provide theoretical basis for the following validation studies.

Firstly, we comparative analysis Herb-Symptom network symptoms targeted by TCM and modern medicine as well as COPD symptoms, and found that the symptoms treated by both TCM and modern medicine of herbs in the formula of ECXB were similar to the symptoms of COPD patients, indicating that ECXB formula treatment of COPD conforms to the symptomatic treatment principle of TCM. Then we analyzed the "Drug-ingredient-target" network, *hederagenin* and *naringenin* (the main ingredients of *Citri reticulatae pericarpium* and *Poria* in Erchen Decoction), and *kaempferol* and *hederagenin* (the main

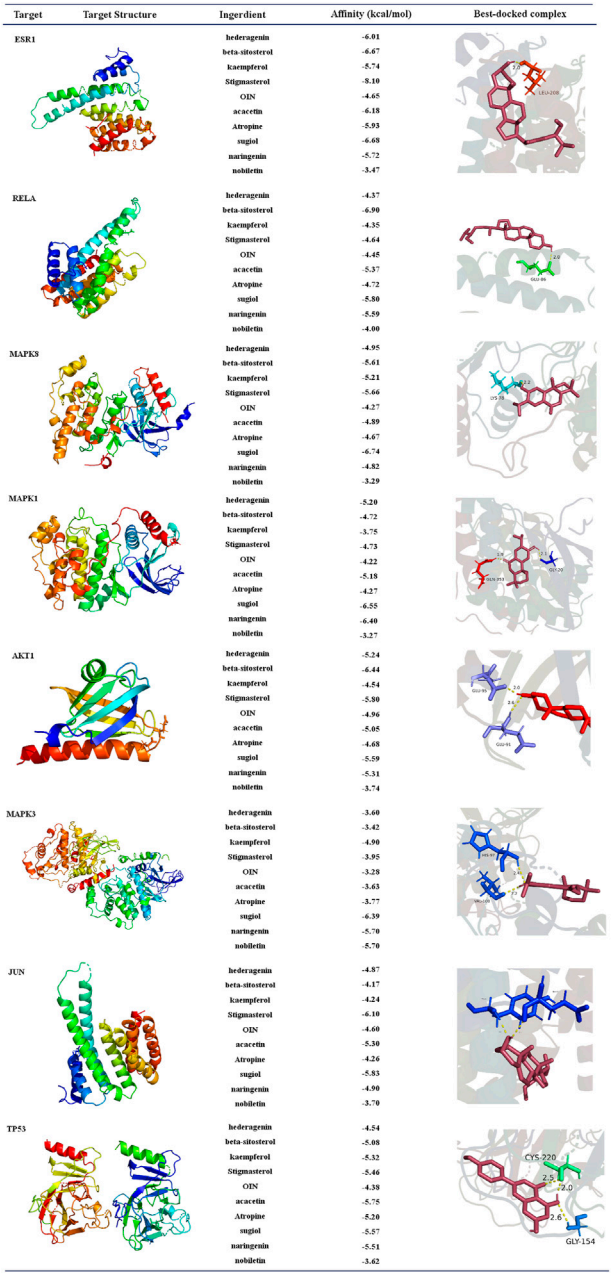

FIGURE 12
Diagram of molecular docking results. Proteins are shown to interact with molecules. The docking scores are shown in the middle. The binding amino acidic sites and other details are shown on the right.

ingredients of *Mori cortex* and *Lycii cortex* in Xiebai Powder), are the core active ingredients of ECXB formula for COPD treatment. *Hederagenin* is a pentacyclic triterpenoid compound isolated from plants, which has been shown to have strong antibacterial, anti-inflammatory, and anti-tumor biological activities (Ndjateu et al., 2014; Fang et al., 2018). Notably, it can reduce the level of proinflammatory cytokines in serum and lung tissue and reduce the damage of oxidative stress response to the lung (Wang and Zhao, 2022). *Naringenin* has anti-inflammatory, scavenging free radicals, inhibiting peroxidation, lowering blood lipids, and inhibiting tumor growth (Annadurai et al., 2013; Alam et al., 2014), and it is thought to be beneficial in COPD due to its anti-inflammatory properties (Chin et al., 2020). Liu et al. (2018) study indicated that *naringenin* attenuates inflammation in COPD in cigarette smoke induced mouse model and involves suppression of NF-κB, and they concluded that it can be a potential therapeutic agent for the treatment of COPD-related inflammation. *Kaempferol* has antioxidant stress activity and anti-inflammatory activity, which significantly inhibits the expression of the MAPK pathway, reduces the production of various inflammatory factors, and effectively inhibits inflammation (Park et al., 2006; Alam et al., 2014). Tsou et al. (2014) study found that *kaempferol* was found to be IKK2 inhibitor and helped prevent COPD occurrence and worsening. In summary, it can be inferred that the core ingredients of ECXB formula play a therapeutic role by affecting inflammatory factors related to COPD.

PPI network analysis results suggest that the core targets of ECXB formula for the treatment of COPD mainly include MAPK8, ESR1, TP53, MAPK3, JUN, RELA, MAPK1, and AKT1. Among them, MAPK8, MAPK3, and MAPK1 are intracellular serine/threonine protein kinases, which can change gene expression by phosphorylation of transcription factors, promote the production of inflammatory factors TNF-α, IL-1, IL-6, and induce a series of inflammatory and immune responses, thus playing a role in the pathogenesis of COPD (Kang et al., 2013; Duan et al., 2020). TP53 is a tumor suppressor that plays a variety of roles in controlling cell cycle checkpoints, apoptosis, and DNA repair. In COPD smokers, downregulation of TP53 - and p53-related signal transduction may lead to lung tumors (Zhou et al., 2021). ESR1 gene can code estrogen receptors, and studies have found that estrogen signaling may play a key role in lung diseases. Overexpression of ESR1 m RNA is closely related to the prognosis of non-small cell lung cancer (Suga et al., 2008), while ESR1 is expressed in lung tissues of patients with COPD, but its specific mechanism remains unclear. JUN is the most widely used protein in activating protein 1 complex, (Bin et al. (2020) discovered that c-Jun is a potential novel therapeutic target for COPD, JNK inhibition by erythromycin restores corticosteroid sensitivity via the inhibition of c-Jun expression. AKT1 is an important factor in the PI3K-AKT signaling pathway, which plays a key role in many physiological processes such as cell growth and survival and is associated with airway inflammation and lung function changes in asthma (gianni, 2019). In conclusion, the core targets may influence the onset and progression of COPD through inflammatory immunity, reducing inflammatory factors and oxidation-reduction reaction, and so on.

We also performed GO function and KEGG pathway enrichment analyses. Response to drug, response to nutrient levels, and response to extracellular stimulation may be the key biological processes in the ECXB formula treatment of COPD (Bidan et al., 2015; Beijers et al., 2022). Membrane raft and amide binding were the most significant cellular component and molecular functions, respectively. It has been reported that preponderance of saturated fatty acids in plasma membrane of erythrocytes of COPD patients which may decrease the membrane fluidity and possibly impair the functions of the plasma membrane in the disease (Gangopadhyay et al., 2012). According to the KEGG analysis, the TNF signaling pathway, cAMP signaling pathway, and VEGF signaling pathway were considered key pathways

TABLE 5 The binding free energy and energy components of MD simulation.

Energy	RELA _ beta-sitosterol	ESR1 _ stigmasterol
Van der Waals Energy (KJ/mol)	−144.687	−135.674
Electrostatic Energy (kJ/mol)	−1.605	1.243
Total Binding Energy (KJ/mol)	−129.870	−121.686

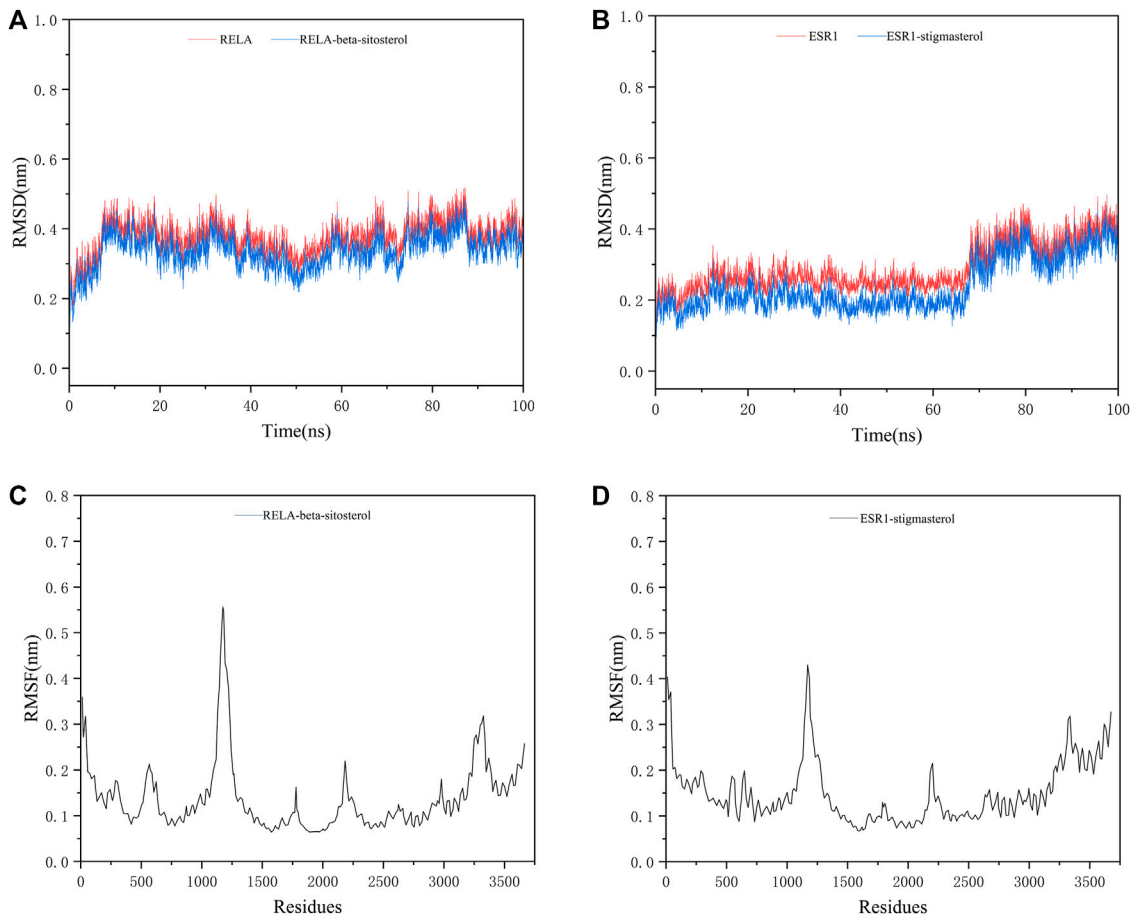

FIGURE 13
The MD simulation results of two complexes. **(A)** The RMSD analysis for the RELA-beta-sitosterol complex. **(B)** The RMSD analysis for the ESR1-stigmasterol complex. **(C)** The RMSF analysis for the RELA-beta-sitosterol complex. **(D)** The RMSF analysis for the ESR1-stigmasterol complex.

in the treatment of COPD by ECXB formula. The TNF pathway is critical in inflammatory response by regulating both apoptosis and proliferation. Lee et al. (2018) display that fisetin is a good therapeutic drug for the treatment of inflammatory lung diseases, such as COPD, by inhibiting the TNF-alpha/NF-kappa B signaling pathway. Arora et al. (2022b) discovered that a significant reduction in TNF-α levels and concomitant suppression of asthma symptoms after oral administration of solasodine in ovalbumin-sensitized rats are indicative of the possible therapeutic role of phytocompound in chronic asthma irresponsive to ICS. Liu et al. (2015) study results suggested that IL-15 inhibited protein degradation in skeletal muscle in COPD rats, which may be mediated by the TNF-alpha and UPP pathway. Arora et al. (2021) and Arora et al. (2022a) studies demonstrate that biomarkers of the inflammatory response, including cell count, immunoglobulin E, cytokines such as interleukin (IL-4), −5, −1β, tumor necrosis factor (TNF)-α, etc. The findings that Mesua ferrea L. and Clerodendrum serratum in allergic asthma may be related to the ability of the plant to attenuate inflammatory cell responses and thus to the production of inflammatory and pro-inflammatory cytokines in the airways. The cAMP pathway plays a major role in COPD signaling. For instance, Dunne et al. (2019) study showed that roflumilast inhibits neutrophil chemotaxis directly via a cAMP-mediated mechanism requiring activation of Epac1 and that Epac1 activators could reduce COPD neutrophilic inflammation. Nabissi et al. (2018) work demonstrated that thyme extract is effective in stimulating CBF by inducing an

increase of cAMP and Ca^{2+} levels, thus supporting its therapeutical use in the treatment of COPD. The VEGF signaling pathway has been related to the pathogenesis of COPD. Zhang et al. (2022) the efficacy of electroacupuncture (EA) with respect to the regulation of microvascular remodeling induced by VEGF/PI3K/Akt was evaluated in a rat model of COPD, showed that reduced pulmonary vascular remodeling via mechanisms possibly related to the VEGF/PI3K/Akt pathway. Willems-Widyastuti et al. (2011) study suggested that TGF-beta (1) could play a key role in bronchial angiogenesis and vascular remodeling via VEGF pathway in asthma. The active ingredients of ECXB formula may act on these signaling pathways in the treatment of COPD.

The network pharmacology results were verified for ECXB formula in the treatment of COPD by the molecular docking of the 8 core targets and the top ten selected active ingredients. The results of the molecular docking indicated that the core active ingredients of ECXB formula in the treatment of COPD could bind well with their core targets. Among them, RELA-beta-sitosterol and ESR1-stigmasterol had the lowest binding scores. MD simulation was employed to further verify the results obtained. The results of molecular dynamics simulation suggested that RELA-beta-sitosterol and ESR1-stigmasterol could bind tightly, and the binding energies of the complexes were −129.870 kcal/mol, and −121.686 kcal/mol, respectively.

However, it should be noted that there were certain limitations of the network pharmacology. The study based on network pharmacology is a static network analysis while the occurrence and development of disease and the action of drugs are both dynamic processes. Therefore, the following experiments *in vivo* or *in vitro* can be carried out on this basis to explore the deeper mechanism of ECXB formula in the treatment of COPD. Despite the limitations of this study, the results revealed that it had certain clinical value and research significance.

5 Conclusion

Altogether, we analyzed the role of ECXB formula in treating COPD from the Herb-Symptom network relationship and utilized network pharmacology, molecular docking, and MD simulation to explore the potential mechanisms of ECXB formula in treating COPD. The results indicated that hederagenin, naringenin, kaempferol, and other effective ingredients of ECXB formula showed therapeutic effects against COPD via multiple targets and multiple pathways. In addition, the good activities of the core active ingredients and the core targets were verified by molecular docking and MD simulation. In summary, the results of this study provided a reference for clinical application and guidance for further experimental verification of ECXB formula for the treatment of COPD.

Data availability statement

The original contributions presented in the study are included in the article/Supplementary Material, further inquiries can be directed to the corresponding authors.

Author contributions

HY: conception and design; designed the research methodology; writing-review and editing. BH: data analysis and interpretation; writing-original draft. YZ: validation; writing-review and editing. ZY: validation; writing-review and editing. YF: data analysis and interpretation collected and sorted data. CW: administrative support. CX: data analysis and editing. QF: administrative support. All author listed have made a substantial, direct, and intellectual contribution to the work and approved it for publication.

Funding

This research was supported by the National Key R&D Program of China (2018YFC1704104); the National Natural Science Foundation of China (82105054); the Natural Science Foundation of Sichuan Province (2023NSFSC1811); the "Xinglin Scholar" Scientific Research Promotion Plan of Chengdu University of TCM (CCZD2021002); the TCM Scientific Research Special project of Sichuan TCM Administration (2021MS559).

Acknowledgments

We sincerely appreciate the databases of SymMap, TCMSP, PubChem, SwissTargetPrediction, Uniport, GeneCards®, OMIM®, STRING, DAVID, Bioinformatics, PDB and Cytoscape, Chem3D, AutoDock 4, PyMol, GROMACS software for provided the data and making the charts. The contents of the manuscript preprint of the first (20 May 2022) and second (03 June 2022) editions are available online (https://www.researchsquare.com/article/rs-1646303/v1).

Conflict of interest

The authors declare that the research was conducted in the absence of any commercial or financial relationships that could be construed as a potential conflict of interest.

Publisher's note

Supplementary material

The Supplementary Material for this article can be found online at: https://www.frontiersin.org/articles/10.3389/fphar.2023.1117238/full#supplementary-material

References

Alam, M. A., Subhan, N., Rahman, M. M., Uddin, S. J., Reza, H. M., and Sarker, S. D. (2014). Effect of citrus flavonoids, naringin and naringenin, on metabolic syndrome and their mechanisms of action. *Adv. Nutr.* 5, 404–417. doi:10.3945/an.113.005603

Amberger, J. S., Bocchini, C. A., Schiettecatte, F., Scott, A. F., and Hamosh, A. (2015). OMIM.org: Online Mendelian Inheritance in Man (OMIM®), an online catalog of human genes and genetic disorders. *Nucleic Acids Res.* 43, D789–D798. doi:10.1093/nar/gku1205

Annadurai, T., Thomas, P. A., and Geraldine, P. (2013). Ameliorative effect of naringenin on hyperglycemia-mediated inflammation in hepatic and pancreatic tissues of Wistar rats with streptozotocin-nicotinamide-induced experimental diabetes mellitus. *Free Radic. Res.* 47, 793–803. doi:10.3109/10715762.2013.823643

Arora, P., Ansari, S. H., and Nainwal, L. M. (2022a). Clerodendrum serratum extract attenuates production of inflammatory mediators in ovalbumin-induced asthma in rats. *Turk. J. Chem.* 46, 330–341. doi:10.55730/1300-0527.3310

Arora, P., Ansari, S. H., and Nainwal, L. M. (2021). Mesua ferrea L. (Calophyllaceae) exerts therapeutic effects in allergic asthma by modulating cytokines production in asthmatic rats. *Turk. J. Bot.* 45, 820–832. doi:10.3906/bot-2111-22

Arora, P., Nainwal, L. M., Gupta, G., Singh, S. K., Chellappan, D. K., Oliver, B. G., et al. (2022b). Orally administered solasodine, a steroidal glycoalkaloid, suppresses ovalbumin-induced exaggerated Th2-immune response in rat model of bronchial asthma. *Chem. Biol. Interact.* 366, 110138. doi:10.1016/j.cbi.2022.110138

Bateman, A., Martin, M. J., Orchard, S., Magrane, M., Agivetova, R., Ahmad, S., et al. (2021). UniProt: The universal protein knowledgebase in 2021. *Nucleic Acids Res.* 49, D480–D489. doi:10.1093/nar/gkaa1100

Beijers, R. J., Iersel, L. E. J. van, Schuurman, L. T., Hageman, R. J. J., Simons, S. O., Helvoort, A. V., et al. (2022). Effect of targeted nutrient supplementation on physical activity and health-related quality of life in COPD: Study protocol for the randomised controlled NUTRECOVER trial. *BMJ Open* 12, e059252. doi:10.1136/bmjopen-2021-059252

Berman, H. M., Westbrook, J., Feng, Z., Gilliland, G., Bhat, T. N., Weissig, H., et al. (2000). The protein data bank. *Nucleic Acids Res.* 28, 235–242. doi:10.1093/nar/28.1.235

Bidan, C. M., Veldsink, A. C., Meurs, H., and Gosens, R. (2015). Airway and extracellular matrix Mechanics in COPD. *Front. Physiol.* 6, 346. doi:10.3389/fphys.2015.00346

Bin, Y. F., Ma, N., Lu, Y. X., Sun, X. J., Liang, Y., Bai, J., et al. (2020). Erythromycin reverses cigarette smoke extract-induced corticosteroid insensitivity by inhibition of the JNK/c-Jun pathway. *Free Radic. Biol. Med.* 152, 494–503. doi:10.1016/j.freeradbiomed.2019.11.020

Blanco, I., Diego, I., Bueno, P., Fernandez, E., Casas-Maldonado, F., Esquinas, C., et al. (2018). Geographical distribution of COPD prevalence in Europe, estimated by an inverse distance weighting interpolation technique. *Int. J. Chronic Obstr. Pulm. Dis.* 13, 57–67. doi:10.2147/COPD.S150853

Buist, A. S., McBurnie, M. A., Vollmer, W. M., Gillespie, S., Burney, P., Mannino, D. M., et al. (2007). International variation in the prevalence of COPD (the BOLD study): A population-based prevalence study. *Lancet* 370, 741–750. doi:10.1016/S0140-6736(07)61377-4

Chin, L. H., Hon, C. M., Chellappan, D. K., Chellian, J., Madheswaran, T., Zeeshan, F., et al. (2020). Molecular mechanisms of action of naringenin in chronic airway diseases. *Eur. J. Pharmacol.* 879, 173139. doi:10.1016/j.ejphar.2020.173139

Daina, A., Michielin, O., and Zoete, V. (2019). Swiss target prediction: Updated data and new features for efficient prediction of protein targets of small molecules. *Nucleic Acids Res.* 47, W357–W364. doi:10.1093/nar/gkz382

Deng, L., Zhang, X., Dong, Y., Wang, L., Chen, K., Zheng, M., et al. (2020). Erchen decoction combined with Sanziyangqin decoction for chronic obstructive pulmonary disease A protocol for systematic review and meta-analysis. *Med. Baltim.* 99, e22315. doi:10.1097/MD.0000000000022315

Duan, R., Niu, H., Yu, T., Cui, H., Yang, T., Hao, K., et al. (2020). Identification and bioinformatic analysis of circular RNA expression in peripheral blood mononuclear cells from patients with chronic obstructive pulmonary disease. *Int. J. Chronic Obstr. Pulm. Dis.* 15, 1391–1401. doi:10.2147/COPD.S252896

Dunne, A. E., Kawamatawong, T., Fenwick, P. S., Davies, C. M., Tullett, H., Barnes, P. J., et al. (2019). Direct inhibitory effect of the PDE4 inhibitor roflumilast on neutrophil migration in chronic obstructive pulmonary disease. *Am. J. Respir. Cell. Mol. Biol.* 60, 445–453. doi:10.1165/rcmb.2018-0065OC

Fang, K., Zhang, X. H., Han, Y. T., Wu, G. R., Cai, D. S., Xue, N. N., et al. (2018). Design, synthesis, and cytotoxic analysis of novel hederagenin-pyrazine derivatives based on partial least squares discriminant analysis. *Int. J. Mol. Sci.* 19, 2994. doi:10.3390/ijms19102994

Gangopadhyay, S., Vijayan, V. K., and Bansal, S. K. (2012). Lipids of erythrocyte membranes of COPD patients: A quantitative and qualitative study. *COPD J. Chronic Obstr. Pulm. Dis.* 9, 322–331. doi:10.3109/15412555.2012.668581

Huang, D. W., Sherman, B. T., and Lempicki, R. A. (2009a). Bioinformatics enrichment tools: Paths toward the comprehensive functional analysis of large gene lists. *Nucleic Acids Res.* 37, 1–13. doi:10.1093/nar/gkn923

Huang, D. W., Sherman, B. T., and Lempicki, R. A. (2009b). Systematic and integrative analysis of large gene lists using DAVID bioinformatics resources. *Nat. Protoc.* 4, 44–57. doi:10.1038/nprot.2008.211

Huang, P., Lin, X., Liu, Y., and Hou, Z. (2022). The efficacy and safety of combined traditional Chinese and Western medicine in the treatment of chronic obstructive pulmonary disease complicated with respiratory failure: A systematic review and meta-analysis study. *Ann. Pallliat. Med.* 11, 1102–1111. doi:10.21037/apm-22-272

Kang, Y., Wang, F., Lu, Z., Ying, H., Zhang, H., Ding, W., et al. (2013). MAPK kinase 3 potentiates Chlamydia HSP60-induced inflammatory response through distinct activation of NF-kappa B. *J. Immunol.* 191, 386–394. doi:10.4049/jimmunol.1300481

Kim, S., Chen, J., Cheng, T., Gindulyte, A., He, J., He, S., et al. (2021). PubChem in 2021: New data content and improved web interfaces. *Nucleic Acids Res.* 49, D1388–D1395. doi:10.1093/nar/gkaa971

Lee, S., Ro, H., Jin, H., Choi, J. H., Kim, M. O., Lee, J., et al. (2018). Fisetin inhibits TNF-α/NF-κB-induced IL-8 expression by targeting PKCδ in human airway epithelial cells. *Cytokine* 108, 247–254. doi:10.1016/j.cyto.2018.01.004

Li, J. (2020). International clinical Practice guideline of Chinese medicine chronic obstructive pulmonary disease. *World Chin. Med.* 15, 39–1092. doi:10.4103/wjtcm.wjtcm_9_20

Li, X., and Luo, X. (2014). Clinical application of qingfei huatan decoction from doctor WANG's. China. *J. TCM.* 29, 3469–3471.

Liu, J., Yao, J., and Zhang, J. (2018). Naringenin attenuates inflammation in chronic obstructive pulmonary disease in cigarette smoke induced mouse model and involves suppression of NF-κB. *J. Microbiol. Biotechnol.* doi:10.4014/jmb.1810.10061

Liu, Z., Fan, W., Chen, J., Liang, Z., and Guan, L. (2015). The role of Interleukin 15 in protein degradation in skeletal muscles in rats of chronic obstructive pulmonary disease. *Int. J. Clin. Exp. Med.* 8, 1976–1984.

Mei, W., and Li, X. (2012). Observation on the curative effect of Xeibai Power combined with Erchen Decoction on acute exacerbation of chronic obstructive pulmonary disease. *Guide. China Med.* 10, 277–278. doi:10.15912/j.cnki.gocm.2012.30.272

Morris, G. M., Huey, R., Lindstrom, W., Sanner, M. F., Belew, R. K., Goodsell, D. S., et al. (2009). AutoDock4 and AutoDockTools4: Automated docking with selective receptor flexibility. *J. Comput. Chem.* 30, 2785–2791. doi:10.1002/jcc.21256

Nabissi, M., Marinelli, O., Morelli, M. B., Nicotra, G., Iannarelli, R., Amantini, C., et al. (2018). Thyme extract increases mucociliary-beating frequency in primary cell lines from chronic obstructive pulmonary disease patients. *Biomed. Pharmacother.* 105, 1248–1253. doi:10.1016/j.biopha.2018.06.004

Ndjateu, F. S. T., Tsafack, R. B. N., Nganou, B. K., Awouafack, M. D., Wabo, H. K., Tene, M., et al. (2014). Antimicrobial and antioxidant activities of extracts and ten compounds from three Cameroonian medicinal plants: Dissotis perkinsiae (Melastomaceae), Adenocarpus mannii (Fabaceae) and Barteria fistulosa (Passifloraceae). *S. Afr. J. Bot.* 91, 37–42. doi:10.1016/j.sajb.2013.11.009

Park, J. S., Rho, H. S., Kim, D. H., Chang, I. S., et al. (2006). Enzymatic preparation of kaempferol from green tea seed and its antioxidant activity. *J. Agric. Food Chem.* 54, 2951–2956. doi:10.1021/jf052900a

Rehman, A. U., Hassali, M. A. A., Muhammad, S. A., Shah, S., Abbas, S., Ali, I. A. B. H., et al. (2020). The economic burden of chronic obstructive pulmonary disease (COPD) in the USA, Europe, and Asia: Results from a systematic review of the literature. *Expert Rev. pharmacoecon. Outcomes Res.* 20, 661–672. doi:10.1080/14737167.2020.1678385

Ru, J., Li, P., Wang, J., Zhou, W., Li, B., Huang, C., et al. (2014). Tcmsp: A database of systems pharmacology for drug discovery from herbal medicines. *J. Cheminformatics* 6, 13. doi:10.1186/1758-2946-6-13

Safran, M., Rosen, N., Twik, M., BarShir, R., Stein, T. I., Dahary, D., et al. (2021). "The GeneCards suite," in *Practical guide to life science databases*. Editors I. Abugessaisa and T. Kasukawa (Singapore: Springer), 27–56. doi:10.1007/978-981-16-5812-9_2

Shannon, P., Markiel, A., Ozier, O., Baliga, N. S., Wang, J. T., Ramage, D., et al. (2003). Cytoscape: A software environment for integrated models of biomolecular interaction networks. *Genome Res.* 13, 2498–2504. doi:10.1101/gr.1239303

Sherman, B. T., Hao, M., Qiu, J., Jiao, X., Baseler, M. W., Lane, H. C., et al. (2022). David: A web server for functional enrichment analysis and functional annotation of gene lists (2021 update). *Nucleic Acids Res.* 50, W216–W221. doi:10.1093/nar/gkac194

Singh, D., Agusti, A., Anzueto, A., Barnes, P. J., Bourbeau, J., Celli, B. R., et al. (2019). Global Strategy for the Diagnosis, management, and prevention of chronic obstructive lung disease: The GOLD science committee report 2019. *Eur. Resp. J.* 53, 1900164. doi:10.1183/13993003.00164-2019

Suga, Y., Miyajima, K., Oikawa, T., Maeda, J., Usuda, J., Kajiwara, N., et al. (2008). Quantitative p16 and ESR1 methylation in the peripheral blood of patients with non-small cell lung cancer. *Oncol. Rep.* 20, 1137–1142.

Szklarczyk, D., Gable, A. L., Lyon, D., Junge, A., Wyder, S., Huerta-Cepas, J., et al. (2019). STRING v11: Protein-protein association networks with increased coverage, supporting functional discovery in genome-wide experimental datasets. *Nucleic Acids Res.* 47, D607–D613. doi:10.1093/nar/gky1131

Tao, W., Xu, X., Wang, X., Li, B., Wang, Y., Li, Y., et al. (2013). Network pharmacology-based prediction of the active ingredients and potential targets of Chinese herbal Radix Curcumae formula for application to cardiovascular disease. *J. Ethnopharmacol.* 145, 1–10. doi:10.1016/j.jep.2012.09.051

Tsou, Y. A., Huang, H. J., Lin, W. W. Y., and Chen, C. Y. C. (2014). Lead screening for chronic obstructive pulmonary disease of IKK2 inhibited by traditional Chinese medicine. *Evid. based Complement. Altern. Med.* 2014, 465025. doi:10.1155/2014/465025

Van Der Spoel, D., Lindahl, E., Hess, B., Groenhof, G., Mark, A. E., and Berendsen, H. J. C. (2005). Gromacs: Fast, flexible, and free. *J. Comput. Chem.* 26, 1701–1718. doi:10.1002/jcc.20291

Wang, L., and Zhao, M. (2022). Suppression of NOD-like receptor protein 3 inflammasome activation and macrophage M1 polarization by hederagenin contributes to attenuation of sepsis-induced acute lung injury in rats. *Bioengineered* 13, 7262–7276. doi:10.1080/21655979.2022.2047406

Willems-Widyastuti, A., Alagappan, V. K. T., Arulmani, U., Vanaudenaerde, B. M., de Boer, W. I., Mooi, W. J., et al. (2011). Transforming growth factor-beta 1 induces angiogenesis *in vitro* via VEGF production in human airway smooth muscle cells. *Indian J. biochem. Biophys.* 48, 262–269.

Wu, Y., Zhang, F., Yang, K., Fang, S., Bu, D., Li, H., et al. (2019). SymMap: An integrative database of traditional Chinese medicine enhanced by symptom mapping. *Nucleic Acids Res.* 47, D1110–D1117. doi:10.1093/nar/gky1021

Xu, X., Zhang, W., Huang, C., Li, Y., Yu, H., Wang, Y., et al. (2012). A novel chemometric method for the prediction of human oral bioavailability. *Int. J. Mol. Sci.* 13, 6964–6982. doi:10.3390/ijms13066964

Zhang, L., Tian, Y., Zhao, P., Jin, F., Miao, Y., Liu, Y., et al. (2022a). Electroacupuncture attenuates pulmonary vascular remodeling in a rat model of chronic obstructive pulmonary disease via the VEGF/PI3K/Akt pathway. *Acupunct. Med.* 40, 389–400. doi:10.1177/09645284221078873

Zhang, Q., Zong, Y., Yang, L., Wang, K., and Wang, Y. (2022b). Clinical evaluation and exploration of mechanisms for modified xiebai powder or modified xiebai powder combined with western medicine in the treatment of pneumonia. *Comput. Math. Method Med.* 2022, 2287470. doi:10.1155/2022/2287470

Zhang, X. W., Liu, W., Jiang, H. L., and Mao, B. (2019b). Dissection of pharmacological mechanism of Chinese herbal medicine yihuo huatan formula on chronic obstructive pulmonary disease: A systems pharmacology-based study. *Sci. Rep.* 9, 13431. doi:10.1038/s41598-019-50064-9

Zhang, Y. Z., Wu, Q. J., Xing, X. X., Chen, Y. Y., and Wang, H. (2019a). Effects of SIRT1/Akt pathway on chronic inflammatory response and lung function in patients with asthma. *Eur. Rev. Med. Pharmacol. Sci.* 23, 4948–4953. doi:10.26355/eurrev_201906_18085

Zhen, G., Yingying, L., and Jingcheng, D. (2018). Traditional Chinese medicine tonifying kidney therapy (Bu shen) for stable chronic obstructive pulmonary disease Protocol for a systematic review and meta-analysis. *Med. Baltim.* 97, e13701. doi:10.1097/MD.0000000000013701

Zhou, L., Gu, W., Kui, F., Gao, F., Niu, Y., Li, W., et al. (2021). The mechanism and candidate compounds of aged citrus peel (chenpi) preventing chronic obstructive pulmonary disease and its progression to lung cancer. *Food Nutr. Res.* 65, 7526. doi:10.29219/fnr.v65.7526

frontiers | Frontiers in Pharmacology

TYPE Original Research
PUBLISHED 12 June 2023
DOI 10.3389/fphar.2023.1139654

OPEN ACCESS

EDITED BY
Lalit Mohan Nainwal,
GD Goenka University, India

REVIEWED BY
Shyamali Mukherjee,
Meharry Medical College, United States
Poonam Arora,
Shree Guru Gobind Singh Tricentenary University, India
Monu Yadav,
Amity Institute of Pharmacy, Amity University Haryana, India

*CORRESPONDENCE
Ruchi Tandon,
ruchi.tandon@thsti.res.in,
ruchitandon.rnd@gmail.com
Madhu Dikshit,
drmadhudikshit@gmail.com

RECEIVED 07 January 2023
ACCEPTED 31 May 2023
PUBLISHED 12 June 2023

CITATION
Sharma PK, Kumar L, Goswami Y, Pujani M, Dikshit M and Tandon R (2023), The aqueous root extract of *Withania somnifera* ameliorates LPS-induced inflammatory changes in the *in vitro* cell-based and mice models of inflammation. *Front. Pharmacol.* 14:1139654. doi: 10.3389/fphar.2023.1139654

The aqueous root extract of *Withania somnifera* ameliorates LPS-induced inflammatory changes in the *in vitro* cell-based and mice models of inflammation

Phulwanti Kumari Sharma[1], Lokesh Kumar[1], Yamini Goswami[1], Mukta Pujani[2], Madhu Dikshit[1,3]* and Ruchi Tandon[1]*

[1]Translational Health Science and Technology Institute, Faridabad, India, [2]ESIC Medical College and Hospital, Faridabad, India, [3]Pharmacology Division, Central Drug Research Institute, Lucknow, India

Introduction: Most critically ill COVID-19 patients have bronchitis, pneumonia, and acute respiratory distress syndrome (ARDS) due to excessive inflammatory conditions. Corticosteroids have largely been prescribed for the management of inflammation in these patients. However, long-term use of corticosteroids in patients with comorbidities such as metabolic, cardiovascular, and other inflammatory disorders is ideally not recommended due to safety issues. A potential and safer anti-inflammatory therapy is therefore the need of the hour. *Withania somnifera* (WS), a well-known herbal medicine used during the pandemic in India to prevent SARS-CoV2 infection, also possesses anti-inflammatory properties.

Methods: In the present study, we, therefore, evaluated the effect of the aqueous extract of the roots of *W. somnifera* in the cell-based assays and in the experimental animal models of LPS-induced inflammation.

Results: In the NCI-H460, A549 cells and human peripheral blood mononuclear cells (PBMCs) pre-treatment with *W. somnifera* reduced the LPS-induced expression of the pro-inflammatory cytokines. In addition, *W. somnifera* extract also showed potent anti-inflammatory activity in the lung tissues of BALB/c mice challenged intranasally with LPS. We observed a marked reduction in the neutrophil counts in the broncho-alveolar lavage (BAL) fluid, inflammatory cytokines, and fibrosis in the mice lungs pre-treated with *W. somnifera*. Results obtained thus suggest the potential utility of *W. somnifera* extract in reducing airway inflammation and recommend the clinical evaluation of *W. somnifera* extract in COVID-19 patients with a high propensity for lung inflammation.

KEYWORDS

***Withania somnifera*, cytokines, lung inflammation, PBMCs, TLR-4, LPS, COVID-19**

Introduction

Coronavirus has got an overwhelming reach in the last 3 years among large populations and has a life-threatening impact on people with existing health issues such as respiratory, cardiac, and metabolic complications (Sanyaolu et al., 2020; Zheng et al., 2020) and those who survived have also been found to have a high prevalence of aberrant airway injuries including pneumonia, bronchitis and acute respiratory distress syndrome (George et al., 2020; Zhou et al., 2020; Allgood et al., 2021).

The hyper-inflammation in Corona-infected patients is a result of cytokine storm due to the excessive production of pro-inflammatory cytokines such as tumor necrosis factor-alpha (TNF-α), interleukin-6 (IL-6), interleukin-8 (IL-8), etc., leading to severe organ damage and may even lead to fatalities in severe cases (Mortaz et al., 2020; Tang et al., 2020; Zhou et al., 2020). The world health organization (WHO) recently released its updated guideline on 16 September 2022, and recommendations for the management of Covid associated complications (Sterne and Murthy, 2020; WHO, 2022). These recommendations suggest the use of remdesivir in combination with corticosteroids, interleukin-6 (IL-6) receptor blockers, and Janus kinase (JAK) inhibitors in patients with severe or critical COVID-19. This guideline has also modified the previous recommendations for the use of neutralizing monoclonal antibodies sotrovimab and casirivimab-imdevimab in patients with non-severe COVID-19.

In order to understand the mechanism of cytokine storm in Corona patients, we found that Corona virus-induced inflammatory profile seems to be similar to the inflammatory trigger induced by Toll-like Receptor 4 (TLR-4) activation. Lipopolysaccharide (LPS), an outer membrane constituent of gram-negative bacteria is a TLR-4 ligand that leads to an increase in the production of pro-inflammatory cytokines such as Tumor necrosis factor alpha (TNF-α), IL-6, and various other cytokines and chemokines in the cell-based models and also the in the mouse models (Park et al., 2004). Several anti-inflammatory drugs and herbal medications have been tried previously to inhibit LPS-induced inflammation in cell-based and mouse models (Yunhe et al., 2012; Huang et al., 2020).

Corticosteroids, as mentioned above, are the choice of medication by a standard medical practitioner to combat inflammation occurring in the lungs and other vital organs of patients infected with Coronavirus due to their potent anti-inflammatory properties (Li et al., 2021). Dexamethasone, a corticosteroid that has been previously shown to inhibit LPS-induced inflammation in both *in vitro* and *in vivo* models have been recommended for use in Corona patients also (RECOVERY Collaborative Group, 2021; Crothers et al., 2021). The unguided use of corticosteroids in patients, however, can be harmful in patients with metabolic diseases such as diabetes, hypertension, and other inflammatory diseases due to their side effects (Sterne and Murthy, 2020). To develop a safer approach for developing therapeutics for Corona patients, WHO has recommended a combination of herbal and modern systems of medicines to achieve the desired pharmacological response with minimal side effects which have also been recommended by the National Board of Medicinal Plants (NBMP) (2021), and Ministry of Ayush, Government of India (ebook, 20 medicinal plants 2021). Ayurveda, which is one of the oldest systems of medicine in the world, offers treatments based on combining products mainly derived from plants and natural resources from ancient Indian medical systems and offers such remedies which can be explored for the management of COVID-19 complications. In addition, several other complementary and traditional medicines have shown potential advantages for the management of various health issues in other countries also (Patwardhan et al., 2004; Ghasemian et al., 2016; Ni, 2020; Patwardhan et al., 2020; Shankar, 2020).

Recent study from this lab have demonstrated the protective effect of the aqueous extract of the *Withania somnifera* (WS) roots in the experimental models of SARS-CoV-2, T cell differentiation, and neutrophil functions (Rizvi et al., 2023) by reducing viral load and inflammation. While the therapeutic potential of Withaferin A (WA) and its derivatives has also been demonstrated in lung cancer. In the lung cancer cells (A549 and H1299), WA pre-treatment suppressed cell adhesion, migration, and invasion by downregulating the expression of tumor growth factor beta 1 (TGFβ1) and tumor necrosis factor *α* (TNFα) expression as well as epithelial-mesenchymal transition (Behl et al., 2020). Similar effects have also been reported in macrophage cell lines (THP-1 and RAW 246.7 cells). In yet another study, WA ameliorated *in vitro* and *in vivo* pulmonary fibrosis by modulating the interplay of fibrotic and matricellular proteins (Bale et al., 2018). Withanolides present in the aqueous extract of WS root inhibited TLR-4 activated innate inflammatory signal utilizing *in silico* and experimental approaches (Purushotham et al., 2017). In a recent study, WA and Withanones were found to inhibit SARS-CoV-2 proteins (Chakraborty et al., 2022). Since lung inflammation is one of the most common concerns in COVID-19 patients, we wanted to test whether WS extract has the potential to inhibit LPS-induced inflammation in the lung-derived cell lines and in the mice model of acute lung inflammation in a TLR-4-dependent manner.

For the *in vitro* studies, we used LPS-stimulated NCI-H460 and A549, lung-derived cell lines as well as human peripheral blood mononuclear cells (PBMCs) to further assess the anti-inflammatory potential of WS. In addition, we also assessed the anti-inflammatory potential of WS in BALB/c mice challenged with LPS by the intranasal route, which led to an increase in the migration of neutrophils in the broncho-alveolar lavage (BAL) fluid and induction of pro-inflammatory cytokines in the lung tissues. Our study demonstrates the potential use of the aqueous extract of WS in combating lung inflammation which can be evaluated further in the planned clinical setups.

Material and methods

Experimental animals

All the experiments were performed as per the guidelines of the Institutional Animal Ethics Committee (IAEC-THSTI/163) of the Translational Health Science and Technology Institute (THSTI), Faridabad, India, and all the experiments were carried out following the control and supervision of experiments on animals (CPCSEA) guidelines (Govt. of India).

8–12 weeks old female BALB/c mice (18–25 g) were procured from the Small Animal Facility (SAF) of Translational Health Science and Technology Institute (THSTI), Faridabad, and housed in individually ventilated cages with controlled air flow as per the institute's experimental animal guidelines. Access to normal chow and water was provided to them *ad libitum*. The animals were acclimatized for 1 week in the above conditions prior to initiating the experiments.

TABLE 1 List of primers.

Gene	Forward primer	Reverse primer
Human primers		
TNF-alpha	CTCTTCTGCCTGCTGCACTTTG	ATGGGCTACAGGCTTGTCACTC
IL-6	AGACAGCCACTCACCTCTTCAG	TTCTGCCAGTGCCTCTTTGCTG
IL-1beta	CCACAGACCTTCCAGGAGAATG	GTGCAGTTCAGTGATCGTACAGG
IL-8	GAGAGTGATTGAGAGTGGACCAC	CACAACCCTCTGCACCCAGTTT
IL-18	GATAGCCAGCCTAGAGGTATGG	CCTTGATGTTATCAGGAGGATTCA
IL-4	CCGTAACAGACATCTTTGCTGCC	GAGTGTCCTTCTCATGGTGGCT
CCL2	AGAATCACCAGCAGCAAGTGTCC	TCCTGAACCCACTTCTGCTTGG
18S	ACCCGTTGAACCCCATTCGTGA	GCCTCACTAAACCATCCAATCGG
Mouse primers		
Tnf-alpha	GGTGCCTATGTCTCAGCCTCTT	GCCATAGAACTGATGAGAGGGAG
Il-6	TACCACTTCACAAGTCGGAGGC	CTGCAAGTGCATCATCGTTGTTC
Il-1beta	TGGACCTTCCAGGATGAGGACA	GTTCATCTCGGAGCCTGTAGTG
Il-18	GACAGCCTGTGTTCGAGGATATG	TGTTCTTACAGGAGAGGGTAGAC
Cxcl1	TCCAGAGCTTGAAGGTGTTGCC	AACCAAGGGAGCTTCAGGGTCA
Il-4	ATCATCGGCATTTTGAACGAGGTC	ACCTTGGAAGCCCTACAGACGA
Ccl2	GCTACAAGAGGATCACCAGCAG	GTCTGGACCCATTCCTTCTTGG
18S	GCAATTATTCCCCATGAACG	GGCCTCACTAAACCATCCAA

Cell culture

NCI-H460 cell line (human lung carcinoma cells) was procured from the National Centre of Cell Science, Pune, India, and was routinely maintained in RPMI-1640 medium containing 10% (v/v) fetal bovine serum (FBS), 100 units/ml penicillin and 100 µg/ml streptomycin (Invitrogen, United States). Cells were maintained in a humidified incubator with 5% CO_2 at 37°C. A549 cells were procured from ATCC and maintained in DMEM containing 10% (v/v) fetal bovine serum (FBS), 100 units/ml penicillin and 100 µg/ml streptomycin (Invitrogen, United States) and maintained in a humidified incubator with 5% CO_2 at 37°C, as above.

Aqueous extract of the *W. somnifera* (WS) roots was prepared in the good manufacturing practice (GMP) facility and was provided by NMPB, and its characterization has been reported previously (Kasarla et al., 2022).

Quantitative real-time PCR (qPCR)

Total RNA was isolated from cells treated with different concentrations of WS and lungs using Trizol Reagent (Thermo Fisher Scientific), according to the manufacturer's protocol and used for the cDNA synthesis. cDNA was synthesized with an iScript cDNA synthesis kit (Applied Biosystems, United States) as per the manufacturer's protocol. The gene-specific primers (Table 1) were designed using NCBI primer blast tool, and qPCR was performed on the QuantStudio 6 (Applied Biosystems, United States) real-time PCR systems. Reactions were carried out in 10 µl volumes containing: 5 µl Sybr green Master Mix (PowerUp SYBR Green mix, Applied Biosystems; Cat. No. A25742), 0.5 µl forward and 0.5 µl reverse primers, 3 µl water, and 1 µl cDNA. Cycling program used was: 7 min at 95°C and then 40 cycles with 10 s at 95°C and 20 s at 60°C. The specificity of the amplicons was analysed by a thermal dissociation curve. Data were normalized against the housekeeping gene, 18S, or GAPDH.

In vitro anti-inflammatory activity of *Withania somnifera* and cell viability assay

NCI-H460 cells were seeded at a density of 1 $\times 10^4$ cells/well in RPMI medium with 10% FBS in a 96-well plate and incubated at 37°C in a CO_2 incubator for 24 h followed by treatment with WS at 10, 3, 1, 0.3, 0.1, and 0.003 mg/ml. LPS (1 µg/ml) was added 30 min after the treatment with WS and the plate was incubated further in the CO_2 incubator for 24 h. Dexamethasone was used as a positive control (10 µM). For gene expression analysis, cells were grown at a density of 4×10^5 cells/well in a 6 well plate. After 24 h, cells were treated with various concentrations of WS (10, 3, and 1 mg/ml) in RPMI 1640 medium with 10% FBS followed by stimulation with LPS (1 µg/ml), and the plate was incubated in the CO_2 incubator for another 24 h. Cells were lysed using the Trizol reagent and total RNA and cDNA was prepared followed by gene expression analysis as mentioned above. Similar experiments were carried out using A549 cells also. To determine the cytotoxicity of WS, 3-(4,5-dimethylthiazol-2-yl)-2,5-diphenyltetrazolium bromide (MTT) assay

was performed. Cells treated as above in the inflammatory profiling setup were treated with MTT (100 µl of 0.5 mg/ml MTT stock in PBS) in an independent experiment, and the plate was incubated for 4 h at 37°C in a CO_2 incubator. The MTT mixture was aspirated and 100 µl of DMSO was added to each well to dissolve the formazan particles. The plate was shaken for 30 min on a plate shaker at 37°C to ensure complete dissolution of formazan crystals and read at 570 nm to measure the probable cytotoxicity of test substances if any.

Cell viability (%) = Total viable cells (unstained)/Total cells (unstained) + blue stained χ 100.

LPS-induced inflammatory response in human peripheral blood mononuclear cells (PBMCs)

Intravenous blood was drawn from healthy individuals and collected in a heparinized tube. Heparinized blood was diluted with 1x PBS (1:1). After dilution, blood was layered on Histopaque-®1077 (2: 1) in a falcon tube and centrifuged at 1,600 rpm for 30 min. The middle layer of the buffy coat containing PBMCs was collected cautiously and washed twice with PBS. The pellet was dissolved in PBS for counting PBMCs using a hemocytometer.

The cells were plated at a cell density of 1×10^6 cells/well in a 24-well plate. Cells were treated with WS (1 mg/ml) and incubated at 37°C in a CO_2 incubator for 30 min followed by treatment with LPS (1 µg/ml) and incubated again at 37°C in a CO_2 incubator for another 16 h. Cell culture supernatant was collected the next day and analyzed for the expression levels of different cytokines by ELISA as per the manufacturer's instructions. Institutional ethics committee approval was obtained prior to initiating experiments with human blood obtained from healthy human volunteers (Institutional ethics approval number: THS1.8.1/100). No experiments were carried out in humans directly.

LPS-induced neutrophilia in BALB/c mice

The effect of WS in LPS-induced neutrophilia was evaluated under two timepoints. In the first healthy mice were randomized based on their body weights and divided into five different groups: 1) Control; 2) LPS (25 µg/mice); 3) Dexamethasone (1 mg/kg); 4–6) WS, (10, 30, and 100 mg/kg). All the groups except the control group were injected intranasally with LPS in 200 µl PBS (pH 7.4). Mice in groups 4, 5, and 6 were treated orally with WS mixed in saline and challenged with LPS after 30 min of drug treatment. Mice in the control group were challenged with saline only and animals were euthanized 4 h after the WS or saline challenge. Broncho-alveolar lavage (BAL) fluid was collected from the lungs of mice in ice-cold Hank's Balanced Salt Solution (HBSS) or 1X Phosphate buffer saline (PBS) and processed for the quantification of total and differential leukocyte counts. Lungs were isolated, homogenized, and lysed with Trizol reagent. Total RNA was isolated as per the manufacturer's protocol. In the second study, the anti-inflammatory potential of WS was analysed in a 4-day LPS challenge model. Mice were treated with WS by oral route followed by intranasal administration of LPS (25 µg/mice) for 4 consecutive days. After 4 days mice were euthanized and analysed for the presence of leukocytes using BAL fluid as in the case of the 4 h study, mentioned above.

BAL fluid analysis

Smears were prepared using 50–100 µl of the freshly isolated BAL fluid on a frosted glass slide using a Cytospin centrifuge (Biotek, Agilent Technologies Inc. Santa Clara, CA United States) by spinning the slides at 1,000 rpm for 10 min. Slides were dried and fixed with 100% ethanol, further stained with Giemsa stain, and cell counts were taken by scientists who were blinded to the treatment groups.

Histological evaluation

Healthy mice were randomized based on their body weights and divided into four different groups: 1) Control; 2) LPS (25 µg/mice); 3) Dexamethasone (1 mg/kg); 4) WS (100 mg/kg). All the groups except the control group were injected intranasally with LPS in 200 µl PBS (pH 7.4). Mice were treated orally with WS mixed in saline after 30 min of LPS challenge. Mice in the control group were challenged with saline only and animals were euthanized 4 days after the WS or saline challenge.

Histological evaluation was done using the lung tissues of different groups of mice. Mice were sacrificed 4 days after the LPS administration and lower lobes from the left lung were dissected and fixed in 10% formalin, dehydrated with ethanol followed by embedding in paraffin and cutting into 5 µm sections. After deparaffinization, the tissues were stained with Hematoxylin and Eosin (H&E) as reported previously (Alwahaibi et al., 2015). Pathological changes among different groups were evaluated under a light microscope and lung injury scores were assessed using a semi-quantitative method.

Statistical analysis

Each experiment was performed three or more times independently with different cell passages. For animal work, each group consisted of $n = 5$ mice. Statistical analysis was performed on GraphPad PRISM 7 software (GraphPad, La Jolla, CA, United States) using one-way ANOVA. The p-values of <0.05 were considered statistically significant. The results were calculated as mean ± S.E.M.

Results

Withania somnifera extract reduces the levels of LPS-induced increase in the levels of pro-inflammatory cytokines in NCI-H460 cells

To recapitulate the anti-inflammatory properties of WS *in vitro*, cell-based assays were conducted using a lung carcinoma cell line, NCI-H460, and lung epithelial cell line A549. WS extract was not found to be toxic in the MTT assay at the concentrations used in the *in vitro* experiments (Figure 1A). Treatment with LPS led to a significant increase in the secretion of TNF-α, IL-8, IL-6, chemokine (c-c)

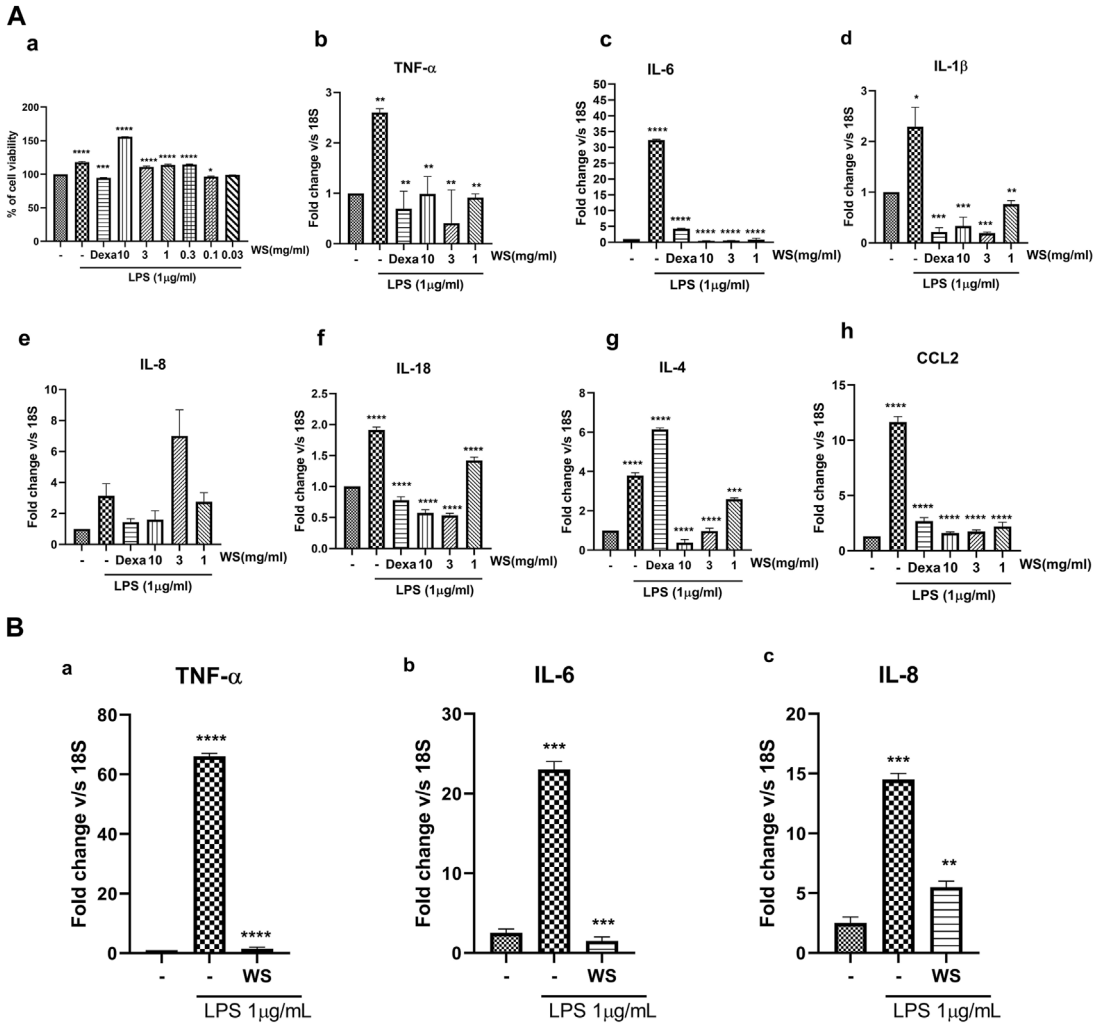

FIGURE 1
WS suppresses the levels of LPS-induced increase in the mRNA expression of inflammatory cytokines and chemokine(s) *in vitro* in the NCI-H460 and A549 cell lines. **(A)** a) Cytotoxicity of WS on NCI-H460 cells expressed as % cell viability. (b–h) mRNA expression levels of various inflammatory markers were analyzed in the cell lysates by semi-quantitative real-time PCR analysis (TNF-α, IL-6, IL-1β, IL-8, IL-18, IL-4 and CCL2) using NCI-H460 cell line. Cells were pre-treated with WS for 30 min, followed by LPS challenge for 4 h. Dexamethasone was used as a positive control. **(B)** mRNA expression levels of a few key inflammatory markers analyzed by semi-quantitative RTPCR using A549 cell line. Data are presented as the mean ± SEM (n = 3). *$p < 0.05$, **$p < 0.001$, ***0.0001 ****$p < 0.00001$ by one-way ANOVA. Significant compared to control (untreated) and ****, ***, ** *significant compared to cells treated with LPS.

motif ligand 2 (CCL2), and IL-8 while pre-treatment of the cells with different concentrations of WS (10–0.03 mg/ml) showed a dose-dependent inhibition of pro-inflammatory cytokines by RT-PCR (NCI-H460: Figure 1A) and in A549 cell line for TNF-α, IL-8, IL-6 (Figure 1B) suggesting the anti-inflammatory properties of WS. Treatment with dexamethasone resulted in a decrease in the levels of pro-inflammatory cytokines.

Withania somnifera extract reduces the levels of LPS-induced increase in the levels of pro-inflammatory cytokines in human PBMCs

Human PBMCs led to an increase in the expression levels of pro-inflammatory cytokines and chemokines such as TNF-α, IL-6, IL-1β, and IL-8, when induced with LPS (1 μg/ml). Pre-treatment of hPBMCs with different concentrations of WS (10, 3, 1, 0.3, 0.1, and 0.03 mg/ml) on the other hand, significantly reduced LPS-induced increase in the cytokines and chemokines (Figure 2).

Withania somnifera (WS) attenuates the LPS-induced increase in the neutrophil counts in the broncho-alveolar lavage (BAL) fluid of BALB/c mice

To explore the beneficial effects of WS on endotoxin-induced airway inflammation *in vivo*, BALB/c mice were treated with three different doses of WS (10, 30, and 100 mg/kg for 30 min, followed by the LPS challenge by the intranasal route, and BAL fluid was collected after 4 h. Total number of leukocytes and differential

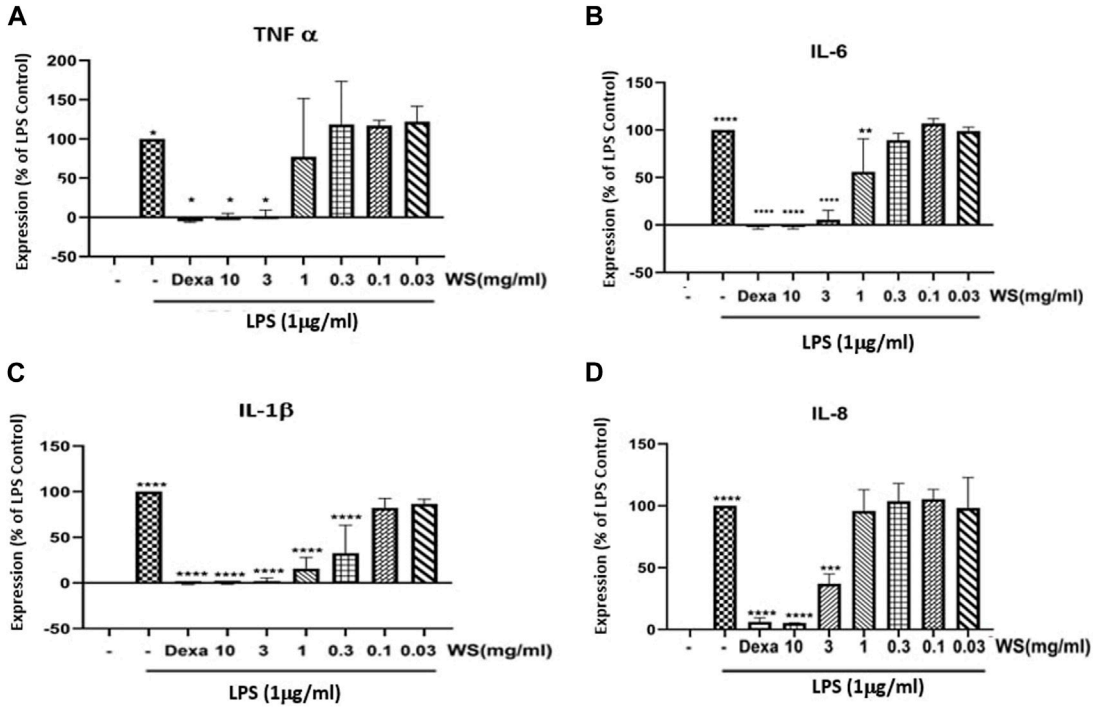

FIGURE 2
WS inhibits the levels LPS induced increase in the levels of pro-inflammatory cytokines in human PBMCs. PBMC cells were pre-treated with various concentrations of WS for 30 min, followed by treatment with LPS for 24 h. Cell culture supernatant was collected and analyzed for the levels of cytokines and chemokines. **(A)** TNF-α, **(B)** IL-6, **(C)** IL-1β, and **(D)** IL-8 by ELISA. Dexamethasone was used as a positive control. Data are presented as the mean ± SEM (n = 3) ****p < 0.00001 by one-way ANOVA. Significant compared to control cells (untreated) and ****, significant compared to cells treated with LPS.

neutrophil counts were analyzed in the BALF (Figure 3A). LPS challenge in mice resulted in a significant increase in the leukocytes influx compared to the unchallenged mice. Treatment with different doses of WS attenuated the number of total leukocytes as well as neutrophil counts in a dose-dependent manner. Dexamethasone was used as a positive control and led to a reduction in neutrophil counts.

Withania somnifera reduces the levels of inflammatory cytokines in the lung tissues of BALB/c mice challenged with LPS

LPS-induced leukocyte infiltration is associated with the levels of pro-inflammatory cytokines secreted into the lungs of mice (Gupta V et al., 2015). To test the effect of WS on LPS-induced inflammation in the lung tissue, mRNA expression studies were done using the lung tissues of mice challenged intranasally with LPS with or without WS by RT-PCR. LPS challenge in mice significantly increased the levels of IL-1β, IL-18, IL-4, IL-6, chemokine (c-x-c) motif ligand 1 (CXCL-1), IL-18, CCL2, and TNF-α (Figure 3B) which was found to be significantly reduced in mice pre-treated with WS in a dose-dependent manner. Treatment with dexamethasone resulted in a significant decrease in all tested cytokines except IL-4.

Withania somnifera ameliorates the LPS-induced lung damage in BALB/c mice in a 4-day study

Intranasal administration of LPS has been reported to cause lung tissue damage in mice. Histological analysis of the lung tissues was carried out to assess the LPS-induced lung damage in a 4-day LPS challenge model using BALB/c mice (Figure 4). The lungs of mice in the control group, showed normal pulmonary architecture whereas the lungs of mice challenged with LPS showed notable inflammatory cell infiltration and alveolar haemorrhage. Treatment with WS significantly attenuated such pathological changes induced by LPS. The positive control dexamethasone also improved the histopathological conditions in LPS-induced mice. For semi-quantitative evaluation, the changes were also evaluated by calculating a lung injury score our data suggests that pre-treatment WS alleviates LPS-induced pathological changes in the mouse model.

Discussion

Inflammation is a crucial event for tissue defense against injury or infection. However, uncontrolled or unresolved inflammation can lead to tissue damage or chronic injury with eventual loss of

10.3389/fphar.2023.1139654

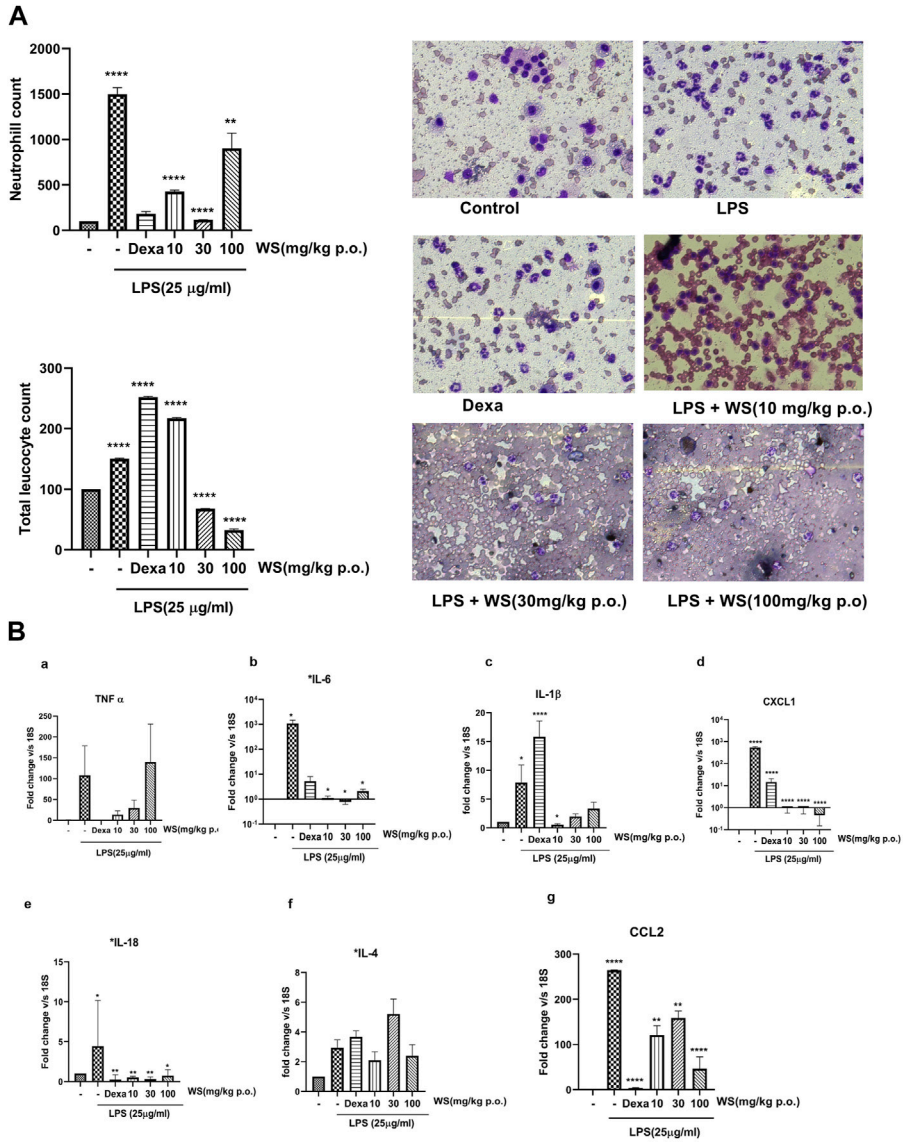

FIGURE 3
WS shows potent anti-inflammatory potential in BALB/c mice challenged intranasally with LPS for 4 h. **(A)** WS reduced the infiltration of LPS-induced increase in the infiltration of total leukocytes and neutrophils in the broncho-alveolar lavage (BAL) fluid of BALB/c mice. Mice (n = 5 mice in each group) were acclimatized, randomized, and prophylactically treated with WS for 30 min followed by LPS challenge for 4 h. Mice were anesthetized after 4 h and BAL fluid was isolated and analysed for a) total neutrophil counts b) total leukocyte counts c) microscopic studies showing the inhibition of neutrophil counts by WS. Data are presented as the mean ± SEM (n = 4–5), *p < 0.05, **p < 0.001, ***0.0001 ****p < 0.00001 by one-way ANOVA. Significant compared to control mice and **, **** significant compared to LPS-treated mice. **(B)** WS inhibits the levels LPS induced increase in the mRNA expression levels of pro-inflammatory cytokines in the lung tissue samples of BALB/c mice by real time-PCR. a) TNF-α, b) IL-6, c) IL-1β, d) CXCL-1, e) IL-18, f) IL-4, and g) CCL2. Dexamethasone was used as a positive control. Data are represented as Mean ± SEM, n = 5–8, and Statistical significance was assessed by one-way ANOVA. Significant compared to control mice and *, **, **** significance compared to LPS-treated mice *p < 0.05, **p < 0.001, ****p < 0.00001).

tissue homeostasis. The COVID-19 pandemic in the last 3 years has swept across the globe and has affected a large number of patients with persistent inflammation in vital tissues such as the lungs, metabolic tissues, and the heart. Since aberrant airway injuries are one of the most common complications in these patients, it is important to identify therapies that can alleviate lung inflammation in these patients.

On the basis of the results of randomized clinical trials, WHO has recommended the guidelines for the treatment of COVID-19-infected patients and prescribed the use of corticosteroids to patients who are admitted to hospitals as a result of severe coronavirus infection (WHO, 2022). There is no data however to support the use of systemic corticosteroids in non-hospitalized patients with COVID-19. Since the use of corticosteroids is associated with several adverse events, e.g., hyperglycemia, neuropsychiatric symptoms, and secondary infections in most patients, they should not be prescribed without the controlled supervision of a clinician.

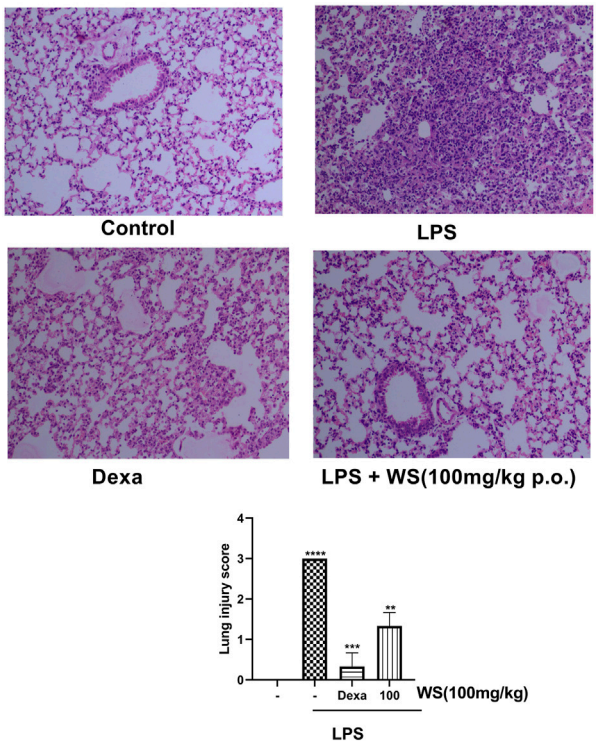

FIGURE 4
WS ameliorates the LPS-induced lung damage in BALB/c mice in a 4 day study. Effect of WS on LPS-induced lung injury was studied in a 4 day LPS challenge model using BALB/c mice. Lungs from each experimental group ((*n* = 5 mice in each group) were obtained 4 days after LPS challenge as described in the Methodology section. Tissue sections were stained with H&E and sections from each group are represented as control (upper left panel), LPS (1 mg/kg, upper right panel), Dexamethasone (1 mg/kg), lower left panel), LPS+WS (100 mg/kg, lower right panel), H&E stained lung sections are shown in original magnification ×200. Assessment of lung injury was done based on the scores obtained as a mark of lung damage (bar diagram). Scores such as 0, 1, 2, 3, and 4 represented no damage, mild damage, moderate damage, severe damage, and very severe damage, respectively. Data have been expressed as means ± SEM. Statistical significance was assessed using Kruskal-Wallis with a Dunn's post test, $^{**}p < 0.001$, $^{**}p < 0.0001$, $^{****}p < 0.00001$). Significant compared to control mice and LPS-treated mice.

Ayurveda an ancient traditional medicinal system that originated and is being practiced in India illustrates the therapeutic potential of many medicinal plants and herbs in curing various kinds of ailments, diseases, and disorders. *W. somnifera*, popularly known as Ashwagandha, is one such medicinal plant mentioned in Ayurveda and is known for its antiviral, anti-inflammatory, anti-diabetic, neuroprotective, analgesic, anti-tumor, and immunomodulatory properties (Fugner, 1973; Singh et al., 2015; Tiwari et al., 2014) including pulmonary hypertension and fibrosis (Kaur et al., 2015). The anti-inflammatory activity of WS extract and its phytoconstituents has been demonstrated in RAW 264.7 cells by the inhibition of LPS-mediated release of nitric oxide following induction of iNOS and COX-2 expression (Orrù et al., 2023) A recently conducted double-blind placebo-controlled clinical trial study (Singh et al., 2022) and recent reviews advocate the benefits of WS extract in the management of COPD patients when given alone or in combination with conventional drugs (Paul et al., 2021; Saggam et al., 2021). A previous study from our lab has shown that WS possesses both antiviral and immunomodulatory properties and was effective in mitigating the pulmonary pathology of COVID-19 in the hamster and transgenic mice models (Rizvi, et al., 2023). In addition, T-cell differentiation was also assessed *in-vitro* to understand the immunomodulatory potential of WS. Effector T helper cell response is central to immunity and health, interferon γ secreted by Th1 cells is important for clearing cellular pathogens (Rizvi, et al., 2023). IL-4 which is primarily secreted by Th2 cells plays a major role in extracellular pathogen clearance and allergic response. Similarly, IL-17 cytokine could act in fungal defense and also leads to cellular injury. We observed that WS was most effective against Th2 cell differentiation suggesting the possible role of WS in limiting COVID-19 pathology. In another study reported recently by us, WS did not have any effect on liver CYP enzymes such as CYP3A4, CYP2C8, and CYP2D6 either alone or in combination with remdesivir suggesting it to be safe without any herb-drug interaction concerns (Kasarla et al., 2022).

Since lung impairment is one of the most common concerns in patients infected with Coronavirus, we, therefore, tested the WS extract for its ability to suppress the inflammation in the cell-based and animal models of acute lung inflammation. The *in vitro* and *in vivo* models used in the present study have wide applicability for testing the anti-inflammatory properties of test substances in alleviating excessive inflammation in respiratory disorders such as asthma, COPD, and bronchitis (Gupta V et al., 2015). The study performed in NCI-H460 and A549 cell lines, demonstrates inhibition of key Th2-dependent cytokines; IL-6 and IL-4, and also a neutrophil function-related cytokine; IL-8 by WS extract in a TLR-4-dependent manner. It is interesting that the level of these cytokines was augmented in COVID-19 patients as well as in the patients with severe asthma and chronic obstructive pulmonary disease (COPD). WS inhibited the expression and generation of the pro-inflammatory cytokines such as IL-6, IL-8, TNF-α, IL-1β, and IL-18 in NCI-H460 cells, human peripheral blood mononuclear cells (PBMCs) and in the lung tissues of Balb/-6 mice challenged intranasally with LPS. Moreover, WS extract pre-treatment reduced neutrophil influx into the LPS-treated mice lungs. Since increased levels of IL-8 have been previously shown to correlate with severe and persistent neutrophil counts in COVID-19 patients, with frequent exacerbations and hospitalizations, we thus evaluated the effect of WS in reducing the LPS-induced neutrophilia in Balb/c mice. Mice challenged intranasally with LPS led to an increase in the total leukocyte and neutrophil counts in the airway which was significantly inhibited by oral administration of WS in both 4-h and 4-day studies along with inhibition of IL-8 in the lung tissues of mice. Ashwagandha thus seems to be efficacious and useful due to its potent immunomodulatory potential.

It is also important to assess the efficacy of Ashwagandha in chronic models of airway inflammation, bronchial asthma in animals (Arora et al., 2021; Arora et al., 2022; Arora et al., 2022; Arora et al., 2022; Visaga et al., 2022), and subsequently in the COPD and COVID-19 patients.

Data availability statement

The original contributions presented in the study are included in the article/supplementary material, further inquiries can be directed to the corresponding authors.

Ethics statement

The animal study was reviewed and approved by the Institutional Animal Ethics Committee (IAEC-THSTI/163) of the Translational Health Science and Technology Institute (THSTI), Faridabad, India, and all the experiments were carried out following the CPCSEA guidelines (Govt. of India).

Author contributions

PS did the *in vitro* and *in vivo* experiments. LK did *in vivo* experiments. YG did experiments using human PBMCs. MP conducted the histopathological studies of mouse lung samples. MD analyzed the experimental data and plan of experiments. RT conceptualised, planned and executed the study and also analysed the data and wrote the manuscript. All authors contributed to the article and approved the submitted version.

Acknowledgments

The authors express their gratitude to the Ministry of AYUSH and the Department of Biotechnology (DBT), Government of India for joint funding to carry out the research work presented in this manuscript (Grant Nos: BT/PR40738/TRM/120/486/2020 and A.11019/03/2020-NMPB-IV-A). MD also acknowledges the financial support from JBR/2020/000034. We acknowledge THSTI Small Animal Facility (SAF) for its services.

Conflict of interest

The authors declare that the research was conducted in the absence of any commercial or financial relationships that could be construed as a potential conflict of interest.

Publisher's note

References

Allgood, S., Peters, J., Benson, A., Maragos, C., McIltrot, K., Slater, T., et al. (2021). Acquired laryngeal and subglottic stenosis following COVID-19-Preparing for the coming deluge. *J. Clin. Nurs.* 2021. doi:10.1111/jocn.15992

Alwahaibi, N. Y., Alkhatri, A. S., and Kumjar, J. S. (2015). Hematoxylin and eosin stain shows a high sensitivity but sub-optimal specificity in demonstrating iron pigment in liver biopsies. *Int. J. Appl. Basic Med. Res.* 5 (3), 169–171. doi:10.4103/2229-516X.165365

Arora, P., Ansari, S. H., and Nainwal, L. M. (2022). Clerodendrum serratum extract attenuates production of inflammatory mediators in ovalbumin-induced asthma in rats. *Turk J. Chem.* 46, 330–341. doi:10.55730/1300-0527.3310

Arora, P., Ansari, S. H., and Nainwal, L. M. (2021). Mesua ferrea L (Calophyllaceae) exerts therapeutic effects in allergic asthma by modulating cytokines production in asthmatic rats. *Turk J. Bot.* 45, 820–832. doi:10.3906/bot-2111-22

Arora, P., Athari, S. S., and Nainwal, L. M. (2022). Piperine attenuates production of inflammatory biomarkers, oxidative stress and neutrophils in lungs of cigarette smoke-exposed experimental mice. *Food Biosci.* 49, 101909. doi:10.1016/j.fbio.2022.101909

Arora, P., Nainwal, L. M., Gupta, G., Singh, S. K., Chellappan, D. K., Oliver, B. G., et al. (2022). Orally administered solasodine, a steroidal glycoalkaloid, suppresses ovalbumin-induced exaggerated Th2-immune response in rat model of bronchial asthma. *Chem. Biol. Interact.* 366, 110138. doi:10.1016/j.cbi.2022.110138

Bale, S., Venkatesh, P., Sunkolu, M., and Godugu, C. (2018). An adaptogen: Withaferin A ameliorates *in vitro* and *in vivo* pulmonary fibrosis by modulating the interplay of fibrotic, matricelluar proteins, and cytokines. *Front. Pharmacol.* 9, 248. doi:10.3389/fphar.2018.00248

Behl, T., Sharma, A., Sharma, L., Sehgal, A., Zengin, G., Brata, R., et al. (2020). Exploring the multifaceted therapeutic potential of withaferin A and its derivatives. *Biomedicines* 8 (12), 571. doi:10.3390/biomedicines8120571

Chakraborty, S., Mallick, D., Goswami, M., Guengerich, F. P., Chakrabarty, A., and Chowdhury, G. (2022). The natural products withaferin A and withanone from the medicinal herb Withania somnifera are covalent inhibitors of the SARS-CoV-2 main protease. *J. Nat. Prod.* 85, 2340–2350. doi:10.1021/acs.jnatprod.2c00521

Crothers, K., DeFaccio, R., Tate, J., Alba, P. R., Goetz, M. B., Jones, B., et al. (2021). Dexamethasone in hospitalised COVID-19 patients not on intensive respiratory support. *Eur. Respir. J.* 60 (1), 2102532. doi:10.1183/13993003.02532-2021

Fugner, A. (1973). Inhibition of immunologically induced inflammation by the plant steroid withaferin A. *Arzneim.* 23 (7), 932–935.

George, P. M., Athol, U., and Jenkins, R. G. (2020). Pulmonary fibrosis and COVID-19: The potential role for antifibrotic therapy. *Respir. Med.* 8 (8), P807–P815. doi:10.1016/S2213-2600(20)30225-3

Ghasemian, M., Owlia, S., and Owlia, M. B. (2016). Review of anti-inflammatory herbal medicines. *Adv. Pharmacol. Sci.* 2016, 9130979–9131011. doi:10.1155/2016/9130979

Gupta, V., Banyard, A., Mullan, A., Sriskantharajah, S., Southworth, T., and Singh (2015). Characterization of the inflammatory response to inhaled lipopolysaccharide in mild to moderate chronic obstructive pulmonary disease. *Br. J. Clin. Pharmacol.* 79 (5), 767–776. doi:10.1111/bcp.12546

Huang, Y. C., Deng, J. S., Huang, W. C., Jiang, W. P., and Huang, G. J. (2020). Attenuation of lipopolysaccharide-induced acute lung injury by hispolon in mice, through regulating the TLR4/PI3K/Akt/mTOR and keap1/nrf2/HO-1 pathways, and suppressing oxidative stress-mediated ER stress-induced apoptosis and autophagy. *Nutrients* 12, 1742. doi:10.3390/nu12061742

Kasarla, S. S., Borse, S. P., Kumar, Y., Sharma, N., and Dikshit, M. (2022). *In vitro* effect of Withania somnifera, AYUSH-64, and remdesivir on the activity of CYP-450 enzymes: Implications for possible herb–drug interactions in the management of COVID-19. *Front. Pharmacol.* 13, 973768. doi:10.3389/fphar.2022.973768

Kaur, G., Singh, N., Samuel, S. S., Bora, H. K., Sharma, S., Pachauri, S. D., et al. (2015). Withania somnifera shows a protective effect in monocrotaline-induced pulmonary hypertension. *Pharm. Biol.* 53 (1), 147–157. doi:10.3109/13880209.2014.912240

Li, H., Yan, B., Gao, R., Ren, J., and Yang, J. (2021). Effectiveness of corticosteroids to treat severe COVID-19: A systematic review and meta-analysis of prospective studies. *Int. Immunopharmacol.* 100, 108121. doi:10.1016/j.intimp.2021.108121

Mortaz, E., Tabarsi, P., Varahram, M., Folkerts, G., and Adcock, I. M. (2020). The immune response and immunopathology of COVID-19. *Front. Immunol.* 11, 1–9. doi:10.3389/fimmu.2020.02037

National Medicinal Plants Board (2021). *Medicinal plants of '21 for COVID-19 care.* India: National Medicinal Plants Board, Ministry of Ayush.

Ni, L., Zhou, L., Zhou, M., Zhao, J., and Wang, D. W. (2020). Combination of Western medicine and Chinese traditional patent medicine in treating a family case of COVID-19. *Front. Med.* 14 (2), 210–214. doi:10.1007/s11684-020-0757-x

Orrù, A., Marchese, G., and Ruiu, S. (2023). Alkaloids in *Withania somnifera* (L) dunal root extract contribute to its anti-inflammatory activity. *Pharmacology* 108, 301–307. doi:10.1159/000527656

Park, H. S., Jung, H. Y., Park, E. Y., Kim, J., Lee, W. J., and Bae, Y. S. (2004). Cutting edge: Direct interaction of TLR4 with NAD(P)H oxidase 4 isozyme is

essential for lipopolysaccharide-induced production of reactive oxygen species and activation of NF-kappa B. *B J. Immunol.* 173, 3589–3593. doi:10.4049/jimmunol.173.6.3589

Patwardhan, B., Chavan-gautam, P., Gautam, M., Gir, T., and Chopra, A. (2020). Ayurveda rasayana in prophylaxis of COVID-19. *Curr. Sci.* 19 (8), 1158–1160. doi:10.1016/j.matpr.2021.03.066

Patwardhan, B., Vaidya, A. D. B., and Mukund, C. (2004). Ayurveda and natural products drug discovery. *Curr. Sci.* 86 (6), 789–799.

Paul, S., Chakraborty, S., Anand, U., Dey, S., Nandy, S., Ghorai, M., et al. (2021). Withania somnifera (L) dunal (Ashwagandha): A comprehensive review on ethnopharmacology, pharmacotherapeutics, biomedicinal and toxicological aspects. *Biomed. Pharmacother.* 143, 112175. doi:10.1016/j.biopha.2021.112175

Purushotham, P. M., Kim, J. M., Jo, E. K., and Senthil, K. (2017). Withanolides against TLR4-activated innate inflammatory signalling pathways: A comparative computational and experimental study. *Phytother. Res.* 31 (1), 152–163. doi:10.1002/ptr.5746

RECOVERY Collaborative GroupHorby, P., and Lim, W. S. (2021). Dexamethasone in hospitalized patients with COVID-19. *N. Engl. J. Med.* 384 (8), 693–704. doi:10.1056/NEJMoa2021436

Rizvi, Z. A., Babele, P., Madan, U., Sadhu, S., Tripathy, M. R., Goswami, S., et al. (2023). Pharmacological potential of *Withania somnifera* (L) Dunal and *Tinospora cordifolia* (Willd) Miers on the experimental models of COVID-19, T cell differentiation, and neutrophil functions. *Front. Immunol. (Viral Immunol.* 14, 1138215–1138220. doi:10.3389/fimmu.2023.1138215

Saggam, A., Limgaokar, K., Borse, S., Gautam, P. C., Dixit, S., Tillu, G., et al. (2021). Withania somnifera (L) dunal: Opportunity for clinical repurposing in COVID-19 management. *Front. Pharmacol.* 12, 623795. doi:10.3389/fphar.2021.623795

Sanyaolu, A., Okorie, C., Marinkovic, A., Patidar, R., Younis, K., Desai, P., et al. (2020). Comorbidity and its impact on patients with COVID-19. *SN Compr. Clin. Med.* 2, 1069–1076. doi:10.1007/s42399-020-00363-4

Shankar, A., Dubey, A., Saini, D., and Prasad, C. P. (2020). Role of complementary and alternative medicine in prevention and treatment of COVID-19: An overhyped hope. *Chin. J. Integr. Med.* 26, 565–567. doi:10.1007/s11655-020-2851-y

Singh, P., Guleri, R., Singh, V., Kaur, G., Kataria, H., Singh, B., et al. (2015). Biotechnological interventions in Withania somnifera (L) dunal. *Biotechnol. Genet. Eng. Rev.* 31 (1-2), 1–20. doi:10.1080/02648725.2015.1020467

Singh, P., Salman, K. A., Shameem, M., and Warsi, M. S. (2022). *Withania somnifera (L.) dunal* as add-on therapy for COPD patients: A randomized, placebo-controlled, double-blind study. *Front. Pharmacol.* 13, 901710. doi:10.3389/fphar.2022.901710

Sterne, J. A. C., Murthy, S., Diaz, J. V., Slutsky, A. S., and Villar, J. (2020). Association between administration of systemic corticosteroids and mortality among critically ill patients with COVID-19: A meta-analysis. *JAMA* 324 (13), 1330–1341. doi:10.1001/jama.2020.17023

Tang, Y., Liu, J., Zhang, D., Xu, Z., Ji, J., and Wen, C. (2020). Cytokine storm in COVID-19: The current evidence and treatment strategies. *Front. Immunol.* 11, 1708. doi:10.3389/fimmu.2020.01708

Tiwari, R., Chakraborty, S., Saminathan, M., Dhama, K., and Singh, S. V. (2014). Ashwagandha (Withania somnifera): Role in safeguarding health, immunomodulatory effects, combating infections and therapeutic applications: A review. *J. Biol. Sci.* 14 (2), 77–94. doi:10.3923/jbs.2014.77.94

Visaga, S. A., Kalonia, H., Verma, V., Sinha, S., Singh, S. K., Upadhyay, S., et al. (2022). Developing selective FPR2 agonists can be a potential approach to treat moderate to severe asthma. *J. Clin. Toxicol.* 12 (3), 1000510.

WHO (2022). COVID-19 therapeutics 2022. Available at: https://www.who.int/teams/health-care-readiness/covid-19/therapeutics.

Yunhe, F., Bo, L., Xiaosheng, F., Fengyang, L., Liang, D., Zhicheng, L., et al. (2012). The effect of magnolol on the toll-like receptor 4/nuclear factor kappa B signaling pathway in lipopolysaccharide-induced acute lung injury in mice. *Eur. J. Pharmacol.* 689, 255–261. doi:10.1016/j.ejphar.2012.05.038

Zheng, K. I., Gong, F., Liu, W. Y., Targher, G., Byrne, C. D., and Zheng, M. H. (2020). Extrapulmonary complications of COVID-19: A multisystem disease? *J. Med. Virol.* 93 (1), 323–335. doi:10.1002/jmv.26294

Zhou, P., Yang, X. L., Wan, X. G., Hu, B., Zhang, L., Zhang, W., et al. (2020). A pneumonia outbreak associated with a new coronavirus of probable bat origin. *Nature* 579 (7798), 270–273. doi:10.1038/s41586-020-2012-7

Zhou, Y., Fu, B., Zheng, X., Wang, D., Zhao, C., Qi, Y., et al. (2020). Pathogenic Tcells and inflammatory monocytes incite inflammatory storms in severe COVID-19 patients. *Nat. Sci. Rev.* 7 (6), 998–1002. doi:10.1093/nsr/nwaa041

frontiers | Frontiers in Pharmacology

TYPE Original Research
PUBLISHED 21 June 2023
DOI 10.3389/fphar.2023.1125414

OPEN ACCESS

EDITED BY
Poonam Arora,
Shree Guru Gobind Singh Tricentenary University, India

REVIEWED BY
Yih Dih Cheng,
China Medical University Hospital, Taiwan
Varisha Anjum,
South Ural State University, Russia

*CORRESPONDENCE
Yuh-Chiang Shen,
yuhcs@nricm.edu.tw
Yi-Chang Su,
sychang@nricm.edu.tw

†These authors have contributed equally to this work and share the first authorship

RECEIVED 16 December 2022
ACCEPTED 12 June 2023
PUBLISHED 21 June 2023

CITATION
Wei W-C, Tsai K-C, Liaw C-C, Chiou C-T, Tseng Y-H, Liao G-Y, Lin Y-C, Chiou W-F, Liou K-T, Yu I-S, Shen Y-C and Su Y-C (2023), NRICM101 ameliorates SARS-CoV-2–S1-induced pulmonary injury in K18-hACE2 mice model.
Front. Pharmacol. 14:1125414.
doi: 10.3389/fphar.2023.1125414

NRICM101 ameliorates SARS-CoV-2–S1-induced pulmonary injury in K18-hACE2 mice model

Wen-Chi Wei[1†], Keng-Chang Tsai[1,2†], Chia-Ching Liaw[1,3†], Chun-Tang Chiou[1], Yu-Hwei Tseng[1], Geng-You Liao[4], Yu-Chi Lin[1], Wen-Fei Chiou[1], Kuo-Tong Liou[1], I-Shing Yu[5], Yuh-Chiang Shen[1*] and Yi-Chang Su[1*]

[1]National Research Institute of Chinese Medicine, Ministry of Health and Welfare, Taipei, Taiwan, [2]Ph.D Program in Medical Biotechnology, College of Medical Science and Technology, Taipei Medical University, Taipei, Taiwan, [3]Department of Biochemical Science and Technology, National Chiayi University, Chiayi, Taiwan, [4]Institute of Physiology, School of Medicine, National Yang Ming Chiao Tung University, Taipei, Taiwan, [5]Laboratory Animal Center, National Taiwan University College of Medicine, Taipei, Taiwan

The coronavirus disease 2019 (COVID-19) pandemic continues to represent a challenge for public health globally since transmission of different variants of the virus does not seem to be effectively affected by the current treatments and vaccines. During COVID-19 the outbreak in Taiwan, the patients with mild symptoms were improved after the treatment with NRICM101, a traditional Chinese medicine formula developed by our institute. Here, we investigated the effect and mechanism of action of NRICM101 on improval of COVID-19-induced pulmonary injury using S1 subunit of the SARS-CoV-2 spike protein-induced diffuse alveolar damage (DAD) of hACE2 transgenic mice. The S1 protein induced significant pulmonary injury with the hallmarks of DAD (strong exudation, interstitial and intra-alveolar edema, hyaline membranes, abnormal pneumocyte apoptosis, strong leukocyte infiltration, and cytokine production). NRICM101 effectively reduced all of these hallmarks. We then used next-generation sequencing assays to identify 193 genes that were differentially expressed in the S1+NRICM101 group. Of these, three (*Ddit4*, *Ikbke*, *Tnfaip3*) were significantly represented in the top 30 enriched downregulated gene ontology (GO) terms in the S1+NRICM101 group versus the S1+saline group. These terms included the innate immune response, pattern recognition receptor (PRR), and Toll-like receptor signaling pathways. We found that NRICM101 disrupted the interaction of the spike protein of various SARS-CoV-2 variants with the human ACE2 receptor. It also suppressed the expression of cytokines IL-1β, IL-6, TNF-α, MIP-1β, IP-10, and MIP-1α in alveolar macrophages activated by lipopolysaccharide. We conclude that NRICM101 effectively protects against SARS-CoV-2-S1-induced pulmonary injury via modulation of the innate immune response, pattern recognition receptor, and Toll-like receptor signaling pathways to ameliorate DAD.

KEYWORDS

COVID-19, NRICM101, traditional Chinese medicine, lung injury, pattern recognition receptors

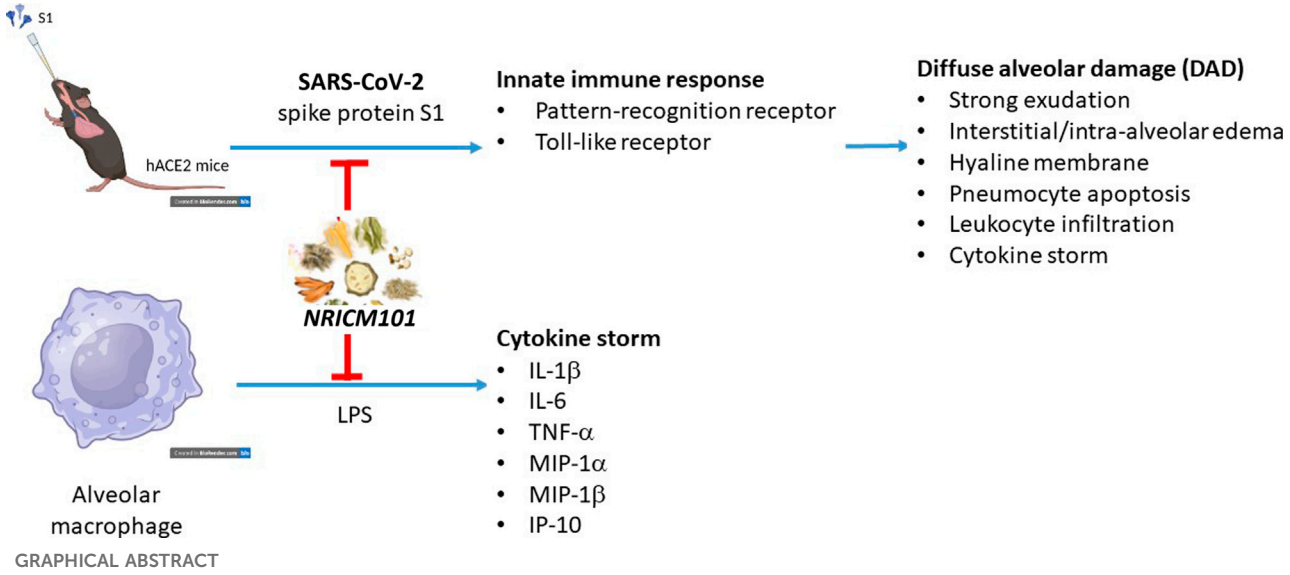

1 Introduction

The coronavirus disease 2019 (COVID-19) pandemic has been recognized as a global health emergency, and reinfections with COVID-19 continue to be reported globally, which may be partially due to mutations of the virus (Harvey et al., 2021; Indari et al., 2021; Ren et al., 2022). COVID-19 is caused by infection with severe acute respiratory syndrome coronavirus 2 (SARS-CoV-2) (Lu et al., 2020; Zhou et al., 2020; Zhu et al., 2020). The virus is transmitted mainly via inhaled droplets and aerosols or via direct exposure to mucus or body fluid from infected symptomatic cases (Amirian, 2020).

Although it can affect a wide range of organs, the respiratory system is the primary target of SARS-CoV-2 infection (Guan et al., 2020; Huang et al., 2020; Wang et al., 2020; Xu et al., 2020; Zhu et al., 2020), and SARS-CoV-2-induced acute respiratory distress syndrome (ARDS) has been suggested to be a major threat to the patient's life. Infection with SARS-CoV-2 causes abnormal lung tissue inflammation, pulmonary oedema, and immune cell infiltration into the lung tissues, leading to lung damage, shortness of breath, and ARDS (Grasselli et al., 2020; Sinha et al., 2020; Tay et al., 2020; Reddy et al., 2021). Angiotensin-converting enzyme 2 (ACE2), which is highly expressed in pulmonary epithelial cells (Li et al., 2003; Gheblawi et al., 2020), has been identified as responsible for the attachment of SARS-CoV-2 to the host (Zhou et al., 2020; Beyerstedt et al., 2021). The virus infects the alveolar type 2 epithelial cells (AT2 cells) via ACE2, adjacent alveolar epithelial cells are then infected in the same manner by newly released viral particles, and this leads to the loss of both AT1 and AT2 cells, causing alveolar damage and eventually ARDS (Mulay et al., 2021; Lamers and Haagmans, 2022). Pathological findings show that inflammation-associated diffuse alveolar damage (DAD) may underlie COVID-19-associated pneumonia and ARDS. Further, SARS-CoV-2-infected cells secret cytokines such as interleukins (e.g., IL-1 and IL-6), tumor necrosis factor-α (TNF-α), interferons (IFNs), chemokine ligands (CXCLs), and monocyte chemoattractant proteins (MCPs) (Smail et al., 2021; Lamers and Haagmans, 2022). The immune system overreaction triggered by SARS-CoV-2 causes acute and excessive production of proinflammatory cytokines, especially in the lung tissue, the so-called "cytokine storm", which may contribute to the lethality of COVID-19 (Ragab et al., 2020; Montazersaheb et al., 2022). Among the types of immune cells found in the alveoli after infection, macrophages have been reported to play a critical role in SARS-CoV-2-associated ARDS and the cytokine storm (Rendeiro et al., 2021; Zhang, et al., 2021). The purpose of the virus-induced inflammatory response is to defend against the invading virus particles; however, the overreaction of the immune system instead causes the subsequent inflammation and lung injury. Suppression of lung inflammation and injury is therefore an effective supportive therapeutic approach for COVID-19 patients.

Currently, several traditional Chinese medicine (TCM)-based formulations are used to treat COVID-19 in Taiwan, including NRICM101 (Tsai et al., 2021), Jing Si Herbal Tea (Hsieh et al., 2022), and Jing Guan Fang (Ping et al., 2022). Under an emergency-use authorization, NRICM101 is a prescription TCM formula commonly used in Taiwan to treat COVID-19 and the associated pulmonary disorders. Our previous study showed that it significantly reduced the formation of plaques that is associated with SARS-CoV-2, disrupted the interaction between the SARS-CoV-2 spike protein and the ACE2 receptor, and inhibited coronavirus 3C-like protease activity (Tsai et al., 2021). In addition, it exhibited a significant regulatory effect on the lipopolysaccharide (LPS)-stimulated secretion of the critical proinflammatory cytokines IL-6 and TNF-α in murine alveolar macrophages.

Clinical observations show that use of NRICM101 alleviates fever, enhances cardiopulmonary function, and reduces the risk of developing severe disease (Tseng et al., 2022). Moreover, chest X-rays showed that NRICM101 administration caused the focal ground-glass opacities to dissipate in most COVID-19 patients. Since NRICM101 possesses important properties for curbing

COVID-19 progression, it may also be able to ameliorate lung inflammation and thus improve ARDS.

2 Materials and methods

2.1 Pulmonary injury in K18-hACE2 mice caused by administering SARS-CoV-2 spike protein S1

There were three treatment groups: sham (sham surgery and saline), S1+saline, and S1+NRICM101. We administered SARS-CoV-2 S1 intratracheally to the mice as described elsewhere (Wei, et al., 2022). Briefly, we anesthetized each mouse by injecting it with xylazine (6 mg/kg) and ketamine (60 mg/kg) intraperitoneally. We then made a small incision in the skin of its neck. We dissolved the S1 (400 μg/kg in 2 mL/kg) in normal sterile saline solution and administered it gradually into the animal's tracheal lumen via the incision. We then closed the incision and the animal was given time for recovery. Each day for 3 days after this procedure, we administered either NRICM101 (3.0 g/kg) or saline solution (the control) to orally the mice. Three days later, we euthanized the mice and measured SO_2 (the concentration of oxygen relative to its maximum possible concentration) in the lungs using an iSTAT G3+ detection kit (Abbott Point of Care, Mississauga, ON, Canada). Finally, we analyzed these results using a video-tracking system (SMART v2.5.21, Panlab, Cornellà, Spain) and calculated the immediate (day 0 after S1 administration) and 72 h (day 3 after S1 administration) rates of survival.

2.2 Histopathology and immunohistochemistry

Fifteen to twenty ~30 μm serial sections were collected from the same part of the lung of mice from all treatment groups for immunohistochemical analysis. Before staining with specific antibodies, we prepared the tissue sections using the general protocol featuring fixation, permeabilization, and blocking. We then randomly selected tissue slices and incubated them overnight at 4°C in phosphate-buffered saline (PBS) containing 3% albumin and stained them for specific protein markers using primary antibodies as follows: SARS-CoV-2 spike protein subunit 1 (S1) RBD (1:100), AT1 (PDPN, 1:100), AT2 (SFTPC, 1:100), F4/80 (macrophage; 1:100), Ly6G (1:100), MPO (1:100), IL1β (1:100), IL-6 (1:100), CD8 (1:100), and TLR4 (1:100) (all from GeneTex, Irvine, CA, United States); CD11b (1:50; Abcam, Cambridge, United Kingdom); the active form of caspase 3 (cCasp3, 1:50; Santa Cruz Biotechnology, Dallas, TX, United States); and phospho(p)-P65NFκB (1:50; BD, San Diego, CA, United States). We washed the tissue sections thoroughly and then stained them with secondary antibodies conjugated with Alexa Fluor 488, 555, or 647 (Cell Signaling Technology, Danvers, MA, United States). We mounted the correctly stained sections on coverslips in medium containing 4′,6-diamidino-2-phenylindole (DAPI) and imaged them using a confocal Zeiss LSM780 laser-scanning microscope (Carl Zeiss, Jena, Germany). Using Zen 2011 (black edition, Carl Zeiss MicroImaging, 1997–2011) and AlphaEase FC (Alpha Innotech, San Leandro, CA, United States) we identified, counted, and calculated the area covered by the immunopositive cells or identified the immunopositive areas and estimated the proportion of the total area they comprised (as a percentage). We applied this procedure to the whole field of view in regions of interest that we sampled from each group. We used 30–1×00 magnification and performed 3–5 independent replicates of each experiment. Finally, we used Masson's trichrome staining method to detect tissue fibrosis.

2.3 RNA sequencing and RNA-seq data analysis

We checked the quality and amount of the RNA samples using a SimpliNano Spectrophotometer (Biochrom, Holliston, MA, United States) and assessed the degradation and integrity of the RNA using a Qsep 100 DNA/RNA Analyzer (BiOptic, New Taipei City, Taiwan). We created sequence libraries using the total RNA with a KAPA mRNA HyperPrep Kit (KAPA Biosystems, Roche, Basel, Switzerland); we produced the raw data via high-throughput sequencing using the NovaSeq 6000 platform (Illumina, San Diego, CA, United States) and ascertained its quality with the FastQC and MultiQC software. We used the Trimmomatic v0.38 tool to produce high-quality raw paired-end read data, which we used in all later analyses. We used HISAT2 v2.1.0 to align the read pairs to the reference genome and then FeatureCounts v2.0.0 to count the number of reads that had been mapped to individual genes. We then used DEGseq v1.40.0 and DESeq2 v1.26.0 to identify DEGs and clusterProfiler v3.14.3 to conduct the GO functional annotation and assess the KEGG pathway enrichment. Finally, we built a protein–protein interaction (PPI) network of the DEGs with STRINGdb (https://string-db.org/).

2.4 BLI (bio-layer interferometry) assay

We conducted a BLI assay according to the previously published procedure (Wei et al., 2022). Briefly, we immobilized several recombinant SARS-CoV-2 variant RBD proteins (GeneTex) on HIS1K sensor tips for 300 s at 50 μg/mL in PBS. We then conducted sequential sample testing, performing the baseline, association, and dissociation steps at 60 s, 180 s, and 180 s, respectively. We used the association signal to align the data and fitted the curves using a 1:1 best-fit model using FortéBio's data analysis software (Sartorius, FortéBio®).

2.5 ACE2-spike protein inhibition ELISA

We conducted an ELISA according to the previously published procedure (Wei et al., 2022). Briefly, we coated the recombinant SARS-CoV-2 variant RBD proteins (0.1–2 μg/well, GeneTex) onto a microplate. We added serial dilutions of NRICM101 (1/10×, 1/50×, 1/100×, 1/150×, 1/300×, 1/600×, 1/900×, 1/1200×, 1/1500×, 1/2000×, 1/3000×, and 1/6000×) to the wells and incubated the microplate at 37°C. We then added recombinant human ACE2 protein (0.2 μg/mL; Sino Biological, Beijing, China) to the

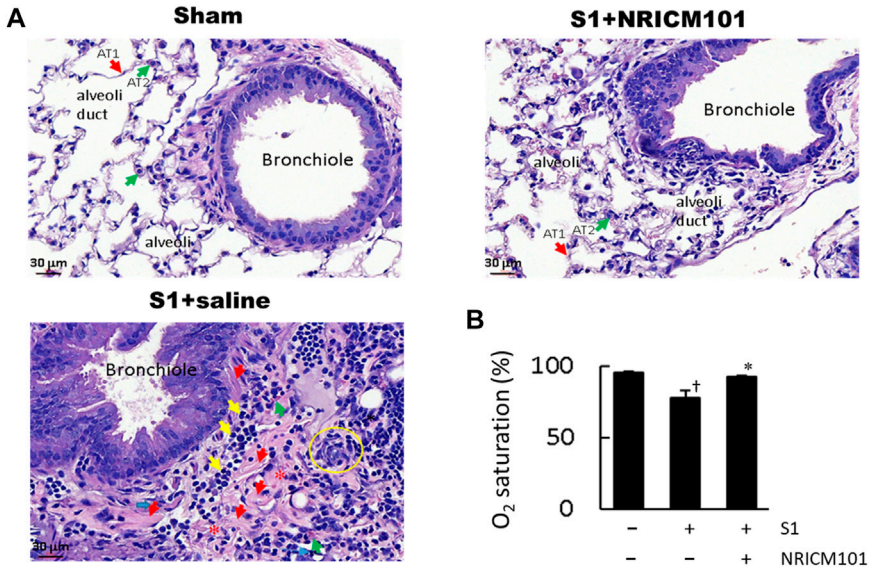

FIGURE 1
Effects of NRICM101 on lung injury symptoms induced by administering SARS-CoV-2 spike S1 protein to K18-hACE2 mice. **(A)**, Hematoxylin and eosin (H&E) staining of lung tissue from the three treatment groups. In the S1+saline group, the hallmarks of diffuse alveolar damage (DAD) can be observed: hyaline membranes (red arrows), pneumocyte hyperplasia (yellow circle), interstitial and alveolar edema (loss of alveoli, red stars), inflammatory cell infiltrate (yellow arrows). These were not observed in the sham (control) or S1+NRICM101 groups. **(B)**, Quantitative summary of the arterial blood oxygen saturation (SO_2) in the three groups. Data presented are the mean ± standard error of the mean (SEM) (n = 5 per group). [1,*] $p < 0.05$ compared with the sham or S1+saline group, respectively; one-way analysis of variance (ANOVA) followed by Student–Newman–Keuls (SNK) *t*-test. We conducted these experiments using hACE2 transgenic mice. The S1 protein was administered intratracheally (400 μg/kg) and the NRICM101 was administered orally (3.0 g/kg). We divided the mice into three treatment groups: sham surgery and saline control (sham), S1 protein administration and vehicle (saline) treatment (S1+saline), and S1 protein administration and NRICM101 treatment (S1+NRICM101).

wells and incubated the plate for 40 min at 37°C. Finally, we incubated it with rabbit anti-human IgG-HRP for a further 40 min, and then quantified the intensity of the signal as optical density at 450 nm using a SPECTROstar Nano microplate reader (BMG LABTECH, Ortenberg, Germany).

2.6 Cytokine inhibition assay

For this assay, we cultured a total of 5×10^5 MH-S CRL-2019 murine alveolar macrophages (ATCC, Manassas, VA, United States) in 12-well culture plates for 24 h. We then treated the cells with various dilutions of NRICM101 in the presence of LPS (1 μg/mL). We prepared the supernatant for cytokine identification and used a Proteome Profiler Mouse Cytokine Array Kit (R&D Systems, Minneapolis, MN, United States), which can detect 40 types of cytokine, to detect cytokine expression.

3 Results

3.1 NRICM101 ameliorated SARS-CoV-2 spike protein S1-induced pulmonary injury and reduction in lung oxygen saturation (SO_2) in K18-hACE2 mice

We investigated the effect of NRICM101 on protection against SARS-CoV-2-associated pulmonary injury using SARS-CoV-2 spike protein S1-induced lung injury in the K18-hACE2 mouse model (Colunga Biancatelli et al., 2021). The mice were pretreated with the S1 for 2 h and then treated with NRICM101 (3.0 g/kg). Hematoxylin and eosin (H&E) staining and microscopic analysis indicated that the S1 had induced acute DAD, as characterized by hyaline membranes lining the alveolar spaces, hyperplastic pneumocytes, the loss of alveolar epithelial cells into the adjacent spaces, interstitial and alveolar edema, congestion and hemorrhaging in the alveolar septa (which contained cellular debris and infiltrating mononuclear inflammatory cells), none of which were evident in the sham group (Figure 1A). Treatment with NRICM101 markedly reduced this S1-induced acute lung injury, as evidenced by reductions in the DAD markers. We also examined the effect of NRICM101 on lung oxygen saturation (SO_2), which is associated with pulmonary function. As suggested by our histological observations, NRICM101 significantly restored the S1-induced decrease in lung SO_2 (Figure 1B; from 78.0% ± 4.6% to 92.6% ± 0.5%). Together, these results suggest that NRICM101 effectively attenuated the S1-induced pulmonary injury, thereby improving lung SO_2, in hACE2 mice.

3.2 NRICM101 reduced SARS-CoV-2 spike protein S1-induced alveolar cell apoptosis in hACE2 mice

Infection with SARS-CoV-2 results in the apoptosis of alveolar epithelial cells and contributes to lung injury (Mulay et al., 2021). As shown in Figure 2, treatment with S1 induced apoptosis of the alveolar epithelial cells throughout the infected tissue of the lung, especially in

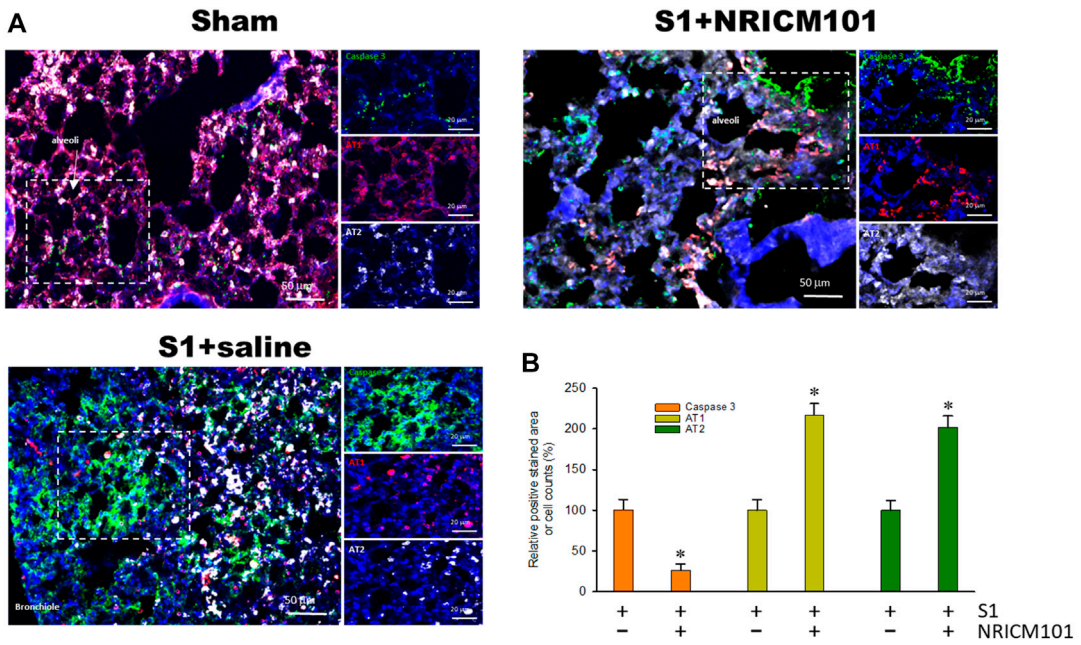

FIGURE 2
The effects of NRICM101 after 72 h on S1-induced alveolar cell apoptosis in K18-hACE2 mice with lung injury symptoms induced by the administration of SARS-CoV-2 spike S1 protein. **(A)**, Representative confocal microscopy images of lung tissue exhibiting truncated (active form) caspase 3 (green fluorescence), type I alveolar cells (AT1, red fluorescence), and type II alveolar cells (AT2, white fluorescence). **(B)**, Quantitative summary of the relative extents of stain-positive area (%) or numbers of cells in the three treatment groups. Data presented are means ± the standard error of the mean (SEM) (n = 5 per group). * $p < 0.05$ compared with the S1+saline group; one-way analysis of variance (ANOVA) followed by Student–Newman–Keuls (SNK) *t*-test. Treatment groups are as described in Figure 1.

the bronchioles and alveoli made up of AT1 and AT2 alveolar cells. However, treatment with NRICM101 significantly reduced the S1-induced lung-tissue cell death and also restored the abundance of AT1 cells. Notably, the abundance of AT2 cells was greatly increased in the S1+NRICM101 group relative to both the S1+saline and sham groups. This shows that NRICM101 significantly inhibited S1-induced alveolar cell apoptosis in hACE2 mice.

3.3 NRICM101 reduced SARS-CoV-2 spike protein S1-induced pulmonary inflammation and leukocyte infiltration in hACE2 mice

The dysregulation of the cytokine response that is induced by SARS-CoV-2 is known to cause abnormal inflammation leading to cell death and lung injury (Mehta et al., 2020; Rodrigues et al., 2020; Varga et al., 2020; Karki et al., 2021). We next investigated whether the protective effects of NRICM101 against SARS-CoV-2-induced lung injury operate via suppression of both inflammation and this S1-induced dysregulation of the cytokine response. Immunohistochemical examination revealed that NRICM101 significantly reduced S1 levels in the lung tissues and attenuated the S1-induced increase in leukocytes, including neutrophils and monocytes/macrophages, as evidenced by positive staining by CD11b (Figure 3A), Ly6G (Figure 3B), and F4/80 (Figures 3C, D), respectively. Moreover, the S1-induced inflammatory response was also strongly suppressed in the S1+NRICM101 group, as evidenced by elevated levels of phosphorylated activated nuclear factor-kappa B (NF-κB) pp65 (Figure 3A), myeloperoxidase (MPO; Figure 3B), IL-1β (Figure 3C), and Toll-like receptor 4 (TLR4) and IL-6 (Figure 3D), relative to the S1+saline group. These results suggest that NRICM101 can ameliorate S1-induced leukocyte infiltration and inflammatory responses in the lung tissues of K18-hACE2 mice.

3.4 NRICM101 inhibits SARS-CoV-2 S1-stimulated gene expression in hACE2 mice

To further investigate the molecular mechanisms underlying the protective effects of NRICM101, we examined differentially expressed genes (DEGs) using next-generation sequencing (NGS) and reverse-transcription polymerase chain reaction (RT-PCR) assays to identify targets that may be specifically affected by NRICM101. To do this, we compared gene expression between the S1+NRICM101 and S1+saline groups. We defined DEGs as those genes that had an adjusted $p <$ 0.005. We identified 1726 genes whose expression was different in the S1+saline groups from that in the sham group. Of these, the expression levels of 1205 (69.8%) were higher and those of 521 (30.2%) were lower. We conducted a principal component analysis (PCA) to produce a visual representation of how the three treatment groups were related in terms of their gene expression patterns. The S1+NRICM101 group was more similar to the sham group than the S1+saline group (Figure 4A). We then produced volcano plots showing which DEGs were up- and downregulated in different comparisons between the groups (Figure 4B). The top 30 enriched downregulated gene ontology (GO) terms between the S1+NRICM101 and S1+saline groups are shown in Figure 4C. The top thirty downregulated GO terms had

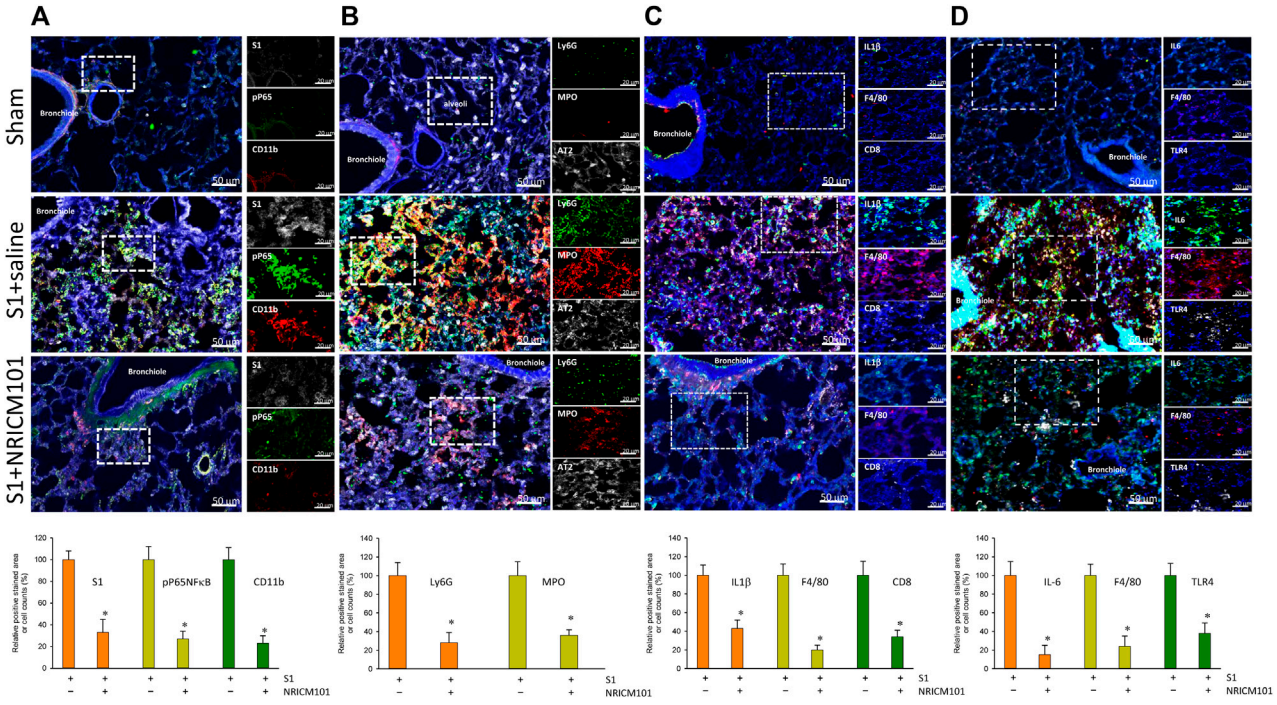

FIGURE 3
The effects of NRICM101 after 72 h on S1-induced pulmonary inflammation and leukocyte infiltration in K18-hACE2 mice with lung injury symptoms induced by the administration of SARS-CoV-2 spike S1 protein. Representative confocal microscopy images of the lung tissue revealing: **(A)**, phospho-P65NFκB (active form) (green fluorescence), CD11b leukocytes (red fluorescence), and S1 protein (S1, white fluorescence); **(B)**, Ly6G (neutrophil marker) (green fluorescence), myeloperoxidase (MPO, red fluorescence), and type II alveolar cells (AT2, white fluorescence); **(C)**, IL-1β (green fluorescence), F4/80 monocytes (red fluorescence), and CD8 lymphocytes (white fluorescence); and **(D)**, IL-6 (green fluorescence), F4/80 monocytes (red fluorescence), and TLR4 (white fluorescence). Bottom row of panels: quantitative summaries of the relative extents of stain-positive area (%) or numbers of cells in the three treatment groups. Data presented are mean ± the standard error of the mean (SEM) (n = 5 per group). * $p < 0.05$ compared with the S1+saline group; one-way analysis of variance (ANOVA) followed by Student–Newman–Keuls (SNK) *t*-test. Treatment groups are as described in Figure 1.

adjusted *p* as shown in the figure; these thirty were thus assumed to be significantly enriched (Figure 4C). They are strongly associated with immune-related functions, which suggests that the S1+NRICM101 group exhibited a reduced immune response. Specifically, the genes whose expression was significantly reduced in response to NRICM101 treatment are associated with the innate immune response, pattern recognition receptor (PRR), and TLR signaling pathways (Figure 4D). The TLR signaling pathway is known to be both involved in inflammation and dysregulated under COVID-19 infection; specifically, evidence has shown that the inflammation that is induced by the SARS-CoV-2 spike protein is activated via TLR2 and TLR4.

The top 15 downregulated genes in the S1+ NRICM101 group are shown in Figure 4E. Of these, DNA-damage-inducible transcript 4 (*Ddit4*) is also known as protein regulated in development and DNA damage response 1 (REDD1). *Ddit4* expression has been shown to be activated by DNA damage (Ellisen et al., 2002) and energy stress (McGhee et al., 2009). Inhibitor of nuclear factor kappa B kinase subunit epsilon (IKBKE, also known as IKKE, IKKI, and IKK-E) is a noncanonical I-kappa-B kinase (IKK) that is essential for regulating antiviral signaling pathways. It is also identified as mediating the signaling involved in the NOD-like receptor, TLR, IL-17, C-type lectin, and Rig-I-like receptor signaling pathways in the KEGG pathway database. TNF-α induced protein 3 (TNFAIP3, also known as A20, AISBL, AIFBL1, OTUD7C, and TNFA1P2) is identified as a gene whose expression is rapidly induced by tumor necrosis factor (TNF). This gene and its associated protein are identified as involved in the cytokine-mediated immune and inflammatory responses and necroptosis in the KEGG pathway database.

3.5 Inhibitory activity of NRICM101 against the ACE2 and the various spike proteins interaction

We examined the anti-SARS-CoV-2 effects of NRICM101 in terms of its binding affinity with the spike receptor-binding domain (RBD) proteins of several variants and its inhibition of the spike protein–ACE2 interaction. As shown in Figure 5A, a bio-layer interferometry (BLI) assay indicated that NRICM101 was able to bind to all the spike RBD protein variants we tested. We also conducted an enzyme-linked immunosorbent assay (ELISA), and this revealed that NRICM101 can disrupt the binding of all the RBD variants we tested to human ACE2 (Figure 5B). For the variants we tested, the half maximal effective concentration (EC_{50}) of NRICM101 (diluted in PBS) was 0.165 mg/mL (wild type), 0.213 mg/mL (Alpha), 0.129 mg/mL (Beta), 0.185 mg/mL (Gamma), 0.110 mg/mL (Delta), 0.132 mg/mL (Omicron), 0.102 mg/mL (BA.2), 0.105 mg/mL (BA.4/BA.5), 0.269 mg/mL Omicron (BA.2.75), 0.225 mg/mL Omicron (BF.7), 0.186 mg/mL Omicron (BQ.1), and 0.159 mg/mL

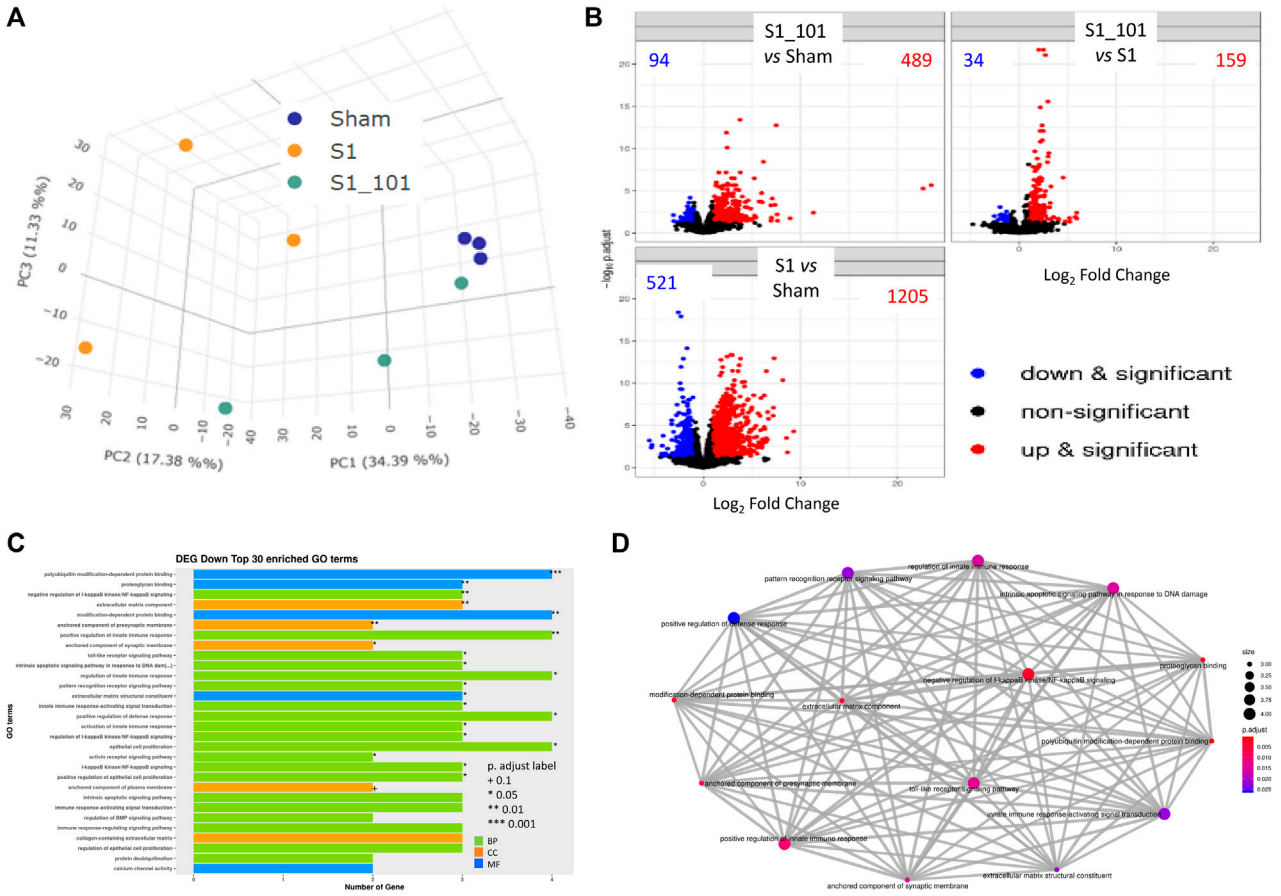

E

Gene symbol	Entrez gene ID	Gene description
Nlrp1c-ps		NLR family, pyrin domain containing 1C, pseudogene [Source:MGI Symbol;Acc:MGI:3582962]
Fst	14313	follistatin [Source:MGI Symbol;Acc:MGI:95586]
Ddit4	74747	DNA-damage-inducible transcript 4 [Source:MGI Symbol;Acc:MGI:1921997]
Tnc	21923	tenascin C [Source:MGI Symbol;Acc:MGI:101922]
Marcksl1	17357	MARCKS-like 1 [Source:MGI Symbol;Acc:MGI:97143]
Ikbke	56489	inhibitor of kappaB kinase epsilon [Source:MGI Symbol;Acc:MGI:1929612]
Bcl2a1b	12045	B cell leukemia/lymphoma 2 related protein A1b [Source:MGI Symbol;Acc:MGI:1278326]
Tnip3	414084	TNFAIP3 interacting protein 3 [Source:MGI Symbol;Acc:MGI:3041165]
Gdf2	12165	growth differentiation factor 2 [Source:MGI Symbol;Acc:MGI:1321394]
Col5a3	53867	collagen, type V, alpha 3 [Source:MGI Symbol;Acc:MGI:1858212]
Tnfaip3	21929	tumor necrosis factor, alpha-induced protein 3 [Source:MGI Symbol;Acc:MGI:1196377]
Tnip1	57783	TNFAIP3 interacting protein 1 [Source:MGI Symbol;Acc:MGI:1926194]
Pkhd1l1	192190	polycystic kidney and hepatic disease 1-like 1 [Source:MGI Symbol;Acc:MGI:2183153]
Tmem37	170706	transmembrane protein 37 [Source:MGI Symbol;Acc:MGI:2157899]
Ntng2	171171	netrin G2 [Source:MGI Symbol;Acc:MGI:2159341]

FIGURE 4
The effects of NRICM101 after 72 h on S1-induced gene expression levels in K18-hACE2 mice with lung injury symptoms induced by the administration of SARS-CoV-2 spike S1 protein. We assessed changes in gene expression using next-generation sequencing (NGS) and reverse-transcription polymerase chain reaction (RT-PCR) assays to identify differentially expressed genes (DEGs) in the S1+NRICM101 group versus the S1+saline group. **(A)**, A principal component analysis (PCA) plot of the DEG profiles of the treatment groups. **(B)**, A Volcano plot showing the DEGs between different treatment groups; comparison between S1+NRICM101 and sham (upper left), S1+NRICM101 and S1+saline (upper right), S1+saline and sham (lower left). **(C)**, The top 30 enriched gene ontology (GO) terms related to the downregulated DEGs. **(D)**, A network plot of the GO terms related to the downregulated DEGs. **(E)**, The top 15 downregulated DEGs.

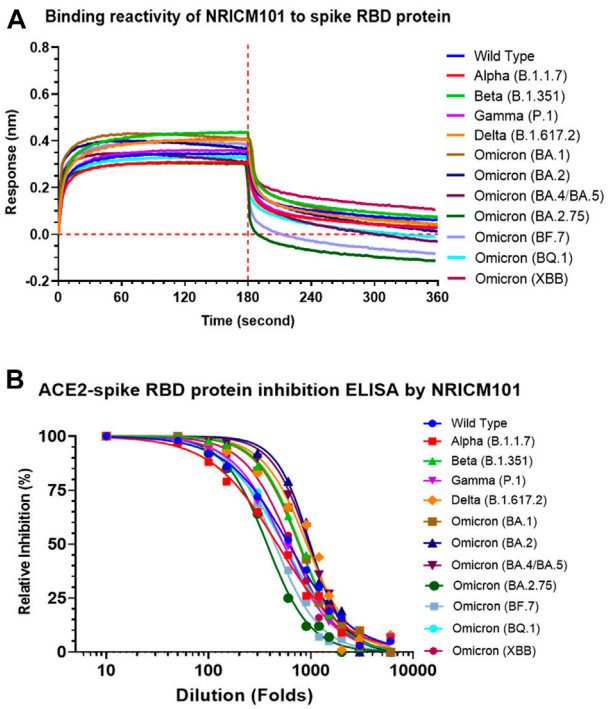

FIGURE 5
The activities of NRICM101 that act to protect against SARS-CoV-2. **(A)**, A bio-layer interferometry (BLI) assay revealing the ability of NRICM101 to bind to the spike receptor-binding domain (RBD) proteins of the following SARS-CoV-2 variants: the wild type, Alpha (B.1.1.7), Beta (B.1.351), Gamma (P.1), Delta (B.1.617.2), Omicron (B.1.1529), Omicron (BA.2), Omicron (BA.4/BA.5), Omicron (BA.2.75), Omicron (BF.7), Omicron (BQ.1), and Omicron (XBB). **(B)**, An enzyme-linked immunosorbent assay (ELISA) showing the inhibition of the binding of the spike RBDs of the same SARS-CoV-2 variants with human angiotensin-converting enzyme 2 (ACE2) by various dilutions of NRICM101. We calculated the percentage inhibition based on the binding signal normalized to that of the same spike RBD in the absence of NRICM101 treatment.

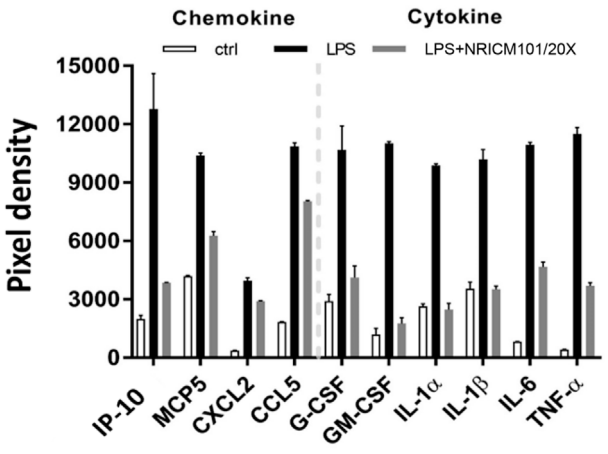

FIGURE 6
Inhibition of LPS-induced cytokine and chemokine production in murine alveolar macrophages by NRICM101. We used a 20-fold dilution of NRICM101 in this assay.

Omicron (XBB). Thus, NRICM101 exhibits strong anti-SARS-CoV-2 properties, despite the existence of many variants of this virus.

3.6 NRICM101 attenuated LPS-induced production of cytokines and chemokines in murine alveolar macrophages

The above results showed that NRICM101 exhibits excellent anti-inflammatory activity in the lung tissues of S1-treated K18-hACE2 mice, and our previous research has shown that it can suppress the LPS-induced production of IL-6 and TNF-α in murine alveolar macrophages (Tsai et al., 2021). To further investigate its regulatory effects on LPS-induced inflammation, we analyzed the profile of inflammation-related cytokines in LPS-stimulated murine alveolar macrophages that had or had not been treated with NRICM101. As shown in Figure 6, NRICM101 significantly suppressed the expression of several LPS-induced cytokines and chemokines, including TNF-α, IL-1α, IL-1β, IL-6, IP-10, MCP-5, CXCL2, CCL5, GM-CSF, and G-CSF.

3.7 RNA-seq profiles of alveolar macrophages activated by LPS

We analyzed the RNA-seq profiles of the mRNA expressed by alveolar macrophages that were activated by LPS to identify the transcriptional changes they had undergone. The first step was to identify the DEGs in LPS-stimulated monocytes versus untreated control alveolar macrophages. As before, DEGs were defined as those for which adjusted $p < 0.005$. In total, we identified 685 DEGs, 426 (62%) of which were upregulated and 259 (38%) of which were downregulated, as shown in the gene expression heatmap in Figure 7A and in the volcano plot in Figure 7B. In Figure 7C, we show a group of 13 selected enriched GO terms that were upregulated in the LPS-stimulated cells. The top three of these GO terms were considered significant because they had adjusted $p < 0.005$. These terms included cellular response to bacterial molecules, cellular response to LPS, viral response, antiviral response, and LPS response. Thus, these terms were strongly linked to the immune response, revealing that the immune response of the LPS-treated cells had increased. We performed a category netplot (cnetplot) analysis to visualize the linkages between the genes and biological concepts (Figure 7D). This showed that the genes that were upregulated in response to LPS stimulation were involved in the signaling pathways of the antiviral defense response, positive regulation of cytokine production, and the response to viruses (Figure 7D).

3.8 Effects of LPS stimulation on alveolar macrophages were inhibited by NRICM101

We identified DEGs in alveolar macrophages treated with LPS+NRICM101 and LPS only, once again defining genes that had adjusted $p < 0.005$ as DEGs. In total, we found 371 DEGs, 274 of which (74%) were downregulated and 97 of which (26%) were upregulated in the cells treated with LPS+NRICM101 relative to those treated with LPS only, as shown in the volcano plot in Figure 8A. The 13 enriched GO terms shown in Figure 8B were

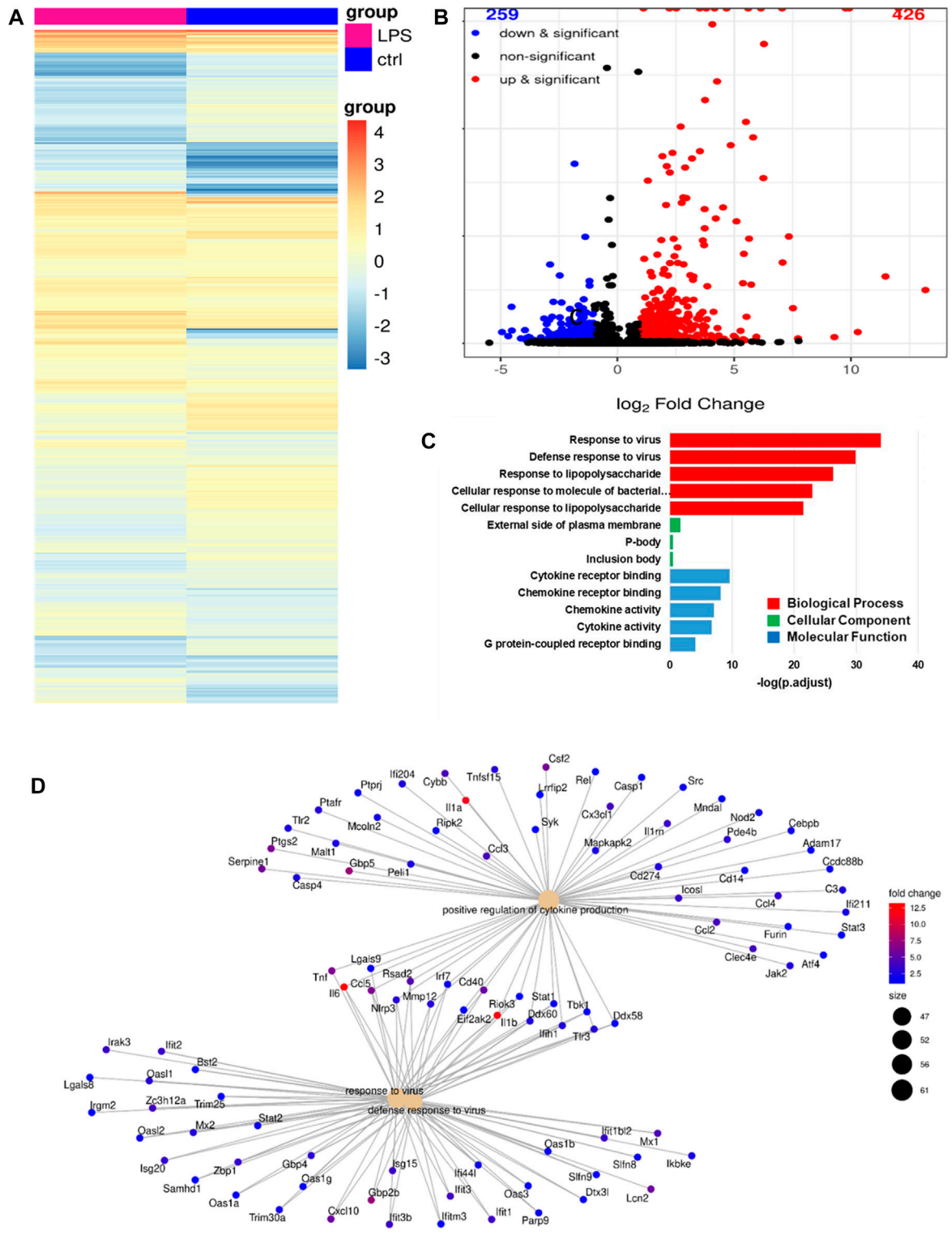

FIGURE 7
RNA-seq analysis revealing the phenotype of LPS-activated alveolar macrophages. **(A)**, A heatmap of the differentially expressed genes (DEGs) in LPS-activated versus untreated alveolar macrophages. **(B)**, A volcano plot showing the same DEGs as in (**A**). **(C)**, The top 13 gene ontology (GO) terms associated with the upregulated DEGs from (**A**). **(D)**, A cnetplot of the upregulated DEGs from (**A**).

downregulated, and the top three had adjusted $p < 0.005$. These terms include IFN-γ response, cellular IFN-γ response, viral response, antiviral response, and LPS response (Figure 8B). All of these terms are thus strongly associated with the immune response, implying that the cells in the LPS+NRICM101 treatment exhibited a diminished immune response. The genes whose expression decreased in response to treatment with NRICM101 are associated with pathways linked to antiviral response, INF-β response, and viral

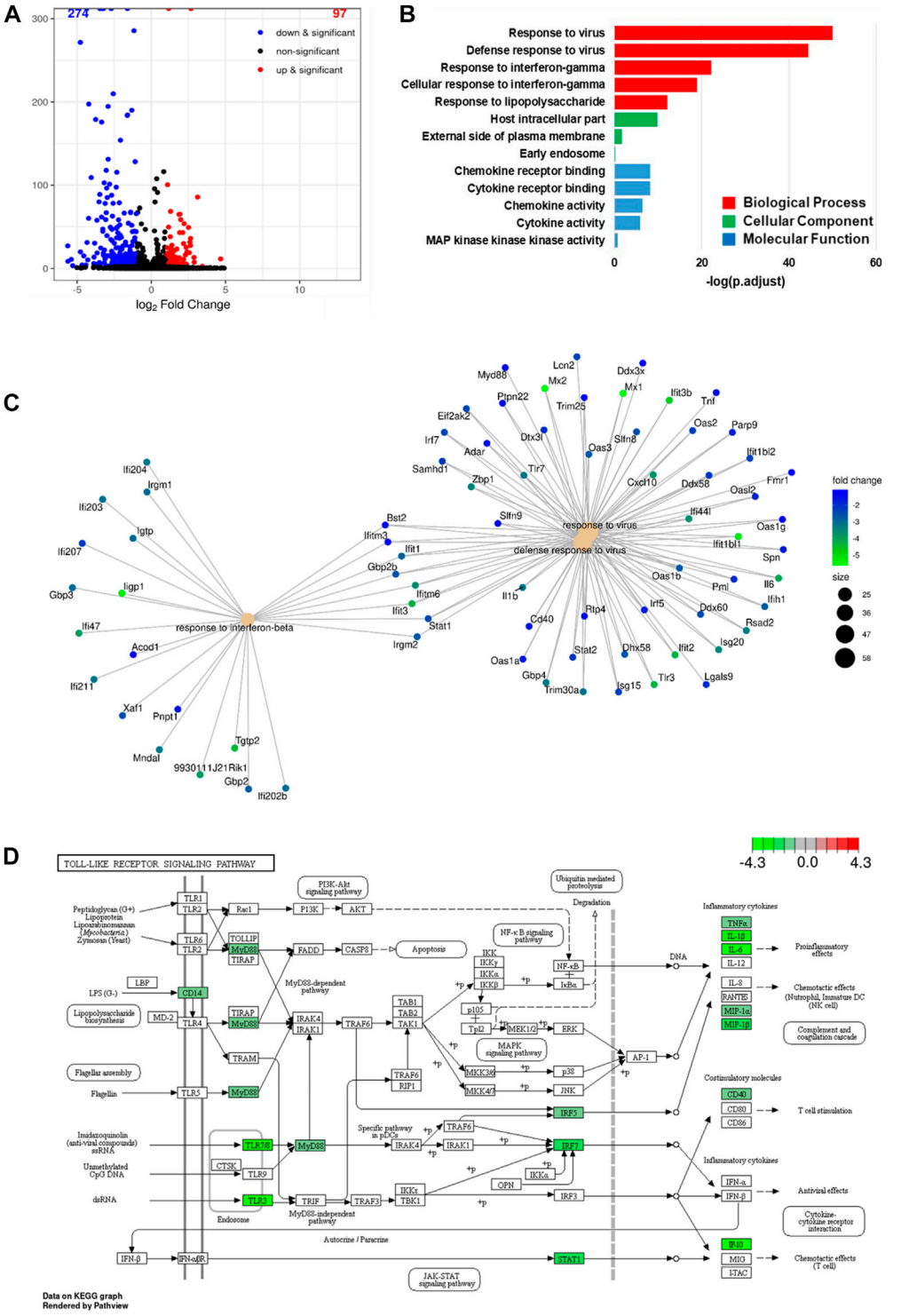

23

FIGURE 8
Inhibitory activities of NRICM101 toward LPS-stimulated alveolar macrophages. (**A**), A volcano plot of the differentially expressed genes (DEGs) in alveolar macrophages treated with LPS versus those treated with LPS and NRICM101. **(B)**, The top 13 gene ontology (GO) terms associated with the downregulated DEGs from (**A**). **(C)**, A cnetplot of the downregulated DEGs from (**A**). **(D)**, KEGG pathway analysis showing how NRICM101 inhibits the Toll-like receptor (TLR) signaling pathway. Genes in the green boxes are significantly downregulated by treatment with NRICM101.

response (Figure 8C). According to a previous study, the inflammatory TLR signaling pathway becomes dysregulated under COVID-19 infection (Tseng et al., 2022). We conducted a KEGG pathway analysis of the DEGs we had identified in this final analysis to investigate the role of NRICM101 in the TLR signaling pathway (Figure 8D). As the KEGG analysis shows, the NRICM101 suppressed the production of inflammatory cytokines that is stimulated by LPS. These cytokines include IL-1β, IL-6, TNF-α, MIP-1β, IP-10, MIP-1α. It also suppressed the costimulatory molecule CD40 via the regulation of several other pathways: MyD88-dependent, MyD88-independent, PI3K–Akt, and JAK–STAT.

4 Discussion

Current clinical and laboratory evidence indicates that SARS-CoV-2-induced lung pathology can be attributed to the combined effects of the direct cytopathic activity of the virus and the dysregulated inflammatory and immune responses that are indirect effects of the virus. Autopsy examinations of patients who have died from COVID-19 reveal that DAD is the most common type of lung injury suffered by these patients (Lamers and Haagmans, 2022). This DAD exhibits signs of the exudative phase, such as edema (both interstitial and intra-alveolar), abnormal pneumocyte apoptosis, hyaline membranes, congestion of the capillaries, and microvascular thrombosis (Carsana et al., 2020; Menter et al., 2020). The abnormal pneumocyte apoptosis has been confirmed by immunostaining the diseased lungs, which contained fewer AT2 and AT1 cells than healthy lungs (Chen et al., 2020; Delorey et al., 2021; Melms et al., 2021).

In this study, using the SARS-CoV-2 spike protein S1 to induce pulmonary injury in hACE2 mice, we successfully established an animal model displaying COVID-19-associated pneumonia (pulmonary injury) and ARDS. We observed severe pulmonary injury in the S1-challenged mice, with a dramatic drop in their SO_2. This pulmonary injury exhibited several of the features of DAD, including strong exudation, edema (both interstitial and intra-alveolar), hyaline membranes, abnormal pneumocyte apoptosis (AT1 and AT2), capillary congestion, and strong inflammation (leukocyte infiltration and cytokine production).

All these DAD features improved significantly as a result of post-treatment with NRICM101 at a dose of 3.0 g/kg (orally administered), which is analogous to the usual clinical dose. Our histological observations showed that in the S1+NRICM101 group, the alveolar damage and collapse of spaces had been effectively prevented: the alveoli were intact and the fragile alveolar septa still included their narrow capillaries, which were lined with flattened AT1 cells and cuboidal AT2 cells. The AT2 cells had retained the potential to self-renew and differentiate into AT1 cells. These features were easily observable throughout the lung tissue and the SO_2 was restored to almost the same level as in the sham group. We also observed that the abundance of AT2 cells was significantly greater in the S1+NRICM101 group than in the S1+saline group, suggesting that NRICM101 may play a role in activating AT2 activity, thus facilitating lung repair.

Accompanying these pathological data, our RNA-seq data analysis revealed that the DAD features in the S1+saline group were strongly associated with signaling pathways linked to activating the innate immune response, PRR, positive regulation of the defense response, and TLR. All of these pathways were downregulated by treatment with NRICM101. Combined, these data suggest that using NRICM101 to treat COVID-19-related pulmonary injury is a reasonable and successful approach.

We also examined the activity of NRICM101 against LPS-induced inflammation. Our results showed that the regulatory effects of NRICM101 against the dysregulation of cytokines and inflammation can be observed not only in S1-treated lung tissue but also in LPS-treated murine alveolar macrophages. The cytokine storm or dysregulated cytokine immune response is not unique to patients with SARS-CoV-2 (Fajgenbaum and June, 2020), but it can be life threatening. Our results indicate that NRICM101 may be also have potential for treating immune-dysregulation–related diseases.

We acknowledge that S1 is insufficient to fully represent all the pathologies of SARS-CoV-2, the spike protein and its S1 subunit have been demonstrated to play a key role in viral pathogenesis, evolution, and transmission. However, some vaccines may instead use highly immunogenic regions like the RBD (receptor binding domain) found within the S1 subunit (Martínez-Flores et al., 2021), as the RBM (receptor binding motif) within the RBD directly interacts with the ACE2 receptor (Shang et al., 2020). The RBD in S1 has received considerable attention since it serves as an intermediary factor in the virus-host cell interaction, specifically by binding to the ACE2 receptor of the host cell. This binding is critical to the viral infection process, and as a result, most of the mutations of SARS-CoV-2 occur within the RBD of S1. Besides, the spike protein S1 subunit is the key immune stimulant in the human body's response to SARS-CoV-2, many strategies, such as antibodies against COVID-19 disorder, have been designed according to anti-S1/RBD. Therefore, in this study, we used the S1 protein - which is the key protein subunit responsible for invading the human system through the ACE2 receptor with the same protein sequence as the original Wuhan strain - as a stimulator to mimic the way SARS-CoV-2 behaves. There are many advantages to using this approach, including the ease and safety of experimental handling, the quick development of a disease model for COVID-19, and the ability to observe typical pathological changes in histology (such as diffused alveolar damage or DAD) and immunology (such as cytokine storm, NET formation, TLR activation, and more). We suggest that the S1-induced animal model represents some but not all of the pathologies of SARS-CoV-2 and is suitable for the quick development and analysis of new drugs against SARS-CoV-2.

SARS-CoV-2-associated respiratory illness is the main challenge for patients with COVID-19, and it can develop into life-threatening pneumonia. However, there is still no effective pharmacologic treatment for SARS-CoV-2-associated ARDS. Our previous study revealed the clinical effectiveness of NRICM101 for treating COVID-19 patients (Tsai et al., 2021). In the present study, we have demonstrated that it can effectively suppress lung inflammation and ameliorate lung injury in SARS-CoV-2 spike protein S1-treated K18-hACE2 mice. These findings provide some mechanistic insights into how NRICM101 functions when used to treat COVID-19.

Data availability statement

The original contributions presented in the study are publicly available. This data can be found here: https://www.ncbi.nlm.nih.gov/PRJNA975698.

Ethics statement

The animal study was reviewed and approved by the Animal Research Committee of the National Research Institute of Chinese Medicine (No. NRICM-IACUC-111-912-2).

Author contributions

Y-CSu and Y-CSh conceived and designed the experiments. Y-CSh, C-CL, W-CW, K-CT, C-TC, Y-CL, G-YL, and K-TL performed the experiments and analyzed the data. I-SY helped to obtain the K18-hACE2 mice. Y-CSu, K-CT, and W-FC supervised the project. C-CL, W-CW, Y-HT, G-YL, Y-CSu, and Y-CSh wrote the manuscript. All authors contributed to the article and approved the submitted version.

Funding

This work was supported by the Ministry of Health and Welfare, Republic of China (NRICM-109T88 and NRICM-110T88).

Acknowledgments

The authors thank the members of the authors' laboratory in the NRICM, who assisted with and supported this study.

Conflict of interest

The authors declare that the research was conducted in the absence of any commercial or financial relationships that could be construed as a potential conflict of interest.

Publisher's note

All claims expressed in this article are solely those of the authors and do not necessarily represent those of their affiliated organizations, or those of the publisher, the editors and the reviewers. Any product that may be evaluated in this article, or claim that may be made by its manufacturer, is not guaranteed or endorsed by the publisher.

References

Amirian, E. S. (2020). Potential fecal transmission of SARS-COV-2: Current evidence and implications for public health. *Int. J. Infect. Dis.* 95, 363–370. doi:10.1016/j.ijid.2020.04.057

Beyerstedt, S., Casaro, E. B., and Rangel, É. B. (2021). Covid-19: Angiotensin-converting enzyme 2 (ACE2) expression and tissue susceptibility to SARS-COV-2 infection. *Eur. J. Clin. Microbiol. Infect. Dis.* 40 (5), 905–919. doi:10.1007/s10096-020-04138-6

Carsana, L., Sonzogni, A., Nasr, A., Rossi, R. S., Pellegrinelli, A., Zerbi, P., et al. (2020). Pulmonary post-mortem findings in a series of COVID-19 cases from northern Italy: A two-centre descriptive study. *Lancet Infect. Dis.* 20 (10), 1135–1140. doi:10.1016/s1473-3099(20)30434-5

Chen, J., Wu, H., Yu, Y., and Tang, N. (2020). Pulmonary alveolar regeneration in adult COVID-19 patients. *Cell. Res.* 30 (8), 708–710. doi:10.1038/s41422-020-0369-7

Colunga Biancatelli, R. M., Solopov, P. A., Sharlow, E. R., Lazo, J. S., Marik, P. E., and Catravas, J. D. (2021). The SARS-CoV-2 spike protein subunit S1 induces COVID-19-like acute lung injury in K18-hACE2 transgenic mice and barrier dysfunction in human endothelial cells. *Am. J. Physiol. Lung Cell. Mol. Physiol.* 321 (2), L477–L484. doi:10.1152/ajplung.00223.2021

Delorey, T. M., Ziegler, C. G., Heimberg, G., Normand, R., Yang, Y., Segerstolpe, Å., et al. (2021). COVID-19 tissue atlases reveal SARS-CoV-2 pathology and cellular targets. *Nature* 595 (7865), 107–113. doi:10.1038/s41586-021-03570-8

Ellisen, L. W., Ramsayer, K. D., Johannessen, C. M., Yang, A., Beppu, H., Minda, K., et al. (2002). REDD1, a developmentally regulated transcriptional target of p63 and p53, links p63 to regulation of reactive oxygen species. *Mol. Cell.* 10 (5), 995–1005. doi:10.1016/s1097-2765(02)00706-2

Fajgenbaum, D. C., and June, C. H. (2020). Cytokine storm. *N. Engl. J. Med.* 383 (23), 2255–2273. doi:10.1056/nejmra2026131

Gheblawi, M., Wang, K., Viveiros, A., Nguyen, Q., Zhong, J. C., Turner, A. J., et al. (2020). Angiotensin-converting enzyme 2: SARS-CoV-2 receptor and regulator of the renin-angiotensin system: Celebrating the 20th anniversary of the discovery of ACE2. *Circ. Res.* 126 (10), 1456–1474. doi:10.1161/circresaha.120.317015

Grasselli, G., Tonetti, T., Protti, A., Langer, T., Girardis, M., Bellani, G., et al. (2020). Pathophysiology of COVID-19-associated acute respiratory distress syndrome: A multicentre prospective observational study. *Lancet Respir. Med.* 8 (12), 1201–1208. doi:10.1016/s2213-2600(20)30370-2

Guan, W. J., Ni, Z. Y., Hu, Y., Liang, W. H., Ou, C. Q., He, J. X., et al. (2020). Clinical characteristics of coronavirus disease 2019 in China. *N. Engl. J. Med.* 382 (18), 1708–1720. doi:10.1056/nejmoa2002032

Harvey, W. T., Carabelli, A. M., Jackson, B., Gupta, R. K., Thomson, E. C., Harrison, E. M., et al. (2021). SARS-CoV-2 variants, Spike mutations and immune escape. *Nat. Rev. Microbiol.* 19 (7), 409–424. doi:10.1038/s41579-021-00573-0

Hsieh, P. C., Chao, Y. C., Tsai, K. W., Li, C. H., Tzeng, I. S., Wu, Y. K., et al. (2022). Efficacy and safety of complementary therapy with jing Si herbal tea in patients with mild-to-moderate COVID-19: A prospective cohort study. *Front. Nutr.* 9, 832321. doi:10.3389/fnut.2022.832321

Huang, C., Wang, Y., Li, X., Ren, L., Zhao, J., Hu, Y., et al. (2020). Clinical features of patients infected with 2019 novel coronavirus in Wuhan, China. *Lancet* 395 (10223), 497–506. doi:10.1016/s0140-6736(20)30183-5

Indari, O., Jakhmola, S., Manivannan, E., and Jha, H. C. (2021). An update on antiviral therapy against SARS-CoV-2: How far have we come? *Front. Pharmacol.* 12, 632677. doi:10.3389/fphar.2021.632677

Karki, R., Sharma, B. R., Tuladhar, S., Williams, E. P., Zalduondo, L., Samir, P., et al. (2021). Synergism of TNF-α and IFN-γ triggers inflammatory cell death, tissue damage, and mortality in SARS-CoV-2 infection and cytokine shock syndromes. *Cell.* 184 (1), 149–168.e17. doi:10.1016/j.cell.2020.11.025

Lamers, M. M., and Haagmans, B. L. (2022). SARS-CoV-2 pathogenesis. *Nat. Rev. Microbiol.* 20 (5), 270–284. doi:10.1038/s41579-022-00713-0

Li, W., Moore, M. J., Vasilieva, N., Sui, J., Wong, S. K., Berne, M. A., et al. (2003). Angiotensin-converting enzyme 2 is a functional receptor for the SARS coronavirus. *Nature* 426 (6965), 450–454. doi:10.1038/nature02145

Lu, R., Zhao, X., Li, J., Niu, P., Yang, B., Wu, H., et al. (2020). Genomic characterisation and epidemiology of 2019 novel coronavirus: Implications for virus origins and receptor binding. *Lancet* 395 (10224), 565–574. doi:10.1016/s0140-6736(20)30251-8

Martínez-Flores, D., Zepeda-Cervantes, J., Cruz-Reséndiz, A., Aguirre-Sampieri, S., Sampieri, A., and Vaca, L. (2021). SARS-CoV-2 vaccines based on the spike glycoprotein and implications of new viral variants. *Front. Immunol.* 12, 701501. doi:10.3389/fimmu.2021.701501

McGhee, N. K., Jefferson, L. S., and Kimball, S. R. (2009). Elevated corticosterone associated with food deprivation upregulates expression in rat skeletal muscle of the mTORC1 repressor, REDD1. *J. Nutr.* 139 (5), 828–834. doi:10.3945/jn.108.099846

Mehta, P., McAuley, D. F., Brown, M., Sanchez, E., Tattersall, R. S., Manson, J. J., et al. (2020). COVID-19: Consider cytokine storm syndromes and immunosuppression. *Lancet* 395 (10229), 1033–1034. doi:10.1016/s0140-6736(20)30628-0

Melms, J. C., Biermann, J., Huang, H., Wang, Y., Nair, A., Tagore, S., et al. (2021). A molecular single-cell lung atlas of lethal COVID-19. *Nature* 595 (7865), 114–119. doi:10.1038/s41586-021-03569-1

Menter, T., Haslbauer, J. D., Nienhold, R., Savic, S., Hopfer, H., Deigendesch, N., et al. (2020). Postmortem examination of COVID-19 patients reveals diffuse alveolar damage with severe capillary congestion and variegated findings in lungs and other organs suggesting vascular dysfunction. *Histopathology* 77 (2), 198–209. doi:10.1111/his.14134

Montazersaheb, S., Hosseiniyan Khatibi, S. M., Hejazi, M. S., Tarhriz, V., Farjami, A., Ghasemian Sorbeni, F., et al. (2022). COVID-19 infection: An overview on cytokine storm and related interventions. *Virol. J.* 19 (1), 92. doi:10.1186/s12985-022-01814-1

Mulay, A., Konda, B., Garcia, G., Yao, C., Beil, S., Villalba, J. M., et al. (2021). SARS-CoV-2 infection of primary human lung epithelium for COVID-19 modeling and drug discovery. *Cell. Rep.* 35 (5), 109055. doi:10.1016/j.celrep.2021.109055

Ping, Y. H., Yeh, H., Chu, L. W., Lin, Z. H., Hsu, Y. C., Lin, L. C., et al. (2022). The traditional Chinese medicine formula Jing Guan Fang for preventing SARS-CoV-2 infection: From clinical observation to basic research. *Front. Pharmacol.* 13, 744439. doi:10.3389/fphar.2022.744439

Ragab, D., Salah Eldin, H., Taeimah, M., Khattab, R., and Salem, R. (2020). The COVID-19 cytokine storm; what we know so far. *Front. Immunol.* 11, 1446. doi:10.3389/fimmu.2020.01446

Reddy, K., Hardin, C. C., and McAuley, D. F. (2021). COVID-19–related acute respiratory distress syndrome subphenotypes and differential response to corticosteroids: Time for more precision? *Am. J. Respir. Crit. Care Med.* 204 (11), 1241–1243. doi:10.1164/rccm.202109-2213ed

Ren, X., Zhou, J., Guo, J., Hao, C., Zheng, M., Zhang, R., et al. (2022). Reinfection in patients with COVID-19: A systematic review. *Glob. Health Res. Policy* 7 (1), 12. doi:10.1186/s41256-022-00245-3

Rendeiro, A. F., Ravichandran, H., Bram, Y., Chandar, V., Kim, J., Meydan, C., et al. (2021). The spatial landscape of lung pathology during COVID-19 progression. *Nature* 593 (7860), 564–569. doi:10.1038/s41586-021-03475-6

Rodrigues, T. S., de Sá, K. S. G., Ishimoto, A. Y., Becerra, A., Oliveira, S., Almeida, L., et al. (2020). Inflammasomes are activated in response to SARS-CoV-2 infection and are associated with COVID-19 severity in patients. *J. Exp. Med.* 218 (3), 20201707. doi:10.1084/jem.20201707

Shang, J., Ye, G., Shi, K., Wan, Y., Luo, C., Aihara, H., et al. (2020). Structural basis of receptor recognition by SARS-CoV-2. *Nature* 581 (7807), 221–224. doi:10.1038/s41586-020-2179-y

Sinha, P., Calfee, C. S., Cherian, S., Brealey, D., Cutler, S., King, C., et al. (2020). Prevalence of phenotypes of acute respiratory distress syndrome in critically ill patients with COVID-19: A prospective observational study. *Lancet Respir. Med.* 8 (12), 1209–1218. doi:10.1016/s2213-2600(20)30366-0

Smail, S. W., Saeed, M., Alkasalias, T., Khudhur, Z. O., Younus, D. A., Rajab, M. F., et al. (2021). Inflammation, immunity and potential target therapy of SARS-CoV-2: A total scale analysis review. *Food Chem. Toxicol.* 150, 112087. doi:10.1016/j.fct.2021.112087

Tay, M. Z., Poh, C. M., Rénia, L., MacAry, P. A., and Ng, L. F. (2020). The trinity of COVID-19: Immunity, inflammation and intervention. *Nat. Rev. Immunol.* 20 (6), 363–374. doi:10.1038/s41577-020-0311-8

Tsai, K. C., Huang, Y. C., Liaw, C. C., Tsai, C. I., Chiou, C. T., Lin, C. J., et al. (2021). A traditional Chinese medicine formula NRICM101 to target COVID-19 through multiple pathways: A bedside-to-bench study. *Biomed. Pharmacother.* 133, 111037. doi:10.1016/j.biopha.2020.111037

Tseng, Y. H., Lin, S. J. S., Hou, S. M., Wang, C. H., Cheng, S. P., Tseng, K. Y., et al. (2022). Curbing COVID-19 progression and mortality with traditional Chinese medicine among hospitalized patients with COVID-19: A propensity score-matched analysis. *Pharmacol. Res.* 184, 106412. doi:10.1016/j.phrs.2022.106412

Varga, Z., Flammer, A. J., Steiger, P., Haberecker, M., Andermatt, R., Zinkernagel, A. S., et al. (2020). Endothelial cell infection and endotheliitis in COVID-19. *Lancet* 395 (10234), 1417–1418. doi:10.1016/s0140-6736(20)30937-5

Wang, D., Hu, B., Hu, C., Zhu, F., Liu, X., Zhang, J., et al. (2020). Clinical characteristics of 138 hospitalized patients with 2019 novel coronavirus–infected pneumonia in Wuhan, China. *JAMA* 323 (11), 1061–1069. doi:10.1001/jama.2020.1585

Wei, W. C., Liaw, C. C., Tsai, K. C., Chiou, C. T., Tseng, Y. H., Chiou, W. F., et al. (2022). Targeting spike protein-induced TLR/net axis by COVID-19 therapeutic NRICM102 ameliorates pulmonary embolism and fibrosis. *Pharmacol. Res.* 184, 106424. doi:10.1016/j.phrs.2022.106424

Xu, Z., Shi, L., Wang, Y., Zhang, J., Huang, L., Zhang, C., et al. (2020). Pathological findings of COVID-19 associated with acute respiratory distress syndrome. *Lancet Respir. Med.* 8 (4), 420–422. doi:10.1016/s2213-2600(20)30076-x

Zhang, J., Wu, H., Yao, X. H., Zhang, D., Zhou, Y., Fu, B., et al. (2021). Pyroptotic macrophages stimulate the SARS-CoV-2-associated cytokine storm. *Cell. Mol. Immunol.* 18 (5), 1305–1307. doi:10.1038/s41423-021-00665-0

Zhou, P., Yang, X. L., Wang, X. G., Hu, B., Zhang, L., Zhang, W., et al. (2020). Addendum: A pneumonia outbreak associated with a new coronavirus of probable bat origin. *Nature* 588 (7836), E6. doi:10.1038/s41586-020-2951-z

Zhu, N., Zhang, D., Wang, W., Li, X., Yang, B., Song, J., et al. (2020). A novel coronavirus from patients with pneumonia in China, 2019. *N. Engl. J. Med.* 382 (8), 727–733. doi:10.1056/nejmoa2001017

Frontiers in Pharmacology

Explores the interactions between chemicals and living beings

The most cited journal in its field, which advances access to pharmacological discoveries to prevent and treat human disease.

Discover the latest Research Topics

See more →

Frontiers

Avenue du Tribunal-Fédéral 34
1005 Lausanne, Switzerland
frontiersin.org

Contact us

+41 (0)21 510 17 00
frontiersin.org/about/contact